Available online at www.sciencedirect.com
SCIENCE DIRECT®
ELSEVIER
Progress in Energy and Combustion Science xx (2004) 1–73
PROGRESS IN ENERGY AND COMBUSTION SCIENCE
www.elsevier.com/locate/pecs

Molecular transport effects on turbulent flame propagation and structure

A.N. Lipatnikov, J. Chomiak*

Department of Thermo and Fluid Dynamics, Chalmers University of Technology, 412 75 Göteborg, Sweden

Received 12 January 2004; accepted 31 July 2004

Abstract

Various experimental and DNS data show that premixed combustion is affected by the differences between the coefficients of molecular transport of fuel, oxidant, and heat not only at weak but also at moderate and high turbulence. In particular, turbulent flame speed increases with decreasing the Lewis number of the deficient reactant, the effect being very strong for lean hydrogen mixtures. Various concepts; flame instability, flame stretch, local extinction, leading point, that aim at describing the effects of molecular transport on turbulent flame propagation and structure are critically discussed and the results of relevant studies of perturbed laminar flames (unstable flames, flame balls, flames in vortex tubes) are reviewed. The crucial role played by extremely curved laminar flamelets in the propagation of moderately and highly turbulent flames is highlighted and the relevant physical mechanisms are discussed.

Keywords: Premixed turbulent combustion; Lewis number; Markstein number; Flame instabilities; Extinction; Critical conditions; Leading points

Contents

* Corresponding author. Tel.: +46 31 772 27 86; fax: +46 31 18 09 76.
E-mail address: comb@tfd.chalmers.se (J. Chomiak).

0360-1285/$ - see front matter © 2004 Published by Elsevier Ltd.
doi:10.1016/j.pecs.2004.07.001

1. Introduction

The current state of the premixed turbulent combustion field can be appraised in polar terms. On the one hand, after the pioneering work of Damköhler [1] and Shchelkin [2], substantial progress was made in revealing the local structure of turbulent flames and a number of interesting physical ideas and approaches have been put forward, such as combustion regime diagrams [3–20]; flame-generated turbulence [21]; counter-gradient transport [22–25]; flamelet library [10]; flamelet stretching and quenching [26–29]; flamelet instabilities [30]; the fractal behavior of local flame surface [31,32]; flame–vortex interaction [12,33]; rapid flame propagation along vortex tubes [34]; leading points [30]; the developing nature of real turbulent flames [21,22,35] with statistical equilibrium at small scales [36]; etc.

Nomenclature

$\mathcal{A}$ flame surface area
a_t flame strain rate (Eq. (15))
c combustion progress variable (Eq. (3))
$\mathcal{D}$ fractal dimension (Eq. (25))
D diffusivity
$Da=\tau_t/\tau_c$ Damköhler number
d_c vortex core diameter
d_f flame diameter in a vortex
e_i inner cut-off scale (Eq. (25))
e_o outer cut-off scale (Eq. (25))
F equivalence ratio
$\mathcal{F}$ arbitrary functions
f disturbance of flame front position (Eq. (24))
G scalar [6,16]
h_m flame curvature (Eq. (15))
I_0 stretch-factor (Eqs. (32) and (A.2))
k wavenumber
k_n marginally stable wavenumber
$Ka'=\tau_c u'/\lambda=0.157Ka$, $Ka''=\tau_c\sqrt{\varepsilon/\nu_u}=\sqrt{15}Ka'$, $Ka=(u'/S_{L,0})^2Re_t^{-1/2}$ Karlovitz numbers [176,10,33]
$\mathcal{L}$ Markstein length (Eq. (8))
L integral length scale of turbulence
$\hat{L}_y$ length scale of the square wave $c(y)$ (Eq. (A.5))
$Le=\kappa/D$ Lewis number
$Ma=\mathcal{L}/\delta_L$ Markstein number
Ma_c Markstein number for consumption speed (Eq. (19))
Ma_d Markstein number for displacement speed (Eq. (20))
$Ma_{h,u}$ Markstein number for $S_{h,u}$ (Eq. (13))
m normalized mass flux through the flame (Eq. (11))
$\vec{n}$ unit normal vector
P pressure
$\mathcal{P}$ probability density function
$\mathcal{P}_q$ probability of flamelet quenching (Eqs. (36) and (37))
$Pr=\nu/\kappa$ Prandtl number
R_c curvature radius
R_f flame radius
$Re_t=u'L/\nu_u$ turbulent Reynolds number
q turbulent kinetic energy
S_c consumption speed
S_d displacement speed
$S_{h,u}$ flame speed with respect to extrapolated flow (Eq. (12))
S_L perturbed laminar flame speed
$S_{L,0}$ unperturbed laminar flame speed
S_t turbulent flame speed
$S_{t,\infty}$ fully developed turbulent flame speed
St mass stoichiometric coefficient
$\dot{s}$ flame stretch rate (Eq. (14))
T temperature
t time
U_t turbulent flame speed and burning velocity
$\mathcal{U}_t$ turbulent burning velocity
u_1 mean flow velocity
$u_i=\{u, v, w\}$ velocity components
u_c consumption velocity, i.e. both consumption and displacement speeds
$u_\eta=u'Re^{-1/4}$ Kolmogorov velocity
u' r.m.s. turbulent velocity
u'_m u' associated with the maximum of a $U_t(u')$-curve
V_f speed of flame propagation along a vortex
$\mathcal{V}$ unburned flow velocity extrapolated to reaction zone
W reaction rate
$\mathcal{W}$ maximum tangential velocity in a vortex
w_h local heat release rate
$x_i=\{x, y, z\}$ spatial coordinates
Y mass fractions
$(\overline{y'^2})^{1/2}$ dispersion of random motion of an inert surface in turbulence (Eq. (5))
$Ze=\beta(\gamma-1)/\gamma$ Zel'dovich number

Greek symbols
$\beta=\Theta/T_b$ normalized activation temperature
$\Gamma=\mathcal{W}d_c$ vortex strength
$\Gamma_{\overline{K}}$ efficiency function [377]
$\gamma=\rho_u/\rho_b$ density ratio
$\Delta_L=(T_b-T_u)/\max|dT/dx|$ preheat zone thickness
$\delta_L=\kappa_u/S_{L,0}$ laminar flame thickness
δ_r reaction zone thickness
δ_t mean turbulent flame brush thickness (Eq. (4))
$\epsilon\sim k\delta_L\sim\tau_c\dot{s}$ small perturbation parameter
$\varepsilon=0.37u'^3/L$ viscous dissipation rate [176]
$\eta=\nu_u^{3/4}\epsilon^{-1/4}=1.28\eta'$, $\eta'=L\cdot Re_t^{-3/4}$ Kolmogorov length scales [10,33]
Θ activation temperature
κ molecular heat diffusivity
Λ_c mean spacing between successive front crests [302]
$\Lambda_n=2\pi/k_n$ marginally stable wave length
$\lambda=u'\sqrt{15\nu_u/\varepsilon}=6.4\lambda'$, $\lambda'=LRe_t^{-1/2}$ Taylor microscales [176,33]
ν molecular viscosity
ξ normalized distance (Eq. (2))
Π flame front perimeter
ρ density
Σ flame surface density
σ dispersion
$\tau_c=\kappa_u/S_{L,0}^2$ laminar flame time scale
τ_{cr}, τ_{ex}, and τ_{lp} time scales for highly curved flames (Eqs. (43)–(45))

$\tau_t = L/u'$	turbulent time scale
$\tau_\eta = \eta'/u_\eta$	Kolmogorov time scale
ψ_0	growth rate for the DL instability (Eq. (7))
ω	growth rate of flame surface disturbances

Subscripts

b	burned
cr	critical
d	deficient reactant
e	excess reactant
F	fuel
f	flame
L	laminar or Lagrangian
le	leading edge
m	maximum
O	oxidant
r	reaction zone
q	quenching
s	steady or relevant to strain
t	turbulent or tangential
u	unburned
0	initial or unperturbed quantities
∞	fully developed, asymptotically steady quantities

A number of physical models for evaluating turbulent flame speed, which are reviewed elsewhere [6,18,37,38], have been proposed based on the above ideas.

Also, different methods for multi-dimensional computations of turbulent flames have been elaborated such as Reynolds- or Favre-averaged numerical simulations (RANS), large eddy simulations (LES) [39–57], direct numerical simulations (DNS), see reviews [14,58] and Refs. [59–66] as recent examples, and the probability density function (PDF) approach discussed elsewhere [19,30,67,68]. To close the Favre-averaged balance equations, a number of numerical models have been developed, such as the eddy-break-up model [69,70], the model of Magnussen and Hjertager [71], the flamelet approach by Bray, Libby, Moss, and Champion [72–76], flame surface density models [19,77,78], and other models [15,16,18,79–85].

In addition, a lot of important experimental data on the instantaneous small-scale structure of turbulent flames have been obtained over the past decade by using advanced diagnostic methods. Certain recent examples are listed below: three-dimensional temperature and two-dimensional OH fields obtained simultaneously with two-sheet Rayleigh scattering and planar laser induced fluorescence (PLIF), respectively [86]; local temperature distributions ahead of thin reaction zones, recorded using two-sheet Rayleigh scattering and laser-induced predissociation fluorescence (LIPF) techniques [87]; three-dimensional measurements of the flamelet surface normal using crossed-plane Mie scattering laser tomography [88]; three-dimensional temperature fields obtained with two-sheet Rayleigh scattering [89–91]; two-dimensional fields of velocity, temperature and density recorded simultaneously using particle image velocimetry (PIV) and filtered Rayleigh scattering thermometry [92]; two-dimensional fields of temperature and OH mole fraction imaged simultaneously using Rayleigh scattering and PLIF, respectively [17,93,94]; two-dimensional fields of velocity and OH, measured simultaneously using PIV and PLIF, respectively [93,95]; two-dimensional temperature fields recorded with Rayleigh scattering [96]; two-dimensional OH fields obtained with PLIF [97]; two-dimensional flame fronts imaged using Mie scattering [98–100]; two-dimensional fields of conditional flow velocities and local flamelet velocity obtained using laser Doppler velocimetry (LDV) and 3- or 4-element electrostatic probes, see Refs. [101,102] and Ref. [103], respectively; line profiles of various species mass fractions and temperature measured simultaneously using UV Raman, Rayleigh, and LIPF techniques [104]; conditional mass fluxes obtained using LDV [105]; local chemiluminescence measurements of OH^*, CH^*, and C_2^* [106]; etc.

On the other hand, despite the substantial progress briefly mentioned above, the combustion community cannot confidently answer even the following simplest question: which mixture, A at r.m.s. turbulent velocity $u' = u'_A$ and integral length scale $L = L_A$ or B at u'_B and L_B, will burn faster? At least two key issues should be resolved to answer this question in a general case.

An increase in turbulent flame speed, U_t, by u' well-documented at moderate ($u' < u'_m$ [18]) turbulence is well known to be followed by a reduction in U_t by strong turbulence [107–113] and global quenching [114]. Since a satisfactory model of the reduction and the quenching has not been elaborated, the value of u'_m associated with the maximum of a $U_t(u'_m)$-curve cannot be predicted. Consequently, we do not know whether turbulent flame speed $U_{t,A} < U_{t,B}$ or $U_{t,A} > U_{t,B}$ if $u'_A < u'_B$, because we do not know whether $u'_B < u'_m$ or $u'_B > u'_m$.

Then, flame speed is well-known to be substantially affected not only by turbulence characteristics and laminar flame speed, $S_{L,0}$, but also by the differences between the molecular diffusion coefficients of the fuel, D_F, the oxidant, D_O, and the molecular heat diffusivity, κ, of the mixture [30,108–112], the effect being of substantial importance not only at weak ($u' < S_{L,0}$) but also at moderate and strong ($u' \approx u'_m$) turbulence.[1] The values of u'_m depend also on $S_{L,0}$, D_F, D_O, and κ. Such experimental data are discussed in Section 3. Although several concepts reviewed in Sections 4–6 have been put forward to explain the effect,

[1] For brevity, we will refer to such effects as molecular transport effects in the following, i.e. the word 'difference' will be omitted.

a physically consistent model capable of predicting the dependence of $U_t(S_{L,0}, D_F, D_O, \kappa)$ has not been elaborated, yet. Consequently, even if $u'_A < u'_B < \min\{u'_{m,A}, u'_{m,B}\}$ (moderate turbulence) and if molecular weights of fuels A and B are substantially different, we do not know whether $U_{t,A} < U_{t,B}$ or $U_{t,A} > U_{t,B}$.

Thus, the influence of molecular transport on turbulent flame speed appears to be one of the two major challenges to the premixed turbulent combustion community and this point explains the choice of subject for the present review. Moreover, the problem referred to appears to be of particular interest due to other, both practical and fundamental, reasons.

First, hydrogen is considered to be a promising energy carrier for future applications, especially in car industry. The most obvious advantages of the use of hydrogen as an alternative fuel are: (1) the potential to produce hydrogen from water or renewable sources, e.g. biomass, and (2) zero emissions of carbon dioxide, carbon oxide and unburned hydrocarbons from the combustion of H_2. Moreover, hydrogen combustion is characterized by high burning velocities at mixture strengths far below the lean flammability limits of hydrocarbon–air mixtures. This implies a relatively low flame temperature and, as a consequence, a drastic reduction in nitrogen oxide emissions and in heat losses to the walls of the combustion device and to the exhaust. The same features of hydrogen combustion (high burning velocity and low lean flammability limit) make H_2 a very promising additive able to substantially improve the performance of the lean burning of conventional hydrocarbon fuels by reducing the lean flammability limit and increasing the burning rate [115–117]. The above benefits of hydrogen call for target-directed studies of the combustion of H_2 and, in particular, for the development of an advanced model for simulating lean hydrogen–air or hydrogen–hydrocarbon–air premixed turbulent flames in future ultra-low emission combustion devices and engines. Since the differences between D_F, D_O, and κ are strong in such flames, a predictive model cannot be developed without understanding of the effects of molecular transport on turbulent flame speed.

Second, a discussion of these effects requires considering other significant issues of turbulent combustion science such as flamelet instabilities (Section 4), weakly perturbed flamelets (Section 5), the extinction of flamelets by turbulent eddies (Section 6.1), and, finally, physical mechanisms that control premixed flame propagation at high turbulence levels (Section 7).

Third, in spite of the avalanche of scientific contributions to the subject, turbulent flame theory should be considered to be in an initial stage of development, close to the 60-year-old concepts of the founding fathers Damköhler [1] and Shchelkin [2]. An increase in the local flame front surface area due to large-scale eddies is commonly recognized to control burning enhancement by moderate turbulence. Although a number of other physical mechanisms mentioned in the beginning of this section have been shown to act locally inside the flame brush, we do not know which mechanisms dominate under particular conditions and which mechanisms can be neglected when estimating U_t.

To some extent, the abundance of phenomena studied and models developed substantially hampers the understanding of turbulent combustion as the key physical factors are buried under a mass of unnecessary details. Emphasizing the key governing processes and cutting-off interesting but marginal phenomena appears to be necessary to make further progress in understanding the subject. This difficult problem cannot be satisfactory resolved today and extensive experimental, numerical, and theoretical investigations are required to do so. Nevertheless, although the *decisive* investigations that establish the *governing* mechanisms of turbulent combustion under different conditions have not yet been performed; the available experimental data on the strong dependence of U_t on D_F, D_O, and κ (see Section 3) appear to be quite sufficient to cut off certain physical mechanisms, while highlighting other ones. We will try to do this in Sections 4–7.

Certainly, the governing mechanisms of turbulent combustion should be established in target-directed experiments. However, discussion of such a characteristic as global as turbulent flame speed may provide sufficient information for supporting a few hypotheses, which further investigations should be focused on. For instance, the dependence of U_t on D_F/D_O in itself implies an important role played by thin laminar zones in turbulent flame propagation; because relatively weak molecular diffusivity (as compared with the turbulent one) may affect the process only if the molecular diffusion is enhanced by the large spatial gradients associated with the zones. Recent experiments have confirmed this hypothesis by showing the existence of such local zones even in highly turbulent flames, as discussed in Section 7.1. Consequently, models that allow for the important role played by thin laminar zones in highly turbulent flames, e.g. the concept of leading points [30] or the concept of reaction sheet [15,16], are of particular interest. Even a farther-reaching hypothesis may be put forward based on the strong dependence of U_t on D_F/D_O, as discussed in Section 7.4.

The above argumentation explains the choice of the subject of this review. To introduce the problem to the reader, to briefly explain the basic concepts and terms, to outline relevant issues and provide links between subsequent sections, we will start the discussion with a brief historical overview. Key experimental and numerical data on the effects of molecular transport on turbulent flame speed, mean flame brush thickness and structure are reviewed in Section 3, where the strong dependence of U_t on D_F/D_O is highlighted. A detailed discussion of physical concepts and models relevant to the subject of this review will be given in Sections 4–6.

2. Historical overview

To the best of the authors' knowledge, the first investigation of the effects of the differences between molecular transport coefficients on premixed turbulent combustion was performed by Wohl et al. [118,119]. They experimentally investigated butane–air flames and found that (1) the equivalence ratio, $F_{L,m} \approx 1$, associated with the maximum laminar flame speed, was markedly less than the equivalence ratio, $F_{t,m} \approx 1.3$, associated with the maximum of $U_t(F)$ (cf. data 2 and 5 in Fig. 1a) and (2) turbulent flame speed in the rich ($F = 1.3$) mixture was much higher than in the lean ($F = 0.8$) one, whereas $S_{L,0}(F = 1.3) \approx S_{L,0}(F = 0.8)$.

Wohl et al. [118,119] associated these results with the difference in molecular diffusivities of butane and oxygen, $D_F < D_O$, and invoked the preceding studies of laminar flame instabilities [120–122] to explain the experimental data referred to. In particular, they pointed out that rich butane–air flames were subject to the instabilities and had 'a tendency to form wrinkles or even to be disrupted under the influence of external disturbances like approach stream turbulence, while lean flame fronts' remained flat [118]. In other words, flame surface area in a turbulent flow is larger in unstable mixtures than in stable ones, all other things being equal.

Such unstable behavior was known to be caused by the increase in the burning rate near the upstream-pointing bulges in a wrinkled laminar flame surface due to local changes in enthalpy and mixture composition. If the molecular diffusivity of the deficient reactant, D_d, is larger than κ, then, the chemical energy supplied to the bulges by molecular diffusion exceed the heat losses due to molecular conductivity and this imbalance results in an increase in local enthalpy, burning rate and propagation speed and, therefore, leads to the growth of the bulge. These local processes cause the so-called diffusive-thermal instability predicted by Zel'dovich [123]. In addition, the concentration of a faster-diffusing reactant increases in the bulges [120–122,124,125]. If this reactant is the deficient one (e.g. the rich butane–air mixtures studied by Wohl et al. [118,119]), then local concentration tends to the stoichiometric one, local propagation speed increases, the bulge grows, and the flame becomes unstable.

The two mechanisms, commonly called 'Lewis number' ($Le \equiv \kappa/D_d$) and 'preferential diffusion' effects, respectively,[2] are considered to substantially affect turbulent flame speed by increasing the local flame surface area. This hypothesis is the first foundation-stone of the current mainstream approach to modeling the dependence of U_t on molecular transport coefficients. Laminar flame instabilities and the effects of them on premixed turbulent combustion are further discussed in Section 4.

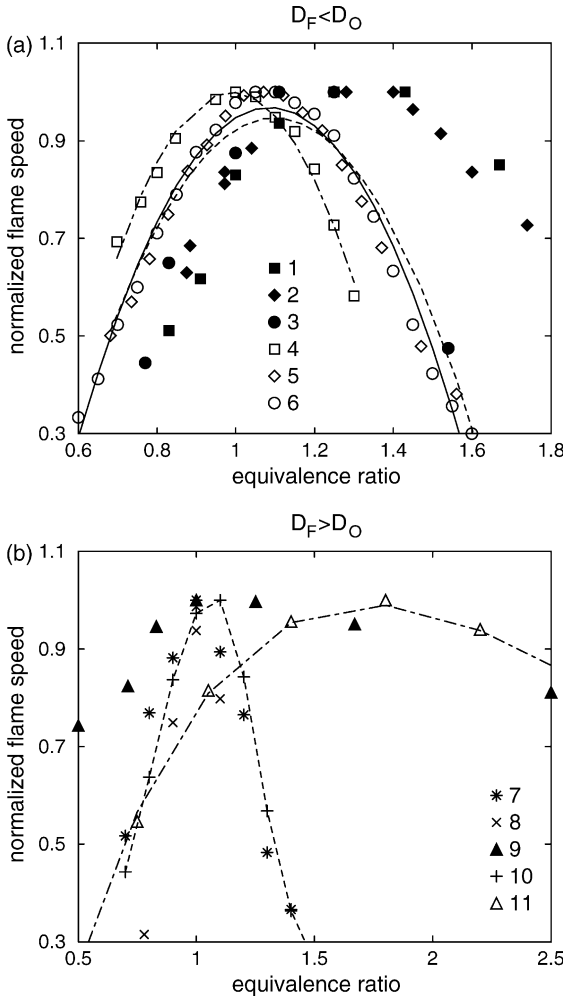

Fig. 1. Flame speed vs. equivalence ratio. Symbols show experimental data. Curves approximate the data on $S_L(F)$ with second-order polynoms. Turbulent and laminar flame speeds are normalized using the maxima of $U_t(F)$ or $S_L(F)$, respectively. (1) U_t for benzene–air mixtures, mean flow velocity $u_1 = 42$ m/s [126]; (2) U_t for butane–air mixtures, No. 8 [118]; (3) U_t for propane–air mixtures, $u' = 2.5$ m/s [144]; (4) $S_L(F)$ for benzene–air mixtures [202]; (5) $S_L(F)$ for butane–air mixtures [203]; (6) $S_L(F)$ for propane–air mixtures [204]; (7) U_t for methane–air mixtures, $u' = 3.7$ m/s [205]; (8) U_t for methane–air mixtures, $u_1 = 5$ m/s [113]; (9) U_t for hydrogen–air mixtures, $u' = 2.5$ m/s [142]; (10) $S_L(F)$ for methane–air mixtures [206]; (11) $S_L(F)$ for hydrogen–air mixtures [207].

The two mechanisms considered above are difficult to distinguish in experimental investigations of premixed combustion or in numerical simulations of complex chemistry flames. When discussing results of such studies in the following, we will use the terms, 'the dependence of turbulent flame speed (or U_t) on the diffusivity of the deficient reactant (or D_d)' or 'the effects of D_d on U_t' if

[2] In the following, we will use a unified term, 'preferential diffusive-thermal (PDT) instability' when discussing the two above basically similar instabilities.

the details of the studies are of minor importance and are not specified in this review. It is worth emphasizing that these terms are introduced solely for the purposes of brevity and they are not completely accurate, because the same effect may be obtained either by varying D_d and keeping constant κ and the diffusivity, D_e, of the excess reactant or by keeping constant D_d and varying κ and D_e. In many theoretical and DNS papers, all chemical reactions in a premixed flame are reduced to a single-step reaction, the rate of which is controlled by temperature and by the concentration of the deficient reactant (the so-called 'single-reactant, single-step chemistry'). Since solely the Lewis number effects are analyzed within the framework of such an approach, we will use the terms, 'the dependence of U_t on *Le*' or 'the effects of *Le* on U_t' when discussing results of such studies.

A few years after the research by Wohl et al. [118,119], Kozachenko [126] (e.g. data 1 in Fig. 1a) and Sokolik and Karpov [107,108] reported a number of experimental data which clearly demonstrate the dependence of U_t on D_d. However, Kozachenko did not discuss this effect and Sokolik tried to explain the data in another way [107,109], as he did not share the concept of thin flame fronts in turbulent flows, widely recognized today [16,19,75].

During the next 15 years, the effects discussed were not studied systematically with the exception of the research by Palm-Leis and Strehlow [127] who investigated statistically spherical, weakly turbulent propane–air flames and documented that the effectiveness of turbulence in increasing flame speed was most pronounced in intrinsically unstable rich flames.

In the late 1960s, Baev and Tretjakov [128] put forward a hypothesis that (1) turbulent flame speed depends on a single physico-chemical parameter of the mixture, a time scale, and (2) the same time scale controls the flashback of the laminar flame of the same mixture into a narrow channel. Based on this, hypothesis, Baev and Tretjakov [128] developed a model for predicting the mean length of premixed jet flames and validated this model using a number of experimental data available in Russia. When testing the approach, Baev and Tretjakov used the time scales obtained by investigating the flashback of laminar flames for different fuels, including hydrogen [129]. It is worth emphasizing that these time scales depended substantially on D_F/D_O.

The findings of Baev and Tretjakov were widely discussed in Russia in the 1970s and were considered to indicate a critical role played by some selected points at flame surface in turbulent combustion. In the vicinity of such points, which control turbulent flame propagation, the local flame structure was assumed to be universal and independent of turbulence characteristics [30], because the aforementioned time scale did not depend on them. Following Zel'dovich and Frank-Kamenetskii [130], Kuznetsov et al. [131–133] and Kuzin and Talantov [134] (1) associated these critical points with the leading points, i.e. those points which penetrated farthest into the unburned mixture, and (2) considered different models of the local flame structure in the vicinity of the leading points. Summarizing the results obtained in this way, Kuznetsov and Sabel'nikov [30] developed the concept of leading points, discussed in Section 6.2. The concept has been further developed and validated over the past decade [117, 135–140].

A number of experimental results on the effects of D_d on U_t were obtained in Russia in the late 1970s and the early 1980s. In particular, Talantov et al. (see reviews [30,141]) experimentally documented differences in $F_{L,m}$ and $F_{t,m}$ in benzene–air mixtures ($D_F < D_O$), $F_{L,m} < F_{t,m}$ similar to the results of Wohl et al. [118,119]. Karpov and Severin [110, 115,142–145] performed extensive experimental investigation of the problem by measuring turbulent flame speeds and burning velocities in a number of mixtures specially prepared to systematically vary $S_{L,0}$, *Le*, D_F, and D_O. They compiled a huge data base on $U_t(u', S_{L,0}, \kappa, Le, D_F/D_O)$ (see Section 3.4.1 in Ref. [18] and Section 3.1 below), the interpretation of which is still a challenge to the combustion community, as discussed in detail in Sections 4–6.

A similar experimental approach was later used by Kido et al. [99,112,116,146–152] who also accumulated an impressive set of data, which clearly indicate strong dependence of U_t on D_d. Large data bases, which show such a dependence have been also compiled by the University of Leeds [100,111], the University of Karlsruhe [153–159], and the University of Michigan [160,161].

At the same time, Sivashinsky [162,163] developed a theory of self-turbulizing flames which accounted for the aforementioned diffusive-thermal instabilities and predicted the substantial effect of *Le* on the process. However, this theory does not address turbulent flames.

Later on, Clavin and Williams [6,23,164,165] developed a theory of wrinkled laminar flames in large-scale turbulence, characterized by a low ratio, $\epsilon = \delta_L/L \ll 1$, of the laminar flame thickness, δ_L, to the turbulent length scale, *L*. In the case of weak turbulence, the theory predicted a certain effect of *Le* on U_t in the second-order (with respect to ϵ) approximation (e.g. Eq. (73), p. 435 [6]), but the first order term did not depend on *Le* and the aforementioned second-order effect was obtained within the limit of negligible density change. No experimental tests of this result are known.

The theory of Clavin and Williams was further extended by Searby and Clavin [166] and Aldredge and Williams [167], who addressed variations of a large-scale ($\epsilon \ll 1$), low-intensity ($u'/S_{L,0} \ll 1$) turbulent flow field in the vicinity of an intrinsically stable laminar flame. The results reported by Aldredge and Williams [167] show a weak effect of *Le* on U_t if the density ratio $\gamma = \rho_u/\rho_b$ is less than 4 (see Fig. 3c in the quoted paper). However, the predicted effect of *Le* on U_t is much more pronounced near the planar-flame stability limit ($\gamma \approx 6$).

In 1981, Peters and Williams [168] introduced the concept of stretched laminar flamelets to model the reaction zones in a turbulent flow and pointed out that the local

burning rate in the flamelets and the local extinction of them depend substantially on the Lewis number.

Later on, Abdel-Gayed et al. [169] extended the so-called two-eddy model, developed originally for $Le=1$ [170], in order to simulate the dependence of $U_t(Le)$. They (1) considered the local changes in laminar burning velocity, caused by the straining of a flame by turbulent eddies, to be the basic physical mechanism that control $U_t(Le)$ and (2) used the theoretical expressions for $S_L/S_{L,0}(a_t, Le, \gamma, \beta)$, obtained by Tromans [171] for strained laminar flames, in order to calculate turbulent burning velocity by replacing $S_{L,0}$ with S_L in the expressions provided by the aforementioned two-eddy model. Here, $S_{L,0}$ is the speed of an unperturbed laminar flame, i.e. of a planar one-dimensional flame which propagates against a stationary and spatially uniform flow of unburned mixture, S_L is the speed of perturbed flames, a_t is the strain rate (see Eq. (15)), $\beta=\Theta/T_b$ is the dimensionless activation temperature, Θ, of a single reaction that models chemical conversion, T is the temperature, and the subscripts 'u' and 'b' label the unburned and burned gas, respectively.

The above idea was generalized by Peters [10] who formulated the concept of 'flamelet library'. The concept is the second foundation-stone of the current mainstream approach to modeling the dependence of U_i on D_d. The approach may be briefly characterized as follows.

In premixed turbulent flames, chemical reactions that control heat release are confined to thin, wrinkled, convoluted and strained reacting fronts that separate unburned reactants from burned products. Such fronts, commonly called flamelets, are typically assumed to have the same local structure as perturbed laminar flames. The basic physical mechanism of the influence of turbulence on combustion consists of the production of flame surface area by turbulent stretching. In unstable laminar flamelets, the increase is more pronounced and turbulent flame speed is higher than in stable ones, all other things being equal. Moreover, the burning rate per unit front surface in flamelets locally stretched[3] by small-scale turbulent eddies differs from $\rho_u S_{L,0}$. The burning rate increases when Le decreases or D_d/D_e increases. If the local stretch rate is sufficiently strong, the burning rate can drop to zero (local extinction), with the probability of this event being increased by Le and D_e/D_d. The dependence of such local variations in the burning rate on molecular transport coefficients contributes also to the dependence of U_t on D_d. The variations might be modeled; (1) by simulating the response of the corresponding laminar flame to simple, well-defined stretching provided by non-planar and non-uniform flows (results of such simulations constitute the so-called 'flamelet library'), and (2) by averaging the library with a PDF for the perturbations in a turbulent flow.

Although the concept of unstable and stretched flamelets has been known about 20 years, it has not been quantitatively tested against representative experimental data on $U_t(Le, D_d/D_e)$.

To the best of the authors' knowledge, few models [167,172,173], which yield a dependence of U_t on D_d due to the instability mechanism, have been developed.

The flamelet library part of the concept is more popular, but the library is typically reduced to one of the two limit cases, either $a_t \to \dot{s}_q$ or $a_t \to 0$. In the former case, the concept of the critical stretch rate, $\dot{s}_q$, which is associated with the extinction of laminar flames by hydrodynamic stretching, was put forward by Bray [174] and Abdel-Gayed et al. [175] and further developed in Refs. [38,176–179] (see Section 6.1).

In the latter case, the concept of the Markstein number, Ma, which characterizes the response of S_L to weak perturbations [165], was invoked to model the effects of molecular transport on U_t [180–182] (see Section 5). This idea initiated an avalanche of scientific contributions aimed at evaluating the Markstein number (see recent reviews [183–185] and Refs. [186–195] as recent examples).

Over the past decade, numerous experimental investigations of the local structure of premixed turbulent flames with substantially different D_F, D_O, and κ were conducted using advanced diagnostic techniques (see Table 1). The structure was also investigated in DNS (see Table 2). The results of these studies support the concept of unstable and stretched flamelets in general terms, but do not allow us to claim that: (1) the concept is fully proven, and (2) the basic physical mechanism that controls the dependence of U_t on D_d is established. In particular, the leading point concept, an alternative to the mainstream approach mentioned above, appears to be not only consistent with recent experimental and numerical results but is also able to predict the strong effect of D_d on U_t (see Section 6.2), which challenges the mainstream approach.

Concluding the historical overview, it is worth mentioning two recent papers which are relevant to the subject of this review but are not discussed in Sections 3–6 due to specific methodology, as well as the lack of follow-up studies and experimental validation of reported numerical results. First, Smith and Menon [196] extended the linear eddy model [197] and predicted a strong acceleration of turbulent flame propagation when Le was decreased from 0.8 to 0.3. Second, Swaminathan and Bilger [198] suggested a submodel of Lewis number effects on premixed turbulent combustion within the framework of the conditional moment technique developed by Klimenko and Bilger [199]. The submodel closes a term in the conditionally averaged progress variable balance equation, which is associated with the differential molecular diffusion of mass and heat. The closure has been validated against

[3] In this paper, we will use the term 'stretching' in order to characterize two types of perturbations, i.e. flame curvature and a straining of the flame by a flow (see Eq. (15) in Section 4.1.3).

Table 1
Methods and conditions of experimental studies of premixed turbulent flames associated with $D_d \neq D_e$ and $Le \neq 1$

Reference	Mixture	$u'/S_{L,0}$	Burner	Technique
Wohl et al. [118,119]	CH_4/air, C_4H_{10}/air	<6	Bunsen flames	Schlieren pictures
Palm-Leis and Strehlow [127]	C_3H_8/air, $F=0.775$	<1	Expanding spherical flames	Flash-Schlieren
Wu et al. [160,161]	H_2/air, $F=0.3$–3.57	0.4–15.5	Jet flames	Flash-Schlieren, 2D laser tomography
Kwon et al. [340,341]	$H_2/O_2/N_2$, $F=1.0$, 1.4, 3.6; C_3H_8/air, $F=0.8$ and 1.8	0.5–2.0	Expanding spherical flames	2D laser tomography
Yoshida and Tsuji [342,343]	C_3H_8/air, $F=0.68$–0.72	0.5–2.0	Bunsen flames	Schlieren pictures, thermocouple
Furukawa et al. [344–346]	CH_4/air, $F=0.95$–1.23, C_3H_8/air, $F=0.85$–1.37	3–10	Bunsen flames	Schlieren pictures, micro-electrostatic probe
Becker et al. [347]	C_3H_8/air, $F=0.67$ and 1.0		Engine simulator $P=1.5$–7.8 bar	2D OH LIF
Lee et al. [223,348]	C_3H_8/air, $F=0.75$–1.25	1.4–5.7	Planar flames	2D OH PLIF
Lee et al. [349,350]	Lean H_2/He/air, lean CH_4/air, lean C_3H_8/air	0	V-shaped flames and Kármán vortex streets	2D OH PLIF
Goix and Shepherd [351]	Lean H_2/air, lean C_3H_8/air	≈ 1	Stagnation point flames	2D laser tomography
Paul and Bray [172]	Rich CH_4/air, rich C_3H_8/air	<0.85	Bunsen flames	2D laser tomography
Kobayashi et al. [97,352–355]	Lean CH_4/air, lean C_2H_6/air, lean C_3H_8/air	0–30	Bunsen flames $P=1$–30 bar	2D laser tomography, 2D OH PLIF, Schlieren
Renou et al. [98,356–358]	CH_4/air, $F=1.0$; C_3H_8/air, $F=1.0$; lean H_2/air	<2	Expanding spherical flames	2D laser tomography
Chang et al. [359]	CH_4/air, $F=0.9$ and 1.2	1.4 and 4.1	Expanding planar flames	2D laser tomography
Haq et al. [360]	CH_4/air, $F=0.7$ and 1.0 C_8H_{18}, $F=0.75$, 1.0, 1.4	1.3–24	Expanding spherical flames, $P=1$ and 5 bar	2D OH PLIF
Soika et al. [361]	CH_4/air, $F=0.7$ and 1.0	10–45	Flames behind a bluff-body, $P=1$–11 bar	OH laser-induced predissociation fluorescence
Chen and Bilger [86,362]	Lean CH_4/air, lean C_3H_8/air, lean H_2/air	2.5–7.1, 12.1–15.1	Bunsen flames	Two-sheet Rayleigh scattering, 2D OH PLIF

Table 2
Methods and conditions of DNS of premixed turbulent flames associated with $Le \neq 1$

Reference	Dimension	Chemistry	Mixture	Density	Turbulence
Ashurst et al. [222]	2D	Single-step, single reactant	$Le=0.5$, 2.0	Constant	Random flow field, $L/\Delta_L=10$
Haworth and Poinsot [209]	2D	Single-step, single-reactant	$Le=0.8$, 1.0, 1.2	Variable	Decaying, $u'_0/S_{L,0}=5.8$–6.6, $L/\Delta_L=3.6$–4.3
Rutland and Trouvé [210]	3D	Single-step, single-reactant	$Le=0.8$, 1.0, 1.2	Constant	Decaying, $u'_0/S_{L,0}=3$–5, $\lambda \approx \Delta_L$
Baum et al. [200]	2D	Complex	Preheated $H_2/O_2/N_2$, $F=0.35$–1.3	Variable	Decaying, $u'_0/S_{L,0}=1.2$–3.2 and 31, $L/\Delta_L=1.26$–4.34
Trouvé and Poinsot [211]	3D	Single-step, single-reactant	$Le=0.3$, 0.8, 1.0, and 1.2	Variable	Decaying, $u'_0/S_{L,0}=10$, $L \approx \Delta_L$
Chen et al. [363–369]	2D	Complex	CH_4/air, $F \leq 1.0$	Variable	Decaying, $u'_0/S_{L,0}=4$–10, $L/\Delta_L=2.9$–4.05
Chen and Im [370,371]	2D	Complex	H_2/air, $F=0.4$, 0.6, 2.0, and 6.5	Variable	Decaying, $u'_0/S_{L,0}=5$ and 10, $L/\Delta_L=2.3$–4.1
de Charentenay and Ern [372]	2D	Complex	$H_2/O_2/N_2$, $F=0.5$, 1.0, 5.0	Variable	Localized turbulence convected through flame
Tanahashi et al. [59,60]	3D	Complex	H_2/air, $F=1.0$, $T_u=700$ K	Variable	Decaying, $u'_0/S_{L,0}=0.85$–3.41, $L/\Delta_L=0.85$–3.38

the DNS data base of Baum et al. [200] obtained for small-scale, high-intensity, 2D turbulence.

3. Experimental evidence

3.1. Turbulent flame speed

The problem of a physically meaningful definition of turbulent flame speed has been addressed in our recent papers [18,201]. In the following, we will use the notation accepted in Ref. [18, p. 7]. In particular, the term 'fully developed turbulent flame speed' and the symbol $S_{t,\infty}$ will denote the speed of a hypothetical unperturbed turbulent flame, i.e. a statistically planar, 1D flame, which has a steady mean flame brush thickness, δ_t, and propagates at a steady velocity against a statistically stationary and uniform flow of unburned mixture. The term, 'turbulent burning velocity' and the symbol $\mathcal{U}_t$ will denote the mass burning rate per unit flame surface area, divided by the density, ρ_u, of unburned mixture ($\mathcal{U}_t = S_{t,\infty}$ for the unperturbed flame, but $\mathcal{U}_t$ is not well-defined for curved flames). The symbol S_t will be used when discussing results obtained definitely for the speed of flame propagation with respect to unburned mixture, although an accurate definition of the speed will not be specified in many such cases (the speed depends on the choice of a reference surface if the flame brush grows). Since the following discussion will often be restricted to solely qualitative trends in the behavior of turbulent flame speed and burning velocity; the common term 'turbulent flame speed' and the common symbol U_t will be used for brevity in order to qualitatively characterize the common features of the behavior of both quantities. In such cases, U_t means either $S_{t,\infty}$, or $\mathcal{U}_t$, or some S_t, which is not well-defined.

The effects of molecular transport on turbulent flame speeds have been observed in numerous experimental investigations. One manifestation of the effects is the aforementioned difference in the values of $F_{L,m}$ and $F_{t,m}$. The negative differences, $F_{L,m} < F_{t,m}$, have been documented by several groups [118,119,126,141,144] (see Fig. 1a) in mixtures with $D_F < D_O$. The positive differences, $F_{L,m} > F_{t,m}$ (see Fig. 1b) have been reported in mixtures with $D_F > D_O$ [113,142,205,208].

The simplest explanation of this effect is as follows: If $D_F > D_O$ ($D_O > D_F$) the local composition in positively (i.e. strained or convex toward unburned mixture) stretched lean (rich) flamelets tends to the stoichiometric one and the local burning rate increases, whereas it decreases in stoichiometric (in the mean) mixtures due to local enrichment (weakening) of the flamelets. Consequently, the local burning rate in positively stretched flamelets, which occur more often in turbulent flows (see Section 5.2.2), reaches the maximum value in leaner (richer) mixtures as compared with $F_{L,m}$.

Other well-documented manifestations of the effects discussed are shown in Figs. 2 and 3. Several research groups selected pairs (or sets—see Figs. 2c and 3) of non-stoichiometric mixtures A and B (C, D, etc.) such that (1) all the mixtures had approximately equal laminar flame speeds, but (2) $D_d < D_e$ (rich, $D_d = D_O < D_F = D_e$, hydrogen– and methane–air mixtures or lean, $D_d = D_F < D_O = D_e$, propane–air ones) and $D_d > D_e$ (lean hydrogen– and methane–air mixtures or rich propane–air ones) for A and B, respectively, and $Le_B < 1 < Le_A$ in the majority of the sets.

First, the data shown in Fig. 2 indicate that $U_{t,A} < U_{t,B}$ under the same turbulent conditions, i.e. turbulent flame speed is reduced by Le and D_e/D_d. The effect is most pronounced in hydrogen–air mixtures (cf. open triangles and filled squares in Fig. 2c), for which the difference in $D_F > D_O$ is quite substantial; but it is pronounced even in methane–air mixtures (see squares and triangles in Fig. 2d), characterized by small differences in $D_F > D_O$. Propane–air mixtures (Fig. 2a and b, circles in Fig. 2c, diamonds and circles in Fig. 2d), characterized by moderate difference in $D_F < D_O$, occupy an intermediate position.

The data have been obtained by four independent groups in fan-stirred bombs. Three sets of data (a, c, and d) definitely characterize burning velocity, because they have been obtained by processing pressure diagrams [110,148, 159]. For this reason, we will use the symbol $\mathcal{U}_t$ when discussing these data. The same behavior of flame speed ($U_{t,A} < U_{t,B}$) has been observed by other groups in confined flames [118,126], jet flames [160,161], and impinging flames stabilized near a stagnation plate [153].

A moderate acceleration of turbulent flames has been also obtained in DNS when decreasing the Lewis number from $Le = 1.2$ to 0.8 [209,210]. The effect is much more pronounced if $Le = 0.3$ [211] (see Fig. 10 in Section 4.2).

Second, Fig. 2c shows that the effect referred to is not associated with a jump transition (like stable–unstable burning). The weakening of lean hydrogen–air mixtures (see filled diamonds, triangles and squares) results in a gradually increasing turbulent burning velocity, all other things being equal. Since, in these three mixtures, D_F is the same and D_O is approximately the same ($D_O = 0.27$, 0.26, and 0.24 cm^2/s for $F = 0.85$, 0.7, and 0.5, respectively), as well as the Lewis number ($Le = 0.57$, 0.53, and 0.47), the data indicate a strong sensitivity of $\mathcal{U}_t$ to Le and D_F/D_O. Fig. 3 also shows that the decrease in D_F (from hydrogen to propane), when keeping the equivalence ratio and laminar flame speed constant, results in a gradually decreasing $\mathcal{U}_t$ without any jumps.

Third, the highest turbulent velocities, u'_q, for which flame propagation can be observed (if $u' = u'_q$, ignition kernel generated by a spark shrinks in 90% of runs) and the turbulent velocities, u'_m, associated with the maxima of $\mathcal{U}_t$ (u') (see Fig. 2a and c), are lower for mixtures with $D_d < D_e$. For instance, the condition of $u' = u'_q$ has been obtained for lean propane–air mixtures (Fig. 2a), but not for rich ones, for which u'_q is outside the investigated range of u'. Fig. 2c shows that u'_q is higher in a rich (filled down triangles)

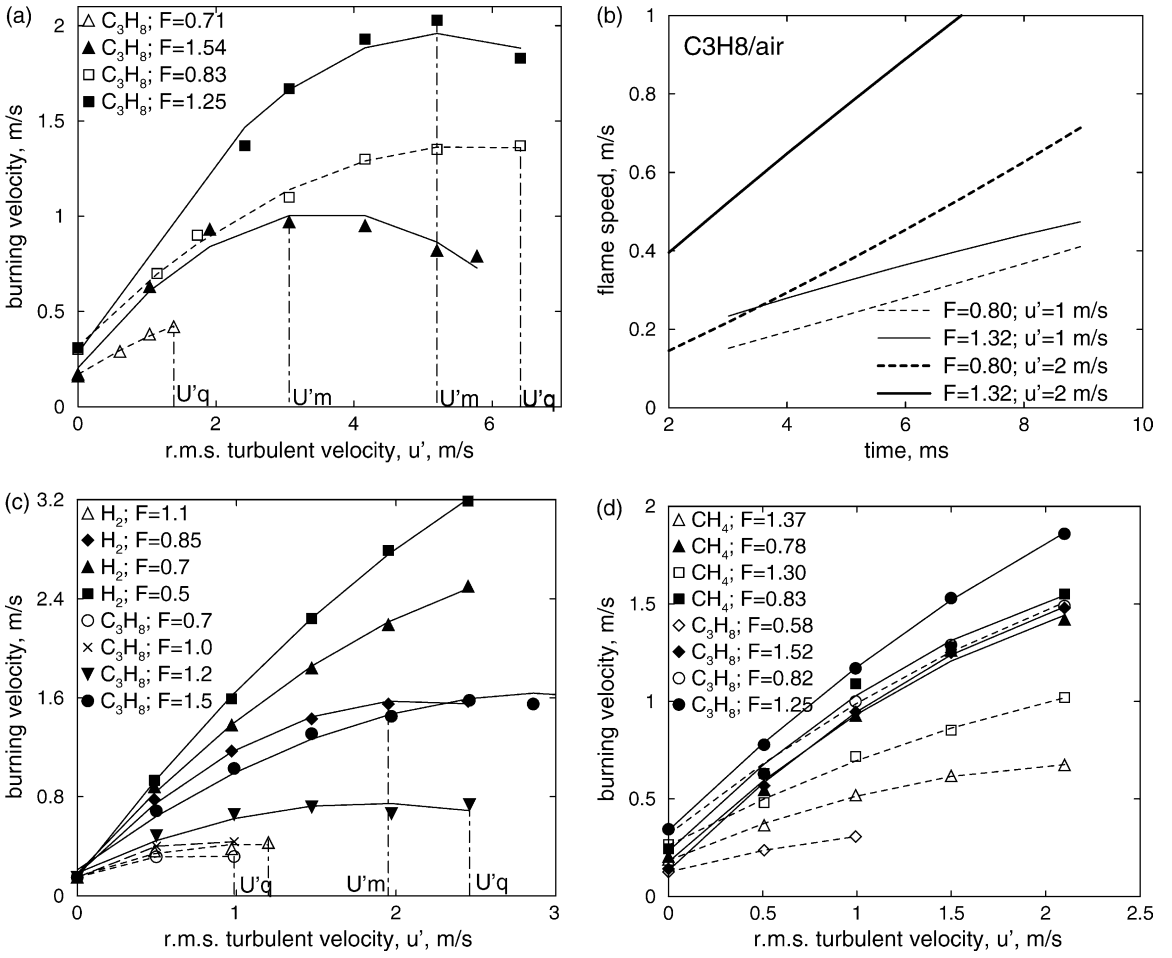

Fig. 2. Turbulent flame speeds measured in fan-stirred bombs. Symbols show raw data approximated with curves. Filled symbols and solid curves correspond to the deficiency of the faster-diffusing reactant. Open symbols and dashed curves correspond to the deficiency of the slower-diffusing reactant. (a) Data by Karpov and Severin [110]; (b) data by Bradley et al. [100], $S_{L,0}=0.28$ m/s for both mixtures; (c) data by Nakahara and Kido [148], $S_{L,0}=0.15$ m/s for all the mixtures; (d) data by Brutscher et al. [159].

propane–air mixture than in the two mixtures (open symbols) characterized by $D_d<D_e$. Moreover, the values of u'_m, obtained in these two mixtures, are markedly lower than the u'_m associated with the mixtures characterized by $D_d>D_e$, these values being reached only in two of five such mixtures (filled symbols).

Fourth, for mixtures with $D_d>D_e$, the maxima of the $\mathcal{U}_t(u')$-curves are well pronounced if the values of u' are sufficiently high (see solid curves in Fig. 2a and c). For mixtures with $D_d<D_e$, the maxima are weakly pronounced and the leveling-off of the curves with no decreasing segments is observed in many such mixtures, as shown in dashed lines in Figs. 2a and c and 4a and b. To the best of the authors' knowledge, the different form of the $\mathcal{U}_t(u')$-curves has not been discussed in the literature.

Figs. 2 and 3 clearly indicate that turbulent flame speed is affected by molecular transport, the effect being observed not only in low-, but also in moderate- and even high-intensity (e.g. the values of u'_m and u'_q) turbulence.

Fig. 4 shows that: (1) the effect can be very strong (cf. mixtures 1 and 2 in Fig. 4a, which are characterized by equal laminar flame speeds, but different Le and D_d/D_e), and (2) the effects observed at moderate ($u'<u'_m$) and high ($u'>u'_m$) turbulence are not correlated.

First, an analysis of a number of experimental data obtained at moderate turbulence for typical hydrocarbon–air mixtures associated with weak ($D_F\approx D_O\approx\kappa$ and $F\approx1$) effects referred to has shown that $U_t\propto S_{L,0}^q$ and $dU_t/du'\propto S_{L,0}^q$ with $q=0.5$–0.8 [18], i.e. the higher the laminar flame speed, the higher U_t and dU_t/du'. Such a correlation fails when the aforementioned flames are compared with lean hydrogen ones characterized by a small Le and a large difference in D_F and D_O. For instance, in very lean hydrogen mixtures 4, 5, and 8 (see Fig. 4a), $S_{L,0}$ is by 4–5 times lower

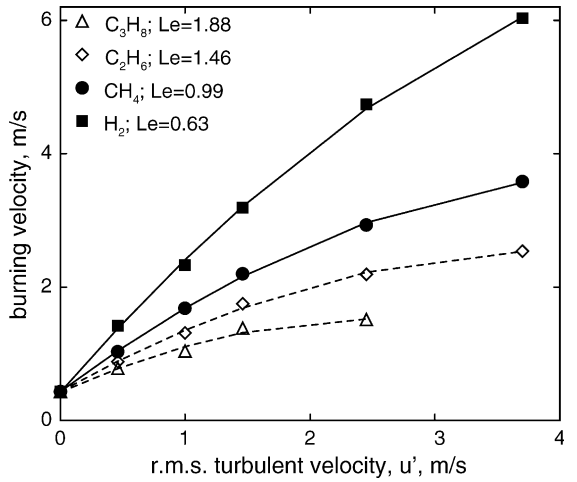

Fig. 3. Burning velocities measured by Kido et al. [112] for fuel/oxygen/nitrogen/helium mixtures with $F=0.5$ and $S_{L,0}=0.43$ m/s. Fuels are specified in legends.

than in the stoichiometric propane–air mixture 6, whereas $\mathcal{U}_t$ is markedly higher in mixtures 4 and 5 than in mixture 6. The effect is even more pronounced when discussing the slopes $d\mathcal{U}_t/du'$ (for $\mathcal{U}_t$, the effect is sometimes masked due to the substantial difference in $S_{L,0}$, e.g. mixtures 6 and 8): the slopes are much steeper in the lean hydrogen mixtures than in mixture 6. In a lean hydrogen mixture 3, $S_{L,0}$ is more than 5 times lower than in a rich mixture 1, whereas the slope shows the opposite behavior and $\mathcal{U}_t$ is markedly higher in the former mixture at $u'>1$ m/s.

Wu et al. [160] investigated jet hydrogen flames and observed that U_t in a lean mixture ($F=0.3$) was higher than in a rich one ($F=3.57$) despite the fact that $S_{L,0}(F=3.57)/S_{L,0}(F=0.3)\approx 6$.

In a stoichiometric methane mixture (see open circles in Fig. 4b), $S_{L,0}$ is 10 times higher than in a lean mixture (filled circles), whereas the slope shows the opposite behavior and $\mathcal{U}_t$ is higher in the latter mixture at $1<u'<3$ m/s.

Finally, the curves of $\mathcal{U}_t$ corresponding to mixtures 1 and 4 (or 5, see Fig. 4a) are close to one another within the interval $u'=2$–3 m/s despite the fact that $S_{L,0}$ in the former mixture is higher by 15 times. The effect is even more pronounced when discussing the slopes: the $\mathcal{U}_t(u')$-curves measured in the lean mixtures have a slope more than twice as high as that in the rich mixture at moderate turbulence ($u'=1$–3 m/s). If $\mathcal{U}_t(u')$ were independent of D_F/D_O and Le, then the slope, $d\mathcal{U}_t/du'\propto S_{L,0}^q$ with $q=0.5$–0.8 [18], would be at least four times higher in mixture 1. Consequently, the molecular transport leads to **very strong** changes in $d\mathcal{U}_t/du'$ (by a factor of 8 or even more!).

A number of other experimental data from Karpov's group [108–110,115,142–145,212], which show strong effects of D_d on $\mathcal{U}_t$, were reported elsewhere [117,136,138, 212]. In these studies, the pairs of mixtures characterized by

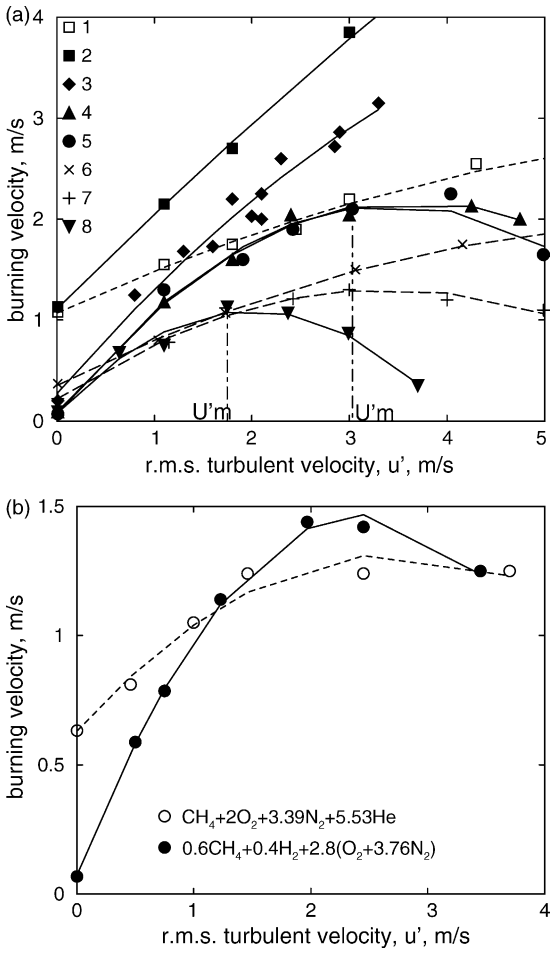

Fig. 4. Strong effect of molecular transport on turbulent burning velocity. Symbols show experimental data. Curves approximate the data with second-order polynoms. Filled symbols and solid lines correspond to the deficiency of the faster-diffusing reactant. Open symbols and dashed line correspond to the deficiency of the slower-diffusing reactant. (a) Data by Karpov and Severin [110]; (1) H_2–air mixture, $F=5.0$, $S_L=1.1$ m/s; (2) H_2–air mixture, $F=0.71$, $S_L=1.1$ m/s; (3) H_2–air mixture, $F=0.26$, $S_L=0.2$ m/s; (4) $H_2+2.8O_2+10.5Ar$, $S_L=0.07$ m/s; (5) $H_2+3O_2+8N_2$, $S_L=0.07$ m/s; (6) C_3H_8–air, $F=1$, $S_L=0.4$ m/s; (7) C_2H_6–air, $F=1.54$, $S_L=0.45$ m/s; (8) H_2–air mixture, $F=0.18$, $S_L=0.09$ m/s. (b) Data by Kido et al. [112,148].

$Le_A>Le_B$, $S_{L,0,A}>S_{L,0,B}$, but $(d\mathcal{U}_t/du')_A<(d\mathcal{U}_t/du')_B$, with well pronounced differences, were selected and analyzed.

Second, as mentioned above, Fig. 2 shows similar effects of D_F/D_O on $d\mathcal{U}_t/du'$ and u'_m. Typically, a higher $\mathcal{U}_t$ or $d\mathcal{U}_t/du'$ is associated with a higher u'_m [110–112,148, 212]. However, in certain pairs of mixtures shown in Fig. 4, this correlation fails (cf. mixtures 6 or 7 and 8; or mixtures 4 or 5 and 1, or 6, or 7 in Fig. 4a; or the two mixtures in Fig. 4b). The lack of a straightforward correlation between $d\mathcal{U}_t/du'$ and u'_m implies that the combustion enhancement caused by moderate turbulence

and the reduction (quenching) caused by strong turbulence depend on different physico-chemical characteristics and, in particular, the effects of molecular transport on moderately and highly turbulent premixed combustion are controlled by different physical mechanisms.

The data shown in Figs. 2–4, with the exception of Fig. 2b, definitely characterize burning velocity, as mentioned, above. As concerns Fig. 2b, these data have been obtained by measuring the speed of a reference surface inside the flame brush, but the surface has been thoroughly determined in order to characterize the burning velocity [100]. Other measurements [109,111,153,208] have indicated substantial effects of D_d on the speeds of certain isotemperature surfaces inside the turbulent flame brush, measured, most often, using the Schlieren technique. In the quoted papers, the observed effect is not as strong as in Fig. 4, but very lean hydrogen mixtures were not used in these experiments. Recently, Betev et al. [212] have demonstrated the strong effect of D_d on the speed of statistically spherical, expanding, turbulent flames, measured using the Schlieren technique in very lean and rich hydrogen–air mixtures (see Fig. 5).

3.2. Mean flame brush thickness and structure

In a recent review [18], we analyzed a number of experimental data on mean flame brush thickness and structure, obtained mainly in hydrocarbon–air mixtures characterized by a minor effect of D_d on turbulent combustion. The analysis has shown the following two important features. First, the spatial profiles of the mean

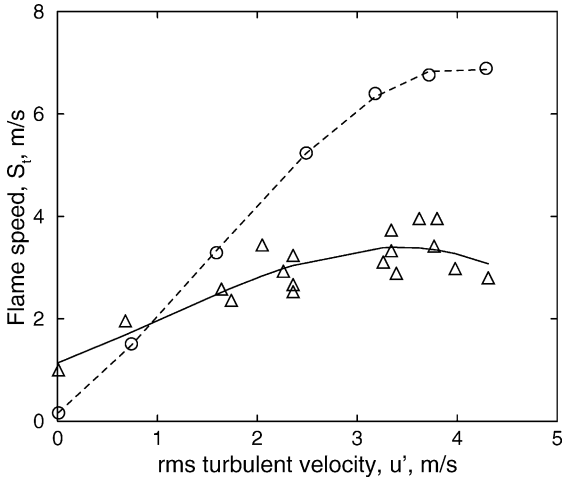

Fig. 5. Flame speed vs. r.m.s. turbulent velocity. The measurements have been performed using the high speed Schlieren technique for statistically spherical flames expanding in the central part of a fan-stirred bomb [212]. Symbols show the experimental data. Curves approximate the data by third-order polynoms. Triangles and circles correspond to rich ($F=5.0$, $S_{L,0}=1.0$ m/s) and lean ($F=0.235$, $S_{L,0}=0.16$ m/s) hydrogen–air mixtures.

combustion progress variable, c, normal to the flame brush, are described by the same function at different instants, t, after ignition in expanding flames or at different distances, x, from flame-holder in stationary flames when using a mean flame brush thickness, $\delta_t(t)$ or $\delta_t(x)$, in order to normalize the spatial coordinate (see Figs. 17–20 in Ref. [18]); the universal profile being well approximated[4] by the complementary error function

$$\overline{c} = 1 - \frac{1}{2}\mathrm{erfc}(\xi\sqrt{\pi}) = 1 - \sqrt{\frac{1}{\pi}}\int_{\xi\sqrt{\pi}}^{\infty} \mathrm{e}^{-\zeta^2}\,\mathrm{d}\zeta; \tag{1}$$

$$\xi = \frac{z - z_f}{\delta_t}. \tag{2}$$

Here, $z_f(t)$ or $z_f(x)$ is the mean flame position, i.e. the coordinate of the surface characterized by $\overline{c}=0.5$, and the Reynolds averages are denoted by overbars, e.g. $\overline{c}$. In the adiabatic and equidiffusive, $D_F=D_O=\kappa$, case, the combustion progress variable can be defined as follows

$$c = 1 - \frac{Y_d}{Y_{d,u}};\ \text{or}\ c = \frac{T - T_u}{T_b - T_u};\ \text{or}\ c = \frac{\rho_u - \rho}{\rho_u - \rho_b}, \tag{3}$$

where Y_d is the mass fraction of the deficient reactant. Consequently, $c=0$ in an unburned mixture and $c=1$ in products. In the case of $D_F\neq D_O\neq\kappa$, discussed here, the Reynolds-averaged progress variable is considered to be equal to the probability of finding combustion products if the probability of finding intermediate (between unburned and burned) states of the mixture is small [22].

Second, the thickness, determined using the maximum gradient method

$$\delta_t^{-1} = \max\left(\frac{\mathrm{d}\overline{c}}{\mathrm{d}z}\right), \tag{4}$$

grows with the time or the distance, the growth being well described by the Taylor theory of turbulent diffusion [214] (see Figs. 21–23 in Ref. [18]), i.e. $\delta_t \approx (2\pi)^{1/2}(\overline{y'^2})^{1/2}$ and the r.m.s. amplitude of random fluctuations of a passive surface in isotropic turbulence scales as follows

$$(\overline{y'^2})^{1/2} = \begin{cases} u't, & \text{if } t \ll \tau_{t,L} \\ \sqrt{2u'L_L t}, & \text{if } t \gg \tau_{t,L} \end{cases} \tag{5}$$

in the two limit cases, Here, $\tau_{t,L}$ is the Lagrangian integral time scale, $L_L=u'\tau_{t,L}$ is the Lagrangian length scale, and, for a typical stationary flame, $t=x/u_1$ where u_1 is the mean flow velocity in the x-direction. The following expression [215–217]

$$\overline{y'^2} = 2u'L_L t\left\{1 - \frac{\tau_{t,L}}{t}\left[1 - \exp\left(-\frac{t}{\tau_{t,L}}\right)\right]\right\}, \tag{6}$$

[4] A theoretical derivation of Eq. (1) is discussed in our recent paper [213].

which results from the insertion of the exponential approximation of the Lagrangian velocity autocorrelation function into the general framework of the turbulent diffusion analysis by Taylor [214], is often used [21,35,37, 218–221] to describe the growth of the thickness. Certain authors [35,220,221] invoked modified length and time scales when applying Eq. (6) to flames, but these modifications appear to be of minor importance for practical flames, as discussed in our review [18].

Are these features affected by the differences in D_F and D_O? To answer this question, the structure of hydrogen–air turbulent flames should be analyzed, because such mixtures are characterized by the largest differences in D_F and D_O. A few data sets reported for such flames are shown in Figs. 6 and 7. The progress variables, measured by Wu et al. [160] and Renou et al. [98] using Rayleigh- and Mie-scattering techniques, respectively, straightforwardly characterize the probability of finding combustion products if local reaction zones are thin. The data have been processed using Eqs. (1), (2), and (6).

Fig. 6 shows that the universal profile of $\overline{c}(\xi)$ is not affected by D_F/D_O. These data have been obtained by two independent groups for two substantially different flames (expanding, spherical, weakly turbulent flames and jet, stationary, highly turbulent ones), the data by Wu et al. [160] include lean and rich or unstable, neutral, and stable

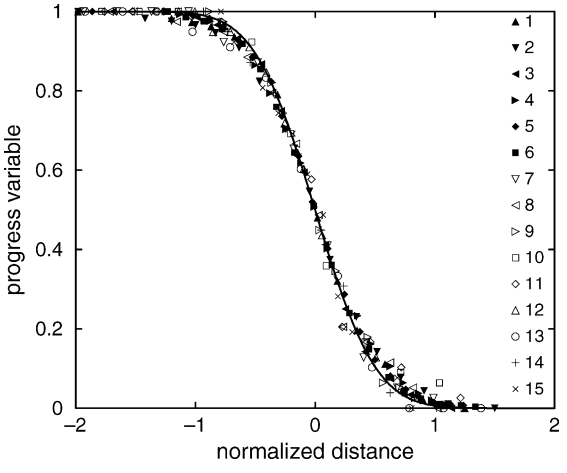

Fig. 6. Reynolds-averaged progress variable profiles normalized with δ_t. Symbols show experimental data obtained in hydrogen–air mixtures. Curve corresponds to the complementary error function approximation (Eq. (1)). 1, 2, 3, 4, 5, and 6—data measured by Renou et al. [98] in expanding, spherical, weakly turbulent lean flames at, respectively, $t=3$, 4, 5, 6, 7, and 8 ms after spark ignition; 7, 8, and 9—data measured by Wu et al. [160] in stationary, jet, highly turbulent, 'unstable' lean ($F=0.8$) flames at, respectively, $x=15$, 29, and 44 mm from burner exit; 10, 11, and 12—data measured by Wu et al. [160] in stationary, jet, highly turbulent, 'neutral' rich ($F=1.8$) flames at, respectively, $x=15$, 29, and 44 mm from burner exit; 13, 14, and 15—data measured by Wu et al. [160] in stationary, jet, highly turbulent, 'stable' rich ($F=3.6$) flames at, respectively, $x=32$, 64, and 97 mm from burner exit.

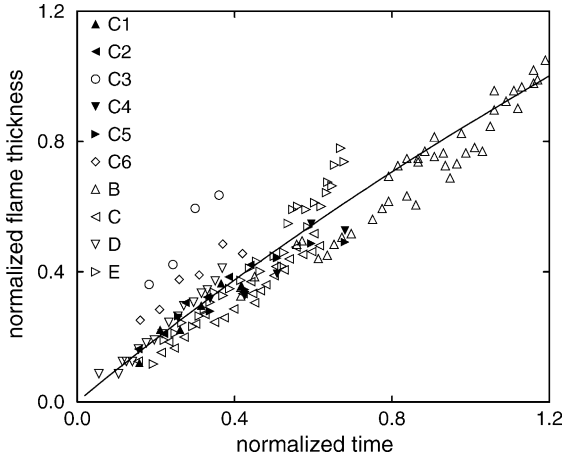

Fig. 7. Normalized mean flame brush thickness, $(2\pi)^{-1/2}\delta_t/L$, vs. normalized time, t/τ_t. Curve corresponds to the turbulent diffusion law (Eq. (6)). Symbols show experimental data. Here, the experimental conditions are labeled following the original papers [98,220]. C1, C2, C3, C4, C5, and C6—data measured by Renou et al. [98] in expanding spherical flames; B, C, D, and E—data measured by Goix et al. [220] in stationary, V-shaped lean hydrogen–air flames.

mixtures. However, the instability does not effect the universal profile of $\overline{c}(\xi)$ in turbulent flows (cf. unstable, 7–9, and stable, 13–15, profiles in Fig. 6).

Fig. 7 shows that the data on the thickness of both lean hydrogen–air[5] (open symbols) and stoichiometric hydrocarbon–air flames (filled symbols) are reasonably well approximated by the turbulent diffusion law (curve). Although the thicknesses measured in expanding, spherical, weakly turbulent lean hydrogen–air flames C3 and C6 by Renou et al. [98] are larger than other data, the effect is markedly reduced by u' (cf. circles and diamonds which correspond to $u'=0.18$ and 0.34 m/s, respectively), All in all, the available data do not indicate any substantial effect of D_F/D_O on the mean flame brush thickness development with the exception of the case C3 with very weak turbulence. Note that the turbulent Reynolds number, $Re_t=u'L/\nu_u$, is as low as 36 in the flame C3 [98]. Here, ν_u is the kinematic viscosity of the unburned mixture.

Paul and Bray [172] have documented that δ_t in rich propane–air flames is larger than in rich methane–air ones, with $S_{L,0}$ being equal. However, the effect is strongly reduced by $u'/S_{L,0}$ and is weakly pronounced at $u'/S_{L,0}=0.85$, the highest velocity ratio investigated. An increase in δ_t when decreasing Le was also observed in the simulations of weakly turbulent flames, performed by Ashurst et al. [222].

[5] Although the profiles of $\overline{c}(z)$, reported by Wu et al. [160] can be also used to calculate $\delta_t(x)$, these results are not shown, because we cannot accurately estimate the flame development time, invoked by Eq. (6), based on the data reported by Wu et al. [160,161] for jet flames.

3.3. Summary

The experimental data reviewed above show that the differences between molecular transport coefficients substantially affect flame speed not only at weak ($u' < S_{L,0}$) but also at moderate ($S_{L,0} < u' < u'_m$) and strong ($u' > u'_m$) turbulence.

No evidence of a marked effect of D_F/D_O on mean flame structure (i.e. the profile of the mean combustion progress variable across the flame brush) has been found in the literature.

Some effect of D_F/D_O on mean flame brush thickness has been reported for weakly turbulent flames, but it is reduced by $u'/S_{L,0}$.

The most intriguing evidence shows very large values of $U_t/S_{L,0}$ and dU_t/du' reported in lean hydrogen flames by, at least, three independent groups [110,148,160] under substantially different conditions and at ratios of $u'/S_{L,0}$ as large as 40 (see mixtures 4 and 5 in Fig. 4a).

We consider such experimental data to be a challenge to contemporary premixed turbulent combustion theory. The focus of the following sections will be on; (1) discussing different concepts aimed at predicting the dependence of U_t on D_d, and (2) assessing the capabilities of the concepts for predicting the above **strong** effect of D_d on $\mathcal{U}_t$.

The experimental data shown in Figs. 1–4 imply a substantial role played by thin laminar zones in turbulent flame propagation and all known concepts aimed at predicting the effects of D_d on U_t are based on studies of perturbed laminar flames with different types of perturbations. The following three chapters deal with unstable laminar flames, weakly perturbed laminar flames, and strongly perturbed laminar flames. Each chapter will start with a brief review of laminar flame studies. In each case, the scope of the review will be restricted to results used in turbulent flame simulations, but some key and recent references will be provided in order to give the interested reader the opportunity to study the problem of perturbed laminar flames in more detail. Then, models of premixed turbulent combustion, which use the results of perturbed laminar flame theories, will be reviewed and assessed by analyzing the recent experimental and DNS data on local structure of premixed turbulent flames. Finally, the ability of such models to predict the **strong** effect of D_d on $\mathcal{U}_t$ will be critically discussed.

4. Unstable laminar flames and premixed turbulent combustion

As discussed in Section 2, the dependence of U_t on D_d is commonly associated with flamelet instabilities [14,118,119,160,161,172,211,222,223] and local variations in the burning rate inside flamelets, with a special emphasis placed on weakly perturbed flamelets [99,159,176,178,180–182]. Models of premixed turbulent combustion, which allow for either unstable laminar flamelets or weakly perturbed ones, are substantially different and are separately discussed in Sections 4 and 5, respectively. However, in the laminar case, theoretical studies of the two problems have been performed using the same methods and sometimes in the same paper (e.g. [224]). For this reason, theoretical results obtained for weakly perturbed laminar flames are briefly reviewed in Section 4.1, whereas the application of these results to premixed turbulent combustion modeling is discussed in Section 5.

4.1. Unstable laminar flames

The problem of the stability of laminar flames with respect to weak perturbations has been discussed in a number of textbooks [6,37,225,226] and review papers [165,227–231], including very recent ones [183,184,232,233]. A very brief and clear summary of the basic results was given by Class et al. [234] (see Table 1 in that paper). Here, we restrict ourselves to an introduction to the issue with the focus on results relevant to modeling of turbulent combustion. To gain deeper insight into the problem, the interested reader is referred to the aforementioned textbooks and reviews, as well as to original papers quoted in this section.

It is worth emphasizing that we will consider only the so-called hydrodynamic or Darrieus–Landau (DL) and the preferential diffusive-thermal (PDT) instabilities. We will restrict the discussion of the two instabilities mainly to an adiabatic and nearly planar flame if the opposite is not specified. Other instabilities (e.g. the pulsating instability predicted by Lewis and von Elbe [218,235], see also recent papers [234,236]) will not be addressed, because such instabilities have not been invoked to explain the dependence of U_t on D_d.

The first observations of the instabilities were reported by Smithells and Ingle [237] in the 19th century, who obtained a flame in the form of a rotating polyhedral pyramid on a Bunsen burner. Similar observations were later done by Smith and Pickering [238]. The so-called cellular flame discovered independently by Drozdov and Zel'dovich [239] and Markstein [120] is another well-known manifestation of the instabilities. The first and many subsequent observations of cellular flames [120–122,125,127,240–249] were in mixtures with a faster diffusive (light) deficient reactant and were associated with the PDT instability. The cellular structure of flames in mixtures with a heavy deficient reactant was reported by Simon and Wang [250], Groff [251], Bradley and Harper [252], Kwon et al. [253]. The latter results are commonly considered to be the manifestation of the DL instability. The first direct measurements of the linear growth rate of the DL instability were recently performed by Searby et al. [254,255].

4.1.1. First theories of hydrodynamic instability

Initially, the theoretical investigations of the two instabilities were performed independently from one

another. Darrieus [256] and Landau [257] developed the following model: a flame is reduced to an infinitely thin surface which propagates at a constant speed and separates unburned and burned mixtures. The flow outside the flame is governed by the non-reacting Euler equations with the density equal to either ρ_u or ρ_b, ahead or behind the flame, respectively. Jump conditions on the flame surface are used to close the model. A stability analysis of such a planar flame, reproduced in many textbooks [37,226,258], shows that, if $S_L = S_{L,0}$, the flame is unconditionally unstable to infinitisemally perturbations of any wavenumber, k, with the linear growth rate of the amplitude of a flame surface disturbance being equal to

$$\frac{\omega}{kS_{L,0}} = \frac{\gamma}{\gamma+1}\left[\sqrt{\gamma+1-\frac{1}{\gamma}}-1\right] \equiv \psi_0(\gamma). \tag{7}$$

This dispersion relation is shown in curve 5 in Fig. 8.

The physical mechanism of the DL instability consists of the following: due to the flame-induced convergence (divergence) of the unburned mixture flow upstream of concave (convex) flame fronts, the flow velocity, u_u, increases (decreases), whereas the flame speed is constant. As a result, both convex (toward unburned gas) and concave bulges, characterized by $u_u < S_{L,0}$ and $u_u > S_{L,0}$, respectively, grow, i.e. the amplitude of the perturbation increases.

Since laminar flames are well known to be stable under a wide range of conditions, the theoretical prediction of the unconditional instability of the flames has been challenging the combustion community. The first attempt to resolve the above contradiction between theory and observations was undertaken by Markstein [121] who suggested that flame speed is not a constant quantity but is affected by the local curvature of the flame surface. He has introduced the following linear relation

$$S_L = S_{L,0}\left(1 - \frac{\mathcal{L}}{R_c}\right), \tag{8}$$

where R_c is the curvature radius ($R_c > 0$ in a flame convex to unburned mixture) and $\mathcal{L}$ is the so-called Markstein length. A stability analysis of the Darrieus–Landau problem using Eq. (8) [37,226] shows that the flame is stable with respect to short-wave ($k > k_n$) perturbations, but unstable with respect to long-wave ($k < k_n$) ones, with the neutral wave number determined from

$$k_n = \frac{\gamma-1}{2\gamma\mathcal{L}}. \tag{9}$$

Consequently, local changes in the speed of a disturbed laminar flame are of importance to flame stability. This finding triggered theoretical studies of perturbed flame speed.

Further contributions to the problem of flame stability were made by analyzing the DL and PDT instabilities together. Before summarizing these results, it is worth briefly mentioning the preceding studies of the PDT instability.

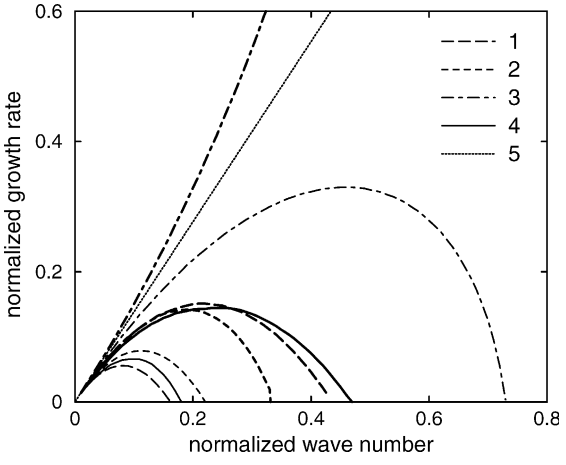

Fig. 8. Normalized linear growth rate, $\omega\tau_c$, for a flame surface disturbance vs. normalized wave-number, $k\delta_L$, of the disturbance, calculated for $\gamma = 6$. Fine and bold lines correspond to $Le = 1.2$ and 0.9, respectively. (1) Eq. (18); (2) Eq. (16); (3) Eq. (11); (4) Eq. (23); (5) Eq. (7).

4.1.2. First theories of diffusive-thermal instabilities

The physical mechanism of the preferential-diffusive-thermal instability consists of the local increase (decrease) in flame speed near upstream- (downstream-) pointing bulges in a wrinkled laminar flame surface due to local changes in enthalpy and mixture composition. If $D_d > \kappa$ (the diffusive-thermal instability [123]) or $D_d > D_e$ (the preferential diffusion instability [120]), then, either the chemical energy supplied to positively curved parts of the flame surface (upstream-pointing bulges) by molecular diffusion exceeds the heat losses due to molecular conductivity, or the mixture composition in the bulges tends to the stoichiometric composition due to the faster diffusion of the deficient reactant as compared with the excess reactant. Both processes increase the flame speed locally and the opposite phenomena occur near the downstream-pointing (negatively curved) bulges. As a result, the upstream-(downstream-) pointing bulges propagate faster (slower) and the amplitude of the flame front perturbations (bulges) grows.

The first theoretical analysis of the diffusive-thermal instability was developed by Barenblatt et al. [259]. The model used by them has introduced the following three assumptions invoked by the majority of subsequent studies: First, combustion chemistry is reduced to a single irreversible reaction (so-called single-step chemistry). Second, the rate of the reaction follows the Arrhenius law, with the activation temperature being very high, $\beta = \Theta/T_b \gg 1$. Third, the mass fraction of the deficient reactant is assumed to be very small, $Y_d \ll Y_e$, so that the mass

fraction, Y_e, of the excess reactant is practically constant in the flame (so-called single-reactant chemistry). Consequently, the preferential diffusion instability is not considered and the results are controlled by the Lewis number, but independent of D_d/D_e.

Since the above three simplifications are used by the majority of the theories discussed in this section, the assumptions will not be repeated for each particular case. If a model does not invoke some of them, this fact will be mentioned.

Barenblatt et al. [259] applied the above model to an analysis of the stability of a planar flame front with respect to long-wave ($k\delta_L \ll 1$) perturbations in the limit of constant density, which showed that the flame was unconditionally unstable if $Le<1$. Here, $\delta_L=\kappa_u/S_{L,0}$ is the laminar flame thickness. Sivashinsky [260] has extended the above analysis and has shown that the flame is stable with respect to short-wave ($k>k_n$) perturbations if $Le>Le_{cr}\equiv 1-2/\beta$. In the limit case of $\beta\gg 1$, $\gamma=1$, and $|1-Le|\ll 1$, the theory yields the following expressions [228,260]

$$\omega = D_d k^2\left[\frac{Ze}{2}(1-Le)-1-4k^2\delta_L^2\right];$$
$$k_n = \frac{1}{2\delta_L}\left[\frac{Ze}{2}(1-Le)-1\right]^{1/2}, \qquad (10)$$

where $Ze=\beta(\gamma-1)/\gamma$ is the Zel'dovich number. The flame is unstable ($\omega>0$) with respect to long-wave ($k<k_n$) perturbations if $Le<Le_c$.

4.1.3. Linear theories of hydrodynamic and diffusive-thermal instabilities

The first theory which accounts for both the DL and the PDT instabilities was developed by Sivashinsky [261] within the framework of the so-called slowly varying flame model. The model, discussed in detail elsewhere [225,262,263], consists of the assumption that flame perturbations are represented by terms on the order of $O(\beta^{-1})$ in the governing equations, which allows researchers to seek solutions in the form of the Taylor series with respect to a single small parameter, $\beta^{-1}\ll 1$. The solution obtained by Sivashinsky [261] in the case of $Le-1=O(1)$ has been recently generalized by Class et al. [234,264][6]

$$\left[1+\frac{Ze}{2}(1-Le^{-1})I_H\omega\right][k^2(\gamma^{-1}-1)+2k\gamma^{-1}\omega + \gamma^{-1}(1+\gamma^{-1})\omega^2] + k^2 Ze(1-Le^{-1})I_H(k+\gamma^{-1}\omega)=0;$$
$$k_n=\frac{1-\gamma^{-1}}{Ze(1-Le^{-1})I_H};$$
$$2m^2\ln m = \frac{Le-1}{Le}ZeI_H\tau_c\left(\frac{1}{m}\frac{\partial m}{\partial t}-\dot{s}\right) \qquad (11)$$

[6] The two papers by Class et al. are further discussed at the end of this section.

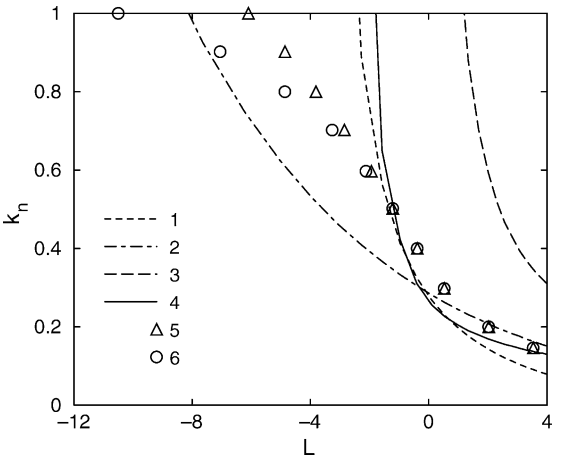

Fig. 9. Normalized neutral wave-number, $k_n\delta_L$, vs. $l=Ze(1-Le^{-1})$, calculated for $\gamma=6$, $Pr=0.75$, $\kappa_b=\kappa_u\gamma^{3/2}$, $\beta\gamma=70$. (1) Eq. (18); (2) Eq. (17); (3) Eq. (11); (4) Eq. (23); (5) numerical results of Jackson and Kapila [325]; (6) numerical results of Sharpe [329].

where the growth rate, ω, and the wavenumber, k, are normalized with the flame time scale, $\tau_c=\kappa_u/S_{L,0}^2$, and thickness, δ_L, respectively, $m\equiv\rho S_L/(\rho_u S_{L,0})$ is the normalized mass flux through the flame, the integral I_H will be specified later (Eq. (22)), and the stretch rate, $\dot{s}$, is the time derivative of a flame surface area element, normalized by the area [26]. This quantity will be discussed later (see Eqs. (14) and (15)). Note that the above solution is not valid if $Le-1=O(\beta^{-1})$ or smaller [261].

For mixtures characterized by $Le>1$ (see fine line 3 in Fig. 8), the theory predicts the stability of short-wave perturbations. The neutral wave number is shown in Fig. 9 (curve 3). If $Le<1$, the flame is unconditionally unstable, the DL instability being enhanced by the PDT instability (cf. bold curve 3 awl curve 5 in Fig. 8).

Bechtold and Matalon [265] extended the model of Sivashinsky by considering near-stoichiometric two-reactant mixture (both Y_F and Y_O change in the flame).

Another approach to jointly analyzing the DL and the PDT instabilities is based on the two-scale singular perturbation technique [164,224,266,267], which consists of the following. In order to obtain the so-called outer (hydrodynamic) solution, the internal structure of the flame is not resolved but the flame is reduced to an infinitely thin surface across which the jump conditions are posed. Then, the flow is analyzed using the incompressible Navier-Stokes equations outside the flame. The jump conditions are derived from the compressible Navier-Stokes, concentration and enthalpy (or energy, or temperature) equations integrated over a thin ($\epsilon\equiv k\delta_L\ll 1$) flame and are asymptotically expanded with respect to ϵ. The expanded jump conditions depend on the speed of the perturbed flame, which is derived by analyzing the inner structure of the flame in the limit of $\beta\gg 1$, i.e. the reaction is assumed to be

confined to a very thin zone located on the burned side of the flame.

Such a model includes three spatial scales;[7] the scale of perturbation, k^{-1}, the thickness of flame, $\delta_L \ll k^{-1}$, and the thickness of the reaction zone, $\delta_r \propto \beta^{-1}\delta_L \ll \delta_L$. The outer and the inner solutions are derived in the zones of the length of $O(k^{-1})$ and $O(\delta_L)$, respectively, with the derivation being performed in the limits of $\epsilon \ll 1$ and $\beta^{-1} \ll 1$, respectively. The model is associated with long-wave perturbations ($\epsilon \ll 1$). It may be applied to; (1) flow velocity perturbations on the order of $S_{L,0}$ or less, and (2) amplitude of flame surface perturbations on the order of k^{-1} or less [224,268].

Similar analytical solutions-have been independently obtained by different groups [164,224,266,267] by analyzing this model in the limit case[8] of $Le-1=O(\beta^{-1})$ and $\rho D=\rho_u D_u$, $\rho\nu=\rho_u\nu_u$, and $\rho\kappa=\rho_u\kappa_u$.

All the groups have obtained similar expressions for perturbed laminar flame speed with respect to unburned gas

$$S_{h,u} = S_{L,0}(1 - Ma_{h,u}\tau_c\dot{s}) + O(\epsilon) \tag{12}$$

and the corresponding Markstein number [224]

$$Ma_{h,u} = \frac{1}{\gamma-1}\left[\gamma\ln(\gamma) + \frac{Ze(1-Le^{-1})I}{2}\right];$$
$$I = \int_0^{\gamma-1}\frac{\ln(1+x)}{x}\mathrm{d}x. \tag{13}$$

As applied to such flames, the term 'weak perturbations' means small changes in flame speed, whereas the flame surface may be strongly perturbed, i.e. the amplitude of bulges may be on the order of $O(k^{-1})$.

The flame stretch rate introduced by Karlovitz et al. [26]

$$\dot{s} = \frac{1}{\mathcal{A}}\frac{\mathrm{d}\mathcal{A}}{\mathrm{d}t} \tag{14}$$

characterizes the rate of change of an elementary area, $\mathcal{A}$, of the flame front associated with the reaction sheet. In the turbulent combustion literature, the flame stretch rate is often rewritten as follows [33,165,269]

$$\dot{s} = S_{L,0}\frac{\partial n_i}{\partial x_i} + n_i n_j\frac{\partial \mathcal{V}_i}{\partial x_j} = 2S_{L,0}h_m + n_i n_j\frac{\partial \mathcal{V}_i}{\partial x_j} - \frac{\partial \mathcal{V}_i}{\partial x_i}$$
$$= 2S_{L,0}h_m + a_t, \tag{15}$$

where $\vec{n} = -\nabla\mathcal{F}/|\nabla\mathcal{F}|$ is the unit normal to the flame front directed to the fresh mixture, $h_m = \nabla\vec{n}/2$ is the flame curvature, the functions $\mathcal{F}$ and f determine the flame position, $\mathcal{F} = x_f - f(y,z,t) = 0$, the flame strain rate, a_t is the tangential gradient of the velocity, $\vec{\mathcal{V}}$, just ahead of the reaction sheet, $\vec{\mathcal{V}}$ is the extrapolation of the velocity of unburned gas to the reaction zone, and $\nabla\vec{\mathcal{V}} = 0$ because the flow ahead of the sheet is considered to be incompressible.

The dispersion relation for the linear growth rate of the amplitude of a flame surface disturbance has been reported in different forms by Frankel and Sivashinsky [266], Matalon and Matkowsky [224], Pelce and Clavin [267]. For instance [267],

$$(\omega\tau_c)^2 A(k\delta_L) + \omega\tau_c B(k\delta_L) + C(k\delta_L) = 0;$$
$$A(x) = \frac{\gamma+1}{\gamma} + \frac{\gamma-1}{\gamma}\left(Ma_{h,u} - \frac{\gamma}{\gamma-1}\ln\gamma\right)x;$$
$$B(x) = 2x + 2\gamma(Ma_{h,u} - \ln\gamma)x^2; \tag{16}$$
$$C(x) = -(\gamma-1)x^2 + (\gamma-1)$$
$$\times\left(1 + \frac{3\gamma-1}{\gamma-1}Ma_{h,u} - \frac{2\gamma}{\gamma-1}\ln\gamma\right)x^3$$

in the case of zero gravity.[9] The theory predicts that a flame is stable with respect to short-wave perturbations, $k > k_n$ if the Lewis number is sufficiently large. The neutral wave number is determined from the condition of $\omega = 0$ and, hence, $C(k_n\delta_L) = 0$:

$$k_n\delta_L = \left(1 + \frac{3\gamma-1}{\gamma-1}Ma_{h,u} - \frac{2\gamma}{\gamma-1}\ln\gamma\right)^{-1}. \tag{17}$$

Matalon and Matkowsky [224] and Sivashinsky [228] have expanded the dispersion relation with respect to $\epsilon = k\delta_L$ as follows

$$\omega = S_{L,0}\psi_0 k - D_{d,u}\psi_1 k^2 + O(\epsilon^3\tau_c^{-1});$$
$$\psi_1 = \frac{\gamma}{2(\gamma-1)}\frac{Ze(Le-1)I(1+\psi_0)(\gamma+\psi_0) + (\gamma-1)^2 + \gamma(\gamma+1+2\psi_0)\ln\gamma}{\gamma + (\gamma+1)\psi_0}; \qquad k_n\delta_L = \frac{\psi_0}{\psi_1}; \tag{18}$$

where the function $\psi_0(\gamma)$ corresponds to the DL solution (Eq. (7)) and the integral I is determined using Eq. (13).

[7] Within the framework of the aforementioned slowly varying flame model, these three scales are not independent, because $k\delta_L \propto \beta^{-1}$.

[8] The slowly varying flame model corresponds to the opposite limit of $Le-1 \gg \beta-1$.

[9] Pelce and Clavin [267] allowed for the effect of gravity on flame stability. Clavin and Garcia [270] obtained more complicated expressions by analyzing the case of temperature-dependent ρD, $\rho\nu$, and $\rho\kappa$.

The above dispersion relations, Eqs. (16) and (18), are shown in curves 2 and 1, respectively, in Fig. 8. The neutral wave numbers, k_n, predicted by Eqs. (17) and (18) are shown in curves 2 and 1, respectively, in Fig. 9.

The following peculiarities of the above solution are of importance to turbulent combustion applications. First, the theory considers the flame surface to be located at the reaction zone, which is infinitely thin, and invokes the outer (constant density) solution outside the flame. Consequently, the flame speed $S_{h,u}$ in Eq. (12) is the difference between the flame speed observed in a laboratory framework and the *extrapolation* of the velocity of unburned gas to the reaction zone. In real flames of a finite thickness, flow velocity differs from the extrapolated velocity, $\mathcal{V}$, due to the gas density variations in the preheat zone, which are neglected when evaluating $\mathcal{V}$. For example, in the simplest case of an expanding spherical flame, $\mathcal{V} = v(R)R^2/r_r^2 > v(r_r)$, where $v(r)$ is the flow velocity, r_r is the radial coordinate of the reaction zone, and $R \gg r_r$ is the radial coordinate of a point far ahead of the flame. To underline the fact that Eqs. (12) and (13) are relevant to hypothetical extrapolated quantities, we use subscript 'h,u'.

Second, if we consider other hypothetical quantities, $\mathcal{V}_b$, $S_{h,b}$, and $Ma_{h,b}$, where $\mathcal{V}_b$ is the extrapolation of the normal velocity of burned gas to the reaction zone ($\mathcal{V}_b = 0$ in the expanding spherical flame discussed above) and $S_{h,b}$ is the difference between the observed flame speed and $\mathcal{V}_b$; then the signs of $Ma_{h,u}$ and $Ma_{h,b}$ may be different under certain conditions [165,271]. Thus, the Markstein number is very sensitive to the definition of flame speed, as discussed, in detail, elsewhere [272].

Third, the response of flame speed to the flame curvature and strain rate is characterized by a single physico-chemical parameter, $Ma_{h,u}$, as far as $S_{h,u}$ is concerned. However, these two types of perturbations (h_m and a_t) differently affect the flame speed associated with another reference surface inside the flame. Consequently, two different Markstein numbers are required to parameterize the response of S_L to weak perturbations [273–276]. Analytical expressions for variations of S_L across the flame were reported by Bechtold and Matalon [275] by extending the analysis of Matalon and Matkowsky [224] to the case of a two-reactant mixture with temperature-dependent ρD, $\rho\kappa$, and $\rho\nu$. Groot et al. [276] have claimed that the strain-relevant Markstein number is not uniquely defined, whereas the stretch- and curvature-relevant Markstein numbers are well defined.

The so-called displacement, S_d, and consumption, S_c, speeds are widely used in turbulent combustion models [33, 277]. The displacement speed is equal to the difference between the observed velocity of the reaction zone, which is asymptotically thin when $\beta \to \infty$, and the mixture velocity just ahead of the zone. The consumption speed is equal to the mass rate of the consumption of the deficient reactant per unit flamelet surface area, integrated across the flamelet and normalized with $\rho_u Y_{d,u}$. Bechtold and Matalon [275] have shown that the response of S_d or S_c to the flame curvature and strain rate is characterized by a single Markstein number, Ma_d or Ma_c, respectively; i.e. the two speeds can be determined using a linear relation[10] similar to Eq. (12)

$$S_c = S_{L,0}(1 - Ma_c\tau_c\dot{s}) + O(\epsilon);$$
$$Ma_c = Ma_{h,u} - \frac{\gamma \ln \gamma}{\gamma - 1}; \tag{19}$$

and

$$S_d = S_{L,0}(1 - Ma_d\tau_c\dot{s}) + O(\epsilon);$$
$$Ma_d = Ma_c + \frac{\ln \gamma}{\gamma - 1} = Ma_{h,u} - \ln \gamma. \tag{20}$$

Since the sign of Ma_c is controlled by $Le - 1$ (cf. Eqs. (13) and (19)), the theory predicts an increase (decrease) in the consumption speed in positively stretched flames for mixtures characterized by low (high) Lewis numbers.

In a two-reactant mixture, the Lewis number used in Eqs. (13), (19), and (20) and associated with the deficient reactant should be replaced with the effective Lewis number [278,279]

$$Le_{eff} = 1 + \frac{(Le_e - 1) + (Le_d - 1)[1 + Ze(\Phi - 1)]}{2 + Ze(\Phi - 1)} \tag{21}$$

where $\Phi = \max(F, 1/F) \geq 1$.

Fourth, if $\tau_c\dot{s}$ becomes comparable with unity for steady perturbations [185,273] or when the frequency of unsteady perturbations becomes comparable with τ_c^{-1} [280], straining and curvature should be considered to be two independent characteristics of the perturbations.

Fifth, the above results have been derived in the limit case of $\epsilon = k\delta_L \ll 1$, $\beta \gg 1$, and $\beta(Le - 1) = O(1)$ and the applicability of Eqs. (13)–(21) outside this range of parameters is questionable. This issue should be borne in mind when invoking a neutral wave number determined using Eq. (17) or (18) for modeling turbulent flames, because $k_n\delta_L$ may be on the order of unity.

Over the past two decades, the theory discussed above has been further extended. The realistic dependence of molecular transport coefficients on temperature has been taken into account [270,275,281,282] and the model of Matalon and Matkowsky [224] was recently extended to a two-reactant mixture with general reaction orders [282].

An analysis of the perturbations and stability of non-adiabatic laminar flames near the flammability limits is another interesting issue, which is not discussed here, because research into the problem has recently been reviewed by Sivashinsky [233] and the obtained results have not been invoked when discussing the dependence of U_t on D_d, to the best of the authors' knowledge.

---

[10] Eqs. (19) and (20) are written in the case of $\rho D = \rho_u D_u$ and $\rho\kappa = \rho_u\kappa_u$, considered above. Bechtold and Matalon [275] have derived more general equations valid for arbitrary temperature-dependencies of D and κ.

Clavin and Joulin [280] extended the theory by Clavin et al. [164,270] of weakly perturbed flame surface ($|\nabla f| \ll 1$ and small flow velocity perturbations in comparison with $S_{L,0}$) to the case of time-dependent perturbations of high frequencies (on the order of τ_c or less).[11] They have shown that: (1) the response of the flame to such perturbations does not depend on *Le* at high frequencies; (2) the response to the strain rate decreases with increasing frequency; (3) whereas the response to the curvature shows the opposite behavior.

Klimenko and Class [284] substantially simplified the derivation of the basic results of both theories discussed above (the theory of Sivashinsky [261] for $Le-1=O(1)$ and $\beta\epsilon=O(1)$ and the theory of Matalon and Matkowsky [224] for $\beta(Le-1)=O(1)$ and ϵ independent of β) by employing tensor calculus. The technique was applied to multi-step chemical reactions in the limit of $\delta_r \ll \delta_L \ll k^{-1}$ and the derived equation for flame propagation speed was reduced by Klimenko and Class [285] to the equations of Matalon and Matkowsky [224] with *Ze* being replaced with an effective Zel'dovich number.

Recently, Class et al. [234,264] developed a unified theory by employing the tensor calculus and the basic ideas of the earlier approach of Matalon and Matkowsky [224]. Contrary to the previous studies limited to either $Le-1=O(1)$ [261] or $\beta(Le-1)=O(1)$ [165,224,266,267], the unified theory is valid for arbitrary Lewis numbers. Moreover, the theory accounts not only for long-wave disturbances of finite amplitude but also short-wave disturbances of small amplitude, which result in new terms in the equation for perturbed flame speed. Finally, the theory introduces a new surface (not the reaction zone used in the previous papers [165,224,266,267]) for evaluating the flame speed. The surface is determined from the condition of the equality of the mass fluxes derived from the hydrodynamic submodel in the unburned and burned mixture, i.e. the unburned mixture velocity extrapolated to the flame sheet should be equal to the burned mixture velocity extrapolated to the sheet. This surface is located in the preheat zone of the flame [264].

The main results of the theory are as follows: First, the mass flux, *m*, through the flame is governed by the normalized non-linear partial differential equation

$$\alpha\left\{I_H\left(\frac{\partial m^{-1}}{\partial t}+\frac{\dot{s}}{m}\right)-I_\Delta\nabla_\perp^2(1/m)+I_{\nabla^2}m[\nabla_\perp(1/m)]^2\right\}+m\ln\left[m+(I_Y-I_X)\frac{\dot{s}}{m}+2h_mI_X\right]=0;$$

$$\alpha=\frac{Ze}{2}(1-Le^{-1});$$

$$I_H=\frac{1}{1-Le^{-1}}\int_0^1\frac{1-\xi^{Le-1}}{[1+(\gamma-1)\xi]^{1/2}}\mathrm{d}\xi;$$

$$I_\Delta=1+Le^{-1}+\frac{3+Le}{4(1+Le)^2}Le(\gamma-1);$$

$$I_{\nabla^2}=\frac{7+Le(4+Le)}{8(1+Le)^3}Le(\gamma-1);$$

$$I_Y=\int_0^1\frac{\xi^{Le-1}\,\mathrm{d}\xi}{[1+(\gamma-1)\xi]^{1/2}}+2(\gamma^{1/2}-1);$$

$$I_X=\frac{2\gamma}{1+\gamma^{1/2}};\qquad(22)$$

where $\nabla_\perp(\ldots)=\vec{n}\times\nabla(\ldots)\vec{n}$ is the surface gradient and $\nabla_\perp^2=\nabla_\perp\cdot\nabla_\perp$ is the surface Laplacian. The following temperature-dependence of molecular transport coefficients, $\kappa\propto T^{3/2}$ and $D\propto T^{3/2}$ has been used for obtaining the above integrals. Eq. (22) is normalized by using the flame velocity, $S_{L,0}$, length, δ_L, and time, τ_c, scales. In the limit case of $\beta(Le-1)=O(1)$, Eq. (22) is reduced to the linear Eq. (12), provided that the flame surface is moved in order for the surface to be located at the reaction zone.

Second, the growth rate of disturbances is governed by the following dispersion relation [234]

$$k^2\left[1+2\kappa_b\gamma^{-1}kPr-\sqrt{1+4\kappa_b\gamma^{-1}Pr(\kappa_b\gamma^{-1}k^2Pr+\gamma^{-1}\omega)}\right]\times B_1-(k-\gamma^{-1}\omega)B_2=0;$$

$$B_1=k^2[\alpha I_H-I_Y+I_X(1+\gamma^{-1})]\{1+\gamma^{-1}+k[2\kappa_bPr-(I_\sigma+2Pr)]\gamma^{-1}\}+[1+\alpha(I_H\omega+I_\Delta k^2)]\times\{2\gamma^{-1}\omega+k[\gamma^{-1}-1+2(\kappa_b\gamma^{-1}-1)\gamma^{-1}\omega Pr]\};$$

$$B_2=k^2[\alpha I_H-I_Y+I_X(1+\gamma^{-1})][2(\gamma^{-1}\omega+k)+k^2(4\kappa_bPr-I_\sigma)\gamma^{-1}]+[1+\alpha(I_H\omega+I_\Delta k^2)]\times[2k\gamma^{-1}\omega+\gamma^{-1}(1+\gamma^{-1})\omega^2+k^2(\gamma^{-1}-1+4\kappa_b\gamma^{-2}\omega Pr)];$$

$$I_\sigma=\frac{4}{3}(Pr+1)(\gamma^{3/2}-1)-2(\gamma-1);\qquad(23)$$

normalized using the aforementioned flame scales. Here, $Pr=\nu/\kappa$ is the Prandtl number.

Curves 4 in Fig. 8 computed from this dispersion relation are quite close to curves 1 calculated from the earlier theory of Matalon and Matkowsky [224] (Eq. (18)). A similar trend is observed in the neutral wave number (cf. curves 1 and 4 in Fig. 9). However, contrary to Eq. (18), the unified theory predicts the stability of short-wave perturbations for any *Le* [234], whereas the previous theory yields the stability only if $Le>Le_c<1$.

Finally, it is worth noting other methods for studying the problem of laminar flame perturbations and instabilities, such as an integral analysis of Chung and Law [286],

[11] A similar problem was investigated by Joulin [283] for a constant density case.

discussed, in detail, in a recent review [184] and the flamelet model developed by de Goey et al. [287–290].

4.1.4. Non-linear models of unstable laminar flames

To simulate the non-linear stage of the development of laminar flame instabilities, Sivashinsky [162] has introduced the so-called potential flow model valid in the limit case of weak heat release, $\gamma \approx 1$. The basic assumption of the model consists of the suppression of the vorticity induced by the flame. Then, for a weakly perturbed flame surface, the following evolution equation for the amplitude of a surface disturbance

$$\frac{\partial f}{\partial t} + \frac{S_{L,0}}{2}(\nabla_t f)^2 = \mathcal{L} S_{L,0} \nabla_t^2 f + \frac{\gamma - 1}{\gamma} \frac{S_{L,0}}{8\pi^2} \int_{-\infty}^{\infty} |\vec{k}| e^{i\vec{k}(\vec{x}-\vec{x}')} f(\vec{x}', t) d\vec{k}\, d\vec{x}' \quad (24)$$

can be asymptotically rigorously ($\gamma \to 1$ and $\beta \to \infty$) derived [162,228,233]. The two terms on the right-hand side (RHS) are associated with the flame speed modification due to the diffusive-thermal mechanism and the growth rate of the DL instability, respectively. The second, non-linear, term on the left-hand side (LHS) stabilizes the disturbances and corresponds to a purely kinematic mechanism (the Huygens principle), emphasized as the main stabilizing mechanism in a number of papers [125,291–294]. Extensions of the above equation were developed by Sivashinsky and Clavin [295], who accounted for the second-order terms with respect to $\gamma - 1$, and by Frankel [296], who considered moderate perturbations.

An important merit of the Sivashinsky equation consists of the opportunity to obtain a number of exact, the so-called pole solutions [297–299], which have substantially contributed to understanding the dynamics of perturbed laminar flames. To apply the equation to weakly ($u' = O(S_L)$ or less) turbulent flames, a forcing function is commonly introduced on the RHS [300–303]. The results of such simulations are briefly discussed in Section 4.1.5. Note that the numerical solutions of the forced Sivashinsky equation are very sensitive to the inevitable numerical noise, as discussed elsewhere [233,304,305].

A number of attempts to develop a non-linear evolution equation for flame front disturbances, valid at arbitrary γ, were recently undertaken [306–313]. These papers are not discussed here, because the analysis was performed for $Le = 1$ and, consequently, the obtained results are not relevant to modeling the dependence of U_t on D_d.

4.1.5. Experimental and numerical studies of unstable laminar flames

Although unstable laminar flames have been observed by numerous groups for more than 120 years [120–122,125,127,237–253,314], the first direct measurements of the linear growth rate of flame front disturbances were made only few years ago [254,255]. The results obtained for $0.04 < k\delta_L < 0.15$ in rich ($F = 1.05 \div 1.33$) $C_3H_8/O_2/N_2$ mixtures have quantitatively confirmed Eq. (16),[12] including the decrease in ω with increasing k for short-wave perturbations. In each mixture, the Markstein number in Eq. (16) was adjusted to obtain the best agreement between theory and experiments, the adjusted values of Ma being in agreement with the data obtained by other groups (see Section 5.1). The stability of short-wave perturbations was not observed, because the neutral wave number predicted by the theory (Eq. (17)) was outside the investigated range of $k\delta_L$.

The first numerical simulations of unstable laminar flames were performed [300] based on the forced Sivashinsky equation. Results have shown that the equation is able to yield a cellular flame, characteristic cell size, and chaotic self-motion of the cells. Based on a similar evolution equation, Filyand et al. [315] numerically demonstrated the self-similar evolution of expanding spherical flames with $R_f \propto t^{3/2}$. The phenomenon is well-known from measurements [253,316–319] and is commonly associated with the growth of unstable laminar flame disturbances [233,318,320,321]. Recently, D'Angelo et al. [322] performed numerical simulations of 3D expanding spherical flames based on an extended Sivashinsky equation and obtained the polygonal network of wrinkles observed in several experiments [244,251] at the onset of instability.

Instabilities of expanding spherical flames were experimentally investigated by Bradley et al. [248,252,314,319] and the obtained results were used [318] to test a theory which had been developed by Bechtold and Matalon [323] by extending the theory of near-planar flames [224] based on ideas put forward by Istratov and Librovich [226,324]. Although qualitative agreement between measurements and theory was obtained, quantitative differences were also reported. For instance, the measured critical flame size at the onset of instability and the smallest measured cell sizes were markedly larger and smaller, respectively, than the corresponding predicted quantities. Recently, the theory was further extended [321] by considering a two-reactant mixture and temperature-dependent ρD, $\rho\kappa$, $\rho\nu$ [282]. The predictions of the extended theory provide better agreement with the experimental data.

Jackson and Kapila [229,325] employed activation energy asymptotic ($\beta \to \infty$) and numerically solved the leading order linearized reactive Navier-Stokes equations for arbitrary γ, Le, and $k\delta_L$. In the simulations, they obtained the stability of short-wave disturbances of the flame front, with the neutral wave number being in acceptable agreement with the predictions of Matalon and Matkowsky [224] (see Eq. (18)) if $Le > 0.9$ (cf. curve 1 and triangles in Fig. 9).

[12] Truffaut and Searby [255] tested a more complicated expression, obtained by Clavin and Garcia [270] in the case of non-zero gravity and temperature-dependent ρD, $\rho\nu$, and $\rho\kappa$.

Denet and Haldenwang numerically investigated the development of the PDT instability at $\gamma=1$ [326] and the DL instability for $Le=0.9\div1.0$ [327]. The computed growth rates of the instabilities tended to the corresponding theoretical solutions (Eqs. (10) and (18), respectively) when the Zel'dovich number was increased from 10 to 20. However, the difference between the theoretical and numerical results was observed even at $Ze=20$.

The problem of the validity of the asymptotic results ($\beta\to\infty$) in real mixtures characterized by finite activation temperature was further investigated by Lasseigne et al. [328] in the case of $\gamma\to1$. The results obtained by them differed from the asymptotic limit but tended to this limit when β was increased.

Recently, Sharpe [329] employed a numerical shooting method for performing a linear stability analysis of planar laminar flames by using the full reactive Navier-Stokes equations for arbitrary values of β, γ, Le, and $k\delta_L$. For $Le>0.9$, the numerical data of Sharpe [329] (see circles in Fig. 9) are in excellent agreement with the data of Jackson and Kapila [325] (triangles) and in reasonably good agreement with the theory of Matalon and Matkowsky [224] (curve 1). The theoretical and numerical growth rates are in excellent agreement if $k\delta_L<0.1$, but Eq. (18) slightly underestimates ω for shorter wave lengths. A similar difference between numerical and analytical results was reported by Denet and Haldenwang [327].

For small Le, the neutral wave numbers computed for $\gamma\beta=70$ [329] are substantially lower than the values calculated by Jackson and Kapila [325] employing activation energy asymptotic and much lower than k_n resulting from Eq. (18). In the limit case of $\gamma\to1$, the values of k_n given by the theory of Sivashinsky [260] (Eq. (10)) differ quantitatively from the numerical results [328,329]. Furthermore, the computed values of both k_n and ω for large k are sensitive to variations in the activation temperature ($\gamma\beta=30\div70$) for small Lewis numbers. For $Le=0.3$, the computed values of $k_n\delta_L\approx1$ [329] are well outside the domain of validity ($k_n\delta_L\ll1$) of most of the theories [165,224,261,266,267] reviewed in Section 4.1.3.

Kadowaki [330,331] performed 2D and 3D numerical simulations of cellular flames by solving the full reactive Navier-Stokes equations for a single-reactant mixture and $Le\geq1$. The computed neutral wave number markedly increases with decreasing Le and $k_n\delta_L=0.4$ for $Le=1$.

Numerical simulations of the DL instability [320,332–334] were also performed by solving the Navier-Stokes equations and the so-called G-equation [6,335,336], which provides a kinematic model of the propagation of an infinitely thin interface, with the flame sheet being treated either as a density sink [320,332,333] or as a surface where jump conditions are prescribed [334]. Although effects associated with the Lewis number were not addressed in these papers, certain results important to our subject were obtained.

In particular, Helenbrook and Law [334] simulated the propagation of stable ($\gamma=1$) and weakly unstable ($\gamma=1.2$ and 2.0) near-planar flames in a large-scale periodic flow and have found that: (1) the scale of flame wrinkling is controlled by the flow rather than by the DL instability; (2) flame wrinkling generated by numerical noise is suppressed by the flow and is not increased by the instability; but (3) flame wrinkling generated by the flow is amplified by the instability, which, thus; (4) manifests itself in a substantial increase in flame speed by γ; (5) the effect is not reduced by u'. The last result is associated with the small values of $u'<S_{L,0}/2$ investigated, because the DL instability growth rate on the scale of the flow is on the order of the strain rate provided by the flow or larger under the conditions of the simulations [334].

Substantially different trends have been reported by Cambray and Joulin [301–303] who numerically solved the forced evolution equation (Michelson–Sivashinsky type [300]) for a single forcing wave number [301] and for the 1D Lorentzian spectrum [302,303] to mimic isotropic turbulence (see Ref. [216, p. 203]). The forcing wave lengths were allowed to be of $O(\delta_l)$ or larger. The flame speeds computed for $\gamma>1$ and $u'/S_{L,0}<5$ were markedly larger than $S_t(\gamma=1)$, the difference being very strong at $u'\ll S_{L,0}$ [301]. The effect was reduced by $u'/S_{L,0}$. The mean spacing between successive front crests tended to a stationary quantity, Λ_c, as the unstable flame developed [302,303]. The Λ_c (1) was mainly controlled by the instability scale (the neutral wave length, $2\pi/k_n$, which was assumed to be known from the linear theory of Clavin and Garcia [270], discussed in Section 4.1.3, see Eq. (17)); (2) decreased approximately linearly when $\ln(u'/S_{L,0})$ increased but $u'<S_{L,0}$; (3) depended very weakly on the flow scale [302]. An analytical expression for $\Lambda_c k_n$ was also suggested [302,303] and it was used by Paul and Bray [172] for modeling premixed turbulent combustion (see Section 4.3). Note that this expression is well approximated by $\Lambda_c k_n=\mathcal{F}(\gamma)$ if $u'<S_{L,0}$.

Denet [337] numerically solved an extended Frankel [296] equation for a 2D flame and found that the DL instability increased the fractal dimension of the flame. For a typical flame, the obtained effect was relatively small, the difference in the fractal dimensions obtained in constant and variable density cases was about 0.1.

Bychkov et al. numerically solved a model non-linear equation that describes the dynamics of a statistically stationary flame front in weakly turbulent 2D [338] and 3D [339] flows. The equation proposed recently by Bychkov [309] combines (1) the linear theory [267] of the DL instability; (2) the non-linear theory [308] of curved flames resulting from the instability,[13] and (3) the linear theory [166] of flame response to weak turbulence. The results of the simulations show that the DL instability markedly

[13] Kazakov and Liberman [312,313] put the self-consistency of this theory into question.

increases flame speed. The effects of D_d on U_t were not addressed in these papers.

4.2. Local structure of unstable flames in a turbulent flow

The goal of this section is to discuss whether or not contemporary experimental and numerical data on the local structure of turbulent flames indicate an important role played by laminar flame instabilities in the premixed turbulent combustion of mixtures with markedly different D_F and D_O.

The methods and conditions of the experimental and numerical investigations of the structure of turbulent flames characterized by substantial differences in D_F and D_O are reported in Tables 1 and 2, respectively. All the DNS studies are associated with small-scale turbulence, characterized by $L = O(\Delta_L)$, where $\Delta_L = (T_b - T_u)/\max|dT/dz|$ is the thickness of the preheat zone of a laminar flame and the z-axis is normal to the flame. This limitation should be borne in mind when discussing the DNS data.

Note that the scope of this section is limited to the discussion of the data directly relevant to the concept of the instability-controlled dependence of $U_t(D_d)$. Other data on the local structure, which are more relevant to another concept of this dependence, will be discussed later, when reviewing the corresponding concept. Tables 1 and 2 summarize not only the measurements and DNS discussed in this section, but also studies reviewed in the following ones.

An increase in local flame surface area by turbulent eddies is commonly recognized to be the basic physical mechanism of burning enhancement caused by turbulence. Such an increase is well documented, flames with $D_d > D_e$ having a higher level of surface distortion [118,119,160] and a larger flame surface area [161,222,348–351] than flames with $D_d < D_e$. Such a behavior is often associated with the PDT instability [118,119,160,161,222].

Wu et al. [161] have reported that the ratio of the perimeters of a wrinkled flame contour and of the mean flame position on 2D images is increased by u' and is larger in lean hydrogen–air flames than in rich ones, other things being equal. They interpreted these results to be evidence of an increase in local flame front area due to the preferential diffusion instability. A similar effect of D_d/D_e on the perimeter ratio was documented by Kwon et al. [340,341] in $H_2/O_2/N_2$ flames and by Lee et al. [348] in rich as compared to lean propane–air flames.

To characterize the degree of local flame surface wrinkling, Renou and Boukhalfa [358] have evaluated the ratio of radii, $R_P = \Pi/(2\pi)$ and $R_A = \sqrt{\mathcal{A}/\pi}$, where Π and $\mathcal{A}$ are the perimeter of a flame contour observed in 2D tomographic images and the area bounded by the contour, respectively. This ratio is increased by u' and is substantially affected by D_d/D_e. In lean hydrogen–air mixtures, it is larger than in stoichiometric hydrocarbon–air ones [358]. However, the same experiments have not revealed any differences between the profiles of flame surface density (local flame front area divided by volume), $\Sigma(\bar{c})$, measured in the aforementioned hydrogen and hydrocarbon flames characterized by roughly equal values of $u'/S_{L,0}$ [98]. The independence of $\Sigma(\bar{c})$ on $Le = 0.8 \div 1.2$ has been also obtained in DNS [211].

The fractal theory [373] is often used to model the increase in local flame surface area caused by turbulence [31,32]

$$\frac{\mathcal{A}}{\mathcal{A}_o} = \left(\frac{e_o}{e_i}\right)^{\mathcal{D}-2}, \tag{25}$$

where $\mathcal{A}$ and $\mathcal{A}_o$ are the areas of wrinkled and smooth flame front surfaces, respectively, e_o and e_i are the so-called outer and inner cut-off scales, respectively (typically, $e_i \ll e_o \approx L$), and $\mathcal{D}$ is the fractal dimension.

Wu et al. [161] reported larger values of $\mathcal{D}$ in lean hydrogen–air ($D_d > D_e$) flames than in rich ($D_d < D_e$) ones, other things being equal. A similar effect of D_d/D_e on $\mathcal{D}$ was documented by Kwon et al. [340,341] in $H_2/O_2/N_2$ flames and by Goix and Shepherd [351] in lean hydrogen–air as compared to lean propane–air stagnation point flames. The inner cut-off scales measured by Goix and Shepherd [351] are weakly sensitive to the fuel.

The experiments performed by Kobayashi and Kawazoe [355] with lean methane– and propane–air ($F = 0.9$ in both cases) flames at elevated pressures did not reveal any effects of D_d/D_e on $\mathcal{D}$ and e_i, probably because such effects are weakly pronounced in near-stoichiometric mixtures.

The DNS of lean and rich $H_2/O_2/N_2$ flames [200] did not indicate any effect of $F = 0.5$–1.3 on the local flame surface area and flame speed. Haworth and Poinsot [209] and Rutland and Trouvé [210] found only a minor effect of $Le = 0.8$–1.2 on the area in DNS.

However, the DNS performed by Trouvé and Poinsot [211] in a similar mixture but with $Le = 0.3$ has shown a strong increase in the area as compared to the results computed at $Le = 0.8$–1.2 (see Fig. 10c). Note that the increase in both the area and the mean consumption velocity (see Fig. 10b) when decreasing Le to 0.3 is roughly equal. As a result of these two effects, the turbulent burning velocity computed for $Le = 0.3$ develops much faster than for $Le = 0.8$ (see Fig. 10a).

In these simulations, finger-like parts of the flame surface were observed at $Le = 0.3$. Similar topologies were also reported by Im and Chen [371] in lean hydrogen–air mixtures.

The increase in the flame surface area with decreasing Le or increasing D_d/D_e is often considered; (1) to be caused by the PDT instability of laminar flamelets, and (2) to be the manifestation of the important role played by the instability in premixed turbulent combustion [118,119,160,161,222]. However, strictly speaking, the experimental data reviewed above are not sufficient to draw such a conclusion. The data show only a substantial increase in flame surface area for flames characterized by the faster-diffusing deficient

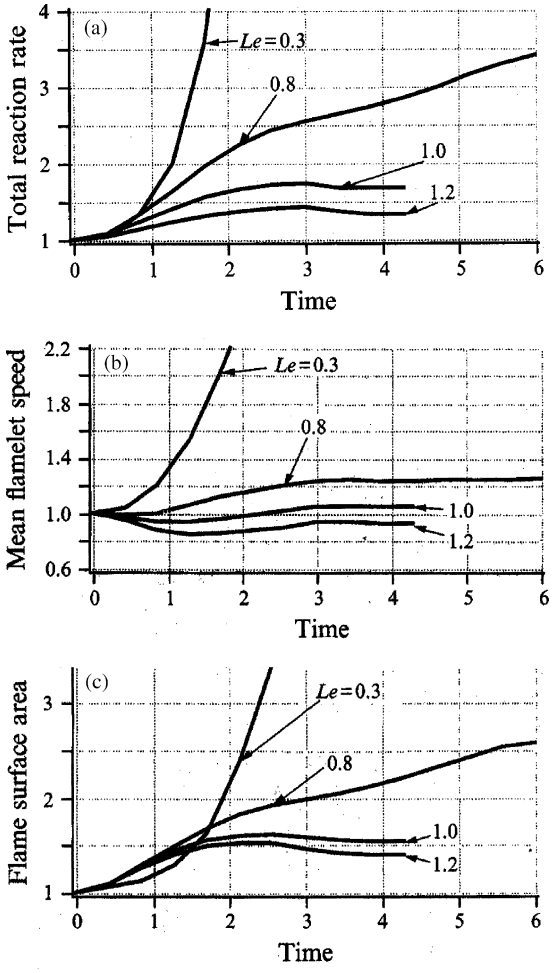

Fig. 10. Development of turbulent burning velocity (a), mean consumption velocity (b), and the relative increase of total flame surface area (c), simulated by Trouvé and Poinsot [211] at different Lewis numbers. The quantities are normalized using $S_{L,0}$ and $\tau_t \sim L/u'$. From the paper by Trouvé and Poinsot [211] © Cambridge University Press, reproduced with permission.

reactant. Although the instability concept is an attractive hypothesis for explaining this effect, this hypothesis is not the only possible one and alternative concepts able to explain the effect will be discussed in Section 6.2.

To prove the important role played by the instabilities in premixed turbulent combustion, more sophisticated measurements and simulations are necessary. For instance, a correlation between the characteristics of the behavior of a flame surface in a turbulent flow and either the growth rate of the instabilities or the relevant wave numbers (e.g. k_n or k_m associated with the maximum of $\omega(k)$) should be demonstrated. Only a few studies of the existence of such a correlation have been performed.

Yoshida and Tsuji [342,343] evaluated local lengths of pockets of unburned and burned mixture by measuring temperature history with a thermal inertia compensated thermocouple at various points inside the turbulent flame brush. They have introduced the so-called mean and eminent length scales. The former scale is equal to the mean length of the pockets at the position where the mean lengths are the same for the unburned and burned mixture. The latter scale is associated with the maximum of the PDF for the aforementioned local length. The two length scales depend weakly on turbulence characteristics (u' and L were varied by 4 and 1.6 times, respectively) and are quantitatively comparable with the length of laminar flame surface wrinkling, measured in the same mixture in the same burner [343]. These observations were interpreted to be the manifestation of the important role played by the DL instability in premixed turbulent combustion [342,343]. It is worth noting that mixture properties were not varied in these experiments.

Goix and Shepherd [351] observed that not only weakly turbulent but also laminar lean hydrogen–air flames had a fractal-like structure, in the latter case, due to the instabilities. However, the fractal dimensions measured by them were $\mathcal{D} = 2.06$ and 2.25 in the unstable laminar and weakly turbulent flames, respectively. Moreover, e_i was smaller by a factor of 2 in the former case. Thus, the local structures of unstable laminar and weakly turbulent flames were substantially different in these experiments.

Kobayashi et al. [352,354] highlighted the DL instability in order to explain the high values of $S_t/S_{L,0}$, obtained by them at elevated pressures.[14] Since k_n scales as δ_L^{-1} (see Eq. (9) or (10), or (17), or (18)), the domain of the instability ($k < k_n$) is expanded by pressure. This effect 'may play an important role in the rapid increase in $S_t/S_{L,0}$ with increasing $u'/S_{L,0}$ at small $u'/S_{L,0}$ in a high-pressure environment' [352].[15]

In subsequent studies, Kobayashi et al. [97,355] have compared the inner cut-off scale of instant flame surface in intense turbulence with the characteristic length scales of the DL instability (π/k_m associated with the maximum of the $\omega(k)$-curve calculated using Eq. (18)) and the turbulence (the measured Kolmogorov length scale η). The reported experimental data indicate a better correlation between e_i and 12η than between e_i and π/k_m. In particular, if $12\eta > \pi/$

[14] Turbulent flame speeds reported by Kobayashi et al. [352,354] for lean methane–, ethane–, and propane–air mixtures also show the dependence of U_t on D_d, as found by Muppala and Dinkelacker [374].

[15] Although Kobayashi et al. [352] made a reservation 'at small $u'/S_{L,0}$,' the hypothesis about the substantial role played by the DL instability in premixed turbulent combustion is sometimes invoked to explain the opposite effects of pressure on laminar and turbulent flame speed at $u'/S_{L,0} > 1$. We may note that the same trends ($S_{L,0}$ increases but U_t decreases with decreasing P) were documented by several independent groups (see Section 3.3.5 in our recent review [18]) at $u'/S_{L,0} > 1$ under *reduced* pressures, i.e. under such conditions that the corresponding laminar flames were stable.

k_m, the inner cut-off scale and the turbulence scale decrease in a similar manner when the turbulent Reynolds number increases. However, if $12\eta < \pi/k_m$, the dependence of e_i on Re_t is not pronounced, whereas η decreases weakly with increasing Re_t. Moreover, if $T_u = 300$ K and $12\eta < \pi/k_m$, Fig. 4 in [97] shows that $e_i \approx \pi/k_m$. On the contrary, if $T_u = 573$ K and $12\eta < \pi/k_m$, Fig. 5 in [97] indicates that e_i is closer to 12η than to π/k_m. Although the independence of e_i on Re_t in intense turbulence characterized by $12\eta < \pi/k_m$ can be interpreted to be indirect evidence of the important role played by the DL instability in premixed turbulent combustion; further studies[16] appear to be necessary for drawing solid conclusions, because (1) 12η and π/k_m are of the same order under the conditions of the measurements discussed; (2) the two scales decrease in a similar manner when pressure increases, and (3) η depends weakly on Re_t when $12\eta < \pi/k_m$.

The data obtained by Soika et al. [361] in methane–air flames at elevated pressures show that the dependence of the mean diameter of the flame front curvature on P is markedly closer to the dependence of the Taylor microscale, $\lambda' = LRe_t^{-1/2}$, on P than to the dependence of $\pi k_m^{-1}(P)$ calculated using Eq. (18) (see Fig. 7 in Ref. [361]). However, the diameter depends also on the equivalence ratio, $F = 0.7$ and 1.0, similarly to the instability scale, whereas the Taylor microscale is independent of F. Under the conditions of these experiments, $\lambda' > \pi k_m^{-1}$ and both scales depend similarly on pressure. It is worth remembering that the numerical simulations of Helenbrook and Law [334] discussed in Section 4.1.5 also show that the flame wrinkling scale is controlled by flow scale if the latter is much larger than k_n^{-1}.

Paul and Bray [172] have reported that the length scale of instant flame front wrinkling is larger in rich methane–air mixtures ($D_d < D_e$) than in rich propane–air ones ($D_d > D_e$), $S_{L,0}$ and turbulence characteristics being the same in the both mixtures. The difference is reduced by $u'/S_{L,0}$. The results were considered to be the manifestation of the effects of the DL instability on turbulent flame structure [172].

A similar but weak (7÷10% difference) effect of $D_d < D_e$ on the wrinkling scale has been documented by Chang et al. [359]. The weakness of the effect is associated with small differences in D_F and D_O in methane–air mixtures investigated by Chang et al. [359].

Recent 3D DNS [375] of premixed flames with single-step, single-reactant chemistry, embedded in decaying small-scale turbulence, have shown that a quasi-developed phase of flame propagation, characterized by a roughly constant total burning rate during several eddy turnover time intervals, is changed to an unstable phase characterized by a rapidly growing burning rate, with this transition being promoted by the increase in γ. These results have been interpreted as a manifestation of the DL instability which controls the burning rate after the decrease of u' to an appropriate value (on the order of $S_{L,0}$) [375]. Note that the simulations have been performed for $Le = 1$.

With the exception of these DNS data, evidence of the important role played by the DL and PDT instabilities in premixed turbulent combustion is indirect, too sparse, few and scattered to draw solid conclusions.

4.3. Models of laminar flame instabilities in turbulent combustion

A widely recognized approach to explaining the dependence of U_t on D_d consists of associating the effect with laminar flame instabilities [14,160,161,172,211, 222,223]. This approach appears to have a solid basis: (1) the laminar flame theory reviewed in Section 4.1 predicts that the instabilities are promoted by a decrease in Le; (2) the increase and more chaotic behavior of the instant flame surface, observed in many experiments and DNS when decreasing either Le or the concentration of the faster-diffusing reactant, looks like the behavior of unstable flames. Nevertheless, the instability concept has not provided a well-recognized model that predicts the effect of D_d on U_t.

To the best of our knowledge, the first model of premixed turbulent combustion, which allowed for the instabilities, was developed by Kuznetsov [133,376] and discussed, in detail, in the book of Kuznetsov and Sabel'nikov [30]. Here, we will restrict ourselves to a brief summary of the main results and refer the interested reader to the book. The model yields the following expression for turbulent flame speed

$$U_t = u'(c_1 + c_2\mu), \tag{26}$$

where c_1 and c_2 are model constants and the parameter

$$\mu = \frac{S_{L,0}}{u'}\psi_0 \ln\left(\frac{L_m}{\gamma\delta_L}\right) \tag{27}$$

characterizes the contribution of the DL instability to flame propagation. Here, the function $\psi_0(\gamma)$ corresponds to the DL solution (Eq. (7)) and L_m is the maximum length scale of perturbations, controlled by burner geometry (e.g. the radius of channel if confined flames are concerned). The model has been validated (see Fig. 11) using the experimental data of Talantov [141], obtained for confined gasoline–air flames under a wide range of conditions ($F = 0.7$–1.25, $u' = 1.5$–7 m/s, tube diameter 25–150 mm, $T_u = 400$–800 K, $P = 0.4$–4.5 bar). In the range of $\mu > 1$, the data (crosses) are well approximated by a straight line, in agreement with Eq. (26).

Note that the model; (1) predicts the reduction of the instability effects by $u'/S_{L,0}$, and (2) includes neither Le nor D_d/D_e, because the short-wave stabilization of flame front disturbances due to molecular transport processes inside

[16] At the 30th Combustion Symposium, Kobayashi et al. reported new experimental data obtained in a wider range of Re_t. The data indicate a correlation between the instability and inner cut-off scales in intense turbulence.

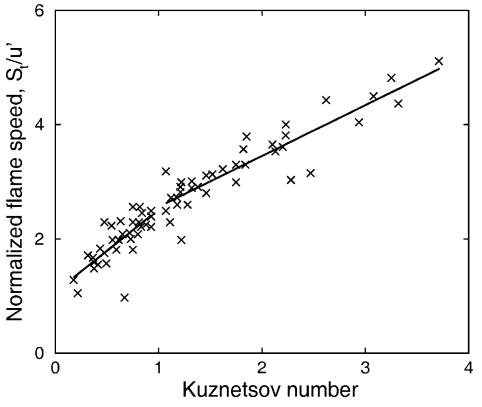

Fig. 11. Normalized turbulent flame speed, S_t/u', vs. the number μ (see Eq. (27)). Crosses show the experimental data reported by Talantov [141] and processed by Kuznetsov [133]. Straight lines approximate the data using a least square fit separately at $\mu<1$ (correlation coefficient 0.74, $c_1=1.1\pm0.2$ and $c_2=1.4\pm0.2$ in Eq. (26)) and at $\mu>1$ (correlation coefficient 0.91, $c_1=1.7\pm0.1$ and $c_2=0.89\pm0.07$).

flamelets, highlighted by the linear theories of laminar flame instabilities (see Section 4.1.3), is not allowed for. Kuznetsov [376] has assumed that the non-linear stabilization of a disturbance with the wavenumber k is controlled by the purely geometrical mechanism connected with propagation (the Huygens principle). The same stabilization mechanism is modeled by the non-linear term on the LHS of the Sivashinsky equation (Eq. (24)). The effect of D_d on U_t was modeled by Kuznetsov et al. [30,131–133] by developing the leading point concept, as discussed in Section 6.2.

Clavin, Williams et al. [6,23,164–167] developed a theory of wrinkled laminar flames in a large-scale, low-intensity turbulent flow field. Although the theory addresses stable flames, the simulations by Aldredge and Williams [167], based on this theory, have shown a substantial increase in flame speed and a considerable effect of Le on $S_{t,\infty}$ near the planar-flame stability limit, which depends on Le.

Another attempt to develop a model of premixed turbulent combustion, which accounts for the instabilities, was undertaken by Paul and Bray [172] who; (1) introduced a new linear production term associated with the DL instability (see the term proportional to H in the RHS of Eq. (A.9)) into the well-known (see recent review by Veynante and Vervish [19] and Appendix A.2) balance equation for flame surface density (FSD), Σ; (2) multiplied the original and the new production terms by $\mathcal{F}$ and $(1-\mathcal{F})$ with the bridging function $\mathcal{F}(u'/S_{L,0})$ tending to 1 or 0 when $u'/S_{L,0}\to\infty$ or 0, respectively, (see Eq. (A.10)); (3) obtained the equilibrium value, Σ_0, of the FSD by assuming that the production and dissipation terms were equal in the balance Eq. (A.9); (4) closed the mean rate of product creation in the combustion progress variable balance equation (see Eq. (A.1)) with $\overline{W}=\rho_u S_{L,0}\Sigma_0$.

Due to numerous assumptions made by Paul and Bray [172] the model needs wide validation. The ability of the model to predict the strong effect of D_d on U_t has not yet been shown. The Lewis number affects the model predictions only through the submodel for the neutral wave number k_n which is assumed to be a known quantity in the parameterization for $\Lambda_c k_n$, reported by Cambray and Joulin [302]. For low Le, the values of k_n were obtained theoretically [234] and numerically [329] recently. Since; (1) the recent numerical results (see circles in Fig. 9) do not indicate a strong dependence of k_n on Le (the values of $k_n(Le=1)$ and $k_n(Le=0.3)$ differ by two times approximately), and (2) $\overline{W}\propto\Sigma_0\propto\Lambda_c^{-1}\propto k_n$ and $U_t\propto\overline{W}^{1/2}\propto k_n^{1/2}$ [172]; the ability of the model to predict this strong effect appears to be questionable, especially as the effect of the instability on U_t, provided by the model, is substantially reduced by $u'/S_{L,0}$ and is weak at $u'/S_{L,0}>1$.

The ideas of Paul and Bray [172] were employed by Boughanem and Trouvé [375]. They have obtained a simple estimate of the domain of the influence of the instability on U_t by comparing characteristic flame stretch rates due to the instability and turbulent eddies. The two stretch rates have been scaled as $S_{L,0}/\Lambda_c$ and $(\varepsilon/\nu_u)^{1/2}\Gamma_{\overline{K}}$, respectively, where ε is the dissipation rate of turbulent kinetic energy and the efficiency function $\Gamma_{\overline{K}}$ has been taken from Meneveau and Poinsot [377] (see also Fig. C1 in our recent review [18]). The parameterization of Cambray and Joulin [302] with k_n determined from the theory of Pelce and Clavin [267] (see Eq. (17)) has been invoked by Boughanem and Trouvé [375] in order to evaluate Λ_c. For a typical case of $\gamma=6$ and $L/\delta_L=10\div1000$, the criterion yields the boundary of the instability-influenced domain close to $u'=S_{L,0}$. In the case of $Le=1$, the criterion has been supported by the DNS results [375] discussed in Section 4.2.

In order to model the effects of gas expansion (the DL-instability) on premixed turbulent combustion, Peters et al. [378] incorporated a gas-expansion term into the G-equation by generalizing the Sivashinsky equation along the lines initiated by Frankel [296]. The generalized G-equation was analyzed following the approach of Peters [15,16,379], i.e. by applying the Reynolds-averaging technique to the G-field, and the developed model was used in simulations. The numerical results show an increase in U_t by γ, but the effect is rather weak (about 40%) even at $u'/S_{L,0}=2/3$ and is substantially reduced by $u'/S_{L,0}$ (see Fig. 3 in Ref. [378]).

Bychkov [173] has developed a simple model of the effects of the DL instability on the propagation speed of a statistically planar, fully developed, premixed turbulent flame. By assuming that (1) the influence of turbulence on flame speed can be modeled using the renormalization ideas [380,381] and (2) the influence of the instability on the speed can be parameterized invoking the fractal approach; he has proposed a linear differential equation with variable coefficients, which combines the two effects in the spectral representation and models the contribution of a length scale l (wavenumber k) to flame speed. Several analytical

solutions to this equation have been provided [173] for $k_n\eta' < 2\pi$ or $k_n\eta' > 2\pi$ and for different values of the fractal dimension $\mathcal{D}$ that characterizes the influence of the DL instability on $S_{t,\infty}$. The obtained expressions for $S_{t,\infty}$ depend substantially on the ratio, k_n/K_m, of the neutral wavenumber, k_n, to the wavenumber, K_m, associated with the largest possible length scale of flame perturbations. For instance, the following expression

$$S_{t,\infty}^2 = S_{L,0}^2\left(\frac{k_n}{K_m}\right)^{2/3} + \frac{4}{3}C_t u'^2 \ln\left(\frac{k_n L}{2\pi}\right),$$

where C_t is a constant on the order of unity, has been obtained in the case of $\mathcal{D} = 7/3$ and $k_n\eta' < 2\pi$ and the structure of expressions reported in other cases (see Eqs. (42), (44), (47), (51), and (52) in Ref. [173]) is similar.

The model predicts considerable influence of the DL instability not only on weakly but also on moderately turbulent flames. For instance, the above expression shows that the effect is of importance even if $1 \ll (u'/S_{L,0})^3 < O(k_n/K_m)$. Other models reviewed in this section predict a substantial effect of the instability on U_t only if $u'/S_{L,0} < O(1)$.[17] This contradiction was not addressed by Bychkov [173] who did not discuss the preceding works [30,172, 375,378].

An assessment and validation of Bychkov's model is difficult, because: (1) the use of two different methods (the renormalization and fractal modes) for modeling the influence of turbulence and the DL instability on flame speed appears to be an arbitrary approach,[18] and (2) the obtained results are sensitive to the quantities k_n, K_m, and $\mathcal{D}$, the values of which are not known in a typical experiment. Moreover, the existence of fully developed premixed turbulent flames in laboratory burners has been put into question in our recent review [18].

Although Bychkov have not studied the effects of *Le* on $S_{t,\infty}$, he mentioned that these effects could be modeled through the dependence of k_n on *Le* [173]. Since (1) k_n is moderately sensitive to *Le*, as discussed above, and (2) $S_{t,\infty}^2 \propto S_{L,0}^2(k_n/K_m)^{(2\mathcal{D}-4)}$ with $\mathcal{D} \approx 7/3$ (see the above expression and Eqs. (42), (44), (47), (51), and (52) in Ref. [173]); the ability of the discussed model to predict the observed strong effect of D_d on $\mathcal{U}_t$ is quite questionable. For instance, in order for the above expression to predict roughly equal turbulent burning velocities for mixtures 1 and 5 in Fig. 4a, a ratio of $(k_n\delta_L)_1/(k_n\delta_L)_5$ should be as low as 15^{-4} for these two mixtures, because $S_{L,0}$ is 15 times higher in mixture 1. The results of the studies of unstable laminar flames, plotted in Fig. 9, show a substantially weaker effect of *Le* on $k_n\delta_L$. Moreover, the model cannot predict the strong effect of D_d on $d\mathcal{U}_t/du'$, well documented in the measurements (cf. mixtures 1 and 3 at $u' = 1$ m/s in Fig. 4a).

All in all, the ability of premixed turbulent combustion models, which allow for the instabilities, for predicting the strong effect of D_d on $\mathcal{U}_t$, observed in the measurements (see Fig. 4) has not yet been shown. Moreover, the majority of these models yield a marked effect of the instabilities on U_t only at weak turbulence, $u' \leq O(S_{L,0})$, whereas the experimental data indicate a strong dependence of $\mathcal{U}_t$ on D_d even for $u' = 40S_{L,0}$ (see mixtures 4 and 5 in Fig. 4a). Consequently, the instability concept cannot explain the experimental data referred to.

Let us keep in mind that the effect of the instabilities on U_t is commonly associated with an increase in flamelet surface area, which scales as $(L/e_i)^{\mathcal{D}-2}$ within the framework of the fractal approach. Various experimental data processed by Gülder and Smallwood [382] indicate that the inner cut-off scale, e_i, is larger than δ_L. A fractal dimension as large as $\mathcal{D} = 7/3$ has been reported [383–385], but certain recent experimental investigations [253,386,387] imply that $\mathcal{D} \leq 9/4$. Even in the extreme case of $e_i = \delta_L$ and $\mathcal{D} = 7/3$, the fractal approach cannot predict an increase in flamelet surface area by more than 3 times in mixtures 4 and 5 in Fig. 4a, whereas the experimental data show a 30-time increase in burning velocity caused by turbulence in these very lean hydrogen mixtures.

Finally, yet another issue is of substantial importance for understanding the role played by the instabilities in turbulent combustion. It is known that laminar flame straining can suppress the instabilities by flattening out the flame surface [225,388,389]. Similar phenomena occur locally inside turbulent flames, e.g. one small eddy wrinkles a flamelet and triggers the instability but another larger eddy locally strains the flame surface and flattens it out, thus, cancelling the effects of the instability. To the best of our knowledge, such interactions have not been addressed in modeling premixed turbulent combustion.

Due to the lack of a general theory, let us apply a very simple phenomenological model. The straining flattens out existing disturbances by providing a convection velocity towards the mean flame surface, equal to $u = a_t x$, where x is the distance from the mean flame position. Thus, we can write the following simple equation

$$\frac{d\zeta}{dt} = (\omega - a_t)\zeta$$

for the growth rate of the amplitude, ζ, of a flame surface disturbance, where ω is the growth rate for the unstrained flame (e.g. Eq. (16), or (18), or (23)). Consequently, the criterion for damping the instability by straining is simply $a_t > \omega$. In the DL solution for ω (Eq. (7)), there are always unstable waves in the short wave range, whatever the stretch

[17] Kuznetsov and Sabel'nikov [30] have pointed out that, even at moderate turbulence characterized by $u' > \mu S_{L,0}$, see Eq. (27), the DL instability might considerably affect local small-scale ($l < l_i < L$) characteristics of premixed flames, with l_i being determined from $u_l' \sim (\varepsilon l_i)^{1/3} < \mu(L_m = l_i)S_{L,0}$.

[18] It is worth noting that a turbulent flame surface shows fractal behavior even in the constant density case, whereas variable density effects and, in particular, the DL instability weakly affect the fractal dimension [337].

rate is. This is not the case for the Markstein and other, more recent, solutions, which predict the stability of short wave perturbations. For low wavenumbers, $\omega \propto k$ is also low and even weak straining can damp the instability. For wave numbers close to k_m, $\omega \approx (0.1–0.2)\tau_c^{-1}$ (see curves 1, 2, and 4 in Fig. 8) and the instability is damped if $\tau_c \overline{a}_t > Ka_{cr} \approx 0.2$ or $Ka' = \tau_c u'/\lambda > Ka_{cr}$ as $\overline{a}_t \propto u'/\lambda$ [30].

The following recent findings are also relevant to the problem of the influence of strain rate on unstable laminar flames. Dao and Linãn [390] and Buckmaster and Short [391] (see also the recent review by Buckmaster [392]) have theoretically and numerically investigated 2D edge premixed flames ignited in the stagnation mixing layer between two opposed streams of the same reactive mixture. The diffusive-thermal instability[19] of such flames can be suppressed by a moderate strain rate, a_t. However, if (1) a_t is close to or larger (e.g. even by 3 times [391]) than the critical value, $a_{t,q}$, associated with the extinction of twin planar flames and (2) the Lewis number is sufficiently small (e.g. $Le = 0.3$ [391]); the instability can return and the flame structure then becomes discontinuous, resulting in multiple, twin, or single 'strings' [391], or 'spots' [390], or 'flame tubes' [249]. These predictions have been experimentally confirmed by Kaiser et al. [249].

4.4. Summary

The asymptotic ($\beta \to \infty$) theories of the DL and PDT instabilities of premixed laminar flames are well elaborated but need more validation for real flames. If the Lewis number is markedly less than unity, the stability limits (neutral wavenumbers) predicted by the asymptotic theories do not agree (see Fig. 9) with the results of numerical simulations performed with finite $\beta \gg 1$, the computed wavenumber depending substantially on β [329].

Experimental data obtained from turbulent flames indirectly support the concept of the important role played by the instabilities in weakly turbulent premixed combustion. However, decisive experimental data have not yet been reported.

Almost all the turbulent combustion models that allow for the instabilities, as well as numerical simulations, indicate that the effects of the instabilities on turbulent flames are substantially reduced by $u'/S_{L,0}$. The ability of such models to predict the dependence of U_t on D_F/D_O has not yet been tested. If $u' \gg S_{L,0}$, no model based on the instability concept can predict the strong dependence of U_t on D_F/D_O, observed in many experiments.

[19] The discussed studies have been performed for single-step, single-reactant chemistry, $Le < 1$, using the approximation of constant density.

5. Weakly perturbed laminar flamelets in premixed turbulent combustion

Another mainstream approach to modeling the dependence of U_t on D_d is based on the concept of flamelet library [10,168], which considers the turbulent flame brush to be an ensemble of laminar flamelets randomly convected and perturbed by turbulent eddies. Within the concept one can: (1) compute a library encompassing the characteristics of variously perturbed laminar flames; (2) average this library by using some approximations of the PDF for the flamelet perturbations produced by turbulence.

Flamelet libraries can be created by simulating various strained and curved laminar flames with realistic molecular transport properties and chemical schemes. Many such computations have been performed for various types of external perturbations (see Refs. [176,178,184,185,393–398] and references quoted therein). However, for premixed turbulent combustion applications, two simplified approaches are commonly used.

The first one, discussed here, is based on the linear Eqs. (12), (13), (19), and (20) derived for weakly (i.e. $S_L/S_{L,0} - 1 = o(1)$) perturbed laminar flames. The second approach, reviewed in Section 6.1, places the focus of consideration on strongly perturbed laminar flamelets under near-quenching conditions.

The basic idea of the concept of weakly perturbed flamelets consists of averaging linear expressions similar to Eq. (12) by invoking a PDF for the flamelet stretch rate in a turbulent flow [180–182].

For instance, Bray and Cant [180] analyzed DNS data available in the early 90s and stressed that the effects of flamelet straining a_t and curvature h_m on flamelets should be separated. They have suggested the following approximation of the DNS results:

$$\mathcal{P}(\dot{s}) = \mathcal{P}_1(a_t) \cdot \mathcal{P}_2(h_m), \tag{28}$$

$$\mathcal{P}_1(a_t) = \frac{1}{\sigma_a\sqrt{2\pi}} \exp\left[-\frac{1}{2}\left(\frac{a_t - \overline{a}_t}{\sigma_a}\right)^2\right], \tag{29}$$

$$\mathcal{P}_2(h_m) = \frac{1}{\sigma_h\sqrt{2\pi}} \exp\left[-\frac{1}{2}\left(\frac{h_m}{\sigma_h}\right)^2\right], \tag{30}$$

where $\sigma_a = 0.45/\tau_\eta$, $\sigma_h = 0.22/\eta'$ and

$$\overline{a}_t = \frac{0.28}{\tau_\eta} \min\left\{1;\ \exp\left[0.25\left(1 - \frac{S_{L,0}}{u_\eta}\right)\right]\right\}; \tag{31}$$

$\tau_\eta = \eta'/u_\eta$, $u_\eta = u' Re_t^{-1/4}$, and $\eta' = L Re_t^{-3/4}$ are the Kolmogorov time, velocity, and length scales, respectively. Recently, Bradley et al. [399] have further contributed to solving the problem of parameterizing $\mathcal{P}(\dot{s})$, $\mathcal{P}_1(a_t)$, and $\mathcal{P}_2(h_m)$.

By averaging Eq. (19) supplemented with Eqs. (15) and (20) and the two independent PDFs for the flamelet strain rate (Eq. (29)) and curvature (Eq. (30)), the following

parameterization for the mean local consumption speed:

$$\overline{S}_c = S_{L,0} I_0(Ka, Ma_c, Ma_d)$$
$$\equiv S_{L,0}[1 - 0.28 Ma_c(\mathcal{F} - 0.69 Ma_d)Ka$$
$$- 0.054 Ma_c Ma_d^2 Ka^2 \mathcal{F}];$$
$$\mathcal{F} = \min\{1;\ \exp[0.25(1 - Ka^{-0.5})]\} \quad (32)$$

has been obtained [181]. Here, $Ka = (u_\eta/S_{L,0})^2 = (u'/S_{L,0})^2 Re_t^{-1/2}$ is the Karlovitz number. Subsequently, $\overline{S}_c$ determined using Eq. (32) can be employed by various turbulent combustion models instead of $S_{L,0}$ and the dependence of U_t on D_d, predicted in such a way, will be controlled by the Markstein numbers, Ma_d and Ma_c.

The stretch-factor, $I_0(Ka, Ma_c, Ma_d)$, depends on two Markstein numbers because the flame speed in Eq. (15) has been determined using Eq. (20). From a theoretical standpoint, this method is inconsistent, because the terms on the order of $O(\varepsilon^2)$ are substituted into Eq. (19) valid with an accuracy of $O(\varepsilon)$.

A simpler, purely phenomenological parameterization

$$S_t = S_t(Ma = 0)\left(1 - b_3 \frac{\mathcal{L}}{l_t} \frac{u'}{S_{L,0}}\right), \quad (33)$$

has been used by Peters [379] to close the $\overline{G}$-equation. Here, b_3 is a constant, and l_t is a turbulence length scale. The more recent model developed by Peters [15,16,378] based on the same $\overline{G}$-equation does not address the effects of D_d on U_t and does not include the Markstein length, $\mathcal{L}$.

The perturbed laminar flame theories, which lead to Eqs. (12)–(15), (19), and (20) are reviewed in Section 4.1.3. In Section 5.1, experimental and numerical results obtained in laminar flames and relevant to these equations are discussed. Then, data on the statistics of local consumption and displacement speeds, flamelet curvature, strain and stretch rates in turbulent flows are reviewed in Section 5.2. Section 5.3 is devoted to a critical discussion of models of premixed turbulent combustion (e.g. Eqs. (28)–(32) or Eq. (33)), which invoke the linear parameterization of the response of laminar flame speed to perturbations (like Eq. (12), (19), or (20)). The focus of the discussion will be placed on the ability of such models to predict the strong dependence of ∂l_t on D_d, shown in Fig. 4.

5.1. Weakly perturbed laminar flames

The validity of the linear Eqs. (12), (19), and (20) has been tested in a number of experimental and numerical studies of perturbed laminar flames. By claiming the importance of the Markstein number for premixed turbulent combustion modeling, the focus of most studies was placed on evaluating *Ma*. Measurements of the response of a laminar flame speed to external perturbations have been performed for counterflow flames [206,400], strongly curved stationary flames in non-uniform flow fields [401–405], expanding spherical flames [186,188,195,207,314,341,406–413], inwardly propagating near-spherical flames [192,194,414,415], collapsing cylindrical flames [187], V-shaped stationary flames [416,417], and tubular flames [418,419]. Searby et al. have evaluated the Markstein number by determining the stability limits of laminar flames [420] or by measuring the growth rate of flame surface disturbances [254,255]. Numerical tests of the aforementioned linear expressions have been conducted for spherical [188,193,194,207,272,398,411,413,421–424], counterflow [189–191,395,424], Bunsen [403], and tubular [418,419] flames.

The linear relation between the flame stretch rate and speed has been confirmed at least for weakly perturbed flames [186–188,190–195,207,276,314,341,395,398,404,407,408,409,411,412,414,415,421–423].

The following issues relevant to the linear relations appear to be of importance for modeling premixed turbulent combustion.

First, the values of *Ma*, obtained by different groups under similar conditions, are widely scattered. This scatter is associated [184,191,274,275,423] with the different definitions of flame speeds employed by the different groups.

Analytical expressions for the dependence of *Ma* on the position of the reference surface have been derived by Matalon et al. [274,275]. The importance of this issue has also been stressed in a numerical study [272]. The problem of defining a reference surface for evaluating flame stretch rate and speed has also been investigated in more recent numerical studies [189–191,193,425] and the strong sensitivity of the value of *Ma* to the definition of the surface has been shown [190,193].

Second, the response of flame speed to perturbations is non-linear if the perturbations are finite. The non-linear dependencies of flame speed on perturbation magnitude have been documented experimentally [405,417,419], obtained numerically [140,272,276,390,421,422,424,425] (e.g. see Fig. 12) and predicted theoretically [261,264,424,426,427,428] (e.g. Eqs. (11) and (22)).

For instance, Mikolaitis [426,427] has theoretically studied strongly curved (the curvature radius, R_c, on the order of the preheat zone thickness, $\gamma\delta_L$), strained, stationary premixed laminar flames in the asymptotic limit of $\beta \to \infty$ and $Le - 1 = O(\beta^{-1})$. Non-linear dependencies of $S_L(a_t)$ have been predicted, the dependencies being different for different R_c. Even for $\dot{s} = 0$, the predicted flame speed can be much smaller than $S_{L,0}$ if both the flame strain rate and curvature are large and have the same magnitude but opposite signs [426]. Consequently, the response of a strongly perturbed flame to the strain rate differs from the response of the flame to curvature. Moreover, the analysis shows that the response is very sensitive to heat losses in strongly stretched concave flames and weakly compressed convex flames. In contrast, in weakly stretched concave and strongly compressed convex flames, the sensitivity disappears.

The well-known flame ball solution [226] discussed in Section 6.2.2 is yet another theoretical example of the non-linear response of laminar flames to strong perturbations.

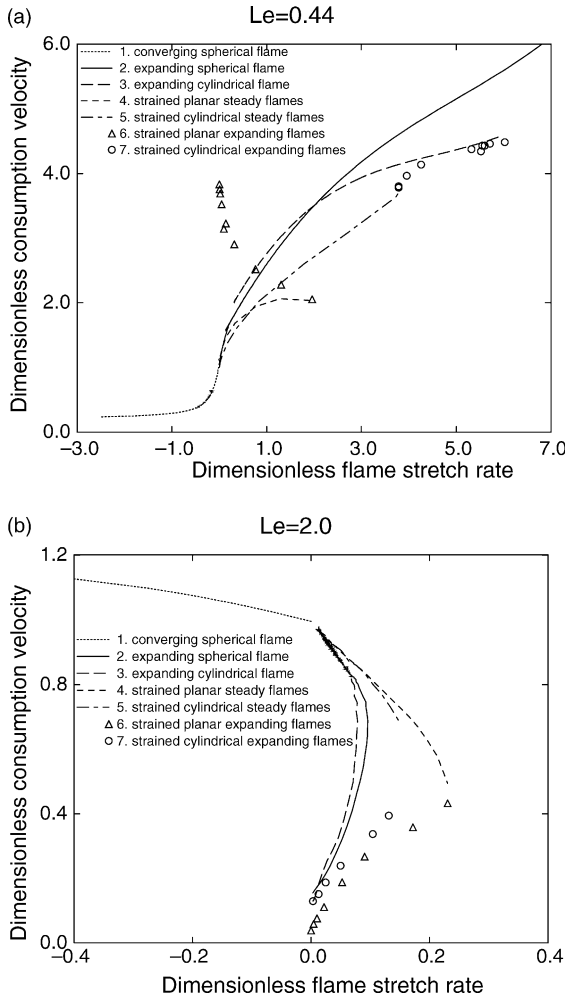

Fig. 12. Normalized consumption speed, $S_c/S_{L,0}$, vs. normalized flame stretch rate, $\dot{s}\tau_c$, computed for (a) $Le=0.44$ and (b) $Le=2.0$ after [140]. Ignition has been simulated by creating a small pocket, $r<r_i$, filled with equilibrium adiabatic combustion products. Curves 1–3 and symbols have been computed for the minimum value of r_i, for which the initial kernel does not shrink. Symbols show the maxima ($Le=0.44$) and minima ($Le=2.0$) of the $S_c(t)$-curves calculated for different a_t.

In this case, S_L, a_t, $S_L h_m$, and $\dot{s}$ are equal to zero, but the consumption velocity depends exponentially on $\beta(1-Le)$ (see Eqs. (41)–(43)).

Large variations in $S_L/S_{L,0}$ are beyond the applicability limits of the linear Eqs. (12), (19), and (20), whereas ratios of $S_L/S_{L,0}$ as large as 6.25 and 20 have been measured at the tip of slot-burner Bunsen flames in stoichiometric [402] and rich ($F=1.7$) [405] methane–air mixtures, respectively. Poinsot et al. [403] numerically simulated the stoichiometric methane–air Bunsen flame and obtained a ratio of $S_L/S_{L,0}$ as large as 10 at the tip. Note that the consumption speed calculated for the same conditions is equal to $S_{L,0}$ ($Le=1$) despite the aforementioned strong increase in S_L.

Several non-linear modifications of Eqs. (12), (19), and (20) have been phenomenologically introduced. For instance, Echekki et al. [402,403] have pointed out that the linear relation between the flame stretch rate and speed may be valid even in strongly perturbed ($S_L/S_{L,0}-1=O(1)$) laminar flames, if the stretch rate (see Eq. (15)) is calculated using S_L, rather than on $S_{L,0}$. In terms of the perturbation technique, this modification is associated with terms on the order of $O(\epsilon^2)$ in the linear Eq. (12). Since such terms have been omitted when deriving Eq. (12), the modification should be considered to be a purely phenomenological one. To support it, Echekki et al. have reported figures (see Figs. 6 and 12 in Refs. [402,403], respectively) where the measured values of $S_L/S_{L,0}$ depend linearly on $|\dot{s}|=(\delta_L/r_c)(S_L/S_{L,0})$ (the modified stretch rate for the tip of a Bunsen flame according to Ref. [402]) in the range of $1<S_L/S_{L,0}\leq 10$. Baillot and Bourehla [414] have reported a similar linear relation for collapsing pockets of unburned mixture in the range of $1<S_L/S_{L,0}<7$. The hypothesis of Echekki et al. [402,403] has been used when deriving Eq. (32) and the second Markstein number, Ma_d in Eq. (32) results from the substitution of $S_d\neq S_{L,0}$ into Eq. (15).

By simulating spherical flames, Mishra et al. [421] have not confirmed the above hypothesis. They have shown that the dependence of S_L on the stretch rate evaluated using S_L is linear only for $\tau_c\dot{s}\ll 1$.

Faeth and co-workers [188,207,341,407–409,411] have further modified the hypothesis of Echekki et al. [402,403] and have assumed that not only $\dot{s}$ but also laminar flame thickness used to normalize the Markstein length should be evaluated using S_L, rather than on $S_{L,0}$, i.e. $\mathcal{L}=Ma\delta'_L\propto Ma\kappa_u/S_L$. To support this assumption, they have reported a number of figures that show, in moderately perturbed flames ($0.7<S_L/S_{L,0}\leq 2.6$), the linear dependence of $S_L^{-1}\propto(dR_f/dt)^{-1}$ on the Karlovitz number defined so that $\mathcal{K}=\dot{s}\delta'_L/S_L\propto(\kappa_u/S_L^2)S_L/R_f\propto\kappa_u/(S_L R_f)$, where R_f is the flame radius.

As pointed out in Ref. [412], such processing of the measured $R_f(t)$-curves leads to the dependence of a quantity on itself ($(dR_f/dt)^{-1}$ vs. $(dR_f/dt)^{-1}$) and this method can (1) mask the wide scatter of experimental data, and (2) convert a non-linear function into a linear-like one (see Figs. 4–6 in Ref. [412]).[20] The same can be said about the aforementioned figures reported by Echekki et al. [402,403] (S_L vs. S_L).

Contrary to the results of Echekki et al. [402,403] concerning the tip a Bunsen flame and the data of Baillot and Bourehla [414] concerning collapsing pockets, Karpov et al. [412] have found that the $R_f(t)$-curves measured in highly curved expanding spherical flames characterized by $S_L\ll S_{L,0}$ are better approximated by a linear Eq. (12) if the stretch rate is evaluated using $S_{L,0}$, rather than on S_L. The same conclusion has been drawn by Ibaretta and Driscoll

[20] Other problems relevant to the interpretation of the data of Faeth et al. are discussed elsewhere [429,430].

[415], Durox et al. [187], and Baillot et al. [192] by processing $R_f(t)$-curves measured in imploding spherical flames.

Third, different Markstein numbers in outwardly and inwardly propagating spherical flames have been reported in the literature [194,421], as well as different values of *Ma* for the response of flame speed to curvature and strain rate [186, 314,398]. Moreover, the behavior of S_L at the tip of the Bunsen flames discussed above implies different responses of strongly perturbed flames to flame strain rate and curvature [402,405,417,426], with the latter dominating.

These experimental results may agree with the theory, because the difference in the Markstein numbers for strain rate and curvature has been theoretically predicted [274,275] for variously defined laminar flame speeds with the exception of $S_{h,u}$, S_d, and S_c. Such a difference may be reduced by properly defining the flame surface [184,423] (e.g. cf. Fig. 29 in Ref. [423], where the two Markstein numbers are the same, with Fig. 4 in Ref. [194], where the numbers are different). However, the non-linear effects discussed above can also contribute to the differences, as well as finite values of β, complex chemistry, transient effects, etc.

Fourth, a low Lewis number and activation energy restrict the validity of the linear theory developed for $\beta \to \infty$ and $\beta|Le-1|=O(1)$. For instance, Mishra et al. [421] pointed out that the simulated response, $dS_L/d\dot{s}$, of spherical flame speed to the stretch rate was proportional to $\beta(Le-1)$, as predicted by the theory [165,224,267] (see Eqs. (12) and (13)), only in the range of $Le \approx 1$. For small *Le*, the response strongly increased with decreasing *Le*.

Fifth, the heat transfer along the surface of a laminar flame can considerably affect the response of the flame to spatially non-uniform perturbations, as shown by Yokomori and Mizomoto [416,431]. They have measured temperature and velocity fields for lean propane–air ($Le > 1$) flames stabilized in a spatially periodic flow in a multiple-slit burner. They have documented that the flame temperature locally decreases (increase in positively (negatively) stretched parts of the flame surface, in the qualitative agreement with the theory. However, the theoretical expressions reported by Sun et al. [423] substantially overestimate the temperature increase measured in strongly negatively stretched flames. Yokomori and Mizomoto [431] (1) have attributed this difference to heat transfer along the flame surface, (2) have extended the aforementioned theory to allow for this effect, and (3) have obtained markedly better agreement between measurements and the extended theory.

Finally, the response of a laminar flame to unsteady perturbations is sensitive to transient effects. For instance, Mueller et al. [432] have experimentally investigated the interaction between a laminar flame and an impinging vortex ring. The obtained instant maximum values of the OH mole fraction are markedly different from the values computed for the same stretch rate in a steady counterflow planar flame (see Fig. 5 in the quoted paper).

Sinibaldi et al. [433,434] have measured the displacement speed of a wrinkled, unsteady, stretched laminar flame perturbed by a toroidal vortex. The results reported in the form of $S_d/S_{L,0}$ vs. the tangential coordinate (e.g. Fig. 8 in Ref. [434]) differ strongly from the curves calculated using the stationary linear theory (Eqs. (12)–(15), (19), and (20)). Ratios of $S_d/S_{L,0}$ as large as 10 have been documented, as well as negative propagation speeds.

Samaniego and Mantel have performed both experimental [435] and numerical [436] investigations of the interaction between a two-dimensional vortex and a planar laminar flame. Figs. 10 and 11 from Ref. [436] do not show any simple relation between the normalized heat release rate and the instant stretch rate.

Hasegawa et al. [437] have simulated interaction between a vortex pair and a premixed laminar flame for $Le = 0.6$, 1.0, and 1.6. Fig. 14 from the quoted paper shows that the dependence of the consumption speed on the local stretch rate cannot be parameterized by a simple function like Eq. (19), the differences being more pronounced for $Le = 0.6$.

In summary, although the linear Eqs. (12), (19), and (20) are an acceptable approximation under certain conditions, their validity is limited by a number of effects, in particular, by the non-linear and transient phenomena. Therefore, the linear expressions are valid only if local burning rate perturbations are weak (a typical limitation of perturbation methods in general), whereas non-linear, strongly perturbed laminar burning structures should be considered to obtain substantial difference in S_c (or S_d) and $S_{L,0}$ and to explain the data shown in Fig. 4 within the framework of the flamelet library concept.

From the theoretical standpoint, the linear Eqs. (12), (19), and (20) are valid only if $Le \approx 1$. In the case of $|Le-1|=O(1)$, which is much more relevant to the subject of this review, both early (Eq. (11)) and recent (Eq. (22)) theories predict the non-linear dependence of S_L on $\dot{s}$.

Thus, just the simplicity of the linear Eqs. (12), (19), and (20) appears to be the main reason for extensively using these expressions in studies relevant to premixed turbulent combustion.

5.2. Statistics of perturbed flamelets in turbulent flows

5.2.1. Local consumption and displacement speeds

A number of experimental data, which show the dependence of the local burning rate on D_d/D_e and *Le* in a turbulent flow and agree qualitatively with the theory of weakly perturbed laminar flames, have been obtained.

Becker et al. [347] have reported that local consumption velocity,[21] u_c, in lean ($F = 0.67$) propane–air mixtures can be less than $S_{L,0}$ by three times, approximately (in fact, they

[21] Here, for brevity, this term unites quantitatively different but qualitatively similar characteristics of the local combustion rate per unit flame front surface area, used by different authors [12,14,33, 277,395], e.g. S_c and S_d.

measured the concentration of OH and assumed that $u_c \propto Y_{OH}$). Becker et al. [347] associated the reduction in $u_c/S_{L,0}$ with local variations in the burning rate in highly curved fronts due to $Le > 1$.

Renou et al. [356,357] obtained larger values of u_c in lean hydrogen–air flames than in hydrocarbon–air flames, the local values being as large as $S_d = 5S_{L,0}$ in the former mixture.

Lee et al. [349,350] have reported that OH LIF intensity is higher (lower) in positively (negatively) curved flame fronts if $D_d > D_e$, whereas the flames characterized by $D_d < D_e$ show the opposite behavior, in line with perturbed laminar flame theory. The effect is more pronounced in hydrogen flames characterized by large differences in D_F and D_O. For these flames, a departure of the peak OH LIF intensity from 20 to 150% of the value at zero flame curvature has been measured, whereas the intensity varies in the range of $\pm 20\%$ in lean propane flames. The correlation between the intensity and the local curvature is well approximated by a linear function after averaging, with the exception of highly positively curved, lean hydrogen flame fronts, for which the correlation tends to level-off [350].

Chen and Bilger [86,362] have documented high probabilities of measuring local OH concentrations higher (lower) than the concentration of OH in the corresponding laminar flame in lean methane– and hydrogen–air (propane–air) mixtures. This result implies substantial variations in the local burning rate inside perturbed flame fronts due to differences in D_d and D_e or κ, $D_d > D_e$ and $Le < 1$ in the methane and hydrogen mixtures, whereas $D_d < D_e$ and $Le > 1$ in the propane ones. In particular, correlations between local flame front curvature and Y_{OH} have been found in the hydrogen flames, but the correlations are not well pronounced, with the exception of strong negatively curved fronts (cusps) characterized by low Y_{OH}, as expected in such mixtures with $D_d > D_e$, and $Le < 1$. Correlations between local flame front curvature and the 3D temperature gradient are more pronounced and have been obtained in all the mixtures investigated. In lean hydrocarbon–air flames, the correlations are negative (positive) if $D_d > D_e$ ($D_d < D_e$), the level of correlation increasing with turbulence [86].

DNS [209,210,370,371] also indicates variations in u_c in line with the theory of perturbed laminar flames, i.e. $u_c > S_{L,0}$ ($u_c < S_{L,0}$) in positively (negatively) curved fronts if $Le < 1$ (single-step chemistry [209,210,371]) or the corresponding laminar flame is unstable (DNS with complex chemistry [60,370]). The opposite behavior is observed in cases of $Le > 1$ or stable laminar flames. Similar trends have been reported for product temperature [210] and enthalpy [222].

The simulations performed by Ashurst et al. [222] have shown a weak effect of Le on $\overline{u}_c$, $\overline{u}_c/S_{L,0} = 0.81$and 1.11 for $Le = 2.0$ and 0.5, respectively. In the case of $Le = 0.8$, the values of $u_c/S_{L,0}$ obtained in other DNS [209,210] are scattered in the range of $0.7-1.7$. In lean ($F = 0.4$) hydrogen–air flames, values of $u_c/S_{L,0}$ and $\overline{u}_c/S_{L,0}$ as large as 5.4 and 2.43, respectively, have been reported [370]. Large ratios of $\overline{u}_c/S_{L,0}$ have been obtained by Trouvé and Poinsot [211] for $Le = 0.3$ (see Fig. 10b).

Although the above data are in general agreement with the theory of perturbed laminar flames, the agreement is mainly qualitative and not universal. In particular, the capabilities of the linear Eqs. (12), (19), and (20) to approximate data obtained locally in turbulent flows is quite questionable.

For instance, the DNS with single-step chemistry have shown no correlation between u_c and a_t for $Le \neq 1$ [209,210], contrary to the theory. Nevertheless, both Haworth and Poinsot [209] and Rutland and Trouvé [210] have considered the averaged effect of the strain rate on u_c to be the primary physical mechanism capable of explaining the moderate increase in U_t with decreasing Le obtained by them, because: (1) the effect of Le on the flame surface area was weak in the simulations, and (2) the effect of the local front curvature on the burning rate was assumed to be canceled after averaging, as discussed in Section 5.3.1.

Baum et al. [200] have found that the local maximum heat release rate, w_h, correlates with the local curvature, but not with the strain rate. The correlation coefficient is negative for $F > 0.5$ and positive for $F = 0.35$ (hydrogen–air mixtures). In the latter case, the heat release rate and Y_{OH} only moderately increase (by factors of 2.5 and 1.7, respectively, or less) in positively curved fronts even if the curvature is high. Contrary to the heat release rate, the consumption speed has been claimed to correlate negatively with the strain rate if $F \geq 0.5$, but the correlation is very weak in lean highly turbulent flames (see Fig. 13a). The ratio of $\overline{S}_c/S_{L,0}$ is decreased by turbulence and is markedly less than unity if $F \geq 0.5$. Note that no correlation between S_c and local curvature and very weak correlations between S_c and Y_{OH} have been found in the simulations.

Ashurst et al. [222] have found a strong correlation between local enthalpy and strain rate for $Le = 2$, but the correlation is weak for $Le = 0.5$.

Echekki and Chen [363,369] have reported that the maximum concentration of H-radicals, the maximum heat release rate, and displacement speed correlate well with curvature. All the correlations are non-linear, but they can be approximated by two straight lines with weak and strong slopes for, respectively, positively and negatively curved flamelets. The displacement speed correlates also with the strain rate, the data being well approximated with a single straight line in the whole range of a_t.

Chen and Im [366,370] have concluded that both displacement and consumption speeds correlate much better with the strain rate than with the curvature, the correlations being well approximated by a linear function even at large strain rates (the best correlations are shown in Fig. 14). As concerns the curvature and stretch rate, the linear approximation is applicable to rich hydrogen–air mixtures, but not lean ones (see Fig. 13b) [370,371]. It is of interest to note that despite well-pronounced correlations between S_d or S_c

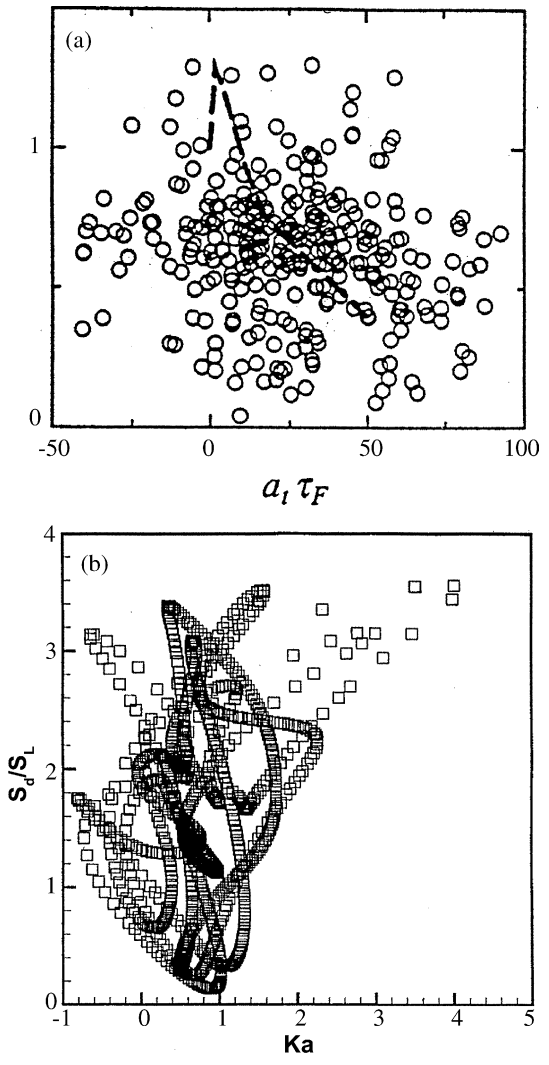

Fig. 13. (a) Normalized consumption speed, $S_c/S_{L,0}$, vs. normalized local strain rate, $a_t\delta_L/S_{L,0}$. From the paper by Baum et al. [200] © Cambridge University Press, reproduced with permission. Case 9, $F=0.5$. Symbols show DNS data, dashed curve has been calculated for a steadily strained laminar flame. (b) Normalized displacement speed, $S_d/S_{L,0}$ vs. normalized local stretch rate, $Ka=\dot{s}\delta_L/S_{L,0}$. Reprinted by permission of Elsevier Science from Ref. [371] © 2002 by The Combustion Institute. Lean ($F=0.4$) hydrogen–air mixture.

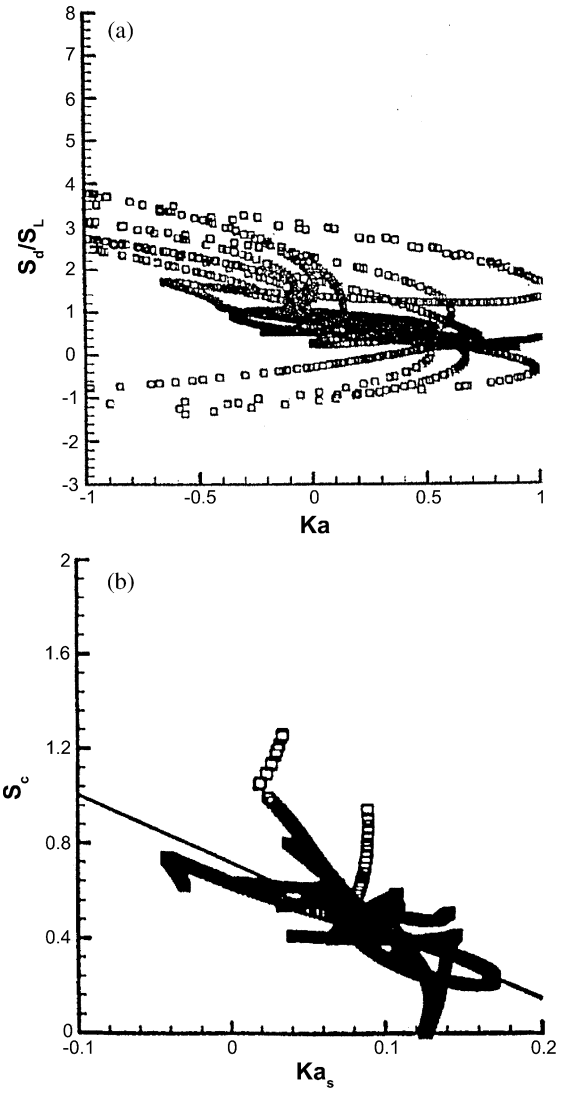

Fig. 14. (a) Correlation of normalized displacement speed, $S_d/S_{L,0}$, with normalized local stretch rate, $Ka=\dot{s}\delta_L/S_{L,0}$. From the paper by Chen and Im [366] © The Combustion Institute, reproduced with permission. Lean ($F=0.7$) methane–air mixture. (b) Correlation of normalized consumption speed, $s_c=S_c/S_{L,0}$ with normalized local strain rate, $Ka_s=a_t\delta_L/S_{L,0}$. From the paper by Chen and Im [370] © The Combustion Institute, reproduced with permission. Rich ($F=6.5$) hydrogen–air mixture.

with h_m, or a_t, or $\dot{s}$ in the rich mixtures, the turbulent flame speed is mainly controlled by the flame surface area increase and is weakly affected by $\overline{u}_c/S_{L,0}$ (see Fig. 4 in Ref. [371]).

Tanahashi et al. [59,60] have claimed that the DNS results they obtained show that the local heat release rate, w_h, correlates well with h_m and correlates also with a_t. From our viewpoint, the original figures reported by them (see Fig. 8 in Ref. [59] or Figs. 8 and 9 in Ref. [60]) show only a weak correlation between w_h and h_m, but no correlation between w_h and a_t.

Chakraborty and Cant [65] have reported that S_d and h_m are negatively correlated in the case of $Le=1$ (3D DNS with single-step, single-reactant chemistry). The instantaneous displacement speed and the tangential strain rate are weakly correlated, whereas the conditionally averaged quantities $S_d(h_m=0)$ and $a_t(h_m=0)$ are negatively correlated.

All in all, quantitative confirmations of the linear Eqs. (12), (19), and (20) are scarce. Even the best correlations reported in the literature for turbulent flames are widely

scattered (see Fig. 14). In many cases, the linear relations are contradicted by DNS data, e.g. u_c vs. a_t for $Le \neq 1$ [209,210], w_h vs. a_t or S_c vs. h_m [200], S_d vs. $\dot{s}$ [371] (see Fig. 13b), w_h vs. a_t [60], etc. The above limitations of the linear Eqs. (12), (19), and (20) are associated with the transient and non-linear phenomena, emphasized in Section 5.1.

5.2.2. Local strain rate and curvature

PDFs for local flamelet strain rate obtained in DNS [59,65,200,209,210,363,366,371] show high probabilities of positive a_t with $\overline{a}_t \propto \tau_\eta^{-1}$, in line with the parameterization of Bray and Cant [180] (Eqs. (28)–(31)). The form of the PDF and $\overline{a}_t$ are weakly sensitive to D_d/D_e and Le [209,210,356].

A strong negative correlation between the strain rate and curvature has been obtained in the DNS by Haworth and Poinsot [209] and Chakraborty and Cant [65,438]. This correlation implies that the two perturbations affect the local consumption rate in opposite directions.

Measured [96,172,223,348,349,351,357,360,361,439, 440] and simulated [62,200,209,210,363,371,439,440] PDFs for flamelet curvature $\mathcal{P}(h_m)$ resemble the Gaussian function with a zero mean value although a certain skewness of the PDFs [59,64,96,209,210,351,356,357,360,361,439] and non-zero mean values [209,349,360,361] have been documented mainly at weak turbulence. Recent 3D DNS using complex chemistry, performed by Tanahashi et al. [59,60] show a substantial deviation of $\mathcal{P}(h_m)$ from the Gaussian function, with the exponential behavior of the tails of $\mathcal{P}(h_m)$ for large curvatures (on the order of η^{-1}).

The variance, σ_h, of $\mathcal{P}(h_m)$ is increased by $u'/S_{L,0}$ [96, 223,344–346,348,360]. Lee et al. [223,348] have reported that the mean positive (fronts convex toward unburned mixture), $\overline{h}_+$, and negative (fronts convex toward burned mixture), $\overline{h}_-$, curvatures show a nearly square-root dependence on $u'/S_{L,0}$ in the range of $u'/S_{L,0} = 1.4 \div 5.7$. Shepherd et al. [96] have shown that the dependence of σ_h on $u'/S_{L,0}$ is well approximated by a linear function in the range of $u'/S_{L,0} = 6 \div 18.7$, whereas the variance they have measured at $u'/S_{L,0} = 3.5$ is substantially lower than the value given by the above approximation. Note that the parameterization of Bray and Cant [180] (Eqs. (28)–(31)) assumes $\sigma_h \propto Re_t^{3/4}/L \propto u'^{3/4}$. The recent empirical expression of Bradley et al. [399] yields $\sigma_h \propto Da^{-1/2} \propto u'^{1/2}$.

Weak sensitivity of the shape of $\mathcal{P}(h)$ to D_d/D_e has been reported [223,348,349,350,351], whereas data on the dependence of σ_h on D_d/D_e are contradictory. On the one hand, Paul and Bray [172] and Haq et al. [360] have reported that the σ_h is larger in mixtures with a faster-diffusing deficient reactant. A similar trend (σ_h increases when Le decreases) has been obtained in DNS [210]. Furukawa et al. [344,345,346] have documented that $\overline{r}_+ = \overline{h}_+^{-1}$ is larger than $\overline{r}_- = \overline{h}_-^{-1}$ and that both radii decrease with decreasing Le. Renou et al. [357] have reported that: (1) $\overline{h}_+$ is increased by Le, whereas $\overline{h}_-$ shows the opposite behavior, (2) the mean radius, $\overline{R}_c = 0.5(\overline{h}_+^{-1} + \overline{h}_-^{-1})$, of flamelet curvature decreases with increasing $u'/S_{L,0}$, the decrease being less pronounced in lean hydrogen–air mixtures. On the other hand, the values of $\overline{h}_+$ and $\overline{h}_-$, measured by Lee et al. [348] in lean ($F = 0.75$, $Le = 1.84$) and rich ($F = 1.25$, $Le = 0.98$) propane–air mixtures with equal $S_{L,0}$, are controlled by $u'/S_{L,0}$ and appear to be independent of F, i.e. of D_d/D_e. The DNS data obtained by Haworth and Poinsot [209] do not show any effect of $Le = 0.8 \div 1.2$ on σ_h, in line with the parameterization of Bray and Cant [180] but contrary to the parameterization of Bradley et al. [399].

Numerical simulations indicate that: (1) the most probable local flame geometry is cylindrical [62,210,439, 440], (2) the most highly curved regions on the flame surface correspond to cylindrical curvature [210], (3) the probability of finding spherically curved flame fronts is low [62,210, 439]. However, the experimental data reported by Chen and Bilger [362] indicate that positively curved parts of a flame front surface are mainly of a dome-like, rather than a cylindrical shape. The results of simulations of passive (zero heat release) flame propagation in 3D turbulence, reported by Ashurst and Shepherd [440], imply that the probability of spherically curved flame fronts increases at the leading edge of the flame brush, although the cylindrical flame front shape dominates the curvature distribution inside the brush. Recent DNS of weakly turbulent spherical flames do not indicate such a tendency [62]. The parameterizations of Bray and Cant [180] and Bradley et al. [399] do not allow for any variations in $\mathcal{P}(\dot{s})$ across the flame brush.

5.2.3. Other data

DNS results [200,209,210] indicate that the local flame front normal aligns with the most compressive strain rate direction, the orientation of the front with respect to the strain rate tensor being independent of Le.

PDFs for the flamelet orientation angle [86,98,223,348, 359,362] and PDFs for the local reaction zone thickness [344] are weakly sensitive to D_d/D_e and Le.

Tanahashi et al. [59] has reported a joint PDF for a_t and local flamelet thickness Δ_L calculated from the local temperature gradient when processing the DNS data base (see Fig. 9b in the quoted paper). The figure indicates a reduction in Δ_L by a_t, the correlation being well pronounced in flamelets thinner than an unperturbed laminar flame.

A dependence of the value of the Reynolds-averaged progress variable, associated with the maximum flamelet crossing frequency (see Ref. [75]), on D_d/D_e has been reported by Chang et al. [359], $\overline{c} = 0.5$ and 0.55 in rich and lean methane–air flames, respectively.

DNS studies performed by Chen et al. [364–367,370,371] indicate a substantial effect of the molecular diffusion of radicals on the local structure of highly perturbed flame fronts.

5.3. Discussion

The above brief review of experimental and DNS results unambiguously shows that differences in and D_F and D_O

substantially affect the local structure of premixed turbulent flames, the effects being in qualitative agreement with the theory of weakly perturbed laminar flames. However, such a qualitative agreement does not mean that the premixed turbulent combustion models that utilize the theoretical results in the form of the linear Eqs. (12), (15), (19), and (20) supplemented with measured or computed values of the Markstein number are a well-developed tool for predicting the dependence of U_t on D_d. On the contrary, a number of important issues straightforwardly relevant to such models are still unresolved.

First, despite a number of experimental and numerical contributions, the data base on *Ma*, available today, appears to be unsatisfactory for turbulent combustion applications. The point is that the majority of premixed turbulent combustion models need either the value of Ma_c or $Ma_{h,u}$. The latter Markstein number appears to be directly relevant to simulations that deal with the instant *G*-equation embedded in a turbulent flow field under the conditions associated with the thin reaction zone regime highlighted recently by Peters [15,16]. The majority of the experimental data characterizes other Markstein numbers, which are well known to depend strongly on the definitions used [189–191,193,272,274,275,425]. For instance, experiments with expanding spherical flames yield Markstein numbers that characterize the flame speed with respect to burned mixture, but these numbers may have a sign opposite to $Ma_{h,u}$ [165,271].

Certainly, this problem appears to be a purely technical one and can be resolved. For instance, experiments with spherical flames are often accompanied by numerical simulations with detailed chemistry [186,188,193,194,207, 314,398,411,413]. Subsequently, the experimental data can be utilized to validate the computations by using the same methods to measure and calculate *Ma*, followed by the numerical evaluation of Ma_c, $Ma_{h,u}$, Ma_d, etc.

In any case, a few data on Ma_c are available today and the lack of reliable data obtained under various conditions strongly impedes testing Eq. (32) or (33) or similar ones and makes any quantitative results questionable.

Second, despite the fact that the non-linear response of laminar flame speed to perturbations is well known in theory (e.g. Eq. (11) or (22)) [226,261,264,424,426–428], simulations [140,272,276,421,422,424,425], and measurements [405,417,419]; the models discussed either do not allow for the non-linear phenomena (Eq. (33)) or mimic them in an arbitrary manner, e.g. by substituting the linear Eqs. (15) and (20) into the linear Eq. (19) when deriving Eq. (32). As discussed in Section 5.1, such a non-linear modification has been contradicted by recent experiments with highly curved flames [187,192, 194,412].

Third, the linear correlation between u_c and $\dot{s}$, a_t, and h_m has been questioned by a number of DNS and experimental investigations (see the last paragraph in Section 5.2.1).

Fourth, the unsteadiness of flamelet perturbations in a turbulent flow is ignored by the models referred to despite the fact that the importance of the transient behavior of stretched laminar flames has been shown experimentally [433–435,441] and numerically [140,436,437]. This issue is further discussed in Section 6.1.1.

Fifth, the assumption of two independent PDFs, for flamelet strain rate and curvature (Eq. (28)), is put into question by DNS (see Fig. 8 in Ref. [209], or Fig. 4c in Ref. [438], or Fig. 9a in Ref. [65]).

Sixth, no approximation for the behavior of $\mathcal{P}(h_m)$ at the leading edge of the mean flame brush has been developed, despite the substantial importance of this issue, as discussed in Section 5.3.1.

5.3.1. Are curved flamelets of importance?

It is well known that (1) the PDF $\mathcal{P}(h_m)$ looks roughly symmetrical with respect to zero, (2) the theory of weakly perturbed laminar flames predicts the linear dependence of u_c on $\dot{s}$ (Eqs. (19) and (20)) and, hence, on a_t and h_m (Eq. (15)), and (3) the linear function reasonably well approximates the correlations between the local burning rate and h_m, measured [349,350] and simulated [209,210] in turbulent flames. Based on these facts, the effect of flamelet curvature on the burning rate averaged over the flamelet surface and, therefore, on U_t is often assumed to be of minor importance, because the variations in the local burning rate tend to cancel in the mean [176,209,210,350]. Subsequently, the main effect of D_d on U_t is associated with enhancing the production of the flame surface area due to flamelet instabilities.

This hypothesis is supported, in part, by the results of DNS, that show a minor increase in the mean consumption velocity with decreasing *Le* from 1.2 to 0.8 (see Fig. 10b) [211]. However, the increase in the velocity with decreasing *Le* down to 0.3 is roughly equal to the increase in the area (cf. Fig. 10b and c). Moreover, the recent DNS data obtained for lean ($F=0.4$) hydrogen–air mixtures indicate that: (1) the dependence of the local displacement speed on the curvature is strongly non-linear [370], and (2) the averaged speed is substantially larger (by a factor of 2) than $S_{L,0}$ [371].

It is worth emphasizing that the concept of small effects of the curvature on $\overline{u}_c$ may be valid inside the mean flame brush, but not at the leading edge ($\tilde{c} \to 0$) of the flame. Indeed, the simplest geometrical consideration implies that solely positively curved flame fronts may exist at the leading edge and, hence, $\mathcal{P}(h_m, \tilde{c} \to 0)$ must be strongly asymmetrical. Consequently, positive and negative variations in $u_c(h_m)$ cannot cancel each other and the curvature effects must manifest themselves not only locally but also in the mean at $\tilde{c} \to 0$. Note that many models of premixed turbulent combustion [18,19,78,277,442–445] predict that U_t is controlled by the mean rate of product creation at the leading edge. Consequently, the behavior of $\mathcal{P}$ at $\tilde{c} \to 0$ is of paramount importance within the framework of such models. However, no research into the behavior of $\mathcal{P}(\tilde{c} \to 0)$ has been performed, to the best of our knowledge.

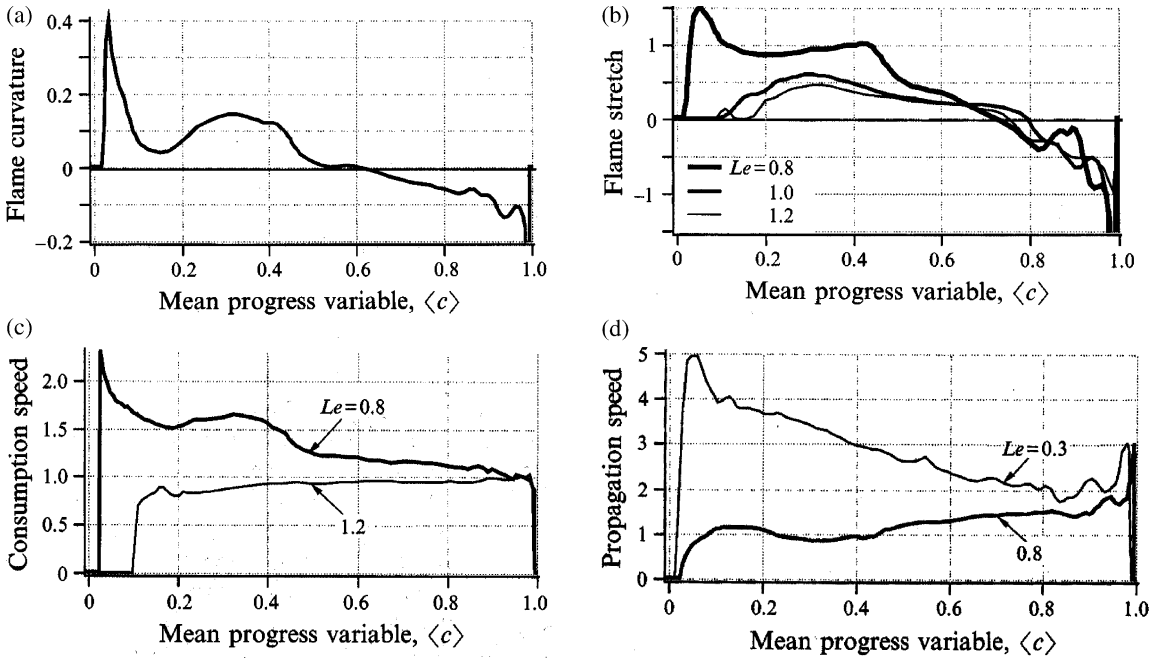

Fig. 15. Results of DNS [211] of the Lewis number effects on turbulent flame structure. The quantities are normalized using δ_L, $S_{L,0}$, ρ_u, and $Y_{f,u}$. From the paper by Trouvé and Poinsot [211] © Cambridge University Press, reproduced with permission. (a) Variations of the mean curvature of the local flame front across the turbulent flame brush. $Le=0.8$, $t/\tau_0\approx 4.3$. (b) Variations of the mean stretch rate of the local flame front across the turbulent flame brush. $t/\tau_0\approx 4.3$. (c) Variations of the mean fuel consumption speed across the brush. $t/\tau_0\approx 4.3$. (d) Variations of the mean displacement speed across the brush. The curves for $Le=0.3$ and 0.8 have been computed at $t/\tau_0\approx 2.5$ and 4.3, respectively.

Numerical simulations [62,211,440] and experiments [440,446–448] indicate that positive curvature dominates at the leading edge (e.g. Fig. 15a). As a result, the difference in $\overline{S}_c$ computed for $Le=0.8$ and $Le=1.2$ increases with decreasing $\tilde{c}$ and becomes quite substantial at $\tilde{c}\approx 0.1$ (see Fig. 15c). A similar trend is observed when comparing $\overline{S}_d(\tilde{c})$ calculated for $Le=0.8$ and $Le=0.3$ (see Fig. 15d). An increase in $\dot{s}_q$, and $\overline{\dot{s}}$ with decreasing $\tilde{c}$ has been also reported by de Charentenay and Ern [372] for lean $H_2/O_2/N_2$ flames, but not for stoichiometric ones.

Furthermore, Swaminathan et al. [449–451] have processed the DNS data bases of Trouvé and Poinsot [211] and Baum et al. [200] and have calculated the dependencies of the reaction rate, $\langle \rho W|\zeta\rangle$, conditionally averaged at $c=\zeta$, on ζ at various $\tilde{c}$. The distributions of $\langle \rho W|\zeta\rangle(\zeta)$, computed from the former data base (see Fig. 16a), are similar to filled circles calculated for the laminar flame if $\tilde{c}\geq 0.34$ (squares), but $\langle \rho W|\xi\rangle(\zeta)$ evaluated at $\tilde{c}=0.13$ (open circles) differs substantially from the other results. This observation also implies substantial changes in local flame front configuration at the leading edge of turbulent flame brush. However, the curves calculated from the latter data base are not affected by $\tilde{c}$ (see Fig. 16b). The difference between the two Figures may be associated either with the fact that the curves shown in Fig. 16b correspond to the mean flame brush ($\tilde{c}\geq 0.29$), rather than the leading edge, or with the differences between the two DNS studies (single-step chemistry and 3D turbulence [211] vs. complex chemistry and 2D turbulence [200]). It is worth noting that both DNS data bases yield substantially larger variations (as compared to the corresponding unperturbed laminar flames) in conditional diffusion, dilatation and scalar dissipation than in $\langle \rho W|\zeta\rangle$ [449–451].

Finally, the concept of the minor effects of the curvature on $\overline{u}_c$ is based on the linearity of the relation between u_c and h_m, which is theoretically supported only in the case of $\beta\gg 1$, $\dot{s}\tau_c\ll 1$, and $\beta(Le-1)=O(1)$ [165,224,266,267]. In the case of $Le-1=O(1)$, which is of more interest for this review, the non-linear dependence of u_c on h_m is predicted by theory [261,264] even for weak perturbations characterized by $\dot{s}\tau_c\ll 1$. For strong perturbations, the non-linear dependence has also been predicted theoretically [226,426,427] even if $Le\approx 1$. The non-linear behavior of S_c and S_d has been documented in a number of numerical [140,272,276,421,422,424,425] and experimental [405,417,419] investigations of perturbed laminar flames.

Consequently, the concept referred to is ill supported due to: (1) the deviations of $\mathcal{P}(h_m)$ from the Gaussian function at $\tilde{c}\to 0$, and (2) the non-linear behavior of $u_c(h_m)$ in mixtures with substantially different D_F and D_O.

5.3.2. Validation

Due to a lack of reliable data on the values of Ma_c, experimental tests of the ability of the concept of

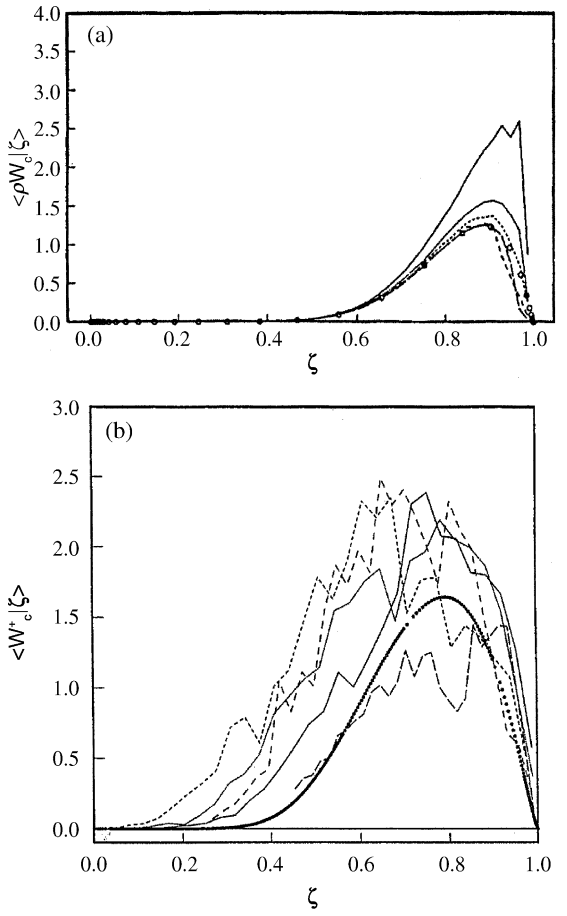

Fig. 16. Variations of the conditionally averaged reaction rate, $\langle \rho W|\zeta\rangle$, with the sample space variable, ζ, at different $\tilde{c}$. The rate is normalized using ρ_u, $S_{L,0}$, and δ_L. (a) DNS data base by Trouvé and Poinsot [211], processed by Swaminathan et al. [450]. © 1997 from Combustion Science and Technology, a paper by Swaminathan et al. [450]. Reproduced by permission of Taylor and Francis, Inc., http://www.taylorandfrancis.com. $Le = 0.81$. Solid, long-dashed, short-dashed, and middle-dashed curves correspond to $\tilde{c} = 0.13$, 0.34, 0.60, and 0.80, respectively. Symbols show the results of unperturbed laminar flame simulations. (b) DNS data base by Baum et al. [200], processed by Swaminathan et al. [451] lean ($F = 0.35$) preheated $H_2/O_2/N_2$ mixture. Solid, dotted, short-dashed, middle-dashed, and long-dashed curves correspond to $\tilde{c} = 0.29, 0.56$, 0.78, 0.88, and 0.94, respectively. Bold curve show the results of unperturbed laminar flame simulations. Reprinted by permission of Elsevier Science from Ref. [451] © 2002 by The Combustion Institute.

the Markstein number to predict the dependence of U_t on D_d are very scarce.

Recently, Brutscher et al. [159] tested the concept by using the dependencies of turbulent burning velocity on u' for lean and rich methane–, ethane–, and propane–air flames expanding in a fan-stirred bomb. The quantitative agreement between the measurements and computations, they reported for 18 mixtures (6 different values of F for each fuel), is impressive but should not be overestimated bearing in mind the following points.

First, Brutscher et al. [159] have used the Markstein numbers measured by Faeth et al. [408,409] and Taylor (see Refs. [406,410]) for expanding spherical flames. Such data are associated with $Ma_{h,b}$ [191,412], whereas the values of Ma_c, required for many premixed turbulent combustion models, may be substantially different, as discussed in Sections 4.1.3 and 5.1. For instance, the experimental data reported by Brutscher et al. (see Fig. 4 in Ref. [159]) show that the effect of D_d on l_t is most pronounced for the richest ($F = 1.37$) methane–air and the leanest ($F = 0.58$) propane–air flames investigated. For these two mixtures, Brutscher et al. [159] have used $Ma = 3.21$ (a similar value is reported in Ref. [409]) and $Ma = 6.0$ (this value appears to be a linear extrapolation of the data Taylor reported for $F = 0.65$ and 0.7), respectively, whereas the recent numerical simulations of differently defined Markstein numbers have yielded $Ma_c \approx 2$ (see Fig. 8 in Ref. [191]) and $Ma_c \approx 4$ (see Fig. 9 in Ref. [191]) for these two mixtures, respectively.

Second, when testing the approach, the dependence of turbulent flame speed on time after spark ignition (or on the flame radius) has not been taken into account, but such effects are of substantial importance to expanding spherical turbulent flames and are able to reduce U_t by 2–3 times as discussed, in detail, elsewhere [18,452,453].

Third, the tests, in fact, question the concept referred to, rather than support it. Indeed, Brutscher et al. [159] have approximated the effect of D_d on U_t by replacing $S_{L,0}$ with the following perturbed laminar flame speed

$$S_L = \frac{S_{L,0}}{1 + Ma\overline{Ka}}, \tag{34}$$

in an expression for U_t, discussed elsewhere [18,80]. It is worth emphasizing that $\overline{Ka}$ has been adjusted for each fuel and does not depend on u'. In the two aforementioned mixtures, the ratios of $S_L/S_{L,0}$, given by Eq. (34), are about 0.5 ($Ma = 3.21$, $\overline{Ka} = 0.32$ and $Ma = 6.0$, $\overline{Ka} = 0.14$ in the rich methane–air and lean propane–air mixtures, respectively) and independent of u'. However, a consistent implementation of the concept of the Markstein number (e.g. Eq. (32) or (33)) should lead to a marked dependence of $S_L/S_{L,0}$ on u', because the stretch rate substituted into Eqs. (12), (19), and (20) depends on u', whereas the Markstein number is a physico-chemical quantity that should not depend on turbulence characteristics.

In summary, the studies performed by Brutscher et al. [159] have shown that even in light paraffin–air mixtures, for which the difference in D_F and D_O is moderate, the dependence of U_t on D_d is well pronounced; the effect being independent of u' but correlating qualitatively with the Markstein number. However, such a correlation does not prove that the effect is controlled by Ma, because the correlation may result from the dependence of U_t on $Le - 1$, rather than on Ma, which is also proportional to $Le - 1$ (see Eq. (13)).

Certainly, turbulent combustion models that utilize various Ma (in the form of a stretch- factor I_0 that parameterizes the mean effect of turbulent stretching on local consumption velocity, e.g. Eq. (32)) can yield the reduction in U_t by Le because Ma depends substantially on $(Le-1)$. Negative (positive) values of Ma and, hence, $I_0>1$ ($I_0<1$) are associated with $Le<1$ ($Le>1$), in line with the increase in $\mathcal{U}_t$ with decreasing Le, shown in Figs. 2–4. It is hard to assess the predictions of these models since they are sensitive to the Markstein numbers used but not reported. The results calculated from Eq. (32) at various combinations of Ma_c and Ma_d are shown by broken lines in Fig. 17. Such results do not seem to explain the strong effect of D_d on $\mathcal{U}_t$, shown in Fig. 4.

Note, that the large values of I_0, calculated for $Ma_c=Ma_d=5$ (dotted line) are controlled by the positive term proportional to Ma_cMa_dKa in Eq. (32). The increase in I_0 by u' for such a mixture is a questionable prediction, because the mean local consumption velocity should be reduced by turbulence for positive Markstein numbers.

In general, any model based on the concept of the Markstein number does not seem to be able to predict the strong effect of D_d on $\mathcal{U}_t$, shown in Fig. 4. First, such a model characterizes the effect by the ratio of $\overline{u}_c/S_{L,0}$ which depends on $KaMa$. In order to yield a strong increase in U_t with decreasing Le, the values of $\overline{u}_c$ in mixtures with a low Le must be larger than in mixtures with a high Le. Since the laminar burning velocities show the opposite behavior, with the ratios of $S_{L,0}(Le>1)/S_{L,0}(Le<1)$ being large (15:6:3:1 for mixtures 1, 6, 3, and 4 or 5, respectively in Fig. 4a); the values of $\overline{u}_c$ must vary by several times as compared with $S_{L,0}$ in order to describe the experimental data. However, a simple linear relation between u_c and the stretch rate $\dot{s}$, which the models are based on, is substantiated only in weakly stretched flames with $Le\approx1$, for which the difference in u_c and $S_{L,0}$ is small. In strongly perturbed laminar flames with $Le-1=O(1)$, the functions $u_c(\dot{s})$ are obviously non-linear and depend on flame geometry and transient effects, as discussed above (e.g. Fig. 12).

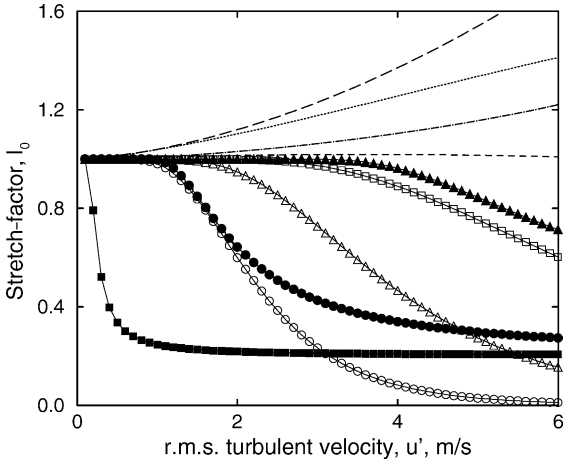

Fig. 17. Stretch-factor I_0 vs. r.m.s. turbulent intensity, u'. Broken lines have been calculated using Eq. (32) at $L=10$ mm, $\tau_c=0.02$ ms, and $Ma_c=-5$, $Ma_d=-5$ (long-dashed line), or $Ma_c=-5$, $Ma_d=-1$ (dotted-dashed line), or $Ma_c=5$, $Ma_d=5$ (dotted line), or $Ma_c=5$, $Ma_d=1$ (dashed line). Open and filled symbols have been calculated at $L=10$ mm using Eqs. (36) and (37), respectively. In the former case, circles, triangles and squares correspond to $\epsilon_q=0.2$, 1.0, and 5.0 ms^{-1}, respectively. $C_\sigma=0.26$. In the latter case, circles, triangles and squares correspond to rich ($F=5.0$, $Le=2.15$, $S_{L,0}=1.1$ m/s), lean ($F=0.71$, $Le=0.6$, $S_{L,0}=1.1$ m/s) and very lean ($F=1/6$, $Le=0.34$, $S_{L,0}=0.07$ m/s) hydrogen–air mixtures, respectively. Turbulent burning velocities measured for the three mixtures by Karpov and Severin [110] are shown by symbols 1, 2 and 5, respectively, in Fig. 4a.

Second, the following qualitative discrepancy between the discussed models and the experimental data is worth emphasizing. The models associate the effect of Le on U_t with the linear dependence of u_c on $Ma\tau_c\dot{s}$, which, after averaging, leads to the dependence of $U_t(KaMa)$ (e.g. Eq. (32) or (33)). Since the Karlovitz number depends substantially on u', $Ka\propto u'^{3/2}$, such models must predict a stronger effect of Le on U_t at a higher u'. In particular, if the model predicts a strong increase in U_t with decreasing Le (or Ma), this implies a substantial dependence of U_t on Ka, because the Lewis number affects flame speed through $KaMa\propto Ka(Le-1)$. Consequently, a decrease in u' and, hence, in Ka, should markedly reduce the effect of Le (or Ma) on U_t, because $dU_t/dLe\propto Ka$. On the contrary, many experimental data shown in Figs. 2–4 exhibit no dependence of the effect on u' at moderate turbulence. The aforementioned studies by Brutscher et al. [159] also support this independence.

In summary, although the concept of the Markstein number yields a dependence of U_t on Le and D_F/D_O, the concept does not seem to be able to quantitatively predict any substantial effect of D_d on Le. This limitation results from a number of assumptions (e.g. weak and steady perturbations, $Le\approx1$), which the concept is based on but which do not hold in practical turbulent flames.

Finally, very lean hydrogen mixtures, for which the discussed effect is most pronounced, are well known to be unstable both due to the DL and PDT mechanisms. Since the linear Eq. (12) and the instability are predicted by the same theory, the use of Eq. (12) without a submodel of flamelet instabilities for turbulent combustion application is inconsistent and underestimates the effect. However, such an instability submodel for flames with low Le and $u'>S_{L,0}$ has not been elaborated, yet, as discussed in Section 4.

5.4. Summary

From a theoretical standpoint, the linear relations between local consumption velocity and stretch rate (Eqs. (12), (19), and (20)) are particular solutions valid in a quite limited range of parameters ($\beta\gg1$, $\beta(Le-1)=O(1)$, $\epsilon\ll1$). A number of other particular solutions

(Eq. (11) or (22), or (41)–(43)) are known to have substantially non-linear form, Eq. (22) being a more general solution than Eq. (12). The simplicity of the linear Eqs. (12), (19), and (20) appears to be the main reason for the wide use of them in premixed turbulent combustion studies.

Experimental and numerical investigations of real laminar flames have shown that the linear relations referred to approximate data obtained in weakly and moderately perturbed laminar flames reasonably well. However, limitations of the linear relations have also been demonstrated in measurements and computations.

Experimental studies and DNS of premixed turbulent flames have shown that local consumption velocity is affected by molecular transport coefficients, in qualitative agreement with the theory of weakly perturbed laminar flames. In particular, if $D_d > D_e$ and $Le < 1$, $u_c > S_{L,0}$ and $u_c < S_{L,0}$ in positively and negatively curved flames, respectively. However, the linear Eqs. (12), (19), and (20) are insufficient to quantitatively correlate such local data (see Figs. 13 and 14) due to the important role played by transient, non-linear, and collective effects in the interaction between a flamelet and turbulent eddies.

If applied to turbulent combustion, the concept of the Markstein number disregards a number of important issues discussed above. Models of premixed turbulent combustion, based on the concept, need validation. No such model has been shown to predict the strong dependence of U_t on D_F/D_O, obtained in various measurements.

6. Strongly perturbed laminar flamelets in premixed turbulent combustion

6.1. The concept of critical stretch rate

In Section 5, we discussed the ability of the concept of the Markstein number to predict the strong dependence of $\mathcal{U}_t$ on D_d. The concept is an asymptotic version of the flamelet library approach, valid for weakly perturbed laminar flames in a turbulent flow. For the opposite limit case of strongly perturbed laminar flamelets, another concept has been developed by Bray [174] and Bradley et al. [38,175,176].

Within the framework of the concept, the critical stretch rate, $\dot{s}_q$, associated with the extinction of laminar flames by external stretching, is utilized for turbulent combustion modeling by using the following simple approach. The flamelet structure is assumed to be unaffected by eddies providing $\dot{s} < \dot{s}_q$, whereas stronger ($\dot{s} > \dot{s}_q$) eddies are assumed to quench the flamelet instantly. Subsequently, the probability, $I_0 \le 1$, of $\dot{s} < \dot{s}_q$ is parameterized and the local burning rate is reduced by a stretch-factor of I_0 as compared to $S_{L,0}$.

To evaluate the stretch-factor, Bray [174] has utilized the well-known, log-normal PDF [30,217,377]

$$\mathcal{P}(\varepsilon_l) = \frac{1}{\sigma_\epsilon \varepsilon_l \sqrt{2\pi}} \exp\left\{ -\frac{1}{2\sigma_\epsilon^2} \left[\ln\left(\frac{\varepsilon_l}{\bar{\varepsilon}}\right) + \frac{\sigma_\epsilon^2}{2} \right]^2 \right\},$$

$$\sigma_{\epsilon,l}^2 = C_\sigma \ln(l/\eta); \tag{35}$$

$$\varepsilon_l = \iiint \left[\frac{\nu}{2} \sum_{i,j=1}^{3} \left(\frac{\partial u_i}{\partial x_j} + \frac{\partial u_j}{\partial x_i} \right)^2 \right] \mathrm{d}\vec{x},$$

for the viscous dissipation ε_l of turbulent energy, locally averaged over a cube of the length l. By integrating this PDF and invoking the critical stretch rate concept, he has suggested the following parameterization

$$\mathcal{P}_q = 1 - \frac{1}{2}\mathrm{erfc}\left\{ -\frac{1}{\sqrt{2}\sigma} \left[\ln\frac{\varepsilon_q}{\bar{\varepsilon}} + \frac{\sigma_\epsilon^2}{2} \right] \right\}, \tag{36}$$

for the probability of flamelet quenching by turbulent stretching. Here, erfc is the complementary error function, $\eta = (\nu_u^3/\varepsilon)^{1/4}$ is the Kolmogorov length scale, ε_q is associated with $\dot{s}_q$, e.g. $\varepsilon_q = 15\nu_u \dot{s}_q^2$, and $\sigma_\varepsilon = \sigma_{\varepsilon,l}$ ($l = L$).

Abdel-Gayed et al. [175] have pointed out that flame stretching is a Lagrangian concept and the flame surface follows the fluid motion in the direction in which the strains are positive. By analogy to the behavior of material line elements in turbulent flows, they have postulated that the flame surface tends to align with the direction of the maximum strain rate. DNS has supported this approach, in part, but has shown a marked probability of negative strain rates for material line elements [14,454,455]. Moreover, when the laminar flame speed is not negligible, the behavior of the flame surface differs substantially from the behavior of material elements due to propagation.

By analyzing the results of DNS and developing the critical stretch rate concept, Bradley et al. [176,177] have suggested the Gaussian approximation of the PDF of the flame stretch rate and have proposed using the following semi-empirical parameterization for the quenching probability

$$\mathcal{P}_q = 1 - \frac{1}{2}\mathrm{erfc}\left\{ -\frac{\dot{s}_q - \bar{\dot{s}}}{\sqrt{2}\sigma} \right\},$$

$$\bar{\dot{s}} = 1.08 \exp\left(-\frac{0.0132}{Ka' Le} \right) \frac{u'}{\lambda},$$

$$\sigma = \left[1 + 0.32 \exp\left(-\frac{0.0132}{Ka' Le} \right) \right] \frac{u'}{\lambda}. \tag{37}$$

Later, a more complicated parameterization was presented by the same group [178] combining the above approach and the concept of the Markstein number. Just a year ago, Bradley et al. [399] further developed the approach by analyzing recent experimental data to generate a more sophisticated PDF for the flame stretch rate.

To close Eq. (36) or (37), the value of $\dot{s}_q$ should be specified.

6.1.1. Extinction of laminar flames

The extinction of laminar flames by flow non-uniformities is a well-known phenomenon first predicted and studied theoretically [26–28]. The subsequent experimental, numerical, and theoretical studies of the issue are discussed in a number of textbooks [6,30,37,225,226,397] and review papers [38,184,185,233,393,394,456].

Following the seminal work of Klimov [28], planar stagnation-point flow is considered to be a well recognized model of laminar flame straining in a turbulent flow. In this case, convective heat and mass fluxes tangential to the flame increase along any iso-scalar surface, whereas the normal fluxes decrease from the unburned to the burned side. If the reaction zone structure of a strained flame is unchanged as compared to the unperturbed flame (e.g. if $\beta \to \infty$, $Le = 1$, and $a_t \tau_c \ll 1$), the temperature gradient in the reaction zone will also be unchanged, but the preheat zone will be thinner due to mass flux increasing with distance from the flame. Moreover, the normal convective mass flux in the reaction zone will be lower than $\rho_u S_{L,0}$, because it balances only a part of the conductive heat flux from the zone while the rest of the heat flux is convected along the flame sheet. As a result, the displacement speed of the reaction zone is lower than $S_{L,0}$, whereas the consumption speed is not affected by low strain rates in the adiabatic case if $Le = 1$ and $\beta \to \infty$ [6,184,226,457]. For finite β, S_c is reduced by the strain due to a decrease in the reaction zone thickness [28]. Moreover, in the counterflowing streams of reactants and products, the reaction zone moves to the product side (with respect to the stagnation plane) if the rate of strain is sufficiently high. Consequently, the creation of products by the flame is severely diminished [457].

If $Le > 1$, the consumption speed is reduced by a_t even for $\beta \to \infty$ [261,263,458–464], because the heat losses from the reaction zone exceed the energy supply to it by the reactant diffusion. Such effects are increased by the strain, because spatial gradients are larger in a thinner flame. As a result, the temperature in the reaction zone and the reaction rate are reduced by a_t and the flame may be quenched by the strain.

The theoretical analysis performed by Libby et al. [462,464] has shown that the Lewis number would have to be unrealistically large in order for the extinction to happen in the adiabatic counterflowing streams of reactants and products [462], whereas the extinction of the adiabatic flames in two counterflowing reactant streams can be obtained for moderately large *Le* [464].

If $Le < 1$, the adiabatic temperature, reaction rate, and consumption speed are increased by the strain. In this case, two adiabatic counterflow flames merge at the plane of symmetry prior to extinction if $\beta \to \infty$ [464]. For finite β, the flames are quenched by the strain due to incomplete reaction when the reaction zones move close to the plane of symmetry [184].

Thus, the quenching strain rates depend substantially on the Lewis number [226,393,458,464]. A dependence of $\dot{s}_q$ on *Le*, substituted into Eqs. (36) and (37), can yield a dependence of U_t on *Le* after implementing the stretch-factor $I_0 = 1 - \mathscr{P}_q$ in a premixed turbulent combustion model, as discussed elsewhere [18,137,177,179,277,452,465].

It is worth emphasizing, however, that the aforementioned theoretical analysis of the counterflowing streams of reactants and products has also shown that the extinction of laminar flames at high rates of strain is mainly controlled by non-adiabaticity, whereas 'non-unity Lewis numbers result in a higher-order effect that may be ignored to a first approximation' [462]. The crucial role played by heat losses in the extinction of premixed flames was recently stressed by Sivashinsky [233].

We will not further discuss the quenching of a laminar flame stabilized in a stationary, non-uniform, laminar flow. The interested reader is referred to the aforementioned textbooks and review papers. For our purposes, it is sufficient to note that the critical strain rate can be computed for a particular mixture, temperature, pressure and flame geometry by numerically solving the mass balance and Navier-Stokes equations supplemented with a complex combustion chemistry mechanism. Refs. [179,190,191,236,466,467] provide recent examples of such simulations for counterflow flames.

If the value of $\dot{s}_q$ is considered to be known from the aforementioned simulations, the models (e.g. Eq. (36) or (37)) of premixed turbulent combustion, based on the concept of the critical stretch rate, are closed and can be used for practical simulations.

The following basic limitations of such an approach are nevertheless worth emphasizing.

First, in a particular mixture, the values of $\dot{s}_q$ depend on flame geometry. For instance, the values of $\dot{s}_q$, computed for symmetrical (unburned against unburned) and asymmetrical (unburned against burned), counterflow, laminar flames differ substantially, all other things being equal [468,469]. Also, theoretical results obtained using the same method are substantially different in these two cases [462,464]. It is quite unclear which geometrical configuration (twin symmetrical planar counter-flow flames? a single planar flame stabilized by the product counter-flow? a strained cylindrical flame?, etc.) is generally relevant in turbulent combustion. For instance, even if the probability of finding the asymmetrical (unburned against burned) flames is much higher than the probability of finding the symmetrical (unburned against unburned) ones inside the turbulent flame brush, the opposite appears to be valid at the leading edge of the brush. As discussed in Section 6.2, the leading edge can control turbulent flame propagation. An important role eventually played by the strained cylindrical flames in premixed turbulent combustion is discussed in Sections 7.3.3 and 7.4.

If *Le* is substantially lower than unity, the curvature of a strained laminar flame allows it to survive under the influence of high strain rates, as documented [249,470] for

the premixed edge flames mentioned at the end of Section 4.3. The simulations of Buckmaster and Short [391] have shown that such flames can survive at values of strain rate about three times larger than the extinction value for twin planar flames stabilized in counterflows of the same mixture with $Le = 0.3$.

Second, the responses of a flame to steady and unsteady strain rates are substantially different [140,184,280,396, 432–437,441,471–483], the difference being more pronounced when the mean strain rate is close to the value of $\dot{s}_{q,s}$, associated with the steady strain rate. A flame needs finite time to respond to variations in the strain rate, and a flame will not respond to rapid changes in $\dot{s}$ even if an instantaneous strain rate is substantially higher than $\dot{s}_{q,s}$. The response time lag can be as long as 1 ms [479].

Numerical simulations have shown that laminar flames can survive when the strain rate oscillates about a value slightly less than $\dot{s}_{q,s}$ [396,476] even if the highest instantaneous strain rate is close to $2\dot{s}_{q,s}$ [140]. The ability to survive under oscillating straining depends substantially on the Lewis number [140,184,476,482].

Mueller et al. [441] have experimentally shown that, for a time lag comparable with τ_c, laminar flames are weakly affected by external stretch rates even if the rates are $2 \div 10$ times greater than $\dot{s}_{q,s}$. Sardi and Whitelaw [480] have also documented that flames can survive under the influence of strong periodic strain rates. Experimental [435] and numerical [436] studies of the interaction between a laminar flame and a strong vortex pair have not indicated any flame quenching at strain rates much higher (by more than 10 times) than the static extinction point of the twin, symmetrical, counterflow laminar flame.

Fourth, since the smallest eddies that provide the highest local stretching in inert turbulent flows are affected by the heat release in flamelets and are rapidly dissipated due to increasing viscosity in the preheat zones, such eddies are non-effective in quenching the flamelets, as predicted theoretically [12,33] and confirmed experimentally [484, 485]. This issue is discussed, in detail, in recent review papers [14,58,486].

In summary, there is no evidence whatsoever that indicates that a steadily strained laminar flame is a good model for perturbed flamelets that occur in real turbulent combustion. On the contrary, the well-pronounced dependence of laminar flame extinction on flame geometry and transient effects, including the viscous dissipation of small eddies in the preheat zone, reveals the deficiency of such a model and implies that neither a PDF for flamelet stretching, nor a joint PDF for flamelet straining and curvature can characterize all flamelet perturbations substantial for premixed turbulent combustion modeling. Moreover, the available parameterization of the above PDFs (Eqs. (28)–(31), or Eq. (35)) depend neither on the coordinate normal to the mean flame brush nor on an averaged progress variable, whereas such a dependence is of paramount importance, as discussed in Sections 5.3.1 and 6.2.

6.1.2. Discussion

As far as we know, there exists only one paper [177] which might be considered to validate the concept of critical stretch rate for premixed turbulent flames. However, this test cannot be recognized as a solid validation for a couple of reasons, discussed, in detail, elsewhere (see Section C.3 in Ref. [18]).

The values of $\dot{s}_q$, used in turbulent combustion simulations, should differ substantially from the values of $\dot{s}_{q,s}$, associated with the extinction of the stationary, counterflow, planar, laminar flames, widely investigated following the pioneering work by Klimov [28]. For instance, values of $\dot{s}_q$ markedly higher than various laminar flame extinction data both for symmetric and asymmetric configurations have been invoked in order to obtain an agreement between the r.m.s. turbulent velocities associated with the maxima of the $\mathcal{U}_t(u')$-curves measured by Karpov and Severin [110] and the values of u'_m, computed with the extended Zimont model (see Appendix A.3) with $I_0 = 1 - \mathcal{P}_q$ determined using Eq. (35) [137,465,487]. However, despite the aforementioned adjustment, an agreement between the measured and computed burning velocities at strong turbulence ($u' > u'_m$), has not been obtained (cf. symbols and solid curves in Fig. 19 in Section 6.2.2), because the computed values of $\mathcal{U}_t$ drop rapidly with increasing $u' > u'_m$. We have also observed similar trends [452].

Certainly, the use of Eq. (36) or (37) may result in a reduction of U_t by Le due to the Lewis number dependence of the critical stretch rate. For example, Eq. (37) yields an increasing function $\mathcal{P}_q(KaLe) \le 1$ and the insertion of this function into an expression for the mean rate of product creation offers the opportunity to calculate the reduction in U_t by Le from the following expressions

$$\overline{W} = \overline{W}_1 I_0(KaLe) = \overline{W}_1[1 - \mathcal{P}_q(KaLe)];$$
$$U_t = U_{t,1} I_1(KaLe); \tag{38}$$

where $\overline{W}_1$ and $U_{t,1}(u'/S_{L,0}, \delta_L/L)$ are associated with $Le = 1$ and discussed in detail elsewhere [18,19]. The functions I_0 and I_1 may be different, e.g. $I_1 = I_0^{1/2}$ for the KPP problem (see Appendix A in Ref. [18]), but both functions are decreasing ones.

For mixtures characterized by the same $S_{L,0}$, such a model yields a strong reduction in I_0 by Le (cf. circles and triangles in Fig. 17) within a certain range of u' and, thus, can predict a higher U_t for lower Le, as observed in the measurements (cf. mixtures 1 and 2 in Fig. 4a). However, if a mixture with a lower Le has a much smaller $S_{L,0}$, Eq. (37) yields a smaller I_0 (cf. filled circles and squares in Fig. 17) and, thus, cannot describe the experimental results (cf. mixtures 1 and 4 or 5 in Fig. 4a).

The effect predicted by the models discussed is much weaker than the measured one. For instance, in mixtures 1 and 5 shown in Fig. 4a, $Le_5/Le_1 \approx 0.16$ but $Ka_5/Ka_1 \approx 225$ under the same turbulent conditions because these two

mixtures have a very strong (by 15 times) difference in $S_{L,0}$. Subsequently, the large ratio of $(KaLe)_5/(KaLe)_1 \approx 35$ is mainly controlled by the laminar flame speed ratio, rather than by the Lewis numbers; Eqs. (37) and (38) yield a much higher U_t in the rich mixture 1 (in this mixture, $U_{t,1}$ is also much higher, because it is increased by $S_{L,0}$ [18]), contrary to experimental data. When comparing the lean hydrogen mixture 4 with the stoichiometric propane–air mixture (No. 6) in Fig. 4a, we have $(KaLe)_6/(KaLe)_4 \approx 0.07$, but the measured $\mathcal{U}_t$ and, especially, $d\mathcal{U}_t/du'$ are markedly higher in the lean mixture. A number of other examples that show a lack of a straightforward correlation between $KaLe$ and U_t are discussed elsewhere [117,138].

Certain trends observed in Figs. 2–4 disagree with the concept of critical stretch rate. First, the key role of $\mathcal{P}_q$ implies that, the effect of Le on U_t must increase with u'. Indeed, the dependence of $I_0 = 1 - \mathcal{P}_q$, as calculated using Eq. (36) or (37), on u' is well pronounced (see symbols in Fig. 17) These models yield $I_0 \approx 1$ at some, mixture-dependent domain of u' but any further increase of u' results in a sharply decreasing stretch-factor. Based on this behavior of I_0, one could expect a lack of influence of Le on U_t at relatively weak turbulence, whereas the effect of Le on U_t should be accompanied by a bending of the $U_t(u')$-curves due to the decrease in I_0. However, the experiments show substantially different trends: (1) the effect of D_d on $\mathcal{U}_t$ is well pronounced in the whole range of moderate turbulence, where the slope of $d\mathcal{U}_t/du'$ is roughly constant; (2) the data exhibit no dependence of the effect on u' in this range.

Second, local flamelet quenching must manifest itself in bending $\mathcal{U}_t(u')$-curves. If the maxima in the curves that correspond to mixtures 4, 5 and 8 in Fig. 4a are attributed to increasing probabilities of quenching, then the values of u'_m associated with these maxima must be related to other effects explained by local quenching, including the effects of D_d on $\mathcal{U}_t$. In particular, the dependencies of $\mathcal{U}_t$ and $d\mathcal{U}_t/du'$ on Le and D_d/D_e at $u' < u'_m$ must correlate with $u'_m(Le, D_d/D_e)$: a weaker slope or a lower burning velocity must be associated with a lower u'_m. However, mixtures 1 and 4 (or 1 and 5, or 6 and 4, or 6 and 5, or 6 and 8, or 7 and 8) show the opposite behavior: a lower u'_m corresponds to a higher slope and, sometimes, to a higher $\mathcal{U}_t$.

In summary, neither the concept of the Markstein number for weakly perturbed flamelets, nor the concept of a critical stretch rate for strongly perturbed flamelets can describe the strong dependence of $\mathcal{U}_t$ on D_d, observed in a number of measurements. The replacement of these two asymptotic concepts with a more general flamelet library concept does not seem to be a remedy, because the above problems of the substantial dependence of the characteristics of perturbed laminar flames on geometry and, especially, on transient phenomena are still unresolved. Flamelet curvature and strain rate are insufficient for creating a flamelet library adequate for modeling turbulent flames. To model the effects of turbulent eddies on flamelet structure and quenching, one has to: (1) utilize a huge number of admissible models of perturbed laminar flames; (2) account for the multi-scale and multi-amplitude nature of turbulent eddies; (3) account for transient phenomena; (4) average the results by invoking a multi-dimensional PDF that depends on flame curvature and strain rate, on flame geometry, on transient processes, on interactions between various perturbations, etc. This very complex task is a matter for the future.

The above problems faced by the flamelet library concept are associated with the fact that a large number of different small-scale reacting structures exist inside the turbulent flame brush. However, this number can be strongly reduced for the leading edge of the brush.

6.2. The concept of leading points

For a steadily propagating, planar turbulent flame, burning velocity $\mathcal{U}_t$ should be equal to the speed, S_{le}, of the leading edge of the flame brush relative to unburned gas. Under this assumption, one can either model the processes inside a mean flame brush to predict $\mathcal{U}_t$ or develop a model for predicting S_{le} based on leading-edge characteristics, and the final result must be the same, $\mathcal{U}_t = S_{le}$. For instance, if local heat release is confined to thin flamelets, the flamelet surface production inside the mean flame brush must provide the balance between $\mathcal{U}_t$ and S_{le}.

Most models of premixed turbulent combustion (as those discussed in the previous sections) follow the former approach, i.e. model $\mathcal{U}_t$. On the one hand, this approach has certain advantages because most available experimental and DNS results have been obtained inside the mean flame brush and little is known about the structure of the leading edge. On the other hand, it is very difficult for a single model to address the problem of substantially different local structures that exist inside the flame brush. If the focus of consideration is placed on the leading edge, certain structures, e.g. negatively curved flamelets, may be omitted. In the best case, one may assume that a few particular structures dominate at the leading edge. For instance, Baev and Tretjakov [128] have argued that $\mathcal{U}_t$, for various turbulent flames, is controlled by u', L, and by a chemical time scale, which (1) is independent of u' and L; (2) depends on mixture composition; (3) is not equal to the chemical time scale τ_c that characterizes the unperturbed laminar flame, and, thus (4) is associated with a perturbed laminar flame of a universal structure.

The crucial role played by the leading points in turbulent flame propagation was highlighted by Zel'dovich [130] and the idea was developed by several groups in Russia [30,117, 128,131–134,136–139]. Note that the well-known KPP solution [488] to the stationary problem of reaction wave propagation, used in many studies of premixed turbulent combustion [78,277,442–445], straightforwardly predicts that propagation speed is controlled by the reaction rate at the leading edge of the flame brush.

Kuznetsov and Sabel'nikov [30] have discussed the physical basis of the concept of leading points in detail and have argued that turbulent flame speed is controlled by the flamelets that advance the furthest into the unburned mixture (leading points) and the structure of the leading kernels is universal (independent of turbulence characteristics), as suggested by Baev and Tretjakov [128]. Here, we restrict ourselves to a brief discussion of the concept and refer the interested reader to the book by Kuznetsov and Sabel'nikov [30].

If u' is substantially larger than $S_{L,0}$, a flamelet element can be a leading point due to the convection of the element by large-scale turbulent eddies. The convection towards the leading edge of the turbulent flame brush is limited by the local combustion extinction caused by strong turbulent eddies. Due to the balance between quenching and convection, critically perturbed (under near-extinction conditions) flamelets appear to dominate at the leading edge. Consequently, the structure of the leading points is assumed to be universal and determined by the strongest possible non-quenching perturbation of flamelets by turbulent eddies.

Such a concept offers the opportunity to substantially simplify modeling premixed turbulent combustion by reducing the flamelet library (a collection of basic characteristics of perturbed laminar flames that allow for all possible perturbations) to a single 'flamelet page' (parameters of a critically perturbed leading kernel). Then, the following issue is of paramount importance: What is the structure of the leading kernels?

6.2.1. Critically strained flamelets

Kuznetsov and Sabel'nikov [30,132] have suggested a critically strained, steady, planar, symmetric, counter-flow laminar flame as a model for the leading kernel structure. By extending the preceding studies of the same problem by Klimov [28] ($D_F = D_O = \kappa$) and by Gremyachkin and Istratov [458] ($D_F = D_O \neq \kappa$), Kuznetsov and Sabel'nikov [132] have theoretically analyzed such a flame in the limit case of single-step, two-reactant chemistry with $\beta \to \infty$ and $D_F \neq D_O \neq \kappa$. They have obtained the following solutions to the temperature, T_r, and the mass fraction of the excess reactant in the critically strained reaction zone

$$\left.\begin{aligned} T_r &= T_u + Y_{F,u} T_1 (1 + \mathrm{St})(D_{F,u}/\kappa_u)^{1/2} \quad F_r \le 1 \\ Y_{O,r} &= Y_{O,u} - \mathrm{St} Y_{F,u} (D_{F,u}/D_{O,u})^{1/2} \end{aligned}\right\};$$

$$\left.\begin{aligned} T_r &= T_u + Y_{O,u} T_1 (1 + \mathrm{St}^{-1})(D_{O,u}/\kappa_u)^{1/2} \quad F_r \ge 1 \\ Y_{F,r} &= Y_{F,u} - \mathrm{St}^{-1} Y_{O,u} (D_{O,u}/D_{F,u})^{1/2} \end{aligned}\right\}; \qquad (39)$$

where St is the mass stoichiometric coefficient, T_r is the local temperature in the reaction zone, and T_1 is the adiabatic combustion temperature of the stoichiometric mixture. Even if $F = 1$, these two temperatures are not equal to one another due to local variations ($Le \neq 1$) in mixture enthalpy in the critically strained reaction zone. Similarly, the local composition in the zone differs from the composition of the unburned mixture far ahead of the flame, because molecular diffusion fluxes of fuel and oxidant into the zone are not equal ($D_F \neq D_O$) to one another.

By arguing that $D_{O,u} \approx \kappa_u$ in typical mixtures, Kuznetsov and Sabel'nikov [30] have proposed to use $S_{L,0}(F_r)$ instead of $S_{L,0}(F_u)$ for premixed turbulent combustion modeling (i.e. to substitute $S_{L,0}(F_r)$ instead of $S_{L,0}(F_u)$ into Eqs. (26) and (27)), where the local equivalence ratio, F_r, in the reaction zone is evaluated from

$$\left.\begin{aligned} F_r &= F_u (D_{F,u}/D_{O,u})^{1/2} \quad F_r \le 1 \\ F_r &= 1 - (D_{O,u}/D_{F,u})^{1/2} + F_u \quad F_r \ge 1 \end{aligned}\right\}. \qquad (40)$$

Eq. (40) results from Eq. (39) in the limit case of $\mathrm{St} \gg 1$ and $D_{O,u}/D_{F,u} = \mathrm{O}(1)$. By testing this method, Kuznetsov and Sabel'nikov [30] succeeded in explaining the differences between $F_{L,m}$ and $F_{t,m}$ reported by Talantov [141] and Karpov and Severin [142] in gasoline– and hydrogen–air mixtures, respectively.

The concept was incorporated into the Zimont model (see Appendix A.3, Eq. (A.12)) by replacing the standard chemical time scale, $\tau_c = \kappa_u / S_{L,0}^2(F_u, T_b)$, with the modified chemical time scale, $\tau_L' = \kappa_u / S_{L,0}^2(F_r, T_r)$, where the leading point speed $S_{L,0}(F_r, T_r)$ was associated with the temperature and equivalence ratio determined using Eq. (39) [487,489]. At moderate turbulence, the extended Zimont model was able to quantitatively predict a considerable number of data on $\mathcal{U}_t(u')$ measured by Karpov and Severin [110] in lean, stoichiometric, and rich hydrocarbon–air mixtures [465]. The predictions were achieved without any variations in the single model constant, A (see Eq. (A.12)). However, the model failed to predict the strong effect of D_d on $\mathcal{U}_t$, measured for lean H_2 flames.

6.2.2. Critically curved flamelets

To predict the strong effect, critically curved laminar flames have been proposed as a model of the leading kernel structure [135] by arguing that: (1) the leading points should be associated with the highest local burning rate, and (2) the highest (for various possible perturbations of a laminar flame with $Le < 1$) local burning rate is reached in such flames. The latter hypothesis has been substantiated by simulations of various perturbed laminar flames (see Fig. 12) [139,140].

We may also note that strongly curved, lean hydrogen–air flames can survive under the influence of high strain rates, as shown for premixed edge laminar flames [249,390–392,470] (see the end of Section 4.3). This behavior is associated with the local increase in temperature in curved laminar flames, because the energy flux into the flame exceeds the heat losses from it if $Le < 1$. The resistance of strongly curved flamelets to local extinction also supports

the choice of such a flamelet as a model of the leading point in the case of $Le<1$.

Strongly curved spherical laminar flames have received plenty of attention recently [428,490–494] in connection with the classical problem of a flame ball [226]. Here, we will restrict ourselves to a very brief introduction to the problem, relevant to the main subject of this review. The interested reader is referred to the reviews by Buckmaster [495] and Ronney [490], as well as to the aforementioned recent papers and to references quoted therein.

The so-called flame ball studied first by Zel'dovich constitutes the asymptotically ($\beta\to\infty$) exact solution of stationary 1D balance equations for the temperature and mass fraction of the deficient reactant, written in the spherical coordinate system. The solution is associated with the adiabatic burning of a motionless mixture at the surface of a small ball with the chemical energy (heat) being transported from infinity to the ball (from the ball to infinity) solely by molecular diffusion (heat conduction) [226]. If the Lewis number is lower (larger) than unity, the temperature in the ball, T_r, will be increased (decreased) as compared with the adiabatic combustion temperature in a planar flame, due to the imbalance between diffusion and heat conduction

$$T_r = T_u + (T_b - T_u)/Le. \tag{41}$$

Eq. (41) yields combustion temperature variations on the order of $T_r/T_b-1=O(Le-1)$, similar to the theory of weakly perturbed laminar flames [165,224,266,267], discussed in Section 4.1.3. However, since the latter theory is valid for $\beta(Le-1)=O(1)$, whereas Eq. (41) has been derived for arbitrary Le (e.g. such that $\beta(Le-1)\gg 1$); the predicted variations in the local burning rate inside the flame ball may be much higher than in weakly perturbed flames with $\beta(Le-1)=O(1)$. As a result, if $Le<1$, the radius of the ball may be very (exponentially) small, as predicted by the following equation

$$R_{cr} = \delta_L Le^{-1}\left(\frac{T_b}{T_r}\right)^{3/2}\exp\left(\frac{\Theta}{2T_b}\frac{T_b-T_r}{T_r}\right), \tag{42}$$

derived for the reaction rate of $W\propto\rho Y\exp(-\Theta/T)$ in the case of $\rho\kappa=\rho_u\kappa_u$ [226,496].

The above solution is unstable [226,497], but flame balls can be stabilized in microgravity [490] due to radiative heat losses [495,498] or under the influence of steady velocity gradients[22] (e.g. rotation, shear or strain) [499], with the stationary flame ball radius depending on the magnitude of the strain rate, but not on its sign. Recently, Joulin et al. [492] have shown that fluctuating velocity gradients with a zero mean can also stabilize flame balls under certain conditions (appropriate amplitude and frequency of fluctuations, $Le<1$).

[22] Recently, Buckmaster and Short [391] have shown that a sufficiently high strain rate can allow steady cylindrical flame structures to exist also.

Since the classical theory of the flame ball [226] predicts a very strong (exponential) increase in the local burning rate due to the increase in the combustion temperature (Eq. (41)) for $Le<1$, the leading points discussed above may be associated with the flame balls. Moreover, since the mass flux of the deficient reactant through the surface of the flame ball scales as R_{cr}^{-1} (see Eq. (6.68) in [226]), the following chemical time scale that characterizes the aforementioned rate

$$\tau_{cr} = \tau_c\frac{R_{cr}}{\delta_L} = \tau_c Le^{-1}\left(\frac{T_b}{T_r}\right)^{3/2}\exp\left(\frac{\Theta}{2T_b}\frac{T_b-T_r}{T_r}\right) \tag{43}$$

has been proposed to be used instead of τ_c for premixed turbulent combustion modeling [135]. Since τ_{cr}/τ_c depends exponentially on $(Le-1)$, see Eq. (41), Eq. (43) predicts that $\tau_{cr}\ll\tau_c$ in mixtures with a low Lewis number. If $Le=1$, Eqs. (41)–(43) yield $\tau_{cr}=\tau_c$.

Eqs. (42) and (43) have been theoretically derived for single-step, single-reactant chemistry with $\beta\to\infty$ and for temperature-independent ρD and $\rho\kappa$. A more general method of determining a chemical time scale that characterizes critically curved laminar flames has been developed numerically in Refs. [117,136,139,140]. For these purposes, the expansion of spherical laminar flames ignited by a ball filled with equilibrium adiabatic combustion products has been simulated. Results show that the dependence of consumption speed on time has a local maximum ($Le<1$) or a local minimum ($Le>1$) if the radius r_i of the igniting ball is close to the critical radius, r_{cr}, that ignites the mixture (when $r_i<r_{cr}$ the initial kernel shrinks and the flame does not develop). A higher maximum ($Le<1$) or a smaller minimum ($Le>1$) correspond to a smaller $r_i>r_{cr}$. Thus, the highest (if $Le<1$) instant combustion rate is reached in expanding spherical flames when $r_i=r_{cr}$, this maximum being the highest rate as compared to the other flame configurations simulated (cf. the right edge of the solid curve with other data shown in Fig. 12a) [139,140].

Based on these numerical results, the following chemical time scale has been introduced [117,136]

$$\frac{\tau_{ex}}{\tau_c} = \frac{S_c(t\to\infty)}{\mathrm{extr}\{S_c(t)\}_{r_i=r_{cr}}}, \tag{44}$$

where extr denotes either the minimum ($Le>1$) or the maximum ($Le<1$) of the computed dependence of $S_c(t)$.

The behavior of both time scales introduced above, τ_{cr} (Eq. (43)) and τ_{ex} (Eq. (44)) is similar but larger quantitative variations are associated with the latter scale. For example, $\tau_{cr}/\tau_c\approx 0.05$ and $\tau_{ex}/\tau_c\approx 0.03$ have been calculated for lean hydrogen–air mixtures [117]. An analysis of the experimental data of Karpov and Severin [110,115,142–145] shows clear-cut correlations between the two time scales and the slopes of $\mathcal{U}_t(u')$-curves at moderate turbulence: a smaller τ_{cr} or a smaller τ_{ex} are associated with a higher $d\mathcal{U}_t/du'$ [117,136,138].

Even this simplified approach, which suggests a similarity of the leading point to a strongly curved laminar

flame, offers the opportunity to explain the most challenging data shown in Fig. 4a. For instance, the following time scales have been reported [117] for certain mixtures shown in Fig. 4a: (1) $\tau_{ex}=0.88$ ms; (2) $\tau_{ex}=0.016$ ms; (3) $\tau_{ex}=0.026$ ms; (5) $\tau_{ex}=0.18$ ms; (6) $\tau_{ex}=0.32$ ms; (7) $\tau_{ex}=0.25$ ms; (8) $\tau_{ex}=0.07$ ms. The values of τ_{ex} and experimental data show the following trend: a smaller time scale is associated with a steeper slope of $\mathcal{U}_t(u')$ at moderate turbulence, $S_{L,0}<u'<u'_m$. This correlation fails in two cases; in very lean hydrogen mixtures 5 and 8, and in rich hydrogen–air mixture 1 as compared with the stoichiometric propane–air mixture 6. In the latter case, this failure may be associated with the overestimation of the effect of $Le>1$, as discussed below. In the former case, this failure may result from the influence of local flame quenching by intense turbulence, because u'_m is too low for mixture 8 which is characterized by a smaller τ_{ex} and a weaker slope as compared with mixture 5. The discussed correlation was supported [117,136] by using τ_{ex} to process a more extensive experimental data base obtained for mixtures showing a well-pronounced effect of D_d on $\mathcal{U}_t$.

Two different physical mechanisms, the convection of a flamelet by a strong eddy [30] and the enhancement of local burning due to diffusive-thermal effects, contribute to the formation of a leading point.

If the latter mechanism is emphasized, strongly curved laminar flamelets are considered to be the leading points only for $Le<1$ [137,139,140]. In such mixtures, the local burning rate in a positively curved flamelet is substantially increased due to the higher chemical energy flux into the flamelet as compared with the heat flux from it. As a result, the flamelet propagates faster[23] and moves to the leading edge of the flame brush.

In the case of $Le>1$, a similar scenario does not seem to be realistic because the local burning rate drops in a positively curved flamelet, but increases in a negatively curved (convex to the burned gas) one. However, the latter flamelet cannot be a leading point due to geometrical consideration. At the leading points, if $Le>1$, the highest local burning rate is associated with planar flamelets compressed by turbulent eddies, but such a planar structure is characterized by the lowest local flamelet surface area $\mathcal{A}/\mathcal{A}_0$ per unit area $\mathcal{A}_0$ of the mean flame surface. Therefore, the balance between an increase in the area due to flamelet wrinkling by small-scale turbulent eddies and a decrease ($Le>1$) in the local burning rate due to the same wrinkling should be reached at the leading points [139,140]. For instance, let us consider the flame surface in the vicinity of the leading point to be the tip of a cone. The acuter the tip, the larger the above area ratio but the lower the consumption velocity, u_c, for $Le>1$. Consequently, the leading point is associated with the tip that has a specific acuteness such that $u_c\mathcal{A}/\mathcal{A}_0$ reaches the maximum (with respect to various acutenesses) value.

Such a leading 'superflamelet' may be described in terms of a chemical time scale, which is higher than τ_c but substantially lower than τ_{ex}. Since no reliable model is currently available, τ_c can be used as the higher estimate. Based on the above reasoning, the following chemical time scale

$$\frac{\tau_{lp}}{\tau_c}=\frac{S_c(t\to\infty)}{\max\{S_c(t)\}_{r_i=r_{cr}}} \tag{45}$$

has been proposed to be used for modeling premixed turbulent combustion [137,139,140]. When $Le<1$, $\tau_{lp}=\tau_{ex}<\tau_c$, but $\tau_{lp}=\tau_c<\tau_{ex}$ if $Le>1$.

We may also note that Eq. (45) appears to provide a reasonable approximation even if another physical mechanism of leading point formation (convection of a flamelet by a strong eddy) is emphasized. Indeed, if $Le>1$, negatively curved flamelets cannot be a leading point, whereas positively curved ones do not reach the leading edge of the mean flame brush, because they are more effectively quenched by strong turbulent eddies.

The use of the 'leading point' time scale offers the opportunity to approximate the whole Karpov data base, as discussed in detail elsewhere [18,140]. Fig. 18 shows that the data base is reasonably well approximated by a function of either the Damköhler, Da, or Karlovitz, $Ka=Re_t^{1/2}/Da$,

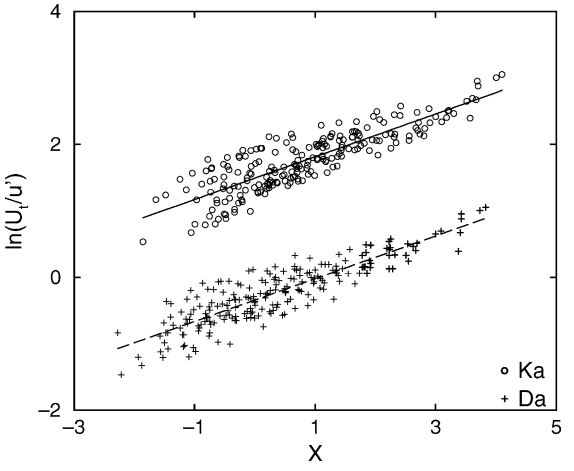

Fig. 18. Processing the experimental data base of Karpov and Severin [110,115,142–144]. After Ref. [139]. Crosses and circles correspond to $X=\ln Da-3$ and $X=-\ln Ka$, respectively. The Karlovitz and Damköhler numbers have been calculated by replacing $\tau_c=\delta_L/S_{L,0}$ with τ_{lp} determined using Eq. (45). Circles are shifted along the ordinate axis and correspond to $\ln(\mathcal{U}_t/u')+2$. Straight lines show the least square fits.

[23] Although the flame ball solution [226,496] yields zero displacement speed at any Le; the numerical simulations [135, 500] and measurements [412,500] indicate a high S_d in highly curved spherical flames with $Le<1$ due to transient processes, such as the instability of the adiabatic flame ball.

numbers if they are calculated by replacing $\tau_c = \delta_L/S_{L,0}$ with τ_{lp} determined using Eq. (45). The latter approximation

$$\mathcal{U}_t \propto u' Ka^{-0.32} \tag{46}$$

yields the least scatter of the experimental data. Similar results but with a slightly larger scatter were obtained when using τ_{cr} or τ_{ex} [117,136,139]. Attempts to correlate this data base by using the standard chemical time scale τ_c resulted in widely scattered graphs which did not exhibit any consistent trend.

The scatter of the experimental data is substantial in Fig. 18 due to a number of causes: (1) τ_{lp} is assumed to be equal to τ_c if $Le > 1$; (2) combustion chemistry is strongly simplified (a single-step chemistry with the activation temperature being independent of the equivalence ratio [139,140,500]); (3) local flamelet quenching by turbulent eddies is neglected; (4) the correlation is not valid for mixtures with a high $S_{L,0}$ (e.g. rich hydrogen–air ones), because it leads, to $U_t \to 0$ when $u' \to 0$; (5) the raw experimental data are scattered; (6) the values of $\mathcal{U}_t$ and $S_{L,0}$, reported by Karpov and Severin [110,115,142–145], have been obtained without any consideration of the transient behavior of $\mathcal{U}_t$ (see [18,452]) and the curvature-dependence of S_L, etc. Nevertheless, Figs. 4 and 18 seem to be quite sufficient in highlighting the crucial role played by strongly curved flamelets in premixed turbulent flame propagation, especially as the transient behavior of $\mathcal{U}_t$ and the overestimated (due to the aforementioned curvature-dependence) values of $S_{L,0}$ for $Le < 1$ only mask this role, as discussed elsewhere [138].

It is worth noting that an expression similar to Eq. (46) has been obtained by Bradley at al. [176] for $Le \approx 1$ and a similar approximation is highlighted in our recent review of the experimental data associated with $D_F \approx D_O \approx \kappa$ [18]. The universal applicability of Eq. (46) has been achieved by using the chemical time scale τ_{lp}, which is smaller by $40 \div 50$ times than τ_c in lean $H_2/O_2/N_2$ mixtures. Since no tuning parameters have been invoked to simulate this very strong effect [139,140,500], the correlations obtained are unlikely to be fortuitous. Even bearing in mind the scatter of the experimental data in Fig. 18, such results should not be underestimated, especially as alternative models discussed in the previous sections do not seem to be able to yield a strong effect of D_d on $\mathcal{U}_t$.

The chemical time scales introduced above for characterizing critically curved flamelets can be straightforwardly used in numerical simulations of premixed turbulent combustion.[24] For instance, they were incorporated into the extended Zimont model (see Appendix A.3) by replacing the standard chemical time scale τ_c with either τ_{ex} [136] or τ_{lp} [137] in Eq. (A.12). The combined models were used [136,137] to simulate the experiments of Karpov and Severin [110,115,142–145]. It is worth emphasizing that no adjustable parameters were invoked to calculate τ_{ex} or τ_{lp} [117,137,139,500]. So, the combined models included a single constant A which affected the burning velocity computed at moderate turbulence (the value of ε_q in Eq. (36) was also adjusted, but this parameter affected the computed results at strong turbulence only—cf. solid[25] and dashed curves in Fig. 19). Almost all the experimental data used in these numerical tests were quantitatively predicted for $u' < u'_m$ by using τ_{lp} and the same value of $A = 0.5$ [137] (see dashed curves in Fig. 19). However, in a few mixtures, it was necessary to tune A to obtain a quantitative agreement between the computed and measured turbulent burning velocities (see dotted curve in Fig. 19d). Fig. 20 shows the best fitted values of A, associated with either τ_c (a) or τ_{lp} (b) [139]. When employing τ_c, A increases strongly with decreasing Le. In contrast, the adjusted values of A are slightly scattered around 0.5 if τ_{lp} is invoked.

In summary, the leading point concept, associated with critically curved flamelets and supplemented with the above submodel of τ_{lp}, allows us not only to explain the strong effect of D_d on $\mathcal{U}_t$ at moderate turbulence but also to quantitatively predict it.

Recent findings by Joulin et al. [492] support the hypothesis as regards the important role played by flame balls in premixed turbulent combustion. The behavior of a laminar flame ball ($Le < 1$) under the influence of fluctuating velocity gradients with a zero mean value has been theoretically and numerically investigated. The stabilization effect of the gradient on the ball has been shown under certain conditions. Based on this finding, Joulin et al. [492] have suggested that: (1) if a turbulent eddy is strong enough to quench a near-planar flamelet, the flame ball can survive, 'while throbbing during its Lagrangian travel and then, later and somewhere else, trigger a self-propagating flame once in a more favorable environment', and (2) such a physical mechanism of 'spotty' turbulent combustion may control a new regime, intermediate between the flamelet and well-stirred reactor ones. We may note that similar arguments are locally applicable as regards the convection of a flamelet by a strong eddy to the leading edge of a turbulent flame brush under the conditions of the flamelet regime.

To the best of our knowledge, direct experimental evidence of the dominating role played by strongly curved flame balls at the leading edge has not yet been reported, probably due to their small size.

6.2.3. Other approaches

The key peculiarity of the concept of leading points consists in the hypothesis that certain universal local structures are formed during interaction between laminar

[24] Note that τ_{cr} can be simply calculated using the analytical Eq. (43), whereas numerical simulations of strongly curved, expanding laminar flames are required to evaluate the time scales τ_{ex} and τ_{lp}.

[25] In certain cases, solid curves are very close to dashed ones and are not shown.

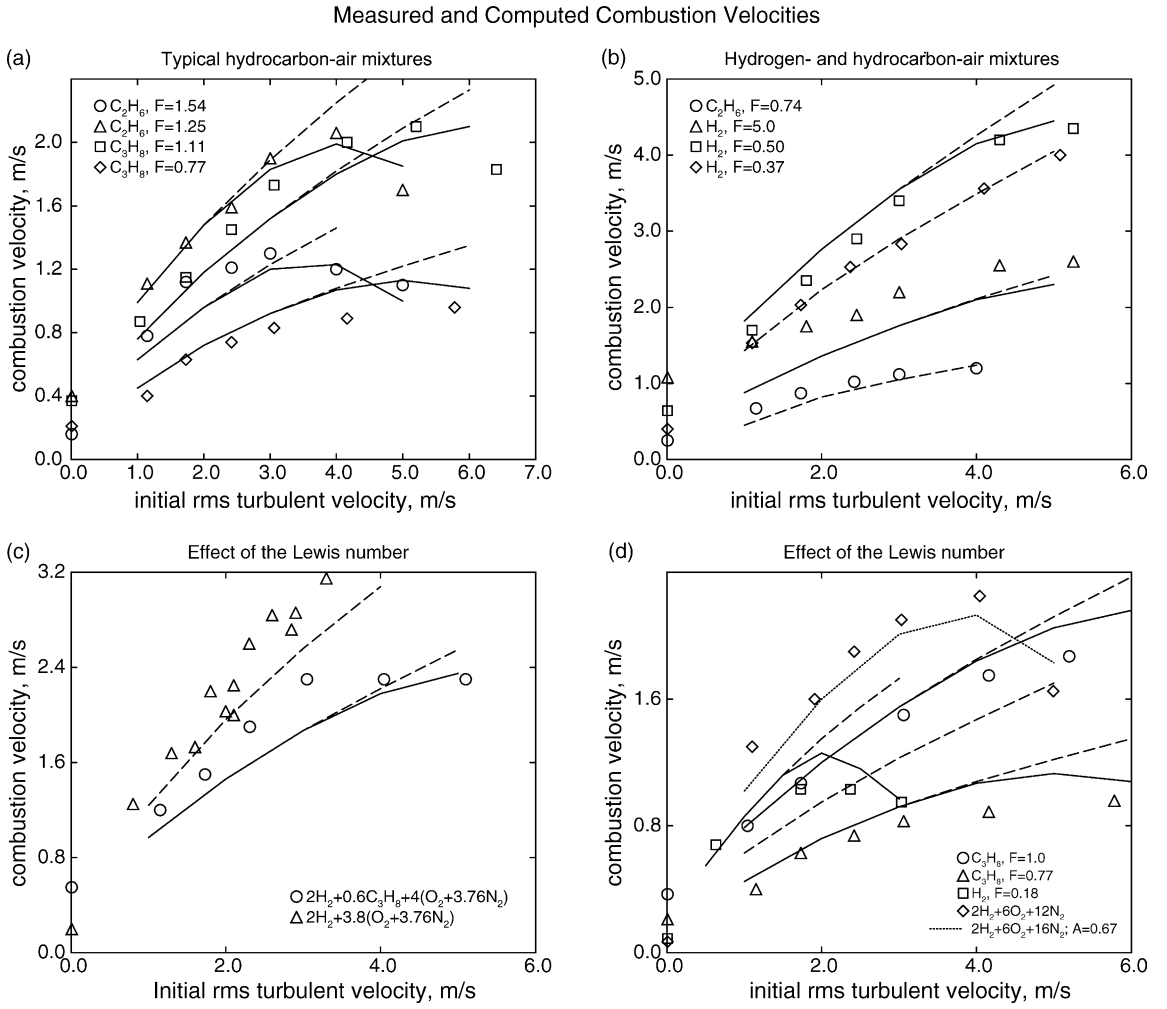

Fig. 19. Turbulent burning velocities measured by Karpov and Severin [110] (symbols) and computed by Karpov et al. [137] using the extended Zimont model (see Appendix A.3) with $I_0=1$ (dashed curves) and I_0 determined using Eq. (36) (solid and dotted curves). All the curves have been computed using the same value of a single model constant $A=0.5$ with the exception of dotted curve in (d), which has been calculated using $A=0.67$.

flame and turbulence, the local burning rate in such structures being controlled by molecular transport, chemistry and instant flow field in the vicinity of the structures. The flow field is assumed to be universal. Therefore, the burning rate is weakly affected by the statistical characteristics of turbulence, because the flow field associated with the aforementioned structures can be produced not only by highly but also by weakly turbulent flows, with the probability of such local events depending on u'. For these reasons, turbulent flame speed may be evaluated by invoking the u_c simulated for the considered laminar structures and independent of u', as discussed in the two previous sections.

In fact, the same strategy is followed by certain other phenomenological models. For instance, the use of Eq. (34) by Brutscher et al. [159] (see Section 5.3.2) implies that turbulent burning velocity is controlled by certain perturbed laminar structures, the characteristics of which are independent of u'. Therefore, the tests discussed in the quoted paper support the concept of leading points, rather than the concept of the Markstein number.

A conceptually similar phenomenological approach has been developed by Nakahara and Kido [148] who invoked $S_{L,0}(F_r \neq F_u)$ to approximate the experimental data on $\mathcal{U}_t(u')$ obtained for a mixture with F_u and $D_F \neq D_O$. Variations in the equivalence ratio, $\Delta F = F_r - F_u$, were considered to be independent of u'. These variations were evaluated by selecting pairs of mixtures such that both mixtures contain the same fuel and exhibit nearly the same $\mathcal{U}_t(u')$ at moderate turbulence, whereas the nitrogen mass fraction, F_u and $S_{L,0}$ were different for the two mixtures. Then, the curves of $S_{L,0}(F_u)$ were measured for both Y_{N_2} and the value

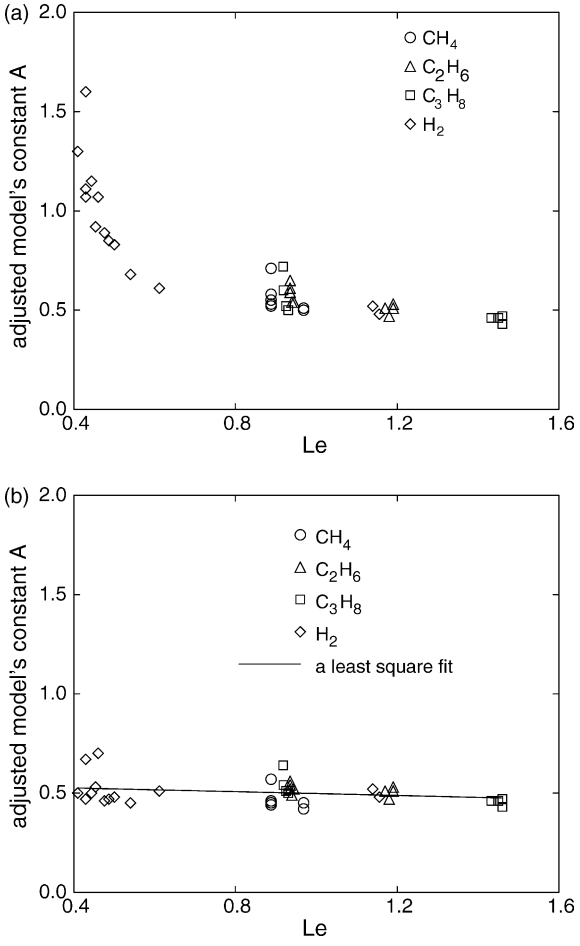

Fig. 20. Adjusted values of the constant A in the extended Zimont model (see Appendix A.3) for two different chemical time scales: (a) $\tau_c = \kappa_u/S_{L,0}^2$ and (b) τ_{lp} determined using Eq. (45). After Ref. [139].

of ΔF was calculated from the condition of $S_{L,0}(F_{u,1} + \Delta F, Y_{N_2,1}) = S_{L,0}(F_{u,2} + \Delta F, Y_{N_2,2})$. The use of such empirically determined values of $S_{L,0}(F_u + \Delta F)$ instead of $S_{L,0}(F_u)$ allowed Kido et al. [146–148,152] to approximate an extensive data base on $\mathcal{U}_t(u')$, obtained for a number of mixtures with substantially different D_d/D_e.

Recently, Chen and Bilger [362] have parameterized the data on the maximum value of the conditional-mean dissipation rate for the temperature-based progress variable, measured in methane–, propane–, and lean hydrogen–air turbulent flames stabilized in a Bunsen-type burner. The data reported as a function of *KaLe* collapse to a universal curve if the dissipation rate is normalized with the quantity computed for a stretched laminar 'flame giving the largest heat release parameter for lean hydrogen/air combustion' [362]. This idea is basically similar to the discussed consequence of the concept of leading points.

Eq. (42) implies that highly curved flame fronts may be locally formed in turbulent flows if $Le < 1$. Experiments [172,344–346,360] also show that the curvature of flame surface is statistically larger for mixtures associated with $D_d > D_e$ or $Le < 1$, as compared with $D_d < D_e$ or $Le > 1$. Such an effect may be modeled within the framework of the fractal approach (see Section 4.2 and Eq. (25)) by assuming that the inner cut-off scale is decreased by Le. Consequently, flamelet surface area and turbulent flame speed should increase as Le decreases. However, such a decrease in e_i does not seem to be strong enough to explain the dependence of $\mathcal{U}_t$ on D_d.

Indeed, let us look at the $\mathcal{U}_t(u')$-curves shown for mixtures 4 and 5 in Fig. 4a. An analysis of these data (see the last paragraph in Section 4.3) has shown that if; (1) unperturbed laminar flame speed is used, and (2) the inner cut-off scale is associated with δ_L, then, the fractal approach cannot predict a ratio of $\mathcal{U}_t/S_{L,0}$ larger than 3, whereas the measured data indicate the 30-time increase in burnin velocity caused by turbulence in mixtures 4 and 5. Consequently, even if the fractal dimension of $\mathcal{D} = 7/3$ is invoked, the ratio of e_i/δ_L must be as small as 0.001 in order to approximate the experimental data for very lean hydrogen mixtures. Since there is no reason to assume such a drastic dependence of e_i/δ_L on D_d, the effect due to the discussed mechanism is not strong enough to explain the experimental data shown in Fig. 4a.

7. Certain basic issues

7.1. Effects of molecular transport on highly turbulent combustion

The effect of the molecular diffusivity of the deficient reactant, D_d, on the behavior of turbulent burning velocity, $\mathcal{U}_t$, at strong turbulence (in the range of $u' > u'_m$ where $\mathcal{U}_t$ is not increased by u') and on the magnitude of u'_m (the rms turbulent velocities associated with the maxima of the $\mathcal{U}_t(u')$-curves) and u'_q (the rms turbulent velocities associated with global flame quenching), shown in Figs. 2a and c and 4a, implies that thin intrinsically laminar zones play an important role in the propagation and quenching of highly turbulent flames. This assumption is also supported by the considerable influence of D_F/D_O and Le on the blow-off limit of flames stabilized by obstacles in high speed turbulent flows [30].

The long-known existence of such effects implies that the front regime of premixed turbulent combustion should be extended to strong turbulence. The regime is identified in classical premixed turbulent combustion diagrams [3–13] with different names, e.g. wrinkled flame [4,9], or reaction sheet [5–7,13], or flamelet [10] regime. The regime is commonly characterized as follows.

The chemical reactions that control heat release are confined to thin, wrinkled, convoluted, and strained reacting fronts that separate unburned reactants from burned products. Such fronts, commonly called flamelets, are

often assumed to have the same local structure as perturbed laminar flames. In the following, we will use the term 'flamelet' exactly in this sense, i.e. we will use this term to identify local burning structures that can be reduced to a perturbed laminar flame. Subsequently, we will use the term 'flamelet regime' to designate a subregime associated with the dominance of flamelets, rather than of other intrinsically laminar reacting structures. The term 'front regime' will be used to summarize all possible subregimes of turbulent flame propagation associated with the important role played by various intrinsically laminar reacting structures, both flamelet and non-flamelet ones (e.g. the thin reaction zone regime introduced by Peters [15,16] is the front regime, but not the flamelet regime; because the structure of the preheat zone can be substantially affected by small-scale turbulent eddies, as documented recently [87]). Note that the dependence of U_t on D_d highlights the front regime, but not necessarily the flamelet one.

Two different physical mechanisms are commonly associated with the strong turbulence limit of the flamelet regime [3–13]. First, laminar flames are well known to be affected by the stretch rates produced by flow non-uniformities, as discussed in Sections 5.1 and 6.1.1. Stretching can quench the flame, with the extinction stretch rate being proportional to τ_c^{-1} for perturbed laminar flames [6,226]. Since the mean strain rate produced by turbulent eddies is on the order of λ/u' [30], local flamelet quenching is assumed to be of importance if the Karlovitz number $Ka' = \tau_c u'/\lambda$ is equal to unity, i.e. the well-known Klimov–Williams criterion.

Second, the smallest eddies can penetrate into flamelets, broaden them, and intensify the heat and mass transfer inside the flamelets [15,36,501]. Such a penetration was considered to be possible only if the flamelet thickness scaled as $\delta_L = \kappa_u/S_{L,0}$ was larger than the scale of the smallest eddies, i.e. the Kolmogorov length scale, $\eta' = LRe_t^{-3/4}$ [8,9]. A comparison of the two scales led to the same Klimov–Williams criterion.[26]

Recent experimental investigations conducted with advanced optical diagnostic methods [20,96,362,502,503] have shown that thin reacting fronts survive even in strong turbulence associated with the Karlovitz numbers markedly larger than unity.

Observations of the existence of the fronts in highly turbulent flames may be associated with the two physical mechanisms discussed in Section 6.1. First, since the smallest eddies rapidly dissipate due to increasing viscosity in flamelets, the eddies, which provide the highest local stretch rates in turbulent inert flows, are non-effective in local combustion quenching [12,14,33,58,484]. Second, since a laminar flame needs finite time to respond to variations in local stretch rates, it can survive under the influence of instantly strong but time-dependent stretching [140,184,396,435,436,441,476].

Other experiments have shown that non-flamelet fronts exist inside a highly turbulent flame brush. Local deviations from a perturbed laminar flamelet structure have been well documented in measurements [17,86,87,89,90,104,502–505] and DNS [60]. The observed deviations may be classified as: (1) local quenching (high temperature but low Y_{OH}) [17,502,503]; (2) a modified preheat zone [17,20,60, 86,87,89,90,104,503–505] but sharp reaction zone as indicated in OH [17,20,86,503] or CH images [504] or in computed local heat release rate fields [60]; (3) the failure of the correlations between temperature and reactant concentration, associated with laminar flames [60,104]. Many DNS performed for large Karlovitz numbers have also indicated the frontal structure of instant heat release rate and concentration fields [200,209,211,368,370,371].

The above observations of thick preheat but thin reaction zones are qualitatively explained with the following simple model. Within the framework of the thermal theory of a planar, 1-D, single-step chemistry, laminar flame [226], the chemical reaction that controls heat release occurs in an asymptotically ($\beta \to \infty$) thin reaction zone. Even if small eddies can; (1) penetrate into the preheat zone of the flame, the thickness of which, Δ_L, is on the order of $\gamma\delta_L$ and much larger than the thickness, δ_r, of the reaction zone; (2) survive inside it; (3) strongly perturb heat and mass transfer processes; the much thinner reaction zone may preserve the intrinsically laminar structure.

Within the framework of such an asymptotic ($\beta \to \infty$) model,[27] the penetration of small turbulent eddies into the reaction zone, rather than into the preheat zone, limits the front regime of premixed turbulent combustion and, in particular, the thin reaction zone subregime as highlighted by Peters [15,16]. Moreover, according to the thermal theory, an intensification of heat and mass transfer in the reaction zone is required to markedly change the burning rate, whereas variations in the diffusivity in the preheat zone are of secondary importance. Consequently, the differentiation between the classical flamelet and the thin reaction zone regimes appears to be of minor importance as far as turbulent flame speed is concerned. In both subregimes, the effects of turbulence on burning velocity consist of (1) an increase in the front (flamelet or reaction zone) surface area by turbulent eddies, and (2) modification of the intrinsic structure of the front by small-scale turbulent stretching. The main difference between the two subregimes consists of the different structures of the fronts, either perturbed flamelet or reaction zone. Since a substantial effect of this difference on turbulent flame speed has not yet been shown, we will not discuss

[26] Since the preheat zone thickness, Δ_L, scales as $\gamma\delta_L$ [226], the boundary of the flamelet regime should be moved to substantially weaker turbulence [17,18].

[27] In many realistic, complex chemistry flames characterized by moderate β, the difference between δ_r and Δ_L is not well pronounced [5,506].

further the fine structure of the fronts. The interested reader is referred to: (1) a recent paper by Chen and Bilger [17], in which several subregimes of the front regime are identified and discussed in detail, and (2) a recent review by Dinkelacker [20], in which the interaction between local flame fronts is considered to be an important process for identifying regimes of highly turbulent combustion.

The dependence of highly turbulent flame speed on D_d, well-documented in measurements, implies that intrinsically laminar zones play a key role in flame propagation even in intense turbulence. Recent experimental and DNS data, briefly reviewed above, confirm the existence of such fronts in highly turbulent flames. Note that these data have been obtained over the past decade, whereas the dependence of $U_t(u' > u'_m)$ on Le has been known at least since 1961 (see Fig. 2 in Ref. [108]).

From our standpoint, the experimental data shown in Figs. 2–5 not only highlight the important role played by intrinsically laminar zones in turbulent flame propagation but are also valuable in discussing the specific structure of the zones that control the propagation.

7.2. Effects of molecular transport on flame speed?

In a fully developed flame, the speed S_{le} (relating to the leading edge only) and burning velocity (that characterizes the mass consumption averaged over the entire flame brush) should be equal. However, most models discussed above do not predict any substantial dependence of S_{le} on D_d in moderately intense turbulent flows. The models based on the effects due to the Markstein number (Section 5), flamelet quenching (Section 6.1), or small-scale wrinkling (the end of Section 6.2.3) provide no clue to predicting the leading-edge speed. The flamelet-instability model can be used to predict an increase in S_{le} due to the local acceleration of unstable laminar flamelets. However, the increase appears to be on the order of $S_{L,0}$ because even unstable flamelets retain a laminar structure, whereas a strong effect of D_d on $\mathcal{U}_t$ is observed in the case of $S_{le} > \mathcal{U}_t > 30S_L$ (mixtures 4 and 5 in Fig. 4a).

Even though the effect of D_d on S_{le} can readily be explained by invoking the concept of leading point, this fact should not be overestimated by highlighting this concept as compared with alternative approaches. The point is that most practical turbulent flames cannot be treated as fully developed since they are characterized by a growing brush thickness (see Section 3.2). In this case, S_{le} must be higher than $\mathcal{U}_t$. We still do not know whether or not S_{le} and $\mathcal{U}_t$ correlate, or whether or not S_{le} depends on D_d. The assumption of the independence of S_{le} on D_d means that $\mathcal{U}_t$ and S_{le} do not correlate. In other words, the difference between them is so large that even the high burning velocities measured in lean hydrogen flames are still much lower than S_{le}. Such a hypothesis is based on the well-documented observation that mean flame brush thickness grows in accordance with the turbulent diffusion law, thus being weakly affected by mixture properties (see Fig. 7); i.e. the difference $S_{le} - \mathcal{U}_t \propto d\delta_{le}/dt$ is mainly controlled by turbulence and is virtually independent of D_d. Here, the thickness $\delta_{le} > \delta_t$ characterizes the distance between the leading edge and the middle of flame brush. Since $\mathcal{U}_t$ is on the order of u' or lower at $u' > 1$ m/s in Figs. 2–4, the hypothesis discussed here can be valid if $d\delta_{le}/dt \sim Cu'$, where C is a constant greater than unity. This estimate agrees with the turbulent diffusion theory [217], which predicts that the speed of the propagation of the leading edge of an admixture cloud is proportional to but larger than u'.

Fig. 5 and other experimental data [109,111,208] show that the flame speed measured using the Schlieren technique depends on D_d. Strictly speaking, this fact does not resolve the discussed issue, because although the $\tilde{c}$-distance between the leading edge and the iso-temperature surface recorded using the Schlieren technique appears to be small, the spatial distance between the two surfaces may be substantial and their speeds may be markedly different.

The hypothesis that S_{le} is not affected by D_d in moderately intense turbulent flows is consistent with most of the models discussed above, with the exception of the leading-point model, for which the dependence of S_{le} on D_d appears to be essential, on the face of it. However, any possible independence of S_{le} on D_d does not invalidate the concept of leading point, as the following physical scenario can be outlined. Although the throws of burning kernels into unburned mixture are controlled by turbulence and the speed of such a front scales as u', the leading kernels trigger combustion and control the flame surface area at the leading edge. Consequently, the flame surface area depends on the characteristics of the leading kernels and on τ_{lp} (see Eq. (45)) in particular. The production of the flamelet surface at the leading edge can affect Σ inside the flame brush and, hence, $\mathcal{U}_t$, provided that the unsteady, convection, and transport terms in the corresponding balance equation (see Eqs. (A.6) and (A.7)) are of substantial importance.

Although the budget for this equation is not well established, yet, the experimental data reported by Veynante

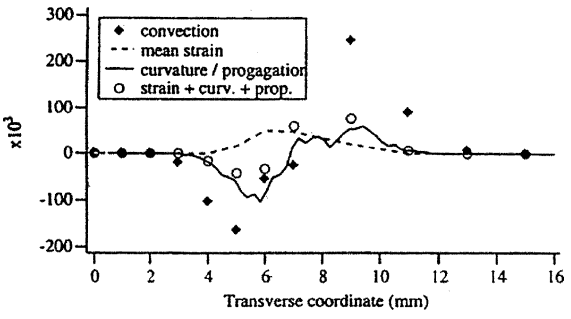

Fig. 21. Comparison of the transverse profiles of mean convection, strain rate due to the mean flow (Q_1 in Eq. (A.7)), and curvature/propagation (III+IV in Eq. (A.6)) terms in flame surface density balance equation. From the paper by Veynante et al. [447] © The Combustion Institute, reproduced with permission. The experimental data have been obtained from a lean ($F=0.9$) propane–air V-shaped flame.

et al. [447] (see Fig. 21) indicate that the convection term is substantially larger than (1) the production of Σ due to flamelet straining by the mean flow (a part of term II in Eq. (A.6) or Q_1 in Eq. (A.7)); (2) the curvature/propagation term (III+IV in Eq. (A.6)), as well as (3) the sum of the three (Q_1 in Eq. (A.7), plus III, plus IV) terms. Consequently, the data support the above scenario.

DNS data [211] (see Fig. 15b) also show that the sum of the strain (II) and the curvature/propagation (III) terms in Eq. (A.6) (this sum normalized with Σ is called the flame stretch in the quoted paper) does not equal zero but is on the same order of each term evaluated separately (see also Figs. 13 and 14 in the quoted paper). This result implies that the unsteady, convection, and transport terms are of substantial importance for the budget. It is also worth noting that the behavior of the discussed sum is strongly affected by *Le* at the leading edge (see Fig. 15b).

Three-dimensional constant-density DNS of premixed flame propagation in a narrow channel [507] also show that the unsteady term is of substantial importance (see Figs. 4–10 in the quoted paper).

7.3. Vortex tubes?

7.3.1. Laminar flame propagation along a vortex

The problem of laminar flame propagation along the axis of a vortex is discussed, in detail, in a recent review by Ishizuka [508]. Here, we will restrict ourselves to a brief summary of the key points relevant to the effects of D_d on U_t.

McCormack et al. [509] have experimentally found that the speed of flame propagation round a laminar vortex ring is linearly proportional to the vortex strength and is much higher than the laminar flame speed. The strong difference between these two speeds has been documented in a number of recent measurements [510–516]. A similar effect has been obtained in experimental [517,518] and numerical [519–525] investigations of laminar flame propagation along the axis of a straight vortex.

The first explanation of this phenomenon was given by Chomiak [34,526] who pointed out that the axial propagation of a flame in a vortex tube is strongly accelerated by the pressure difference between hot products and cold unburned mixture, which results from the reduction of swirling motion due to the volume expansion of the products (so-called bursting). The following expression for the speed of flame propagation along the vortex axis.

$$V_f = \gamma^{1/2}\mathcal{W}, \tag{47}$$

has been suggested, where $\mathcal{W}$ is the maximum tangential velocity in the vortex. Over the past decade, this phenomenon has been analyzed by different authors [508, 510,512–514,519–521,523,524,527–530], however, a theory that predicts all the effects observed in the measurements has not yet been elaborated. For this reason,

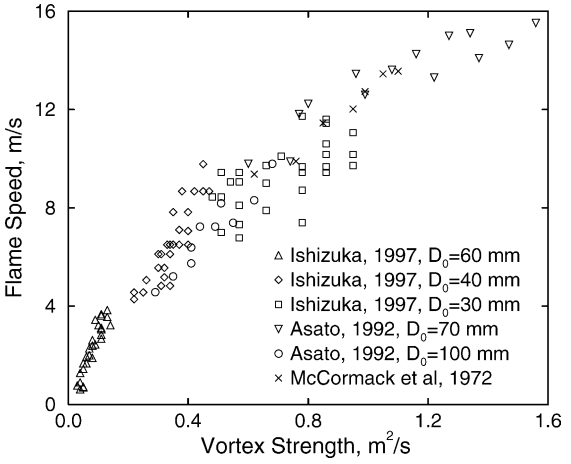

Fig. 22. Speed of flame propagation round vortex rings vs. vortex strength. D_0 is the diameter of the nozzle. The vortex core diameter is proportional to D_0.

we will not discuss the models quoted above, but refer the interested reader to the recent review [508].

The aforementioned experimental and numerical investigations show the following trends, important to the subject of this paper.

First, the flame speed V_f is much higher than $S_{L,0}$ and is almost linearly increased by the vortex strength, $\Gamma = \mathcal{W}d_c$, or by the maximum tangential velocity, $\mathcal{W}$, in the vortex at moderate magnitudes of $\mathcal{W}$ (see Fig. 22). Here, d_c is the vortex core diameter. The bending and leveling-off of the $V_f(\mathcal{W})$-curves have been also documented at higher $\mathcal{W}$ [510, 512,516], followed by flame quenching [512,516], (see filled symbols in Fig. 23a).

Second, an increase in V_f by γ has been obtained in recent numerical simulations [521]. However, the experimental data reported by Ishizuka et al. [514–516] show that the dependence of V_f on $\mathcal{W}$ is well approximated by a straight line, $V_f \propto \mathcal{W}$, at moderate tangential velocities (see Fig. 23). The slope of the straight line appears to be independent of mixture composition, i.e. on $S_{L,0}$ and γ, whereas the values, $\mathcal{W}_m$ and $\mathcal{W}_q$, of the tangential velocity, associated with the bending and quenching, respectively, depends substantially on *F*.

Third, the propagation of flames along vortices or in other rotating flows depends substantially on D_d/D_e and *Le*. For example, the expansion in the rich limit of flame propagation caused by rotation has been documented in propane–air ($D_d > D_e$, $Le < 1$) flames [511,531,532], whereas no substantial effect of rotation on the rich limit has been found in methane–air flames ($D_F \approx D_O \approx \kappa$).

The Schlieren images of flames in vortex rings [512,514, 516] show that the diameter, d_f, of a flame (1) is less than the vortex diameter; (2) decreases when $\mathcal{W}$ increases (see Fig. 23); (3) depends on mixture composition. The diameters of rich ($D_d > D_e$, $Le < 1$) propane–air ($D_F < D_O$)

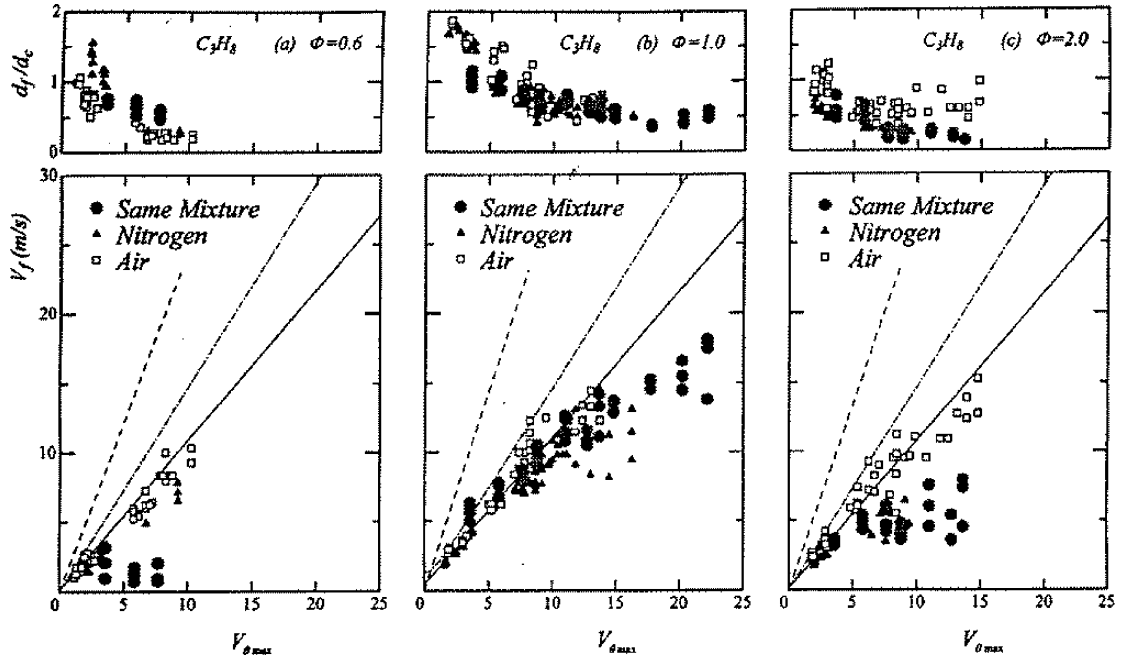

Fig. 23. Speed of flame propagation round a vortex ring vs. the maximum tangential velocity after Ishizuka et al. [516]. Lean, $F=0.6$ (a), stoichiometric (b), and rich, $F=2.0$ (c), propane–air flames in the atmosphere of air, or nitrogen, or the same mixture. Symbols show experimental data, curves correspond to various theories not discussed in the present review. From the paper by Ishizuka et al. [516] © The Combustion Institute, reproduced with permission.

flames are substantially smaller than lean ones ($D_d<D_e$, $Le>1$) and the tips of the former flames are very acute (see Fig. 44 in Ref. [508]). The opposite trend has been observed in methane–air ($D_F>D_O$) flames but the effect is less pronounced. Similar results have been documented in laminar flames in other rotating flows [531,532].

Note that most theories of laminar flame propagation along the axis of a vortex predict that flame speed will be increased by the flame diameter if $d_f<d_c$ (see Section 6.2.3 in Ref. [508]). Consequently, the effect of D_d on d_f, discussed above, should yield an increase in V_f by Le or D_e/D_d, a trend opposite to the dependence of $U_t(D_e/D_d, Le)$. Decisive experimental evidence of the increase has not yet been found, to the best of the authors' knowledge.

The effect of D_d on V_f can be pronounced in other rotating flows. For instance, Sakai and Ishizuka [532] have investigated the propagation of laminar flames in a rotating tube. Results (see Fig. 24) show that the slope the $V_f(\mathcal{W})$-curves measured for a rich ($F=2.0$) propane–air mixture is much higher than the $dV_f/d\mathcal{W}$ of a lean mixture ($F=0.65$), although $S_{L,0}$ is lower by more than three times in the former mixture and the density ratios are almost equal in both mixtures. Moreover, the discussed slope is even higher in the rich mixture than the $dV_f/d\mathcal{W}$ of the stoichiometric mixture although $S_{L,0}$ is much higher in the latter mixture.

Recent numerical simulations [525] of the propagation of a lean ($F=0.5$) hydrogen–air flame along the axis of a decaying Burgers vortex have shown that the displacement speed of the tip of the flame is much higher than $S_{L,0}$ and is

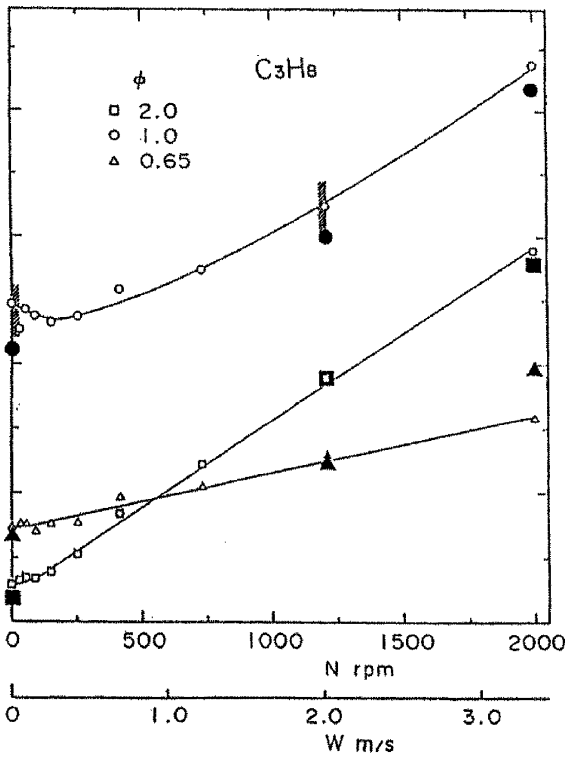

Fig. 24. Flame velocities in a rotating tube vs. rotational speed. From the paper by Sakai and Ishizuka [532] © The Combustion Institute reproduced with permission.

increased by rotation velocity. These observations are associated with the PDT effects (see Fig. 5 in the quoted paper), which are particularly strong in lean hydrogen–air mixtures. For instance, a local temperature as high as 2100 K has been computed at the tip of the flame at $\mathcal{W} = 10$ m/s, whereas the adiabatic combustion temperature is equal to 1652 K for this mixture [525]. Such temperature variations[28] can strongly increase the local burning rate.

Finally, Fig. 23 indicates that rich propane–air flames are more resistant to quenching than lean ones, $\mathcal{W}_q(F = 2.0) \approx 2\mathcal{W}_q(F = 0.6)$, whereas the laminar flame speed is higher in the lean mixture. As a result, although flame speeds measured at $\mathcal{W} < 3$ m/s are roughly the same in both mixtures, the maximum flame speed $V_{f,m} = V_f(\mathcal{W}_q)$ is much higher in the rich one. This behavior associated with an increase (decrease) in the curved flame temperature if $Le < 1$ ($Le > 1$) is similar to the behavior of premixed laminar edge flames characterized by a sufficiently low Lewis number, which can survive under the influence of high stretch rates [249,390–392,470].

In summary, when Le decreases and D_d/D_e increases, the diameter of a laminar flame that propagates along the axis of a vortex decreases, the curvature of the flame tip increases, the flame becomes more resistant to quenching, and higher values of $\mathcal{W}$ and $V_{f,m}$ can be reached. For a constant maximum tangential velocity, the effect of D_d on V_f is not established in vortex rings, but V_f is substantially increased by D_d/D_e for flames that propagate in a rotating tube (Fig. 24).

7.3.2. Vortex tubes in turbulent flows

A laminar flame in a vortex is an example of a strongly curved reacting zone which (1) has an intrinsically laminar structure; (2) propagates at a speed much higher than $S_{L,0}$; (3) is substantially affected by D_d. Such a structure appears to be the best candidate for explaining the strong dependence of $\mathcal{U}_t$ on D_d, based on the concept of leading point. Do such structures exist in turbulent flows?

Tennekes [533] has developed a simple model of small-scale turbulence structure by considering vortex tubes which have a diameter of the Kolmogorov scale, η, a circumferential velocity on the order of, u', and are stretched by eddies on the scale of the Taylor length scale, λ. The model correctly represents the mean dissipation rate and the ratio of η/λ in isotropic turbulence. Recent studies have supported this model in part.

DNS [534–546] of various, constant density, turbulent flows have shown that strong vorticity tends to be organized in elongated, coherent structures (so-called 'vortex filaments,' or 'worms').[29] Moreover, based on local cavitation effects due to the pressure drop in the vortex core, these filaments have been visualized in several experimental studies [547–550].

Cylindrical-, sheet- and ribbon-like structures have been documented in DNS. She et al. [538] have pointed out that the cylindrical structures (vortex tubes) are associated with very high vorticity amplitudes, whereas sheet- and ribbon-like structures dominate in moderate-amplitude vorticity regions. Ruetsch and Maxey [537] have documented tube-like regions of intense vorticity surrounded by moderate-valued energy dissipation regions and have found that the most intense regions of a scalar gradient occur as large flat sheets. Tanaka and Kida [542] have concluded that vortex tubes and sheets correspond to high vorticity with a relatively low and with comparable strain rate, respectively. Jimenez et al. [544] have reported that the vortex tubes appear to dominate at high Reynolds numbers, while sheet- and ribbon-like structures are predominant at lower Re_t.

There is a substantial probability of finding compressive strains along the filaments [544–546]. No substantial differences between the statistics of stretching along the filament axis and in the bulk of the flow have been found in the quoted papers, i.e. the filaments are not statistically correlated with high stretching. As a result, the filaments contribute a little to the total dissipation rate ε, which is a quantity originating at large scales. The minor contribution of the filaments to ε has been experimentally confirmed by Cadot et al. [551] who added polymers to a flow to destroy the filaments, but observed no effects of the polymers on the dissipation rate.

Although the individual sections of the filaments are locally characterized by various radial and axial distributions of vorticity, the radial distribution of the azimuthally averaged vorticity in the filaments can be well approximated with the Gaussian function [544–546]. In sections associated with positive local axial strain rates, $a_t > 0$, the obtained local radius of the radial vorticity distribution scales as $(\nu/a_t)^{1/2}$ which corresponds to the equilibrium Burgers' vortex. The mean diameter $\overline{d}_f$ of the filaments scales as the Kolmogorov length scale [536,544–546] and is on the order of 10 η [59].

The maximum tangential velocity in the filament cross-section scales as u' [59,544–546,549]. Velocity fluctuations of the magnitude of u' and of a length on the order of η have been experimentally documented [552,553].

The length of vortex tubes on the order of λ has been evaluated from DNS data [536]. Long filaments on the order of the integral length scale L of turbulence have been experimentally visualized [549,550]. Jimenez et al. [544–546] have used different quantities in order to characterize the filament length. The length of the spatial domain characterized by the local vorticity higher than the background level scales as L. The axial correlation lengths for the filament radius and for the vorticity scale as λ, whereas the axial correlation length for the axial stretching scales as η.

[28] Recently, Mosbacher et al. [418] have measured the considerable increase in the local temperature (by 420 K as compared with the adiabatic combustion temperature equal to 875 K) in highly curved, very lean ($F = 0.175$) hydrogen–air tubular flames.

[29] Turbulence external to such structures is commonly called background turbulence.

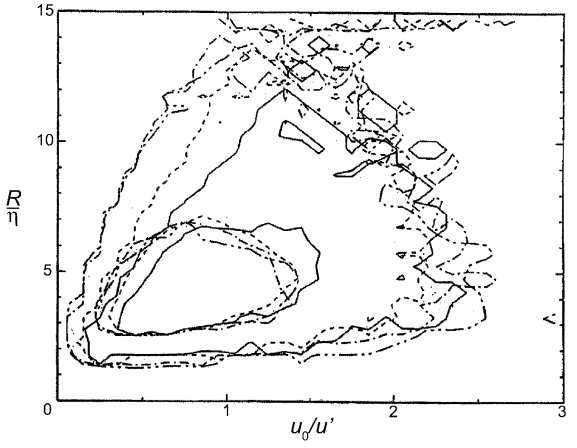

Fig. 25. Joint PDFs of maximum tangential velocity and filament radius after Jimenez and Wray [546]. Different lines show the results of DNS with different $Re_\lambda = 37 \div 168$. For each Re_λ, two probability isolines are included, $\mathcal{P} = 0.1$ and $\mathcal{P} = 0.001$. From the paper by Jiminez and Wray [546] © Cambridge University Press, reproduced with permission.

The above scaling laws are discussed, in detail, elsewhere [546,554].

The scaling laws reviewed above characterize averaged quantities, whereas instant characteristics of filaments are distributed in a wide domain. Jimenez and Wray [546] have shown that the tangential velocity in vortex tubes may be as large as $2.5u'$ and the radius of the tube varies from η to 15η (see Fig. 25). The highest velocity is associated with thin tubes. The minimum and maximum values of $\mathcal{W}$ measured at a fixed probability level scale as u_η and u. The minimum radius has been estimated [546] to scale as $\eta Re_t^{1/8}$. The thickest filaments are on the order of λ [546,549].

7.3.3. Vortex tubes in turbulent flames

Although rapid flame propagation along vortex tubes was suggested to be a possible physical mechanism of premixed turbulent combustion many years ago [526,555], little is known about the role played by such structures in turbulent flames.

Some indirect experimental evidence of vortex tubes in turbulent flames has been pointed out in a few papers [353, 361,502,526,556,557]. In particular, small-scale parts of flame front, convex to the unburned mixture, have been reported to move at a speed much higher than u' or $S_{L,0}$ [353] in weakly turbulent flames under elevated pressures. Recently, Soika et al. [361] published a 2D OH-LIPF image which looks like a vortex tube (see Fig. 4, $F = 0.7$, $P = 0.3$ MPa in the quoted paper). Nevertheless, decisive experimental data which prove an important role played by vortex tubes in premixed turbulent combustion have not yet been reported.

Recent three-dimensional, variable density DNS has confirmed the existence of vortex tubes in premixed turbulent flames and showed a tube-like structure of the regions characterized by a high local heat release rate [59]. However, such regions were observed near vortex tubes, rather than inside them, whereas no penetration of the flame into the tubes was observed, probably because the turbulence simulated was of a too small scale and the diameters of the tubes were smaller than the laminar flame thickness (see p. 535 in Ref. [59]).

Other published DNS data provide no information about vortex tubes in premixed turbulent flames.

It is worth emphasizing that the role played by the rapid propagation of laminar flames along vortex tubes in premixed turbulent combustion may be assessed only in three-dimensional and variable density studies, because the tubes are 3D structures, and rapid propagation is possible only if $\rho_b < \rho_u$ [34]. Consequently, the recent results of DNS, reported by Ulitsky and Collins [558], who found a minor contribution of coherent structures (e.g. vortex tubes) in turbulent flame speed by numerically eliminating these structures; should not be considered to be a test, because the DNS were performed in the case of $\rho_b = \rho_u$.

Let us note that the following observation may be relevant to this discussion. Ronney et al. measured the propagation of constant density aqueous chemical fronts [559] and of various methane–air flames [560] in the same type of turbulent Taylor–Couette flow. In the former case, the results agree well with the predictions of the renormalization group theory [380] developed for passive self-propagating interfaces, whereas markedly higher speeds have been recorded for methane–air flames. This difference implies that some physical mechanisms affect variable density flames but not the passive interfaces in turbulent flows. Rapid flame propagation along vortex tubes may be such a mechanism, side by side with the DL instability or the flame-generated turbulence.

Several models of turbulent flame speed [34,170,527, 561] have been developed based on the vortex tube mechanism considered above. The models are not discussed here because they do not address the effects of D_d on U_t.

It is worth noting that the small radius of vortex tubes and considerable viscous dissipation associated with such small-scale structures do not invalidate the hypothesis, as regards the important role played by the tubes in turbulent flame propagation.

First, in constant density flows, vortex tubes survive a long time on the order of the time scale of the largest structures of the flow [550]; because the dissipation is balanced by the energy flux from background turbulence due to stretching of the tubes. Vortex tubes most often disappear by catastrophic breaking events and due to merging with other tubes, but not by viscosity [539]. Since $V_f \propto u'$, a laminar flame can propagate a long way (on the order of L) during the tube life time that scales as τ_t.

Second, in flames, viscosity increases in high-temperature products, and this process might shorten the life-time of vortex tubes. However, a recent three-dimensional, variable

density DNS [59] has indicated that vortex tubes survive in combustion products. Even simulations of laminar flame propagation along the axis of an isolated, decaying Burgers vortex have shown that, despite the viscous decay of the vortex, the flame propagates a long way (at least 10 mm) before the decay begins to markedly affect the process [525].

Finally, vortex tubes can substantially affect turbulent flame speed not only due to the rapid propagation of laminar flamelets along the axes of the tubes, as discussed above, but also due to the random motion of the tubes themselves. The motion is controlled by stretch rates produced by background turbulence and the mean speed of the tubes appears to scale as a small-scale turbulence velocity, e.g. the Kolmogorov velocity, u_η. A similar phenomenon is well known in free turbulent flows, where the boundary between turbulent fluid and the external region of irrotational motion is a thin (its thickness is on the order of η) and convoluted interface (the so-called 'viscous superlayer') that moves at a speed on the order of u_η [562–566].

If $u_\eta \gg S_{L,0}$ and a flamelet is inside a vortex tube, the motion of the tube substantially accelerates the propagation of the flamelet and, thus, contributes to turbulent flame speed.

One may argue that the probability of finding vortex tubes is too low for them to play an important role in turbulent flame propagation. According to DNS of constant density flows [544–546], the volume fraction occupied by vortex tubes scales as Re_t^{-1}. If the mean volume of a single tube scales as $\eta^2 L \propto L^3 Re_t^{-3/2}$ (the mean radius and the length of the tube scale as η and L, respectively, see Section 7.3.2), the number of the tubes per cube of $L\times L\times L$ scale as $Re_t^{1/2}$, quite a sufficient number of potentially leading points.

We may also note that if a flamelet is inside a vortex tube, the local flame surface area associated with such a burning structure scales as $d_f L$ and the corresponding flame surface density scales as $d_f L Re_t^{1/2}/L^3$. In the two limit cases of $d_f \propto \delta_L$ and $d_f \propto \eta$, we obtain the following estimate

$$Ka^q \frac{1}{L}\left(\frac{\delta_L}{L}\right)^{1/3}$$

for the density associated with flamelets inside vortex tubes, where $q = 1/3$ and $-1/6$, respectively. For comparison, the experimental data reported by Deshamps et al. [567] show that the maximum flamelet surface density scales as

$$\Sigma_m \propto \frac{1}{L}\left(\frac{\delta_L}{L}\right)^{1/3}$$

(see Fig. 6 in the quoted paper). A difference between the two scalings consists of a factor of Ka^q, which is of minor importance if $Ka \approx 1$. Consequently, the flamelet surface area associated with flamelets captured by vortex tubes may be comparable to the flamelet surface area associated with flamelets that propagate in background turbulence.

Since the former flamelets are strongly curved, the local burning rate that characterizes these flamelets depends substantially on Le and D_F/D_O. However, it is worth noting that this effect is (in part?) counteracted by a decrease in d_f and, hence, in Σ with decreasing Le. Consequently, the mean effect of the random motion of vortex tubes on turbulent flame speed may depend weakly on molecular transport coefficients.

7.4. Governing physical mechanisms of premixed turbulent flame propagation

The above discussion allows us to outline the following physical scenario:

1. Processes at the leading edge of a developing flame brush affect substantially turbulent burning velocity by triggering combustion and flame surface area production and affecting the balance of Σ in the whole flame brush.
2. The structure of leading kernels is controlled by the local velocity field and by the characteristics of strongly perturbed reaction zones, which depend substantially on D_d/D_e and Le. Such zones dominate at the leading edge due to one of the two following physical mechanisms:
   - (2.a) The random convection of local reaction zones towards the leading edge of the turbulent flame brush is limited by the local extinction caused by strong turbulent eddies. Due to the balance between the quenching and convection, critically perturbed zones dominate at the leading edge. In mixtures with $Le < 1$ and $D_d > D_e$, the strongest known perturbations of laminar flames are associated with a critically curved spherical kernel. Consequently, such kernels appear to survive under the influence of eddies which are so strong they quench other laminar burning structures.
   - (2.b) A laminar flame that penetrates into a vortex tube, which exists in a turbulent unburned mixture, propagates along the tube at a speed, $V_f = O(\mathcal{W})$, on the order of tangential velocity and much higher than laminar flame speed. For any mixture, the highest local speed of the propagation, $V_{f,m}$, (see Fig. 23) is associated with critical conditions (the highest $\mathcal{W} = \mathcal{W}_q$ and extremely curved tip of the flame, for which the flame barely survives inside the tube), which strongly depend on Le and D_d/D_e. Consequently, $V_{f,m}$ increases with decreasing Le and increasing D_d/D_e (see Fig. 23). Since the basic characteristics of vortex tubes in a turbulent flow constitute a continuous spectrum (see Fig. 25), the aforementioned critical conditions are reached locally in certain vortex tubes for a wide range of u', L, and mixture characteristics. If the critical conditions are reached in a tube, the laminar flame moves fast along it and advances furthest into the unburned mixture, provided that the tube axis is not parallel to the mean flame surface. Thus, the structure and propagation of the leading edge of turbulent

flame brush are controlled by the propagation of the strongly curved tip of a laminar flame along the axis of critically strong vortex tubes.

3. As a result, the dependence of the characteristics of the critically curved reaction zones on Le and D_d/D_e controls the dependence of $U_t(Le, D_d/D_e)$.
4. Moreover, the random motion of vortex tubes that capture flamelets at a speed on the order of u_η can also affect turbulent burning velocity. Since flamelets inside the tubes are strongly curved, the effect depends on the Lewis number.

The above scenario is a hypothesis capable of explaining the strong effect of D_d on $\mathcal{U}_t$ in moderately and highly turbulent flames in a consistent manner. The ability to explain and even quantitatively predict (see Figs. 18–20) the effect is the key merit of this hypothesis as compared to the alternative approaches discussed in Sections 4, 5 and 6.1. It is worth emphasizing again that: (1) these approaches are not able to yield a substantial effect of D_d on the speed of the leading edge of a turbulent flame if $u' \gg S_{L,0}$; (2) the available models based on these approaches cannot predict the strong effect of D_d on $\mathcal{U}_t$, indicated by experimental data (e.g. Fig. 4a).

The above discussion highlights strongly curved reaction zones to be a suitable candidate for explaining the considerable effect on D_d on $\mathcal{U}_t$. Certainly the behavior of such a coarse characteristic as turbulent flame speed is insufficient to establish the governing physical mechanism of premixed turbulent combustion, but the existence of a paradox not resolved by most known approaches appears to be quite sufficient in order to point out a certain physical mechanism as the potentially governing one, based on the ability of this mechanism to resolve the paradox.

The strong effect of D_d on $\mathcal{U}_t$ should definitely be associated with the important role played by some thin, intrinsically laminar reaction zones in the propagation of turbulent flames. Since the characteristics of the different types of such zones are substantially different and depend strongly on D_d, the magnitude of the effect of D_d on U_t, predicted by different models, must substantially depend on the type of the zone, which the model is based on. This distinction offers the opportunity to select from a range of potentially important zones and to gain insight into the basic mechanism of premixed turbulent combustion.

The hypotheses put forward above strongly need validation and development. The validation could be performed by obtaining new experimental and DNS data on the fine structure of non-equidiffusive premixed turbulent flames and by comparing the predicted behavior of turbulent flame speed with experimental data. Figs. 18–20 provide a validation of the latter type by indicating that strongly curved laminar flamelets play an important role in turbulent flame propagation. A more decisive test could be done if an expression for U_t could be derived by developing the above hypotheses. To do so, studies of the structure of the tip of a laminar flame that propagates along the axis of a vortex tube under near-critical rotation velocity appear to be of paramount importance.

8. Conclusions

1. Various experimental and DNS data show that premixed combustion is affected by the differences between the coefficients of molecular transport of fuel, oxidant and heat, not only at weak but also at moderate and high turbulence.
   - Turbulent flame speed increases with decreasing Lewis number and/or increasing D_d/D_e. In lean hydrogen mixtures characterized by substantial differences in κ, D_F, and D_O, the effect is very strong even if $u' \gg S_{L,0}$.
   - The mean structure of a premixed turbulent flame does not depend on these differences.
   - The mean flame brush thickness increases with decreasing Lewis number and/or increasing D_d/D_e, but the effect appears to be well pronounced at weak turbulence only.
   - The local structure of a premixed turbulent flame is sensitive to Le and D_d/D_e. The local burning rate is increased in positively curved flamelets if $Le<1$ and/or $D_d>D_e$ and the local flame surface area increases with decreasing Lewis number and/or increasing D_d/D_e.
2. The concept of laminar flame instabilities associates the above effects with enhanced production of flame surface area due to the instabilities. However, such phenomena appear to be of importance at weak turbulence only. Moreover, despite the substantial progress obtained in the studies of flame instabilities in laminar flows, the development of the concept has not led to a model capable of predicting a strong dependence of $U_t(Le, D_d/D_e)$.
3. The concept of flamelet library associates the above effects with (i) local variations of burning rate inside laminar flamelets stretched and wrinkled by turbulent eddies (the concept of Markstein number) and (ii) local quenching of flamelets by sufficiently strong turbulent eddies (the concept of critical stretch rate). The ability of such models to predict a strong dependence of $U_t(Le, D_d/D_e)$ has not been shown yet. The concept cannot predict any substantial effect of Le and D_d/D_e on the speed of the leading edge of the flame brush if turbulence is strong ($u' \gg S_{L,0}$).
4. The concept of leading point associates the above effects with (i) the crucial role played by the leading edge of the turbulent flame brush in the propagation of the flame and (ii) the dominance of critically perturbed thin reaction zones at the leading edge. If the structure of leading kernels is modeled with a critically curved spherical, laminar flame, the concept is able to predict the strong dependence of $\mathcal{U}_t(Le, D_d/D_e)$ both qualitatively and

quantitatively. To do so in a consistent manner, several hypotheses about physical mechanisms that control the structure of the leading edge (a flame ball or a critically curved tip of a laminar flame propagating along a vortex tube at near-critical rotational velocities) have been put forward and discussed. These hypotheses need further validation.

Acknowledgements

This work was supported by the Swedish Research Council for Engineering Sciences. The authors are grateful to Prof. V.P. Karpov and A.S. Betev for providing experimental data and for fruitful discussions.

Appendix A. Models discussed in the review

Here, we restrict ourselves to a brief summary of three approaches to multi-dimensional simulations of premixed turbulent combustion, which have been used to simulate the dependence of U_t on D_d. The interested reader is referred to recent reviews by Bray [75] (the flamelet approach), by Bradley [179] (the flamelet approach), by Veynante and Vervish [19] (the flamelet and flame surface density approaches), and by us [18] (the extended Zimont model) for more details.

All the models discussed below pertain to adiabatic, completely premixed flames.

A.1. Flamelet models

Flamelet models characterize the combustion process by a single progress variable ($c=0$ in the unburned gas and $c=1$ in the products) following the well-known Bray–Moss method [72]. The balance equation for the Favre-averaged progress variable is as follows [74]

$$\frac{\partial\overline{\rho}\tilde{c}}{\partial t}+\frac{\partial}{\partial x_j}(\overline{\rho}\tilde{u}_j\tilde{c})=-\frac{\partial}{\partial x_j}(\overline{\rho u_j'' c''})+\overline{\rho}\tilde{W}, \tag{A.1}$$

where t is the time, x_j and u_j are the coordinates and flow velocity components, respectively; $\tilde{W}$ is the mean rate of product creation, and the Reynolds averages denoted by overbars, as well as the Favre averages, such as $\overline{\rho}\tilde{c}=\overline{\rho c}$, are used where $c''=c-\tilde{c}$ and $c'=c-\overline{c}$.

The progress variable may be defined by any of Eq. (3) in the adiabatic and equidiffusive, $D_F=D_O=\kappa$, case. In the case of $D_F\neq D_O\neq\kappa$ and in the flamelet regime of turbulent combustion, a more consistent interpretation of the progress variable is to associate this quantity with the probability of finding combustion products. In the equidiffusive case, the probability tends to the Reynolds-averaged progress variable as the probability of finding intermediate (between unburned and burned) states of the mixture vanishes [72].

Bradley [177–179] has closed the mean reaction rate as follows

$$\overline{\rho}\tilde{W}=\int_0^1\int_{-\infty}^{\infty}\rho W_L(c,\dot{s})\mathscr{P}(c,\dot{s})\mathrm{d}\dot{s}\,\mathrm{d}c\approx I_0\int_0^1\rho W_L(c,0)\mathscr{P}_f(c)\mathrm{d}c;$$
$$I_0\equiv\int_{-\infty}^{\infty}w(\dot{s})\mathscr{P}_s(\dot{s})\mathrm{d}\dot{s}; \tag{A2}$$

where the PDFs $\mathscr{P}_f(c)$ and $\mathscr{P}_s(\dot{s})$ are assumed to be statistically independent, i.e. $\mathscr{P}(c,\dot{s})=\mathscr{P}_f(c)\cdot\mathscr{P}_s(\dot{s})$, the rate $W_L(c,\dot{s})$ corresponds to a stretched laminar flame and is provided by a flamelet library, and the ratio of $w(\dot{s})\equiv W_L(c,\dot{s})/W_L(c,0)$ is considered to be independent of c. The PDF $\mathscr{P}_f(c)$ is assumed a priori to be a beta function evaluated from computed first and second moments of the PDF [177].

If $w(\dot{s})=1$ for $\dot{s}_{q,-}<\dot{s}<\dot{s}_{q,+}$ and $w(\dot{s})=0$ otherwise, then [177]

$$I_0=\int_{\dot{s}_{q,-}}^{\dot{s}_{q,+}}\mathscr{P}_s(\dot{s})=1-\mathscr{P}_q, \tag{A.3}$$

where $\mathscr{P}_q$ is the probability of flamelet quenching and the quantities $\dot{s}_{q,-}$ and $\dot{s}_{q,+}$ are associated with flamelet quenching by negative (compression) and positive stretching, respectively.

Bray [74,75,277] has closed the mean reaction rate as follows

$$\overline{\rho}\tilde{W}=\rho_u I_0 S_{L,0}\Sigma, \tag{A.4}$$

where the stretch-factor, I_0, characterizes averaged variations in the local burning rate in stretched flamelets (see Sections 5 and 6.1) and the mean flamelet surface density, Σ, is evaluated by assuming that the square wave spatial distribution $c(y)$ along a contour $\overline{c}=\text{const}$ is a random telegraph signal [568,569]

$$\Sigma=\frac{g\overline{c}(1-\overline{c})}{\overline{\sigma}_y\hat{L}_y}, \tag{A.5}$$

where g is a number of the order unity, $\hat{L}_y$ is the integral length scale of the square wave $c(y)$, and $\overline{\sigma}_y$ is the mean of a direction cosine that defines the flamelet orientation relative to the aforementioned contour.

Within the framework of flamelet models, the transport term in the RHS of Eq. (1) is typically closed by invoking balance equations for $\overline{\rho u_j'' c''}$ [19,25,73–75,82,177,568].

A.2. Flame surface density models

Eq. (A.4) is often closed by determining Σ using an additional balance equation for the mean flamelet surface

density, which reads [19,211,269,570,571]

$$\frac{\partial \Sigma}{\partial t} + \underbrace{\frac{\partial}{\partial x_i}(\langle u_i \rangle_S \Sigma)}_{\mathrm{I}} = \underbrace{\langle \frac{\partial u_i}{\partial x_i} - n_i n_j \frac{\partial u_i}{\partial x_j} \rangle_S \Sigma}_{\mathrm{II}} + \underbrace{\langle S_d \frac{\partial n_i}{\partial x_i} \rangle_S \Sigma}_{\mathrm{III}} - \underbrace{\frac{\partial}{\partial x_i}(\langle S_d n_i \rangle_S \Sigma)}_{\mathrm{IV}}, \tag{A.6}$$

where $\vec{n}$ is the unit vector normal to the surface, pointing towards the unburned mixture, $\nabla \vec{n}$ is the flamelet curvature, and $\langle f \rangle_S = \langle f \Sigma' \rangle / \Sigma$ denotes a surface mean, where Σ' is the local flamelet surface density, i.e. $\langle \Sigma' \rangle = \Sigma$.

Flame surface density models provide various closures of Eq. (A.6), which can be written in the following general form [19,78]

$$\frac{\partial \Sigma}{\partial t} + \frac{\partial}{\partial x_j}(\tilde{u}_j \Sigma) = \frac{\partial}{\partial x_j}\left(D_\Sigma \frac{\partial \Sigma}{\partial x_j} \right) + Q_1 + Q_2 - R \tag{A.7}$$

where the convection and gradient transport terms originate in term I in Eq. (A.6) after the standard decomposition, $u_i = \tilde{u}_i + u_i''$; the source terms Q_1 and Q_2 originate in term II after the same decomposition and are associated with flamelet straining by mean and turbulent flows, respectively, and the sink term R models the consumption of the area due to flamelet propagation and is associated with the so-called curvature-propagation [19] term III in Eq. (A.6) (term IV is often neglected). Particular closures for R, Q_1, and Q_2 are reported in Table 5 in Ref. [19], where an improved version of the closed balance equation is also proposed (see Eq. (210) in the quoted paper).

Note that the majority of flame surface density models invoke the gradient closure of the transport term in Eq. (A.1)

$$\overline{\rho u_j'' c''} = -\overline{\rho} D_t \frac{\partial \tilde{c}}{\partial x_j}, \tag{A.8}$$

where D_t is the turbulent diffusivity.

In order to allow for the DL instability, Paul and Bray [172] have introduced an additional source term into Eq. (A.7). The extended equation that they use reads

$$\frac{\partial \Sigma}{\partial t} + \frac{\partial}{\partial x_j}(\tilde{u}_j \Sigma) - \frac{\partial}{\partial x_j}\left(D_\Sigma \frac{\partial \Sigma}{\partial x_j} \right) = \alpha \Sigma \left[\frac{\mathcal{F}}{\tau_t} + (1 - \mathcal{F}) \frac{S_{L,0}}{\Lambda_n} aH \right] - \beta \frac{S_{L,0} \Sigma^2}{\tilde{c}(1 - \tilde{c})}, \tag{A.9}$$

where the instability function $H(\gamma, u'/S_{L,0}, L/\Lambda_n)$ has been parameterized by Cambray and Joulin [302], the neutral wavelength, Λ_n, is provided by the theory of unstable laminar flames (e.g. Eq. (17)), α and β are constants of the original flame surface density model, the bridging function is approximated by

$$\mathcal{F} = 1 - \exp(-bu'/S_{L,0}), \tag{A.10}$$

a and b are new constants, a being assumed to be equal to $\beta g/(\alpha \overline{\sigma}_y)$ (see Eq. (A.5)).

A.3. Extended Zimont model

The extended Zimont model discussed, in detail, elsewhere [18,36,83,136,137,465,487,489] provides the following closed balance equation for the mean combustion progress variable

$$\frac{\partial \overline{\rho} \tilde{c}}{\partial t} + \frac{\partial}{\partial x_j}(\overline{\rho} \tilde{u}_j \tilde{c}) = \frac{\partial}{\partial x_j}\left(\overline{\rho} D_t \frac{\partial \tilde{c}}{\partial x_j} \right) + \rho_u \mathcal{U}_t |\nabla \tilde{c}|,$$
$$|\nabla \tilde{c}| \equiv \left\{ \sum_{j=1}^{3} \left(\frac{\partial \tilde{c}}{\partial x_j} \right)^2 \right\}^{1/2}, \tag{A.11}$$

where turbulent burning velocity is determined using

$$\mathcal{U}_t = A u' Da^{1/4} I_0 = A u' \left(\frac{\tau_t}{\tau_c'} \right)^{1/4} I_0, \tag{A.12}$$

where $A = 0.5$ is a constant, Da is the Damköhler number, the stretch-factor $I_0 = 1 - \mathcal{P}_q$ has been determined using Eq. (36) [137,465,487], and different submodels for the flame time scale, τ_c', have been used, in particular, $\tau_c' = \tau_c = \kappa_u / S_{L,0}^2$ [36,83], $\tau_c' = \tau_c(F_r)$ with F_r calculated using Eq. (40) [465,487,489], $\tau_c' = \tau_{cr}$ (see Eq. (43)) [136], $\tau_c' = \tau_{lp}$ (see Eq. (45)) [137].

References

[1] Damköhler G. Der einfuss der turbulenz auf die flammengeschwindigkeit in gasgemischen. Zs Electrochemie 1940;6:601–52.
[2] Shchelkin KI. Combustion in turbulent flow. Zhournal Tekhnicheskoi Fiziki 1947;13:520–30 (English translation NACA TM, 1112, 1947).
[3] Barrére M. Modéles de combustion. Revue Gén Thermique 1974;148:295–308.
[4] Bray KNC. Turbulent flows with premixed reactants. In: Libby PA, Williams FA, editors. Turbulent reacting flows. Berlin: Springer; 1980. p. 115–83.
[5] Abraham J, Williams FA, Bracco FV. A discussion of turbulent flame structure in premixed charges. SAE Paper 1985;850343.
[6] Williams FA. Combustion theory. Menlo Park, CA: Benjamin/Cummings; 1985.
[7] Williams FA. Turbulent combustion. In: Buckmaster JD, editor. The mathematics of combustion. Philadelphia, PA: SIAM; 1985. p. 97–128.
[8] Borghi R. On the structure and morphology of turbulent premixed flames. In: Bruno C, Casci S, editors. Recent advances in aerospace science. New York: Plenum; 1985. p. 117–38.
[9] Borghi R. Turbulent combustion modeling. Prog Energy Combust Sci 1988;14:245–92.

[10] Peters N. Laminar flamelet concepts in turbulent combustion. 21st Symposium (international) on combustion. Pittsburgh, PA: The Combustion Institute; 1986 p. 1231–49.
[11] Abdel-Gayed RG, Bradley D, Lung FKK. Combustion regimes and the straining of turbulent premixed flames. Combust Flame 1989;76:213–8.
[12] Poinsot T, Veynante D, Candel S. Diagrams of premixed turbulent combustion based on direct simulation 23rd Symposium (international) on combustion. Pittsburgh, PA: The Combustion Institute; 1990 p. 613–9.
[13] Libby PA, Williams FA. Fundamental aspects and a review. In: Libby PA, Williams FA, editors. Turbulent reactive flows. London: Academic Press; 1994. p. 1–61.
[14] Poinsot T, Candel S, Trouvé A. Applications of direct numerical simulations to premixed turbulent combustion. Prog Energy Combust Sci 1995;21:531–76.
[15] Peters N. The turbulent burning velocity for large-scale and small-scale turbulence. J Fluid Mech 1999;384:107–32.
[16] Peters N. Turbulent combustion. Cambridge, UK: Cambridge University Press; 2000.
[17] Chen YC, Bilger R. Simultaneous 2-D imaging measurements of reaction progress variable and OH radical concentration in turbulent premixed flames: instantaneous flame-front structure. Combust Sci Technol 2001;167: 187–222.
[18] Lipatnikov AN, Chomiak J. Turbulent flame speed and thickness: phenomenology, evaluation, and application in multi-dimensional simulations. Prog Energy Combust Sci 2002;28:1–73.
[19] Veynante D, Vervish L. Turbulent combustion modeling. Prog Energy Combust Sci 2002;28:193–266.
[20] Dinkelacker F. Experimental validation of flame regimes for highly turbulent premixed flames. In: European Combustion Meeting; 2003, Paper 158. CD.
[21] Karlovitz B, Denniston DW, Wells FE. Investigation of turbulent flames. J Chem Phys 1951;19:541–7.
[22] Prudnikov AG. Combustion of homogeneous fuel–air mixtures in turbulent flows. In: Raushenbakh BV, editor. Physical basis of processes in combustion chambers of air-breathing engines. Moscow: Mashinostroenie; 1964. p. 255–347 (in Russian).
[23] Clavin P, Williams FA. Theory of premixed-flame propagation in large-scale turbulence. J Fluid Mech 1979;90: 589–604.
[24] Moss JB. Simultaneous measurements of concentration and velocity in an open premixed turbulent flame. Combust Sci Technol 1980;22:119–29.
[25] Libby PA, Bray KNC. Countergradient diffusion in premixed turbulent flames. AIAA J 1981;19:205–13.
[26] Karlovitz B, Denniston Jr. DW, Knapschaefer DH, Wells FE. Studies of turbulent flames. 4th Symposium (international) on combustion. Baltimore: Williams and Wilkins; 1953. p. 613–20.
[27] Kovasznay LCG. Combustion in turbulent flow. Jet Propulsion 1956;26:485–97.
[28] Klimov AM. Laminar flame in a turbulent flow. Zhournal Prikladnoi Mekchaniki i Tekhnicheskoi Fiziki 1963;3:49–58.
[29] Williams FA. Criteria for existence of wrinkled laminar flame structure of turbulent premixed flames. Combust Flame 1976;26:269–70.
[30] Kuznetsov VR, Sabel'nikov VA. Turbulence and combustion. New York: Hemisphere; 1990.
[31] Gouldin FC. An application of fractals to modelling premixed turbulent flames. Combust Flame 1987;68:249–66.
[32] Gülder L. Turbulent premixed combustion modelling using fractal geometry. 23rd Symposium (international) on combustion. Pittsburgh, PA: The Combustion Institute; 1990. p. 835–41.
[33] Poinsot T, Veynante D, Candel S. Quenching processes and premixed turbulent combustion diagrams. J Fluid Mech 1991;228:561–606.
[34] Chomiak J. Basic considerations of the turbulent flame propagation in premixed gases. Prog Energy Combust Sci 1979;5:207–21.
[35] Scurlock AL, Grover JH. Propagation of turbulent flames 4th Symposium (international) on combustion. Baltimore: Williams and Wilkins; 1953 p. 645–58.
[36] Zimont VL. Theory of turbulent combustion of a homogeneous fuel mixture at high Reynolds number. Combust, Explos, Shock Waves 1979;15:305–11.
[37] Chomiak J. Combustion: a study in theory, fact and application. New York: Gordon and Breach; 1990.
[38] Bradley D. How fast can we burn? 24th Symposium (international) on combustion Pittsburgh, PA: The Combustion Institute; 1992 p. 247–62.
[39] Menon S, Jou WH. Large-eddy simulations of combustion instability in an axisymmetric ramjet combustor. Combust Sci Technol 1991;75:53–72.
[40] Im HG, Lund TS, Ferziger JH. Large eddy simulation of turbulent front propagation with dynamic subgrid models. Phys Fluids 1997;9:3826–33.
[41] Colucci PJ, Jaberi FA, Givi P, Pope SB. Filtered density function for large eddy simulation of turbulent reacting flows. Phys Fluids 1998;10:499–515.
[42] Boger M, Veynante D, Boughanem H, Trouvé A. Direct numerical simulation analysis of flame surface density concept for large-eddy simulation of turbulent premixed combustion. 27th Symposium (international) on combustion. Pittsburgh, PA: The Combustion Institute; 1998. p. 917–25.
[43] Weller HG, Tabor G, Gosman AD, Fureby C. Application of a flame-wrinkling LES combustion model to a turbulent mixing layer. 27th Symposium (international) on combustion. Pittsburgh, PA: The Combustion Institute; 1998. p. 899–907.
[44] Colin O, Ducros F, Veynante D, Poinsot T. A thickened flame model for large eddy simulations of turbulent premixed combustion. Phys Fluids 2000;12:1843–63.
[45] Fureby C. Large eddy simulation of combustion instabilities in a jet engine afterburner model. Combust Sci Technol 2000; 161:213–43.
[46] Kim WW, Menon S. Numerical modeling of turbulent premixed flames in the thin-reaction-zones regime. Combust Sci Technol 2000;160:119–50.
[47] Hawkes ER, Cant RS. A flame surface density approach to large-eddy simulations of premixed turbulent combustion. Proc Combust Inst 2000;28:51–8.
[48] Nwagwe IK, Weller HG, Tabor GR, Gosman AD, Lawes M, Sheppard CGW, et al. Measurements and large eddy simulations of turbulent premixed flame kernel growth. Proc Combust Inst 2000;28:59–65.

[49] Chakravarthy VK, Menon S. Large-eddy simulation of turbulent premixed flames in the flamelet regime. Combust Sci Technol 2001;162:175–222.
[50] Charlette F, Meneveau C, Veynante D. A power-law flame wrinkling model for LES of premixed turbulent combustion part I: non-dynamic formulation and initial tests. Combust Flame 2002;131:159–80.
[51] Charlette F, Meneveau C, Veynante D. A power-law flame wrinkling model for LES of premixed turbulent combustion part II: dynamic formulation. Combust Flame 2002;131: 181–97.
[52] Pitsch H, de Lageneste LD. Large-eddy simulation of premixed turbulent combustion using a level-set approach. Proc Combust Inst 2002;29:2001–8.
[53] Stone C, Menon S. Swirl control of combustion instabilities in a gas turbine combustor. Proc Combust Inst 2002;29: 155–60.
[54] Tullis S, Cant RS. Scalar transport modeling in large eddy simulation of turbulent premixed flames. Proc Combust Inst 2002;29:2097–105.
[55] Kaufmann A, Nicoud F, Poinsot T. Flow forcing techniques for numerical simulation of combustion instabilities. Combust Flame 2002;131:371–85.
[56] Pope SB. Ten questions concerning the large-eddy simulation of turbulent flows. New J Phys 2004;6:1–24.
[57] Selle L, Lartigue G, Poinsot T, Koch R, Schildmacher KU, Krebs W, et al. Compressible large eddy simulation of turbulent combustion in complex geometry on unstructured meshes. Combust Flame 2004;137:489–505.
[58] Poinsot T. Using direct numerical simulations to understand premixed turbulent combustion. 26th Symposium (international) on combustion. Pittsburgh, PA: The Combustion Institute; 1996. p. 219–232.
[59] Tanahashi M, Fujimura M, Miyachii T. Coherent fine-scale eddies in turbulent premixed flames. Proc Combust Inst 2000;28:529–35.
[60] Tanahashi M, Nada Y, Ito Y, Miyachii T. Local flame structure in the well-stirred reactor regime. Proc Combust Inst 2002;29:2041–9.
[61] Bell JB, Day MS, Grcar J. Numerical simulation of premixed turbulent methane combustion. Proc Combust Inst 2002;29: 1987–93.
[62] Jenkins KW, Cant RS. Curvature effects on flame kernels in a turbulent environment. Proc Combust Inst 2002;29:2023–9.
[63] Nishiki S, Hasegawa T, Borghi R, Himeno R. Modeling of flame-generated turbulence based on direct numerical simulation databases. Proc Combust Inst 2002;29:2017–22.
[64] Thévenin D, Gicquel O, Charentenay JD, Hilbert R, Veynante D. Two- versus three-dimensional direct simulations of turbulent methane flame kernels using realistic chemistry. Proc Combust Inst 2002;29:2031–9.
[65] Chakraborty N, Cant S. Unsteady effects of strain rate and curvature on turbulent premixed flames in an inflow–outflow configuration. Combust Flame 2004;137:129–47.
[66] Im YH, Huh KY, Nishiki S, Hasegawa T. Zone conditional assessment of flame-generated turbulence with DNS database of a turbulent premixed flame. Combust Flame 2004;137: 478–88.
[67] Pope SB. PDF methods for turbulent reacting flows. Prog Energy Combust Sci 1985;11:119–92.
[68] Pope SB. Lagrangian PDF methods for turbulent flows. Annual Rev Fluid Mech 1994;26:23–63.
[69] Spalding DB. The spread of turbulent flame confined in ducts. 11th Symposium (international) on combustion. Pittsburgh, PA: The Combustion Institute; 1967. p. 807–15.
[70] Spalding DB. Mixing and chemical reaction in steady confined turbulent flame. 13th Symposium (international) on combustion. Pittsburgh, PA: The Combustion Institute; 1971. p. 649–57.
[71] Magnussen BF, Hjertager BH. On mathematical modeling of turbulent combustion with special emphasis on soot formation and combustion. 16th Symposium (international) on combustion. Pittsburgh, PA: The Combustion Institute; 1976. p. 719–29.
[72] Bray KNC, Moss JB. A unified statistical model for the premixed turbulent flame. Acta Astronautica 1977;4: 291–319.
[73] Libby PA. Theory of normal premixed turbulent flames revisited. Prog Energy Combust Sci 1985;11:83–96.
[74] Bray KNC. Turbulent transport in flames. Proc R Soc Lond 1995;A451:231–56.
[75] Bray KNC. The challenge of turbulent combustion. Proc Combust Inst 1996;26:1–26.
[76] Bray KNC, Champion M, Libby PA. Premixed flames in stagnating turbulence part IV: a new theory for the Reynolds stresses and Reynolds fluxes applied to impinging flows. Combust Flame 2000;120:1–18.
[77] Candel S, Veynante D, Lacas F, Maistret E, Darabiha N, Poinsot T. Coherent flame model: applications and recent extensions. In: Larrouturou BE, editor. Advances in combustion modeling. Singapore: World Scientific; 1990. p. 19–64.
[78] Duclos JM, Veynante D, Poinsot T. A comparison of flamelet models for premixed turbulent combustion. Combust Flame 1993;95:101–17.
[79] Weller HG. The development of a new flame area combustion model using conditional averaging. TF/9307, Mechanical Engineering Department, Imperial College; 1993.
[80] Schmidt HP, Habisreuther P, Leuckel W. A model for calculating heat release in premixed turbulent flames. Combust Flame 1998;113:79–91.
[81] Lindstedt RP, Váos EM. Second moment modeling of premixed turbulent flames stabilizing in impinging jet geometries. 27th Symposium (international) on combustion. Pittsburgh, PA: The Combustion Institute; 1998. p. 957–62.
[82] Lindstedt RP, Váos EM. Modeling of premixed turbulent flames with second moment methods. Combust Flame 1999; 116:461–85.
[83] Zimont VL. Gas premixed combustion at high turbulence. Turbulent flame closure combustion model. Exp Thermal Fluid Sci 2000;21:179–86.
[84] Zimont VL, Biagioli F. Gradient, counter-gradient transport and their transition in turbulent premixed flames. Combust Theory Modell 2002;6:79–101.
[85] Biagioli F, Zimont VL. Gasdynamics modelling of counter-gradient transport in open and impinging turbulent premixed flames. Proc Combust Inst 2002;29:2087–95.
[86] Chen YC, Bilger R. Experimental investigation of three-dimensional flame-front structure in premixed turbulent combustion—I: hydrocarbon/air Bunsen flames. Combust Flame 2002;131:400–35.

[87] Kortschik C, Plessing T, Peters N. Laser optical investigation of turbulent transport of temperature ahead of the preheat zone in a premixed flame. Combust Flame 2004;136:43–50.

[88] Knaus DA, Gouldin FC. Measurements of flamelet orientations in premixed flames with positive and negative Markstein numbers. Proc Combust Inst 2000;28:367–73.

[89] O'Young F, Bilger RW. Scalar gradient and related quantities in turbulent premixed flames. Combust Flame 1997;109:682–700.

[90] Chen YC, Mansour MS. Investigation of flame broadening in turbulent premixed flames in the thin reaction zone regime. 27th Symposium (international) on combustion. Pittsburgh, PA: The Combustion Institute; 1998. p. 811–8.

[91] Soika A, Dinkelacker F, Leipertz A. Measurement of the resolved flame structure of turbulent premixed flames with constant Reynolds number and varied stoichiometry. 27th Symposium (international) on combustion. Pittsburgh, PA: The Combustion Institute; 1998. p. 785–92.

[92] Most D, Dinkelacker F, Leipertz A. Direct determination of the turbulent flux by simultaneous application of filtered Rayleigh scattering thermometry and particle image velocimetry. Proc Combust Inst 2002;29:2669–77.

[93] Plessing T, Kortschik C, Peters N, Mansour MS, Cheng RK. Measurements of the turbulent burning velocity and of the structure of premixed flames on a low-swirl burner. Proc Combust Inst 2000;28:359–66.

[94] Most D, Dinkelacker F, Leipertz A. Lifted reaction zones in premixed turbulent bluff-body stabilized flames. Proc Combust Inst 2002;29:1801–8.

[95] Kalt PAM, Chen YC, Bilger RW. Experimental investigation of turbulent scalar flux in premixed stagnation-type flames. Combust Flame 2002;129:401–15.

[96] Shepherd IG, Cheng RK, Plessing T, Kortschik C, Peters N. Premixed flame front structure in intense turbulence. Proc Combust Inst 2002;29:1833–40.

[97] Kobayashi H, Kawahata T, Seyama K, Fujimari T, Kim JS. Relationship between the smallest scale of flame wrinkles and turbulence characteristics of high-pressure, high-temperature turbulent premixed flames. Proc Combust Inst 2002; 29:1773–80.

[98] Renou B, Mura A, Samson E, Boukhalfa A. Characterization of the local flame structure and flame surface density for freely-propagating premixed flames at various Lewis numbers. Combust Sci Technol 2002;174:81–117.

[99] Kido H, Nakahara M, Nakashima K. Influence of local flame displacement velocity on turbulent burning velocity. Proc Combust Inst 2002;29:1855–61.

[100] Bradley D, Haq MZ, Hicks RA, Kitagawa T, Lawes M, Sheppard CGW, et al. Turbulent burning velocity, burned gas distribution, and associated flame surface definition. Combust Flame 2003;133:415–30.

[101] Furukawa J, Noguchi Y, Hirano T, Williams F. Anisotropic enhancement of turbulence in large-scale, low-intensity turbulent premixed propane–air flames. J Fluid Mech 2002; 462:209–43.

[102] Furukawa J, Williams F. Flamelet effects on local flow in turbulent premixed Bunsen flames. Combust Sci Technol 2003;175:1835–58.

[103] Furukawa J, Suzuki T, Hirano T, Williams F. Investigation of flamelets in a turbulent premixed flame with a 4-element electrostatic probe and a 2-D LDV. Combust Sci Technol 2001;170:151–68.

[104] Mansour MS, Chen YC, Peters N. Highly strained turbulent rich methane flames stabilized by hot combustion products. Combust Flame 1999;116:136–53.

[105] Shepherd IG, Cheng RK. The burning rate of premixed flames in moderate and intense turbulence. Combust Flame 2001;127:2066–75.

[106] Ikeda Y, Kojima J, Nakajima T, Akamatsu F, Katsuki M. Measurement of the local flame-front structure of turbulent premixed flames by local chemilumenscence. Proc Combust Inst 2000;28:343–50.

[107] Sokolik AS. Self-ignition, flame and detonation in gases. Moscow: AN SSSR; 1960 (in Russian; translated from Russian by Kaner N, edited by Hardin R, Jerusalem: Israel Program for Scientific Translations; available from the Office of Technical Services, U.S. Dept. of Commerce, Washington).

[108] Karpov VP, Sokolik AS. Ignition limits in turbulent gas mixtures. Doklady Phys Chem 1961;141:866–9.

[109] Sokolik AS, Karpov VP, Semenov ES. Turbulent combustion of gases. Combust, Explos, Shock Waves 1967;3:36–45.

[110] Karpov VP, Severin ES. Effects of molecular-transport coefficients on the rate of turbulent combustion. Combust, Explos, Shock Waves 1980;16:41–6.

[111] Abdel-Gayed RG, Bradley D, Hamid MN, Lawes M. Lewis number effects on turbulent burning velocity 20th Symposium (international) on combustion. Pittsburgh, PA: The Combustion Institute; 1984 p. 505–12.

[112] Kido H, Kitagawa T, Nakashima K, Kato K. An improved model of turbulent mass burning velocity. Mem Fac Eng, Kyushu Univ 1989;49:229–47.

[113] Bourguignon E, Kostiuk LW, Michou Y, Gökalp I. Experimentally measured burning rates of premixed turbulent flames. 26th Symposium (international) on combustion. Pittsburgh, PA: The Combustion Institute; 1998. p. 447–53.

[114] Yang SI, Shy SS. Global quenching of premixed CH_4/air flames: effects of turbulent straining, equivalence ratio, and radiative heat loss. Proc Combust Inst 2002;29:1841–7.

[115] Karpov VP, Severin ES. Turbulent combustion of hydrogen–hydrocarbon–air mixtures. Fizika Goreniya i Vzryva 1981; 17(1):137–8 (in Russian).

[116] Kido H, Huang S, Tanoue K, Nitta T. Improvement of lean hydrocarbon mixtures combustion performance by hydrogen addition and its mechanisms. Proceedings of the fourth international symposium on diagnostics and modeling of combustion in internal combustion engines—COMODIA94. Yokohama: JSME; 1994. p. 119–24.

[117] Betev AS, Karpov VP, Lipatnikov AN, Vardosanidze ZP. Hydrogen combustion in engines and preferential diffusion effects in laminar and turbulent flames. Archivum Combust 1995;15:199–227.

[118] Wohl K, Shore L. Experiments with butane–air and methane–air flames. Ind Eng Chem 1955;47:828–34.

[119] Wohl K, Shore L, von Rosenberg H, Weil CW. The burning velocity of turbulent flames. 4th Symposium (international) on combustion. Baltimore: Williams and Wilkins; 1953. p. 620–35.

[120] Markstein GH. Cell structure of propane flames in tubes. J Chem Phys 1949;17:428–9.

[121] Markstein GH. Experimental and theoretical studies of flame front stability. J Aeronaut Sci 1951;18:199–220.
[122] Markstein GH. Instability phenomena in combustion waves 4th Symposium (international) on combustion. Baltimore: Williams and Wilkins; 1953 p. 44–59.
[123] Zel'dovich YB. Theory of gas combustion and detonation. Moscow: AN SSSR; 1944 (in Russian).
[124] Clusius K. Die verwendung von deuterium und 'flammen-flammenfärbern' zur aufklärung des mechanismus der wasserstoffverbrennung in der nähe der unteren zündgrenze. Chimia 1950;4(7):151–4 (in German).
[125] Manton J, von Elbe G, Lewis B. Nonisotropic propagation of combustion waves in explosive gas mixtures and the development of cellular flames. J Chem Phys 1952;20:153–7.
[126] Kozachenko LC. Burning of benzene–air mixtures in turbulent flow. The third all-union congress on combustion theory, vol. 1. Moscow: AN SSSR; 1960. p. 126–37 (in Russian).
[127] Palm-Leis A, Strehlow RA. On the propagation of turbulent flames. Combust Flame 1969;13:111–29.
[128] Baev VK, Tretjakov PK. Calculation of flame position in turbulent flow. Izvestia SO AN SSSR 1969;3(1):32–7 (in Russian).
[129] Baev VK, Tretjakov PK. Characteristic burning times of fuel–air mixtures. Combust, Explos, Shock Waves 1968;4: 208–14.
[130] Zel'dovich YB, Frank-Kamenetskii DA. Turbulent and heterogeneous combustion. Moscow: MMI; 1947 (in Russian).
[131] Buriko YY, Kuznetsov VR. Effect of diffusional stratification on the combustion of a homogeneous mixture in laminar and turbulent flow. Combust, Explos, Shock Waves 1976;12: 348–55.
[132] Kuznetsov VR, Sabel'nikov VA. Combustion characteristics of mixed gases in a strongly turbulent flow. Combust, Explos, Shock Waves 1977;13:425–34.
[133] Kuznetsov VR. Limiting laws of propagation of a turbulent flame. Combust, Explos, Shock Waves 1982;18:172–9.
[134] Kuzin AF, Talantov AV. On the mechanism and characteristics of combustion in turbulent flow of homogeneous mixture. In: Combustion and explosion. Moscow: Nauka; 1977. p. 356–60 (in Russian).
[135] Karpov VP, Lipatnikov AN. On effect of molecular thermal conductivity and diffusion on premixed combustion. Doklady Phys Chem 1995;341:83–5.
[136] Karpov VP, Lipatnikov AN, Zimont VL. Influence of molecular heat and mass transfer processes on premixed turbulent combustion. In: Chan SH, editor. Transport phenomena in combustion, 1. Washington, DC: Taylor & Francis; 1996. p. 629–40.
[137] Karpov VP, Lipatnikov AN, Zimont VL. A test of an engineering model of premixed turbulent combustion. 26th Symposium (international) on combustion. Pittsburgh, PA: The Combustion Institute; 1996. p. 249–57.
[138] Karpov VP, Lipatnikov AN, Zimont VL. Flame curvature as a determinant of preferential diffusion effects in premixed turbulent combustion. In: Sirignano WA, Merzhanov AG, De Luca L, editors. Advances in combustion science: in honor of Ya.B. Zel'dovich. Progress in astronautics and aeronautics, vol. 173, 1997. p. 235–50.
[139] Lipatnikov AN. Modeling of the influence of mixture properties on premixed turbulent combustion. In: Roy GD, Frolov SM, Givi P, editors. Advanced computation and analysis of combustion. Moscow: ENAS; 1997. p. 335–59.
[140] Lipatnikov AN, Chomiak J. Lewis number effects in premixed turbulent combustion and highly perturbed laminar flames. Combust Sci Technol 1998;137:277–98.
[141] Talantov AV. Combustion in flows.. Moscow: Mashinostroenie; 1978 (in Russian).
[142] Karpov VP, Severin ES. Turbulent combustion velocities of gas mixtures for describing combustion in engines. In: Combustion of heterogeneous and gas systems. Chernogolovka: OIKhF; 1977. p. 74–76 (in Russian).
[143] Karpov VP, Severin ES. Turbulent burning of nearly limiting mixtures of hydrogen. Doklady Phys Chem 1978;239: 208–10.
[144] Karpov VP, Severin ES. Turbulent burn-up rates of propane–air flames determined in a bomb with agitators. Combust, Explos, Shock Waves 1978;14:158–63.
[145] Karpov VP, Severin ES. Turbulent combustion of mixtures of hydrogen and carbon monoxide. Combust, Explos, Shock Waves 1982;18:643–4.
[146] Kido H, Tanoue K, Nakahara M, Kido H, Inoe T. Experimental study of the turbulent combustion mechanism of non-stoichiometric mixtures. JSAE Rev 1996;17:361–7.
[147] Kido H, Nakahara M. A model of turbulent burning velocity taking the preferential diffusion effect into consideration. JSME Int J 1998;41:666–73.
[148] Nakahara M, Kido H. A study of the premixed turbulent combustion mechanism taking the preferential diffusion effect into consideration. Mem Fac Eng, Kyushu Univ 1998;58:55–82.
[149] Kido H, Nakahara M, Hashimoto J. A turbulent burning velocity model taking account for preferential diffusion effect. Proceedings of the fourth international symposium on diagnostics and modeling of combustion in internal combustion engines—COMODIA98. Tokyo: JSME; 1998. p. 249–54.
[150] Kido H, Nakahara M, Barat D, Hashimoto J. Effect of preferential diffusion on turbulent burning velocity of fuel/oxygen/inert gas mixtures. Mem Fac Eng, Kyushu Univ 1999;59:231–41.
[151] Kido H, Nakashima K, Nakahara M, Hashimoto J. Experimental study of the configuration and propagation characteristics of premixed turbulent flame. JSAE Rev 2001;22: 131–8.
[152] Kido H, Nakahara M, Hashimoto J, Barat D. Turbulent burning velocities of two-component fuel mixtures of methane, propane, and hydrogen. JSME Int J 2002;45: 355–62.
[153] Liu Y, Lenze B. The influence of turbulence on the burning velocity of premixed CH_4–H_2 flames with different laminar burning velocities. 22nd Symposium (international) on combustion. Pittsburgh, PA: The Combustion Institute; 1988. p. 747–54.
[154] Leuckel W, Nastoll W, Zarzalis N. Experimental investigation of the influence of turbulence on the transient premixed flame propagation inside closed vessels. 23rd Symposium (international) on combustion. Pittsburgh, PA: The Combustion Institute; 1990. p. 729–34.
[155] Liu Y, Ziegler M, Lenze B. Burning velocity of premixed flames as a function of turbulence and physico-chemical fuel

properties. In: Proceedings of the Anglo-German combustion symposium. Cambridge: The British Section of the Combustion Institute; 1993. p. 64–7.

[156] Ziegler M, Lenze B. The influence of turbulence conditions and molecular transport phenomena on turbulent burning rates of premixed flames in a stagnation flow system. In: Book of abstracts, Joint meeting of the French and German sections of the combustion institute. Mulhouse: The French Section of the Combustion Institute; 1995.

[157] Ziegler M, Lenze B. Lewis number effects on turbulent premixed combustion investigated using LDV and laser tomography. In: Chan CH, editor. Transport phenomena in combustion, vol. 1. Washington, DC: Taylor & Francis; 1996. p. 617–28.

[158] Ziegler M. Untersuchungen zur ansbreitung stationärer, turbulenter vormischflammen unter besonderer berücksichtigung bevorzugter diffusion. Dissertation, Universität Karlsruhe; 1998 (in German).

[159] Brutscher T, Zarzalis N, Bockhorn H. An experimentally based approach for the space-averaged laminar burning velocity used for modeling premixed turbulent combustion. Proc Combust Inst 2002;29:1825–32.

[160] Wu M-S, Kwon A, Driscoll JF, Faeth GM. Turbulent premixed hydrogen/air flames at high Reynolds numbers. Combust Sci Technol 1990;73:327–50.

[161] Wu M-S, Kwon A, Driscoll JF, Faeth GM. Preferential diffusion effects on the surface structure of turbulent premixed hydrogen/air flames. Combust Sci Technol 1991; 78:69–96.

[162] Sivashinsky GI. Nonlinear analysis of hydrodynamic instability in laminar flames. I. Derivation of basic equations. Acta Astronautica 1977;4:1177–206.

[163] Sivashinsky GI. On self-turbulization of a laminar flame. Acta Astronautica 1979;6:569–91.

[164] Clavin P, Williams FA. Effects of molecular diffusion and of thermal expansion on the structure and dynamics of premixed flames in turbulent flows of large scale and low intensity. J Fluid Mech 1982;116:251–82.

[165] Clavin P. Dynamical behavior of premixed flame fronts in laminar and turbulent flows. Prog Energy Combust Sci 1985; 11:1–59.

[166] Searby G, Clavin P. Weakly turbulent, wrinkled flames in premixed gases. Combust Sci Technol 1986;46:167–93.

[167] Aldredge RC, Williams FA. Influence of wrinkled premixed-flame dynamics on large-scale, low-intensity turbulent flow. J Fluid Mech 1991;228:487–511.

[168] Peters N, Williams FA. Coherent structures in turbulent combustion. In: Jimenez J, editor. The role of coherent structures in modelling turbulence and mixing. Lecture notes in physics, vol. 136. Berlin: Springer; 1981. p. 364–93.

[169] Abdel-Gayed RG, Al-Khishali KJ, Bradley D. Turbulent burning velocities and flame straining in explosions. Proc R Soc Lond 1984;A391:391–414.

[170] Abdel-Gayed RG, Bradley D. A two-eddy theory of premixed turbulent flame propagation. Phil Trans R Soc Lond 1981;A301:1–25.

[171] Tromans PS. The ASME symposium on fluid mechanics of combustion systems. Boulder: ASME; 1981 p. 201–6.

[172] Paul RN, Bray KNC. Study of premixed turbulent combustion including Landau–Darrieus instability effects. 26th Symposium (international) on combustion. Pittsburgh, PA: The Combustion Institute; 1996. p. 259–66.

[173] Bychkov V. Importance of the Darrieus–Landau instability for strongly corrugated turbulent flames. Phys Rev E 2003; 68:066304.

[174] Bray KNC. Methods of including realistic chemical reaction mechanisms in turbulent combustion models. In: Complex chemical reaction systems. Mathematical modelling and simulation. Berlin: Springer; 1987. p. 356–75.

[175] Abdel-Gayed RG, Bradley D, Lau AKC. The straining of premixed turbulent flames. 22nd Symposium (international) on combustion. Pittsburgh, PA: The Combustion Institute; 1988. p. 731–8.

[176] Bradley D, Lau AKC, Lawes M. Flame stretch rate as a determinant of turbulent burning velocity. Phil Trans R Soc Lond 1992;A338:359–87.

[177] Bradley D, Gaskell PH, Gu XJ. Application of a Reynolds stress, stretched flamelet, mathematical model to computations of turbulent burning velocities: comparisons with experiments and the predictions of other models. Combust Flame 1994;96:221–48.

[178] Bradley D, Gaskell PH, Gu XJ. The modeling of aerodynamic strain rate and flame curvature effects in premixed turbulent combustion. 27th Symposium (international) on combustion. Pittsburgh, PA: The Combustion Institute; 1998. p. 849–56.

[179] Bradley D. Problems of predicting turbulent burning rates. Combust Theory Modell 2002;6:361–82.

[180] Bray KNC, Cant RS. Some applications of Kolmogorov's turbulence research in the field of combustion. Proc R Soc Lond 1991;A434:217–40.

[181] Bray KNC, Peters N. Laminar fiamelets in turbulent flames. In: Libby PA, Williams FA, editors. Turbulent reacting flows. London: Academic Press; 1994. p. 63–113.

[182] Kostiuk LW, Bray KNC. Mean effects of stretch on laminar flamelets in a premixed turbulent flame. Combust Sci Technol 1994;95:193–212.

[183] Clavin P. Dynamics of combustion fronts in premixed gases: from flame to detonation. Proc Combust Inst 2000;28: 569–85.

[184] Law CK, Sung CJ. Structure, aerodynamics, and geometry of premixed flames. Prog Energy Combust Sci 2000;26: 459–505.

[185] Williams FA. Progress in knowledge of flamelet structure and extinction. Prog Energy Combust Sci 2000;26:657–82.

[186] Gu XJ, Haq MZ, Lawes M, Woolley R. Laminar burning velocity and Markstein lengths of methane–air mixtures. Combust Flame 2000;121:41–58.

[187] Durox D, Ducruix S, Candel S. Experiments on collapsing cylindrical flames. Combust Flame 2001;125:982–1000.

[188] Kwon S, Faeth GM. Flame/stretch interactions of premixed hydrogen-fueled flames: measurements and predictions. Combust Flame 2001;134:590–610.

[189] Davis SG, Quinard J, Searby G. A numerical investigation of stretch effects in counterflow, premixed laminar flames. Combust Theory Modell 2001;5:353–62.

[190] Davis SG, Quinard J, Searby G. Determination of Markstein numbers in counterfiow premixed flames. Combust Flame 2002;130:112–22.

[191] Davis SG, Quinard J, Searby G. Markstein numbers in counterflow, methane– and propane–air flames: a computational study. Combust Flame 2002;130:123–36.

[192] Baillot F, Durox D, Demare D. Experiments on imploding spherical flames: effects of curvature. Proc Combust Inst 2002;29:1453–60.

[193] Groot GRA, de Goey LPH. A computational study of propagating spherical and cylindrical flames. Proc Combust Inst 2002;29:1445–51.

[194] Ibaretta AF, Driscoll JF, Feikema DA. Markstein numbers of negatively stretched premixed flames: microgravity measurements and computations. Proc Combust Inst 2002;29: 1435–43.

[195] Rozenchan G, Zhu DL, Law CK, Tse SD. Outward propagation, burning velocities, and chemical effects of methane flames up to 60 atm. Proc Combust Inst 2002;29: 1461–9.

[196] Smith TM, Menon S. Model simulations of freely propagating turbulent premixed flames. 26th Symposium (international) on combustion. Pittsburgh, PA: The Combustion Institute; 1996. p. 299–306.

[197] Kerstein AR. Linear-eddy modelling of turbulent transport. Part 6. Microstructure of diffusive scalar mixing fields. J Fluid Mech 1991;231:361–94.

[198] Swaminathan N, Bilger RW. Analyses of conditional moment closure for turbulent premixed flames. Combust Theory Modell 2001;5:241–60.

[199] Klimenko AY, Bilger RW. Conditional moment closure for turbulent combustion. Prog Energy Combust Sci 1999;25: 595–687.

[200] Baum M, Poinsot T, Haworth DC, Darabiha N. Direct numerical simulation of $H_2/O_2/N_2$ flames with complex chemistry in two-dimensional turbulent flows. J Fluid Mech 1994;281:1–32.

[201] Lipatnikov AN, Chomiak J. Turbulent burning velocity and speed of developing, curved, and strained flames. Proc Combust Inst 2002;29:2113–21.

[202] Wang CH, Ueng GJ, Tsay MS. An experimental determination of the laminar burning velocities and extinction stretch rates of benzene/air flames. Combust Flame 1998;113:242–8.

[203] Davis SG, Law CK. Determination of and fuel structure effects on laminar flame speeds of C_1 to C_8 hydrocarbons. Combust Sci Technol 1998;140:427–49.

[204] Vagelopoulos CM, Egolfopoulos FN, Law CK. Further considerations on the determination of laminar flame speeds with the counterflow twin flame technique. 25th Symposium (international) on combustion. Pittsburgh, PA: The Combustion Institute; 1994. p. 1341–7.

[205] Shy SS, Lin WJ, Wei JC. An experimental correlation of turbulent burning velocities for premixed turbulent methane–air combustion. Proc R Soc Lond 2000;A456:1997–2019.

[206] Vagelopoulos CM, Egolfopoulos FN. Direct experimental determination of laminar flame speeds. 27th Symposium (international) on combustion. Pittsburgh, PA: The Combustion Institute; 1998. p. 513–9.

[207] Aung KT, Hassan ML, Faeth GM. Effects of pressure and nitrogen dilution on flame/stretch interactions of laminar premixed $H_2/O_2/N_2$ flames. Combust Flame 1998;112:1–15.

[208] Koroll JW, Kumar RK, Bolwles EM. Burning velocities of hydrogen–air mixtures. Combust Flame 1993;94:330–40.

[209] Haworth DC, Poinsot T. Numerical simulations of Lewis number effects in turbulent premixed flames. J Fluid Mech 1992;244:405–36.

[210] Rutland CJ, Trouvé A. Direct simulations of premixed turbulent flames with nonunity Lewis numbers. Combust Flame 1993;94:41–57.

[211] Trouvé A, Poinsot T. Evolution equation for flame surface density in turbulent premixed combustion. J Fluid Mech 1994;278:1–31.

[212] Betev AS, Karpov VP, Semenov ES. Nonsteady phenomena in propagation of highly curved flames. Chem Phys Reports 1997;16:1861–8.

[213] Lipatnikov AN, Chomiak J. A theoretical study of premixed turbulent flame development. Proc Combust Inst 2004;30 (in press).

[214] Taylor GI. Statistical theory of turbulence. IV. Diffusion in a turbulent air stream. Proc R Soc Lond 1935;A151:465–78.

[215] Brodkey RS. The phenomena of fluid motions. London: Addison-Wesley; 1967.

[216] Hinze JO. Turbulence. 2nd ed. New York: McGraw-Hill; 1975.

[217] Monin AS, Yaglom AM. Statistical fluid mechanics: mechanics of turbulence, vol. 2. Cambridge: The MIT Press; 1975.

[218] Lewis B, von Elbe G. Combustion, flames and explosions of gases. New York: Academic Press; 1961.

[219] Shchetinkov ES. Physics of gas combustion. Moscow: Nauka; 1965 (English translation FTD-HT-23-496-48).

[220] Goix P, Paranthoen P, Trinite M. A tomographic study of measurements in a V-shaped H_2-air flame and a Lagrangian interpretation of the turbulent flame brush thickness. Combust Flame 1990;81:229–41.

[221] Boyer L, Quinard J. On the dynamics of anchored flames. Combust Flame 1990;82:51–65.

[222] Ashurst WT, Peters N, Smooke MD. Numerical simulation of turbulent flame structure with non-unity Lewis number. Combust Sci Technol 1987;53:339–75.

[223] Lee T-W, North GL, Santavicca DA. Curvature and orientation statistics of turbulent premixed flame fronts. Combust Sci Technol 1992;84:121–32.

[224] Matalon M, Matkowsky BJ. Flames as gas dynamic discontinuities. J Fluid Mech 1982;124:239–60.

[225] Buckmaster JD, Ludford GSS. Theory of laminar flames. Cambridge: Cambridge University Press; 1982.

[226] Zel'dovich YB, Barenblatt GI, Librovich VB, Makhviladze GM. The mathematical theory of combustion and explosions. New York: Plenum; 1985.

[227] Markstein GH. Nonsteady flame propagation. Oxford: Pergamon; 1964.

[228] Sivashinsky GI. Instabilities, pattern formation, and turbulence in flames. Annual Rev Fluid Mech 1983;15:179–99.

[229] Jackson TL, Kapila AK. Thermal expansion effects on perturbed premixed flames: a review. In: Ludford GSS, editor. Reacting flows. Lectures in applied mathematics, vol. 24. Berlin: Springer; 1986. p. 325–47.

[230] Hertzberg M. Selective diffusional demixing: occurrence and size of cellular flames. Prog Energy Combust Sci 1989;15: 203–39.

[231] Clavin P. Premixed combustion and gas dynamics. Annual Rev Fluid Mech 1994;26:321–52.

[232] Joulin G, Vidal P. Introduction to the instabilities of flames, shocks, and detonations. In: Godréche G, Manneville P, editors. Hydrodynamics and nonlinear stabilities. Cambridge: Cambridge University Press; 1998. p. 493–673.

[233] Sivashinsky GI. Some developments in premixed combustion modeling. Proc Combust Inst 2002;29:1737–61.
[234] Class AG, Matkowsky BJ, Klimenko AY. Stability of planar flames as gasdynamic discontinuities. J Fluid Mech 2003; 491:51–63.
[235] Lewis B, von Elbe G. On the theory of flame propagation. J Chem Phys 1934;2:537–46.
[236] Minaev SS, Fursenko R, Ju Y, Law CK. Stability analysis of near-limit stretched flames. J Fluid Mech 2003;488:225–44.
[237] Smithells S, Ingle K. The structure and chemistry of flames. J Chem Soc 1882;61:204–17.
[238] Smith FA, Pickering SF. Bunsen flames with unusual structure. Ind Eng Chem 1928;20:1012–3.
[239] Drozdov IP, Zel'dovich YB. Diffusion phenomena near flammability limits. Zhournal Fizicheskoi Khimii 1943; 17(3):134–44 (in Russian).
[240] Kokochashvili VI. Specific nature of combustion of hydrogen–bromine mixtures. Zhournal Fizicheskoi Khimii 1951; 25(2):445–53 (in Russian).
[241] Troshin YK, Shchelkin KI. Spherical flame-front structure and normal burning instability. Izvestia Akademii Nauk USSR, Otdelenie Tekhnicheskikh Nauk 1955;9:160–6 (in Russian).
[242] Karpov VP. Cellular flame structure under conditions of a constant-volume bomb and its relationship with vibratory combustion. Combust, Explos, Shock Waves 1965;1(3): 39–44.
[243] Babkin VS, V'yun AV, Kozachenko LS. Determination of burning velocity from the pressure record in a constant-volume bomb. Combust, Explos, Shock Waves 1967;3: 221–5.
[244] Gussak LA, Sprintsina EN, Shchelkin KT. Stability of the normal flame front. Combust, Explos, Shock Waves 1968;4: 202–7.
[245] Gussak LA, Istratov AG, Librovich VB, Sprintsina EN. Development of perturbations at the surface of a flame propagating from a central point ignition source in a closed vessel. Combust, Explos, Shock Waves 1977;13:15–18.
[246] Sabathier F, Boyer L, Clavin P. Experimental study of a weak turbulent premixed flame. Prog Astronautics Aeronautics 1981;76:246–58.
[247] Karpov VP. Cellular flame structure and turbulent combustion. Combust, Explos, Shock Waves 1982;18:109–11.
[248] Bradley D, Sheppard CGW, Woolley R, Greenhalgh DA, Lockett RD. The development and structure of flame instabilities and cellularity at low Markstein number explosions. Combust Flame 2000;122:195–209.
[249] Kaiser C, Liu J-B, Ronney PD. Diffusive-thermal instability of counterflow flames at low Lewis number. AIAA Paper, 2000-0576; 2000.
[250] Simon DM, Wong EL. Burning velocity measurement. J Chem Phys 1953;21:936–6.
[251] Groff EG. The cellular nature of confined spherical propane–air flames. Combust Flame 1982;48:51–62.
[252] Bradley D, Harper CM. The development of instabilities in laminar explosion flames. Combust Flame 1994;99:562–72.
[253] Kwon OC, Rozenchan G, Law CK. Cellular instabilities and self-acceleration of outwardly propagating spherical flames. Proc Combust Inst 2002;29:1775–83.
[254] Clanet C, Searby G. First experimental study of the Darrieus–Landau instability. Phys Rev Lett 1998;27:3867–70.
[255] Truffaut JM, Searby G. Experimental study of the Darrieus–Landau instability on an inverted-V flame, and measurement of the Markstein number. Combust Sci Technol 1999;149: 35–52.
[256] Darrieus G. Propagation d'un front de flamme. Unpublished work presented at La Technique Moderne, Paris; 1938.
[257] Landau LD. On the theory of slow combustion. Acta Psysicochimica USSR 1944;19:77–85.
[258] Landau LD, Lifshitz EM. Fluid mechanics. Oxford: Pergamon; 1987.
[259] Barenblatt GI, Zel'dovich YB, Istratov AG. On heat and diffusion effects in stability of laminar flames. Zhournal Prikladnoi Mekchaniki i Tekhnicheskoi Fiziki 1962;4:21–6 (in Russian).
[260] Sivashinsky GI. Diffusional-thermal theory of cellular flames. Combust Sci Technol 1977;15:137–46.
[261] Sivashinsky GI. On a distorted flame front as a hydrodynamic discontinuity. Acta Astronautica 1976;3:889–918.
[262] Buckmaster JD. Slowly varying laminar flames. Combust Flame 1977;28:225–39.
[263] Buckmaster JD. The quenching of a deflargation wave held in front of a bluff body 17th Symposium (international) on combustion. Pittsburgh, PA: The Combustion Institute; 1979 p. 835–42.
[264] Class AG, Matkowsky BJ, Klimenko AY. A unified model of flames as gasdynamic discontinuities. J Fluid Mech 2003; 491:11–49.
[265] Bechtold JK, Matalon M. Effects of stoichiometry on stretched premixed flames. Combust Flame 1999;119: 217–32.
[266] Frankel ML, Sivashinsky GJ. The effect of viscosity on hydrodynamic stability of a plane flame front. Combust Sci Technol 1982;29:207–24.
[267] Pelce P, Clavin P. Influence of hydrodynamics and diffusion upon the stability limits of laminar premixed flames. J Fluid Mech 1982;124:219–37.
[268] Clavin P, Joulin G. Premixed flames in large-scale and high intensity turbulent flow. J Phys Lett 1983;44:L-1.
[269] Candel S, Poinsot T. Flame stretch and the balance equation for the flame area. Combust Sci Technol 1990;170:1–15.
[270] Clavin P, Garcia-Ybarra P. The influence of the temperature dependence of diffusivities on the dynamics of flame fronts. J Mechanique Appliquee 1983;2:245–63.
[271] Frankel ML, Sivashinsky GJ. On effects due to thermal expansion and Lewis number in spherical flame propagation. Combust Sci Technol 1983;31:131–8.
[272] Lipatnikov AN. Some issues of using Markstein number for modeling premixed turbulent combustion. Combust Sci Technol 1996;119:131–54.
[273] Clavin P, Joulin G. Flamelet library for turbulent wrinkled flames. In: Borghi R, Murthy SNB, editors. Turbulent reactive flows. Lecture notes in engineering. Berlin: Springer; 1989. p. 213–40.
[274] Tien JH, Matalon M. On the burning velocity of stretched flames. Combust Flame 1991;84:238–48.
[275] Bechtold JK, Matalon M. The dependence of the Markstein length on stoichiometry. Combust Flame 2001;127:1906–13.
[276] Groot GRA, van Qijen JA, de Goey LPH, Seshardi K, Peters N. The effects of strain and curvature on the mass burning rate of premixed laminar flames. Combust Theory Modell 2002;6:675–95.

[277] Bray KNC. Studies of the turbulent burning velocity. Proc R Soc Lond 1990;A431:315–35.
[278] Joulin G, Mitani T. Linear stability analysis of two-reactant flames. Combust Flame 1981;40:235–46.
[279] Jackson TL. Effect of thermal expansion on the stability of two-reactant flames. Combust Sci Technol 1987;53:51–4.
[280] Clavin P, Joulin G. High-frequency response of premixed flames to weak stretch and curvature: a variable density analysis. Combust Theory Modell 1997;1:429–46.
[281] Keller D, Peters N. Transient pressure effects in the evolution equation for premixed flame fronts. Theor Comput Fluid Dynam 1994;6:141–59.
[282] Matalon M, Cui C, Bechtold JK. Hydrodynamic theory of premixed flames: effects of stoichiometry, variable transport coefficients and arbitrary reaction orders. J Fluid Mech 2003; 487:179–200.
[283] Joulin G. On the response of premixed flame to time-dependent stretch and curvature. Combust Sci Technol 1994; 97:219–29.
[284] Klimenko AY, Class AG. On premixed flames as gasdynamic discontinuities: a simple approach to derive their propagation speed. Combust Sci Technol 2000;160:23–33.
[285] Klimenko AY, Class AG. Propagation of nonstationary curved and stretched premixed flames with multistep reaction mechanisms. Combust Sci Technol 2002;174(8):1–43.
[286] Chung SH, Law CK. An integral analysis of the structure and propagation of stretch premixed flames. Combust Flame 1988;72:325–36.
[287] de Goey LPH, ten Thije Boonkkamp JHM. A mass-based definition of flame stretch for flames with finite thickness. Combust Sci Technol 1997;122:399–405.
[288] de Goey LPH, Mallens RMM, ten Thije Boonkkamp JHM. An evaluation of different contributions to flame stretch for stationary premixed flames. Combust Flame 1997;110: 54–66.
[289] de Goey LPH, ten Thije Boonkkamp JHM. A flamelet description of premixed laminar flame and the relation with flame stretch. Combust Flame 1999;119:253–71.
[290] ten Thije Boonkkamp JHM, de Goey LPH. A flamelet model for premixed stretched flames. Combust Flame 1999;149: 183–200.
[291] Markstein GH. Nonisotropic propagation of combustion waves. J Chem Phys 1952;20:1051–3.
[292] Petersen RE, Emmons KW. The stability of laminar flames. Phys Fluids 1961;4:456–64.
[293] Shchelkin KI. Instability of combustion and detonation in gases. Uspekhi Fizicheskikh Nauk 1965;87:273–302 (in Russian).
[294] Zel'dovich YB. On some effect stabilizing the distorted flame front. Zhournal Prikladnoi Mekchaniki i Tekhnicheskoi Fiziki 1966;1:102–4 (in Russian).
[295] Sivashinsky GI, Clavin P. On the nonlinear theory of hydrodynamic instability in flames. J Phys (France) 1987; 48:193–8.
[296] Frankel ML. An equation of surface dynamics modeling flame fronts as density discontinuities in potential flows. Phys Fluids A 1990;2:1879–83.
[297] Thual O, Frish U, Henon M. Application of the pole-decomposition to an equation describing the dynamics of wrinkled flame fronts. J Phys (France) 1985;46:1485–94.
[298] Renardy M. A model equation in combustion theory exhibiting an infinite number of secondary bifurcations. Physica D 1987;28:155–67.
[299] Minaev SS, Pirogov EA, Sharypov OV. Velocity of flame propagation upon development of hydrodynamic instability. Combust, Explos, Shock Waves 1993;26:679–84.
[300] Michelson DM, Sivashinsky GI. Nonlinear analysis of hydrodynamic instability in laminar flames. Part II. Numerical experiments. Acta Astronautica 1977;4:1207–21.
[301] Cambray P, Joulin G. On moderately-forced premixed flames. 24th Symposium (international) on combustion. Pittsburgh, PA: The Combustion Institute; 1992. p. 61–7.
[302] Cambray P, Joulin G. Length scales of wrinkling of weakly-forced, unstable premixed flames. Combust Sci Technol 1994;97:405–28.
[303] Cambray P, Joulain K, Joulin G. Mean evolution of wrinkle wavelengths in a model of weakly turbulent premixed flame. Combust Sci Technol 1994;103:265–82.
[304] Joulin G. On the hydrodynamic stability of curved premixed flames. J Phys (France) 1989;50:1069–82.
[305] Karlin V. Cellular flames may exhibit a non-modal transient instability. Proc Combust Inst 2002;29:1537–42.
[306] Zhdanov SK, Trubnikov BA. Nonlinear theory of instability of a flame front. J Exp Theor Phys 1989;68:65–77.
[307] Matalon M, Metzener P. The propagation of premixed flames in closed tubes. J Fluid Mech 1997;336:331–50.
[308] Bychkov V. Nonlinear equation for a curved stationary flame and the flame velocity. Phys Fluids 1998;10:2091–8.
[309] Bychkov V. Velocity of turbulent flamelets with realistic fuel expansion. Phys Rev Lett 2000;84:6122–5.
[310] Bychkov V, Liberman M, Reinmann R. Velocity of turbulent flamelets of finite thickness. Combust Sci Technol 2001;168: 113–29.
[311] Kazakov KA, Liberman MA. Nonlinear theory of flame front instability. Combust Sci Technol 2002;174(7):129–51.
[312] Kazakov KA, Liberman MA. Effect of vorticity production on the structure and velocity of curved flames. Phys Rev Lett 2002;88:064502.
[313] Kazakov KA, Liberman MA. Nonlinear equation for curved stationary flames. Phys Fluids 2002;14:1166–81.
[314] Bradley D, Hicks RA, Lawes M, Sheppard CGW, Woolley R. The measurement of laminar burning velocities and Markstein numbers for iso-octane–air and iso-octane-*n*-heptane–air mixtures at elevated temperatures and pressures in an explosion bomb. Combust Flame 1998;115:126–44.
[315] Filyand L, Sivashinsky G, Frankel ML. On self-acceleration of outward propagating wrinkled flames. Physica D 1994;72: 110–8.
[316] Gostintsev YA, Istratov AG, Shulenin YV. Self-similar propagation of a free turbulent flame in mixed gas mixtures. Combust Explos, Shock Waves 1988;24:563–8.
[317] Gostintsev YA, Istratov AG, Kidin NI, Fortov VE. Self-turbulization of gas flames: an analysis of experimental results. High Temp 1999;37(2):282–8.
[318] Bradley D. Instabilities and flame speeds in large-scale premixed gaseous explosions. Phil Trans R Soc Lond 1999; 357:3567–81.
[319] Bradley D, Cresswell TM, Puttock JS. Flame acceleration due to flame-induced instabilities in large-scale explosions. Combust Flame 2001;124:551–9.

[320] Aldredge RC, Zuo B. Flame acceleration associated with the Darrieus–Landau instability. Combust Flame 2001;127: 2091–101.

[321] Addabbo R, Bechtold JK, Matalon M. Wrinkling of spherically expanding flames. Proc Combust Inst 2002;29: 1527–35.

[322] D'Angelo Y, Joulin G, Boury G. On model evolution equations for the whole surface of three-dimensional expanding wrinkled premixed flames. Combust Theory Modell 2000;4:317–38.

[323] Bechtold JK, Matalon M. Hydrodynamic and diffusion effects on the stability of spherically expanding flames. Combust Flame 1987;67:77–90.

[324] Istratov AG, Librovich VB. On the stability of gasdynamic discontinuities associated with chemical reaction. The case of a spherical flame. Astronautica Acta 1969;14:453–67.

[325] Jackson TL, Kapila AK. Effect of thermal expansion on the stability of a plane, freely propagating flame. Combust Sci Technol 1984;41:191–201.

[326] Denet B, Haldenwang P. Numerical study of thermal-diffusive instability of premixed flames. Combust Sci Technol 1992;86:199–221.

[327] Denet B, Haldenwang P. A numerical study of premixed flames Darrieus–Landau instability. Combust Sci Technol 1995;104:143–67.

[328] Lasseigne DG, Jackson TL, Jameson L. Stability of freely propagating flames revisited. Combust Theory Modell 1999; 3:591–611.

[329] Sharpe GJ. Linear stability of premixed flames: reactive Navier-Stokes equations with finite activation temperature and arbitrary Lewis number. Combust Theory Modell 2003; 7:45–65.

[330] Kadowaki S. The influence of hydrodynamic instability on the structure of cellular flames. Phys Fluids 1999;11: 3426–33.

[331] Kadowaki S. Numerical study on the formation of cellular premixed flames at high Lewis numbers. Phys Fluids 2000; 12:2352–9.

[332] Chomiak J, Zhou G. A numerical study of large amplitude baroclinic instabilities of flames 26th Symposium (international) on combustion. Pittsburgh, PA: The Combustion Institute; 1996 p. 883–9.

[333] Ma LZ, Chomiak J. Flame shapes and speeds for hydrodynamically unstable laminar flames. 27th Symposium (international) on combustion. Pittsburgh, PA: The Combustion Institute; 1998. p. 545–54.

[334] Helenbrook BT, Law CK. The role of Landau–Darrieus instability in large scale flows. Combust Flame 1999;117: 155–69.

[335] Ashurst WT, Sivashinsky GI, Kerstein AR. Flame front propagation in nonsteady hydrodynamic fields. Combust Sci Technol 1988;62:273–84.

[336] Kerstein AR, Ashurst WT, Williams FA. Field equation for interface propagation in an unsteady homogeneous flow field. Phys Rev A 1988;37:2728–31.

[337] Denet B. Frankel equation for turbulent flames in the presence of a hydrodynamic instability. Phys Rev E 1997; 55:6911–6.

[338] Zaitsev M, Bychkov V. Effect of the Darrieus–Landau instability on turbulent flame velocity. Phys Rev E 2002;66: 026310.

[339] Akkerman V, Bychkov V. Turbulent flame and the Darrieus–Landau instability in a three-dimensional flow. Combust Theory Modell 2003;7:767–94.

[340] Kwon S, Wu MS, Driscoll JF, Faeth GM. Flame surface properties of premixed flames in isotropic turbulence: measurements and numerical simulations. Combust Flame 1992;88:221–38.

[341] Aung KT, Hassan ML, Kwon S, Tseng LK, Kwon OC, Faeth GM. Flame/stretch interactions in laminar and turbulent premixed flames. Combust Sci Technol 2002;174: 61–99.

[342] Yoshida A, Tsuji H. Characteristic scale of wrinkles in turbulent premixed flames. 19th Symposium (international) on combustion. Pittsburgh, PA: The Combustion Institute; 1982. p. 403–11.

[343] Yoshida A, Tsuji H. Mechanism of flame wrinkling in turbulent premixed flames. 20th Symposium (international) on combustion. Pittsburgh, PA: The Combustion Institute; 1984. p. 445–51.

[344] Furukawa J, Maruta K, Nakamura T, Hirano T. Local reaction zone configuration of high intensity turbulent premixed flames. Combust Sci Technol 1993;90:267–80.

[345] Furukawa J, Hirano T. Fine structure of small-scale and high-intensity turbulent premixed flames. 25th Symposium (international) on combustion. Pittsburgh, PA: The Combustion Institute; 1994. p. 1233–9.

[346] Furukawa J, Maruta K, Hirano T. Flame front configuration of turbulent premixed flames. Combust Flame 1998;112: 293–301.

[347] Becker H, Monkhouse PB, Wolfrum J, Cant RS, Bray KNC, Maly R, et al. Investigation of extinction in unsteady flames in turbulent combustion by 2D-LIF of OH radicals and flamelet analysis. 23rd Symposium (international) on combustion. Pittsburgh, PA: The Combustion Institute; 1990. p. 817–23.

[348] Lee TW, North GL, Santavicca DA. Surface properties of turbulent premixed propane/air flames at various Lewis numbers. Combust Flame 1993;93:445–56.

[349] Lee TW, Lee JG, Nye DA, Santavicca DA. Local response and surface properties of premixed flames during interactions with Karman vortex streets. Combust Flame 1993;94: 146–60.

[350] Lee JG, Lee TW, Nye DA, Santavicca DA. Lewis number effects on premixed flames interacting with turbulent Karman vortex streets. Combust Flame 1995;100:161–8.

[351] Goix P, Shepherd IG. Lewis number effects in turbulent premixed flame structure. Combust Sci Technol 1993;91: 191–206.

[352] Kobayashi H, Tamura T, Maruta K, Niioka T. Burning velocity of turbulent premixed flames in a high-pressure environment. 26th Symposium (international) on combustion. Pittsburgh, PA: The Combustion Institute; 1996. p. 389–96.

[353] Kobayashi H, Nakashima T, Tamura T, Maruta K, Niioka T. Turbulence measurements and observations of turbulent premixed flames at elevated pressures up to 3.0 MPa. Combust Flame 1997;108:104–17.

[354] Kobayashi H, Kawabata Y, Maruta K. Experimental study on general correlation of turbulent burning velocity at high pressure. 27th Symposium (international) on combustion. Pittsburgh, PA: The Combustion Institute; 1998. p. 941–8.

[355] Kobayashi H, Kawazoe H. Flame instability effects on the smallest wrinkling scale and burning velocity of high-pressure turbulent premixed flames. Proc Combust Inst 2000;28:375–82.

[356] Renou B, Boukhalfa A, Puechberty D, Trinite M. Effects of stretch on the local structure of freely-propagating premixed low turbulent flames with various Lewis numbers. 27th Symposium (international) on combustion. Pittsburgh, PA: The Combustion Institute; 1998. p. 841–7.

[357] Renou B, Boukhalfa A, Puechberty D, Trinite M. Local scalar flame properties of freely propagating premixed turbulent flames at various Lewis numbers. Combust Flame 2000;123:507–21.

[358] Renou B, Boukhalfa A. An experimental study of freely propagating premixed flames at various Lewis numbers. Combust Sci Technol 2001;162:347–70.

[359] Chang NW, Shy SS, Yang SI, Yang TS. Spatially resolved flamelet statistics for reaction rate modeling using premixed methane–air flames in near-homogeneous turbulence. Combust Flame 2001;127:1880–94.

[360] Haq MZ, Sheppard CGW, Woolley R, Greenhalgh DA, Lockett RD. Wrinkling and curvature of laminar and turbulent premixed flames. Combust Flame 2002;131:1–15.

[361] Soika A, Dinkelacker F, Leipertz A. Pressure influence on the flame front curvature of turbulent premixed flames: comparison between experiment and theory. Combust Flame 2003;132:451–62.

[362] Chen YC, Bilger R. Experimental investigation of three-dimensional flame-front structure in premixed turbulent combustion—II: lean hydrogen/air bunsen flames. Combust Flame 2004 (in press).

[363] Echekki T, Chen JH. Unsteady strain rate and curvature effects in turbulent premixed methane–air flames. Combust Flame 1996;106:184–202.

[364] Echekki T, Chen JH, Gran I. The mechanism of mutual annihilation of stoichiometric premixed methane–air flames 26th Symposium (international) on combustion. Pittsburgh, PA: The Combustion Institute; 1996 p. 855–63.

[365] Chen JH, Echekki T, Kollman W. The mechanism of two dimensional pocket formation in lean premixed methane–air flames with implications to turbulent combustion. Combust Flame 1998;116:15–48.

[366] Chen JH, Im HG. Correlation of flame speed with stretch in turbulent premixed methane–air flames. 27th Symposium (international) on combustion. Pittsburgh, PA: The Combustion Institute; 1998. p. 819–26.

[367] Kollman W, Chen JH. Pocket formation and the flame surface density equation. 27th Symposium (international) on combustion. Pittsburgh, PA: The Combustion Institute; 1998. p. 927–34.

[368] Peters N, Terhoeven P, Chen JH, Echekki T. Statistics of flame displacement speeds from computations of 2-D unsteady methane–air flames. 27th Symposium (international) on combustion. Pittsburgh, PA: The Combustion Institute; 1998. p. 833–9.

[369] Echekki T, Chen JH. Analysis of the contribution of curvature to premixed flame propagation. Combust Flame 1999;118:308–11.

[370] Chen JH, Im HG. Stretch effects on the burning velocity of turbulent premixed hydrogen–air flames. Proc Combust Inst 2000;28:211–8.

[371] Im HG, Chen JH. Preferential diffusion effects on the burning rate of interacting turbulent premixed hydrogen–air flames. Combust Flame 2002;131:246–58.

[372] de Charentenay J, Ern A. Multicomponent transport impact on turbulent premixed H_2/O_2 flames. Combust Theory Modell 2002;6:439–62.

[373] Mandelbrot BB. On the geometry of homogeneous turbulence with stress on the fractal dimension of iso-surfaces of scalars. J Fluid Mech 1975;72:401–16.

[374] Muppala SRP, Dinkelacker F. Numerical calculation of turbulent premixed methane, ethene, and propane/air flames at pressures up to 10 bar. Proceedings of the european combustion meeting, Orleans; 2003, CD.

[375] Boughanem H, Trouvé A. The domain of influence of flame instabilities in turbulent premixed combustion. 27th Symposium (international) on combustion. Pittsburgh, PA: The Combustion Institute; 1998. p. 971–8.

[376] Kuznetsov VR. Effect of flame instability on turbulent combustion of a homogeneous mixture. In: Combustion of gases and natural fuels. Chernogolovka: OIKhF; 1980. p. 32–7 (in Russian).

[377] Meneveau C, Poinsot T. Stretching and quenching of flamelets in premixed turbulent combustion. Combust Flame 1991;86:311–32.

[378] Peters N, Wenzel H, Williams FA. Modification of the turbulent burning velocity by gas expansion. Proc Combust Inst 2000;28:235–43.

[379] Peters N. A spectral closure for premixed turbulent combustion in the flamelet regime. J Fluid Mech 1992;242: 611–29.

[380] Yakhot V. Propagation velocity of premixed turbulent flames. Combust Sci Technol 1988;60:191–214.

[381] Pocheau A. Scale invariance in turbulent front propagation. Phys Rev E 1994;49:1109–22.

[382] Gülder L, Smallwood GJ. Inner cutoff scale of flame surface wrinkling in turbulent premixed flames. Combust Flame 1995;103:107–14.

[383] Mantzaras J, Felton PG, Bracco FV. Fractals and turbulent premixed engine flames. Combust Flame 1989;77:295–310.

[384] North GL, Santavicca DA. The fractal nature of premixed turbulent flames. Combust Sci Technol 1990;72:215–32.

[385] Yoshida A, Kasahara M, Tsuji H, Yanagisawa T. Fractal geometry application in estimation of turbulent burning velocity of wrinkled laminar flame. Combust Sci Technol 1994;103:207–18.

[386] Das AK, Evans RL. An experimental study to determine fractal parameters for lean premixed flames. Exp Fluids 1997;22:312–20.

[387] Gülder L, Smallwood GJ, Wong R, Snelling DR, Smith R, Deschamps BM, et al. Flame front surface characteristics in turbulent premixed propane/air combustion. Combust Flame 2000;120:407–16.

[388] Sivashinsky GI, Law CK, Joulin G. On stability of premixed flames in stagnation-point flow. Combust Sci Technol 1982; 28:155–9.

[389] Korsarts Y, Brailovsky J, Sivashinsky GI. On hydrodynamic instability of stretched flames. Combust Sci Technol 1997; 123:207–21.

[390] Dao J, Linān A. Ignition and extinction fronts in counter-flowing premixed reactive gases. Combust Flame 1999;118: 479–88.

[391] Buckmaster JD, Short M. Cellular instabilities, sublimit structures and edge-flames in premixed counterflows. Combust Theory Modell 1999;3:199–214.
[392] Buckmaster JD. Edge flames. Prog Energy Combust Sci 2002;28:435–75.
[393] Law CK. Dynamics of stretched flames 22nd Symposium (international) on combustion. Pittsburgh, PA: The Combustion Institute; 1988 p. 1281–302.
[394] Dixon-Lewis G. Structure of laminar flames 23rd Symposium (international) on combustion. Pittsburgh, PA: The Combustion Institute; 1990 p. 305–24.
[395] Cant RS, Bray KNC, Kostiuk LW, Rogg B. Flow divergence effects in strained laminar flamelets for premixed turbulent combustion. Combust Sci Technol 1994;95:261–76.
[396] Egolfopoulos FN. Dynamics and structure of unsteady, strained, laminar premixed flames 25th Symposium (international) on combustion. Pittsburgh, PA: The Combustion Institute; 1994 p. 1365–73.
[397] Warnatz J, Maas U, Dibble RW. Combustion: physical and chemical fundamentals, modeling and simulation, experiments, pollutant formation. Berlin: Springer; 1996.
[398] Bradley D, Gaskell PH, Gu XJ. Burning velocities, Markstein lengths, and flame quenching for spherical methane–air flames: a computational study. Combust Flame 1996;104: 176–98.
[399] Bradley D, Gaskell PH, Sedaghat A, Gu XJ. Generation of PDFs for flame curvature and for flame stretch rate in premixed turbulent combustion. Combust Flame 2003;135: 503–23.
[400] Law CK, Zhu DL, Yu G. Propagation and extinction of stretched premixed flame. 21st Symposium (international) on combustion. Pittsburgh, PA: The Combustion Institute; 1986. p. 1419–26.
[401] Deshaies B, Cambray P. The velocity of a premixed flame as a function of the flame stretch: an experimental study. Combust Flame 1990;82:361–75.
[402] Echekki T, Mungal MG. Flame speed measurements at the tip of a slot burner: effects of flame curvature and hydrodynamic stretch. 23rd Symposium (international) on combustion. Pittsburgh, PA: The Combustion Institute; 1990. p. 455–61.
[403] Poinsot T, Echekki T, Mungal MG. A study of the laminar flame tip and implications for premixed turbulent combustion. Combust Sci Technol 1992;81:45–73.
[404] Choi CW, Puri IK. Flame stretch effects on partially premixed flames. Combust Flame 2000;123:119–39.
[405] Choi CW, Puri IK. Contribution of curvature to flame-stretch effects on premixed flames. Combust Flame 2001;126: 1640–54.
[406] Dowdy DR, Smith DB, Taylor SC, Williams A. The use of expanding spherical flames to determine burning velocities and stretch effects in hydrogen–air mixtures. 23rd Symposium (international) on combustion. Pittsburgh, PA: The Combustion Institute; 1990. p. 325–32.
[407] Kwon S, Tseng LK, Faeth GM. Laminar burning velocities and transition to unstable flames in $H_2/O_2/N_2$ and $C_3H_8/O_2/N_2$ mixtures. Combust Flame 1992;90:230–46.
[408] Tseng LK, Ismail MA, Faeth GM. Laminar burning velocities and Markstein numbers of hydrocarbon/air flames. Combust Flame 1993;95:410–26.
[409] Aung KT, Tseng LK, Ismail MA, Faeth GM. Response to comment by S.C. Taylor and D.B. Smith on 'laminar burning velocities and Markstein numbers of hydrocarbon/air flames'. Combust Flame 1995;102:526–30.
[410] Brown MJ, McLean IC, Smith DB, Taylor SC. Markstein lengths of CO_2/H_2/air flames, using expanding spherical flames. 26th Symposium (international) on combustion. Pittsburgh, PA: The Combustion Institute; 1996. p. 875–81.
[411] Aung KT, Hassan ML, Faeth GM. Flame stretch interactions of laminar premixed hydrogen/air flames at normal temperature and pressure. Combust Flame 1997;109:1–24.
[412] Karpov VP, Lipatnikov AN, Wolanskii P. Finding the Markstein number using the measurements of expanding spherical laminar flames. Combust Flame 1997;109:436–48.
[413] Hassan ML, Aung KT, Faeth GM. Measured and predicted properties of laminar premixed methane/air flames at various pressures. Combust Flame 1998;115:539–50.
[414] Baillot F, Bourehla A. Burning velocity of pockets from a vibrating flame experiment. Combust Sci Technol 1997;126: 201–24.
[415] Ibaretta AF, Driscoll JF. Measured burning velocities of stretched inwardly propagating premixed flames. Proc Combust Inst 2000;28:1783–91.
[416] Yokomori T, Mizomoto M. Interaction of adjacent flame surfaces on the formation of wrinkling laminar premixed flame. Proc Combust Inst 2002;29:1511–7.
[417] Choi CW, Puri IK. Response of flame speed to positively and negatively curved premixed flames. Combust Theory Modell 2003;7:205–20.
[418] Mosbacher DM, Wehrmeyer JA, Pitz RW, Sung CJ, Byrd JL. Experimental and numerical investigation of premixed cylindrical flames. AIAA Paper, 2002-0481; 2002.
[419] Mosbacher DM, Wehrmeyer JA, Pitz RW, Sung CJ, Byrd JL. Experimental and numerical investigation of premixed tubular flames. Proc Combust Inst 2002;29:1479–86.
[420] Searby G, Quinard J. Direct and indirect measurements of Markstein numbers of premixed flames. Combust Flame 1990;82:298–311.
[421] Mishra DP, Paul PJ, Mukunda HS. Stretch effects extracted from inwardly and outwardly propagating spherical premixed flames. Combust Flame 1994;97:35–47.
[422] Mishra DP, Paul PJ, Mukunda HS. Stretch effects extracted from propagating spherical premixed flame with detailed chemistry. Combust Flame 1994;99:379–86.
[423] Sun CJ, Sung CJ, He L, Law CK. Dynamics of weakly stretched flames: quantitative description and extraction of global flame parameters. Combust Flame 1999;118:108–28.
[424] Sun CJ, Law CK. On the nonlinear response of stretched premixed flames. Combust Flame 2000;121:236–48.
[425] Mukhopadhyay A, Puri IK. An assessment of stretch effects on a flame tip using the thin flame and thick flame formulations. Combust Flame 2003;133:499–502.
[426] Mikolaitis DW. The interaction of flame curvature and stretch, part 1: the concave premixed flame. Combust Flame 1984;57:25–31.
[427] Mikolaitis DW. Stretched spherical cap flames. Combust Flame 1986;63:95–111.
[428] He L. Critical conditions for spherical flame initiation in mixtures with high Lewis numbers. Combust Theory Modell 2000;4:159–72.

[429] Poinsot T. Comments on 'Flame stretch interactions of laminar premixed hydrogen/air flames at normal temperature and pressure' by K.T. Aung, M.J. Hassan, and G.M. Faeth. Combust Flame 1998;113:279–81.

[430] Aung KT, Hassan ML, Faeth GM. Response to comment by T. Poinsot on 'Flame stretch interactions of laminar premixed hydrogen/air flames at normal temperature and pressure'. Combust Flame 1998;113:282–4.

[431] Yokomori T, Mizomoto M. Flame temperatures along a laminar premixed flame with a non-uniform stretch rate. Combust Flame 2003;135:489–502.

[432] Mueller CJ, Driscoll JF, Sutkus DJ, Roberts WL, Drake MC, Smoke MD. Effect of unsteady stretch rate on OH chemistry during a flame-vortex interaction: to assess flamelet models. Combust Flame 1995;100:323–31.

[433] Sinibaldi JO, Mueller CJ, Driscoll JF. Local flame propagation speeds along wrinkled, unsteady, stretched premixed flames. 27th Symposium (international) on combustion. Pittsburgh, PA: The Combustion Institute; 1998. p. 827–32.

[434] Sinibaldi JO, Driscoll JF, Mueller CJ, Donbar JM, Carter CD. Propagation speeds and stretch rates measured along wrinkled flames to assess the theory of flame stretch. Combust Flame 2003;133:323–34.

[435] Samaniego JM, Mantel T. Fundamental mechanisms in premixed turbulent flame propagation via flame-vortex interactions part I: experiment. Combust Flame 1999;118: 537–56.

[436] Mantel T, Samaniego JM. Fundamental mechanisms in premixed turbulent flame propagation via flame-vortex interactions part II: numerical simulation. Combust Flame 1999;118:557–82.

[437] Hasegawa T, Morooka T, Nishiki S. Mechanism of interaction between a vortex pair and a premixed flame. Combust Sci Technol 2000;150:115–42.

[438] Chakraborty N, Cant RS. Tangential strain rate and curvature effects on the displacement speed of an unsteady turbulent premixed flame in a quasi-stationary configuration. In: European Combustion Meeting; 2003, Paper 142. CD.

[439] Shepherd IG, Ashurst WT. Flame front geometry in premixed turbulent flames. 24th Symposium (international) on combustion. Pittsburgh, PA: The Combustion Institute; 1992. p. 485–91.

[440] Ashurst WT, Shepherd IG. Flame front curvature distributions in turbulent premixed flame zone. Combust Sci Technol 1997;124:115–44.

[441] Mueller CJ, Driscoll JF, Reuss DL, Drake MC. Effects of unsteady stretch on the strength of a freely-propagating flame wrinkled by a vortex. 26th Symposium (international) on combustion. Pittsburgh, PA: The Combustion Institute; 1998. p. 347–55.

[442] Hakberg B, Gosman AD. Analytical determination of turbulent flame speed from combustion models. 20th Symposium (international) on combustion. Pittsburgh, PA: The Combustion Institute; 1984. p. 225–32.

[443] Catlin CA, Lindstedt RP. Premixed turbulent burning velocities derived from mixing controlled reaction models with cold front quenching. Combust Flame 1991;85:427–39.

[444] Sabel'nikov VA, Corvellec C, Bruel P. Analysis of the influence of cold front quenching on the turbulent burning velocity associated with an eddy-break-up model. Combust Flame 1998;113:492–7.

[445] Corvellec C, Bruel P, Sabel'nikov VA. Turbulent premixed flames in the flamelet regime: burning velocity spectral properties in the presence of countergradient diffusion. Combust Flame 2000;120:585–8.

[446] Veynante D, Duclos JM, Piana J. Experimental analysis of flamelet models for premixed turbulent combustion 25th Symposium (international) on combustion. Pittsburgh, PA: The Combustion Institute; 1994 p. 1249–56.

[447] Veynante D, Piana J, Duclos JM, Martel C. Experimental analysis of flame surface density models for premixed turbulent combustion. 26th Symposium (international) on combustion. Pittsburgh, PA: The Combustion Institute; 1996. p. 413–20.

[448] Kostiuk LW, Shepherd IG, Bray KNC. Experimental study of premixed turbulent combustion in opposed streams part III—spatial structure of flames. Combust Flame 1999;118:129–39.

[449] Swaminathan N, Bilger RW. Scalar dissipation, diffusion and dilatation in turbulent H_2–air premixed flames with complex chemistry. Combust Theory Modell 2001;5:429–46.

[450] Swaminathan N, Bilger RW, Ruetsch GR. Interdependence of the instantaneous flame front structure and the overall scalar flux in turbulent premixed flames. Combust Sci Technol 1997;128:73–97.

[451] Swaminathan N, Bilger RW, Cuenot B. Relationship between turbulent scalar flux and conditional dilatation in premixed flames with complex chemistry. Combust Flame 2001;126:1764–79.

[452] Lipatnikov AN, Chomiak J. Transient and geometrical effects in expanding turbulent flames. Combust Sci Technol 2000;154:75–117.

[453] Lipatnikov AN, Chomiak J. Application of the Markstein number concept to curved turbulent flames. Combust Sci Technol 2004;176:331–58.

[454] Yeung PK, Girimaji SS, Pope SB. Straining and scalar dissipation of material surfaces in turbulence: implications for flamelets. Combust Flame 1990;79:340–65.

[455] Girimaji SS, Pope SB. Propagating surfaces in isotropic turbulence. J Fluid Mech 1992;234:247–77.

[456] Williams FA. The role of theory in combustion science 24th Symposium (international) on combustion. Pittsburgh, PA: The Combustion Institute; 1992 p. 1–17.

[457] Libby PA, Williams FA. Structure of laminar flamelets in premixed turbulent flames. Combust Flame 1982;44: 287–303.

[458] Gremyachkin VM, Istratov AG. On a steady flame in a stream with a velocity gradient. In: Gorenie i Vzriv. Moscow: Nauka; 1972. p. 305–8 (in Russian).

[459] Buckmaster JD, Mikolaitis D. The premixed flame in a counterflow. Combust Flame 1982;47:191–204.

[460] Durbin PA. The premixed flame in uniform straining flow. J Fluid Mech 1982;121:141–61.

[461] Daneshyar H, Mendes-Lopes JMC, Ludford GSS. Effect of strain rate fields on burning rate 19th Symposium (international) on combustion. Pittsburgh, PA: The Combustion Institute; 1982 p. 413–21.

[462] Libby PA, Linãn A, Williams FA. Strained premixed laminar flames with nonunity Lewis numbers. Combust Sci Technol 1983;34:257–93.

[463] Sato J, Tsuji H. Extinction of premixed flames in a stagnation flow considering general Lewis number. Combust Sci Technol 1983;33:193–205.

[464] Libby PA, Williams FA. Strained premixed laminar flames with two reaction zones. Combust Sci Technol 1984;37: 221–52.

[465] Zimont VL, Lipatnikov AN. A numerical model of premixed turbulent combustion. Chem Phys Reports 1995;14: 993–1025.

[466] Ren JY, Qin W, Egolfopoulos FN, Tsotsis TT. Strain-rate effects on hydrogen-enhanced lean premixed combustion. Combust Flame 2001;124:717–20.

[467] Seiser R, Truett L, Seshadri K. Extinction of partially premixed flames. Proc Combust Inst 2002;29:1551–7.

[468] Rogg B. Response and flamelet structure of stretched premixed methane–air flames. Combust Flame 1988;73: 45–65.

[469] Lebedev VN. Numerical calculation of the quenching of stretched laminar flames in H_2+ and CH_4+air mixtures. Combust, Explos, Shock Waves 1991;27:184–7.

[470] Liu JK, Ronney PD. Premixed edge flames in spatially varying straining flows. Combust Sci Technol 1999;144: 21–46.

[471] Saitoh T, Otsuka Y. Unsteady behavior of diffusion flames and premixed flames for counterflow geometry. Combust Sci Technol 1976;12:135–46.

[472] Rutland CJ, Ferziger JR. Unsteady strained premixed laminar flames. Combust Sci Technol 1990;73:305–26.

[473] Stahl C, Warnatz J. Numerical investigation of time-dependent properties and extinction of strained methane– and propane–air flames. Combust Flame 1991;85:285–99.

[474] Ghoniem AF, Soteriou MC, Knio OM, Cetegen B. Effect of steady and periodic strain on unsteady flamelet combustion. 24th Symposium (international) on combustion. Pittsburgh, PA: The Combustion Institute; 1992. p. 223–30.

[475] Pearlman HG, Sohrab SH. Extinction of counterflow premixed flames under periodic variation of the rate of stretch. Combust Sci Technol 1995;105:19–32.

[476] Im HG, Bechtold JK, Law CK. Response of counterflow premixed flames to oscillating strain rates. Combust Flame 1996;105:358–72.

[477] Petrov C, Ghoniem A. A uniform strain model of elemental flames in turbulent combustion simulations. Combust Flame 1997;111:47–64.

[478] Huang Z, Bechtold JK, Matalon M. Weakly stretched premixed flames in oscillating flows. Combust Theory Modell 1998;2:115–33.

[479] Najm HN, Knio OM, Paul P, Wyckoff PS. Response of stoichiometric and rich premixed methane–air flames to unsteady strain rate and curvature. Combust Theory Modell 1999;3:709–26.

[480] Sardi K, Whitelaw JH. Extinction timescales of periodically strained, lean counterflow flames. Exp Fluids 1999;27: 199–209.

[481] Hirasawa T, Ueda T, Matsuo A, Mizomoto M. Response of flame displacement speeds to oscillatory stretch in wall-stagnating flow. Combust Flame 2000;121:312–22.

[482] Sung CJ, Law CK. Structural sensitivity, response, and extinction of diffusion and premixed flames in oscillating counterflow. Combust Flame 2000;123:375–88.

[483] Najm HN, Paul P, McIlroy A, Knio OM. A numerical and experimental investigation of premixed methane–air flame transient response. Combust Flame 2001;125:879–92.

[484] Roberts WL, Driscoll JF, Drake MC, Goss LP. Images of the quenching of a flame by vortex—to quantify regimes of turbulent combustion. Combust Flame 1993;94:58–69.

[485] Renard PH, Rolon JC, Thévenin D, Candel S. Wrinkling, pocket formation and double premixed flame interaction processes. 27th Symposium (international) on combustion. Pittsburgh, PA: The Combustion Institute; 1998. p. 659–66.

[486] Renard PH, Thévenin D, Rolon JC, Candel S. Dynamics of flame/vortex interactions. Prog Energy Combust Sci 2000; 26:225–82.

[487] Zimont VL, Lipatnikov AN. To computations of the heat release rate in turbulent flames. Doklady Phys Chem 1993; 332:592–4.

[488] Kolmogorov AN, Petrovsky EG, Piskounov NS. A study of the diffusion equation with a source term and its application to a biological problem. Bjulleten' MGU, Moscow State University, USSR, Section A 1937;1(6) (in Russian; English translation In: Pelcé P, editor. Dynamics of curved fronts. San Diego: Academic Press; 1988)..

[489] Zimont VL, Lipatnikov AN. A model of heat release in premixed turbulent combustion. In: Kondranin TV, editor. Applied problems of aeromechanics and geospase physics. Moscow: MIPT; 1992. p. 48–58 (in Russian).

[490] Ronney PD. Understanding combustion processes through microgravity research. 27th Symposium (international) on combustion. Pittsburgh, PA: The Combustion Institute; 1998. p. 2485–506.

[491] Minaev SS, Kagan L, Joulin G, Sivashinsky G. On self-drifting flame balls. Combust Theory Modell 2001;5:609–22.

[492] Joulin G, Cambray P, Jaouen N. On the response of a flame ball to oscillating velocity gradients. Combust Theory Modell 2002;6:53–78.

[493] Dold JW, Thatcher RW, Omon-Arancibia A, Redman J. From one-step to chain-branching premixed flame asymptotics. Proc Combust Inst 2002;29:1519–26.

[494] Gerlinger W, Schneider K, Fröhlich J, Bockhorn H. Numerical simulations on the stability of spherical flame structure. Combust Flame 2003;132:247–71.

[495] Buckmaster JD. The structure and stability of laminar flames. Annual Rev Fluid Mech 1993;25:21–53.

[496] Champion M, Deshaies B, Joulin G, Kinoshita K. Spherical flame initiation: theory versus experiments for lean propane–air mixtures. Combust Flame 1986;65:319–37.

[497] Deshaies B, Joulin G. On the initiation of a spherical flame kernel. Combust Sci Technol 1984;37:99–116.

[498] Buckmaster JD, Joulin G, Ronney P. The structure and stability of non-adiabatic flame balls; II: effects of far-field losses. Combust Flame 1991;84:411–22.

[499] Buckmaster JD, Joulin G. Flame balls stabilized by suspension in fluids with steady linear ambient velocity distributions. J Fluid Mech 1991;227:407–27.

[500] Karpov VP, Lipatnikov AN. Premixed turbulent combustion and thermodiffusional effects in laminar flames. In: Merzhanov AG, Frolov SM, editors. Combustion, detonation, shock waves. Proceedings of the Zel'dovich memorial, vol. 1. Moscow: ENAS; 1994. p. 168–80.

[501] Ronney PD, Yakhot V. Flame broadening effects on premixed turbulent flame speed. Combust Sci Technol 1992;86:31–43.

[502] Buschmann A, Dinkelacker F, Schäfer T, Schäfer M, Wolfrum J. Measurement of the instantaneous detailed

flame structure in turbulent premixed combustion 26th Symposium (international) on combustion. Pittsburgh, PA: The Combustion Institute; 1996 p. 437–45.

[503] Dinkelacker F, Soika A, Most D, Hofmann D, Leipertz A, Polifke W, et al. Structure of locally quenched highly turbulent lean premixed flames. 27th Symposium (international) on combustion. Pittsburgh, PA: The Combustion Institute; 1998. p. 857–65.

[504] Mansour MS, Peters N, Chen YC. Investigation of scalar mixing in the thin reaction zone regime using a simultaneous CH-LIF/Rayleigh laser technique. 27th Symposium (international) on combustion. Pittsburgh, PA: The Combustion Institute; 1998. p. 767–73.

[505] Chen YC, Bilger R. Simultaneous 2-D imaging measurements of reaction progress variable and OH radical concentration in turbulent premixed flames: experimental methods and flame brush structure. Combust Sci Technol 2001;167:131–67.

[506] Bilger RW. Future progress in turbulent combustion research. Prog Energy Combust Sci 2000;26:367–80.

[507] Bruneaux G, Poinsot T, Ferziger JH. Premixed flame–wall interaction in a turbulent channel flow: budget for the flame surface density evolution equation and modelling. J Fluid Mech 1997;349:191–219.

[508] Ishizuka S. Flame propagation along a vortex axis. Prog Energy Combust Sci 2002;28:477–542.

[509] McCormack PD, Scheller K, Mueller G, Tisher R. Flame propagation in a vortex core. Combust Flame 1972;19: 297–303.

[510] Asato K, Takeuchi Y, Kawamura T. Fluid dynamic effects on flame propagation in a vortex ring. In: Proceedings of the 11th Australian fluid mechanics conference. Hobart: University of Tasmania; 1992. p. 167–70.

[511] Asato K, Takeuchi Y, Wada H. Effects of the Lewis number on characteristics of flame propagation in a vortex core. In: Proceedings of the Russian–Japanese seminar on combustion. Chernogolovka: The Russian Section of the Combustion Institute; 1993. p. 73–6.

[512] Asato K, Wada H, Hiruma T, Takeuchi Y. Characteristics of flame propagation in a vortex core: validity of a model for flame propagation. Combust Flame 1997;110:418–28.

[513] Ishizuka S, Murakami T, Hamazaki T, Koumura K, Hasegawa R. Flame speeds in combustible vortex rings. Combust Flame 1998;113:542–53.

[514] Ishizuka S, Hamazaki T, Koumura K, Hasegawa R. Measurements of flame speeds in combustible vortex rings: validity of the back-pressure drive flame propagation mechanism. 27th Symposium (international) on combustion. Pittsburgh, PA: The Combustion Institute; 1998. p. 727–34.

[515] Ishizuka S, Koumura K, Hasegawa R. Enhancement of flame speed in vortex rings of rich hydrogen/air mixtures in air. Proc Combust Inst 2000;28:1949–56.

[516] Ishizuka S, Ikeda M, Kameda K. Vortex ring combustion in an atmosphere of the same mixture as the combustible. Proc Combust Inst 2002;29:1705–12.

[517] Hasegawa T, Goton D, Nishiki S, Michikami S, Nakamichi R, Nomura T. Experimental and numerical studies of flame propagation along a straight vortex tube. In: Proceedings of the third international symposium on scale modeling. Nagoya: JSME; 2000.

[518] Hasegawa T, Michikami S, Nomura T, Goton D, Sato T. Flame development along a straight vortex. Combust Flame 2002;129:294–304.

[519] Hasegawa T, Nishikado K, Chomiak J. Flame propagation along a fine vortex tube. Combust Sci Technol 1995;108: 67–80.

[520] Hasegawa T, Nishikado K. Effect of density ratio on flame propagation along a fine vortex tube. 26th Symposium (international) on combustion. Pittsburgh, PA: The Combustion Institute; 1996. p. 291–7.

[521] Hasegawa T, Nakamichi R, Nishiki S. Mechanism of flame evolution along a fine vortex. Combust Theory Modell 2002; 6:413–24.

[522] Dwyer HA, Hasegawa T. Some flows associated with premixed laminar flame propagation in a rotating tube flow. Proc Combust Inst 2002;29:1471–7.

[523] Umemura A, Takamori S. Wave nature in vortex-bursting initiation. Proc Combust Inst 2000;28:1941–8.

[524] Takamori S, Umemura A. Behaviors of a flame ignited by a hot spot in a combustible vortex (vortex bursting initiation revisited). Proc Combust Inst 2002;29:1729–36.

[525] Nishioka M, Ogura R. A numerical study of the high-speed flame propagation in a vortex tube. In: Proceedings of the 19th international colloquium on the dynamics of explosions and reactive systems, July 27–August 1, Hakone, Japan. CD ISBN4-9901744-1-0-c3053; 2003.

[526] Chomiak J. Dissipation fluctuations and the structure and propagation of turbulent flames in premixed gases at high Reynolds numbers 16th Symposium (international) on combustion. Pittsburgh, PA: The Combustion Institute; 1977 p. 1665–73.

[527] Daneshyar H, Hill PG. The structure of small-scale turbulence and its effect on combustion in spark ignition engines. Prog Energy Combust Sci 1987;13:47–73.

[528] Atobiloye RZ, Britter RE. On flame propagation along vortex tubes. Combust Flame 1994;98:220–30.

[529] Ashurst WT. Flame propagation along a vortex: the baroclinic push. Combust Sci Technol 1996;112:175–85.

[530] Umemura A, Tomita K. Rapid flame propagation in a vortex tube in perspective of vortex breakdown phenomena. Combust Flame 2001;125:820–38.

[531] Ishizuka S. On the flame propagation in a rotating flow field. Combust Flame 1990;82:176–90.

[532] Sakai Y, Ishizuka S. The phenomena of flame propagation in a rotating tube. 26th Symposium (international) on combustion. Pittsburgh, PA: The Combustion Institute; 1996. p. 847–53.

[533] Tennekes H. Simple model for the small-scale structure of turbulence. Phys Fluids 1968;11:669–71.

[534] Siggia ED. Numerical study of small scale intermittency in three dimensional turbulence. J Fluid Mech 1981;107: 375–406.

[535] Kerr RM. Higher order derivative correlation and the alignment of small-scale structures in isotropic numerical turbulence. J Fluid Mech 1985;153:31–58.

[536] Hosokawa I, Yamamoto K. Fine structure of a directly simulated isotropic turbulence. J Phys Soc Jpn 1989;58:20–3.

[537] Ruetsch GR, Maxey MR. Small-scale features of vorticity and passive scalar fields in homogeneous isotropic turbulence. Phys Fluids A 1991;3:1587–97.

[538] She ZS, Jackson E, Orszag A. Structure and dynamics of homogeneous turbulence: models and simulations. Proc R Soc Lond A 1991;434:101–24.

[539] Vincent A, Meneguzzi M. The spatial structure and statistical properties of homogeneous turbulence. J Fluid Mech 1991; 225:1–25.

[540] Vincent A, Meneguzzi M. The dynamics of vorticity tubes in homogeneous turbulence. J Fluid Mech 1994;258:245–54.

[541] Kida S, Ohkitani K. Spatiotemporal intermittency and instability of a forced turbulence. Phys Fluids A 1992;4: 1018–27.

[542] Tanaka M, Kida S. Characterization of vortex tubes and sheets. Phys Fluids A 1993;5:2079–81.

[543] Pumir A. A numerical study of pressure fluctuations in three-dimensional, incompressible, homogeneous, isotropic turbulence. Phys Fluids 1994;6:2071–83.

[544] Jimenez J, Wray AA, Saffman PG, Rogallo RS. The structure of intense vorticity in isotropic turbulence. J Fluid Mech 1993;255:65–90.

[545] Jimenez J, Wray AA. Columnar vortices in isotropic turbulence. Meccanica 1994;29:453–64.

[546] Jimenez J, Wray AA. On the characteristics of vortex filaments in isotropic turbulence. J Fluid Mech 1998;373: 255–85.

[547] Douady S, Couder Y, Brachet ME. Direct observation of the intermittency of intense vorticity filaments in turbulence. Phys Rev Lett 1991;67:983–6.

[548] Abry P, Fauve S, Flandrin P, Laroche C. Analysis of pressure fluctuations in swirling turbulent flows. J Phys II (France) 1994;4:725–33.

[549] Cadot O, Douady S, Couder Y. Characterization of the low-pressure filaments in a three-dimensional turbulent shear flow. Phys Fluids 1995;7:630–46.

[550] Villermaux E, Sixou B, Gagne Y. Intense vortical structures in grid-generated turbulence. Phys Fluids 1995;7:2008–13.

[551] Cadot O, Bonn D, Douady S. Turbulent drag reduction in a closed system: boundary layer versus bulk effects. Phys Fluids 1998;10:426–36.

[552] Belin F, Maurer J, Tabeling F, Willaime H. Observation of intense filaments in fully developed turbulence. J Phys II (France) 1996;6:573–83.

[553] Noullez A, Wallace G, Lempert W, Miles RB, Frisch U. Transverse velocity increments in turbulent flow using the RELIEF technique. J Fluid Mech 1997;339:287–307.

[554] Verzicco R, Jimenez J, Orlandi P. On steady columnar vortices under local compression. J Fluid Mech 1995;299: 367–88.

[555] Chomiak J. A possible propagation mechanism of turbulent flames at high Reynolds numbers. Combust Flame 1970;15: 319–21.

[556] Abdel-Gayed RG, Bradley D, McMahon M. Turbulent flame propagation in premixed gas: theory and experiment. 17th Symposium (international) on combustion. Pittsburgh, PA: The Combustion Institute; 1979. p. 245–54.

[557] Yoshida A, Narisawa M, Tsuji H. Structure of highly turbulent premixed flames. 24th Symposium (international) on combustion. Pittsburgh, PA: The Combustion Institute; 1992. p. 519–25.

[558] Ulitsky M, Collins LR. Relative importance of coherent structures vs background turbulence in the propagation of a premixed flame. Combust Flame 1997;111:257–75.

[559] Ronney PD, Haslam BD, Rhys NO. Front propagation rates in randomly stirred media. Phys Rev Lett 1995;74:3804–7.

[560] Aldredge RC, Vaezi V, Ronney PD. Premixed-flame propagation in turbulent Taylor–Couette flow. Combust Flame 1998;115:395–405.

[561] Tabaczynski RJ, Trinker FH, Shannon BAS. Further refinement and validation of a turbulent flame propagation model for spark-ignition engines. Combust Flame 1980;39: 111–21.

[562] Corrsin S, Kistler AL. Free stream boundaries of turbulent flows NACA Report 1244 1955.

[563] Kovasznay LSG, Kibens V, Blackwelder RF. Large-scale motion in the intermittent region of a turbulent boundary layer. J Fluid Mech 1970;41:283–325.

[564] Philips OM. The entrainment interface. J Fluid Mech 1972; 51:97–118.

[565] Turbulence. In: Bradshaw P, editor. Topics in applied physics, vol. 42. Berlin: Springer; 1976.

[566] Chevray R. Entrainment interface in free turbulent shear flow. Prog Energy Combust Sci 1982;8:303–15.

[567] Deschamps B, Smallwood GI, Prieur J, Snelling DR, Gülder L. Surface density measurements of turbulent premixed flames in a spark-ignition engine and a Bunsen-type burner using planar laser-induced fluorescene. 26th Symposium (international) on combustion. Pittsburgh, PA: The Combustion Institute; 1996. p. 427–35.

[568] Bray KNC, Champion M, Libby PA. The interaction between turbulence and chemistry in premixed turbulent flames. In: Borghi R, Murthy SNB, editors. Turbulent reacting flows. Lecture notes in engineering, vol. 40. Berlin: Springer; 1989. p. 541–63.

[569] Bray KNC, Libby PA. Recent developments in the BML model of premixed turbulent combustion. In: Libby PA, Williams FA, editors. Turbulent reacting flows. London: Academic Press; 1994. p. 115–51.

[570] Pope SB. The evolution of surface in turbulence. Int J Eng Sci 1998;26:445–69.

[571] Cant RS, Pope SB, Bray KNC. Modelling of flamelet surface-to-volume ratio in turbulent premixed combustion. 23rd Symposium (international) on combustion. Pittsburgh, PA: The Combustion Institute; 1990. p. 809–15.